Department of AERONAUTICS and ASTRONAUTICS
STANFORD UNIVERSITY

FRANK J. REES
I. FLÜGGE-LOTZ

MINIMUM FUEL CONTROL OF A PITCH MOTION OF A SATELLITE IN CIRCULAR ORBIT

AUGUST
1968

This research was sponsored by
the National Aeronautics and Space Administration
under Research Grant NsG 133

SUDAAR
NO. 352

Department of Aeronautics and Astronautics
Stanford University
Stanford, California

MINIMUM FUEL CONTROL OF A PITCH MOTION OF A SATELLITE IN CIRCULAR ORBIT

by

Frank J. Rees

and

I. Flügge-Lotz

SUDAAR No. 352
AUGUST 1968

This research was sponsored by
the National Aeronautics and Space Administration
under Research Grant NsG 133

ACKNOWLEDGMENT

The contribution of the National Aeronautics and Space Administration is gratefully acknowledged; the work was sponsored by NASA under Research Grant NsG 133-61.

ABSTRACT

The pitch motion of a satellite in circular orbit can be described by the normalized differential equation

$$\ddot{x}(t) + \sin x(t) = u(t)$$

whenever a principal axis of the satellite remains normal to the orbit plane. The controlling torque $u(t)$ is bounded ($|u(t)| \leq A$), and $x(t)$ is twice the pitch coordinate. Our goal is to find that control $u(t)$ which zeros the pitch error and error rate within a prescribed fixed time t_f while minimizing the fuel expended ($\int_{t_o}^{t_f} |u(t)|\,dt$). The condition that the bound A of the control be greater than one is essential for the results obtained.

A time varying feedback control law $u(x(t), \dot{x}(t), t)$ is derived by examining the backward time pseudoextremals of Pontryagin's Maximum Principle emanating from the origin and eliminating all candidates except one for each initial disturbance $(x(t_o), \dot{x}(t_o))$ and fixed times t_f. With the existence of an optimal controller guaranteed by a separate argument, our derived control law is both optimal and unique.

The fuel optimal control $u(t)$ is a piecewise constant function of time which can attain only the values $+A$, 0, and $-A$. For finite times of solution t_f, the backwards time trajectories approach is then justified. Singular solutions are not optimal.

The most important facts encountered are

1) For $t_f \leq \pi$ only one switching may occur in the pathological minimum time solution.

2) For $t_f < \pi/2 + \text{arcsinh } 1$ at most two switchings may occur in any control sequence containing both the values $+A$ and $-A$.

3) In contrast to the linear problem, the control sequences $(+A,0,+A,0,\ldots)$ or $(-A,0,-A,0,\ldots)$ are optimal for appropriate initial disturbances.

4) Only pseudoextremals with a vanishing Hamiltonian may arrive at the origin earlier than the specified time of solution t_f and still be fuel optimal for that specific time t_f.

The solution is then applied to solve the actual earth-pointing satellite problem where one now desires to zero the pitch rate while driving the pitch coordinate in time t_f to that integral multiple of 2π which is most economical of fuel. Time varying indifference curves, defined by the locus of those states $(x,\dot{x})$ which may be driven to $(4k\pi,0)$ or $(4(k+1)\pi,0)$ in time t_f with identical fuel expenditure, then subdivide the state space into periodic segments. The pitch coordinate of any state within one such segment is driven to the same multiple of 2π.

The results of this nonlinear analysis are compared to the solution of the linearized problem. An efficient suboptimal control design is proposed and its performance is evaluated.

TABLE OF CONTENTS

TABLE OF CONTENTS (Continued)

LIST OF FIGURES

LIST OF FIGURES (Continued)

LIST OF FIGURES (Continued)

LIST OF FIGURES (Continued)

LIST OF FIGURES (Continued)

INTRODUCTION

The problem of designing an attitude control system to maintain the orientation of a communication satellite so that its antenna points earthward is of great practical interest. In order to evaluate the merit of a proposed design, one first must establish some overall performance criterion for the system. The selection of which factors to include in such a criterion is in itself a difficult value judgment. However, upon agreeing on a performance criterion, it would be useful to determine the optimal control policy and thereby the optimal performance for the system.

The results of such an optimal control study are of importance to the designer for two reasons. Firstly, it may be possible to implement the optimal control strategy directly. If such an implementation is unfeasible, the study would indicate how an efficient suboptimal control scheme might be devised. Secondly, it would establish an optimal performance index by which to gauge the effectiveness of a proposed design.

The dynamical system to be controlled consists of six state variables which completely describe the motion of the satellite; namely, the coordinates of the mass center and the Euler angles. The evolution in time of these states is governed by a strongly coupled system of nonlinear differential equations. Finding a complete feedback fuel optimal control law for the most general satellite motion would involve near insurmountable technical difficulties. Instead this study is a thorough treatment of the full nonlinear equations for a particular satellite motion; namely, the attitude motions of a satellite in circular orbit

when one principal axis remains normal to the orbital plane. This motion is Lyapunov stable and an approximate solution for more general motions for sufficiently small roll and yaw errors and error rates.

The method proposed for providing the control torques is the use of cold gas reaction jets. Such a system is very reliable in a full thrust or zero thrust operation. The so called minimum effort performance criterion was chosen because it corresponds directly to minimizing the amount of gas expended in executing the desired earthpointing maneuver. Inasmuch as only a limited amount of fuel is available for such maneuvers once the satellite is in orbit, such a performance measure is most appropriate. The fact that the optimal control policy for this problem is indeed of the bang-coast or full thrust, zero thrust type further supports the proposal for cold reaction jet controllers.

Since the satellite may spin as well as oscillate, the pitch angle does not remain small. Design studies based on linear analysis may lead to grossly erroneous conclusions. In Chapter V the results of this nonlinear investigation are compared to those obtained from an optimal linearized solution to indicate the caution that must be used in extending conclusions based on a linear model into regions where such a model is no longer valid.

Pontryagin's Maximum Principle is the basic tool employed in this investigation. With the differential equations describing the satellite dynamics at hand, the Maximum Principle provides candidates for the optimal control as a function of the adjoint variables. At this point

the difficulty posed by the nonlinearity becomes most pronounced. For linearized dynamics the adjoint system of differential equations is decoupled from the dynamics system. In this event one may in principle determine the optimal control as a function of time, once one solves the most difficult task of determining appropriate initial conditions for the adjoint variables corresponding to the particular satellite state to be corrected. However, in the nonlinear problem the coupling between the control, state, and adjoint variables is complete. The optimal control depends on the adjoint variables which depend upon the state variables which in turn depend upon the control history.

The goal of this study is to exhibit the fuel optimal control law in the form of a feedback control law. In this form the effects of outside disturbances occurring during the reorientation maneuver are minimized. Actually the feedback control law is time dependent as the time remaining for completing the mission is an essential parameter. The realization of such a time dependent bang-coast control law depends upon the determination of switching surfaces in the cartesian product space $X \times t$ where the time t as well as the state variables X is a coordinate.

For the actual earthpointing satellite problem the number of summersaults through which the satellite has tumbled is of little consequence. The solution for zeroing the pitch error and error rate is then applied to the real satellite problem where one now desires to zero the pitch error rate while driving the pitch coordinate in time t_f to that integral multiple $2K\pi$ which is most economical of fuel. Time varying

indifference curves, defined by the locus of those states in the plane $(x,\dot{x})$ which may be driven to $(2K\pi,0)$ or $(2(K+1)\pi,0)$ in time t with identical fuel expenditure, then subdivide the state space into periodic segments. The pitch coordinate of all states within each segment at time t are driven to the same multiple $2K\pi$.

CHAPTER I

THE SYSTEM - A system consists of a plant or process to be controlled and a means for providing a control input. The dynamical behavior of our plant is governed by the differential equation:

$$\ddot{x}(t) + \sin x(t) = u \tag{1-1}$$

where dots denote differentiation with respect to time t and u is the control input. Let

$$\begin{aligned} x_1(t) &= x(t) \\ x_2(t) &= \dot{x}(t) \end{aligned} \tag{1-2}$$

Then the state variables $x_1(t)$ and $x_2(t)$ are the solutions of the differential equations

$$\begin{aligned} \dot{x}_1(t) &= x_2(t) \\ \dot{x}_2(t) &= u(t) - \sin x_1(t) \end{aligned} \tag{1-3}$$

The scalar control function $u(t)$ shall satisfy the conditions:

i) $u(t)$ is a piecewise continuous function of time (1-4)

ii) $u(t)$ is bounded; that is $|u(t)| \leq A$ for all $t\epsilon(-\infty, +\infty)$ (1-5)

where A is a fixed number greater than one.

THE CONTROL PROBLEM - For the plant described by equations (1-3), we seek a control $u(t)$ satisfying (1-4) and (1-5) which transfers the

system from some known initial state $(x_1(t_o),x_2(t_o))$ to the terminal state $(x_1(t_f),x_2(t_f)) = (0,0)$ within a specified time $T = t_f - t_o$. Since equations (1-3) are stationary, i.e. invariant under change of time reference, t_o may be chosen to be zero. Therefore the boundary conditions may be written as

$$\begin{aligned} (x_1(0),x_2(0)) &= (x_{10},x_{20}) \\ (x_1(T),x_2(T)) &= (0,0) \end{aligned} \tag{1-6}$$

DEFINITION 1-1 Any control $u(t)$ satisfying conditions (1-5), (1-6), and (1-7) shall be designated an admissible control. In other words any piecewise continuous function of time whose absolute value is bounded by a given number A, which drives the system from some prescribed initial state (x_{10},x_{20}) to the origin of state space within a prescribed time T is an admissible control for the given boundary conditions.

THE OPTIMAL CONTROL PROBLEM One frequently desires that the control optimize the system performance in a particular sense while meeting the objectives of the control problem; namely, minimize a performance index while transfering the phase point $(x_1(t),x_2(t))$ to the origin within a prescribed time. For the present case, the criterion to be used in evaluating system performance is

$$J = \int_0^T |u(t)|\,dt \tag{1-7}$$

the so called minimum effort criterion. We may introduce an auxiliary state $x_o(t)$ satisfying

$$\dot{x}_o(t) = |u(t)| \tag{1-8}$$

with initial condition $x_o(0) = 0$ to measure the effort or fuel expended along a trajectory. The optimal control problem then is to minimize the final value of this auxiliary state variable $x_o(T)$. The problem as posed is of practical interest for it describes the pitch motion of a satellite in a circular orbit when one principal axis of the satellite is parallel to the normal of the orbital plane. In that case the pitch motion, as shown in Appendix A, is described by the differential equation

$$I_3\ddot{\theta} - 3\Omega^2 K_3 I_3 \cos\theta \sin\theta = M \tag{1-9}$$

with the symbols to be defined below. The principal moments of inertia of the satellite about its mass center are denoted by I_1, I_2 and I_3. The vectors $\bar{b}_1, \bar{b}_2, \bar{b}_3$ along the principal axes define a reference frame B fixed in the satellite at its mass center. Reference frame A is defined by the orthogonal set of unit vectors $\bar{a}_1, \bar{a}_2$, and $\bar{a}_3$ where

$\bar{a}_1$ is along the line of centers (yaw axis).

$\bar{a}_2$ is along the tangent to the orbital plane (roll axis).

$\bar{a}_3$ is the normal to the orbital plane (pitch axis).

$$K_3 = \frac{I_1 - I_2}{I_3}$$

M = controlling torque about the pitch axis.

Ω = angular velocity of reference frame A with respect to a non-rotating inertial reference frame R at the earth's center.

θ = angle between $\bar{a}_1$ and $\bar{b}_1$; the pitch coordinate.

These quantities are illustrated in Figure 1-1 for the particular motion under consideration; namely, $\bar{b}_3 \equiv \bar{a}_3$. Introducing the change of variables $x = 2\theta$ equation (1-9) becomes

$$\ddot{x} - 3\Omega^2 K_3 \sin x = \frac{M}{2I_3} \tag{1-10}$$

The practical consideration of a stable satellite configuration in the absence of the controlling torque M dictates that K_3 should be negative. The geometric properties of the inertial ellipsoid further restrict K_3 to the closed interval $[-1,1]$. Thus

$$-1 < K_3 < 0 \tag{1-11}$$

Introducing a nondimensional variable $\tau = \sqrt{-3K_3}\Omega t$ equation (1-10) may be rewritten:

$$\frac{d^2x(\tau)}{d\tau^2} + \sin x(\tau) = \frac{M}{6I_3K_3\Omega^2} = u \tag{1-12}$$

where $\frac{\tau}{\sqrt{-3K_3}}$ now corresponds to radians of orbit traversed by the satellite. The right hand side of equation (1-12) is the control variable u of our originally posed problem and is bounded by A as before. The bound A is greater than one to guarantee complete controllability of the satellite. In those satellites where the controlling torque M is generated by jets whose thrust is proportional to rate of

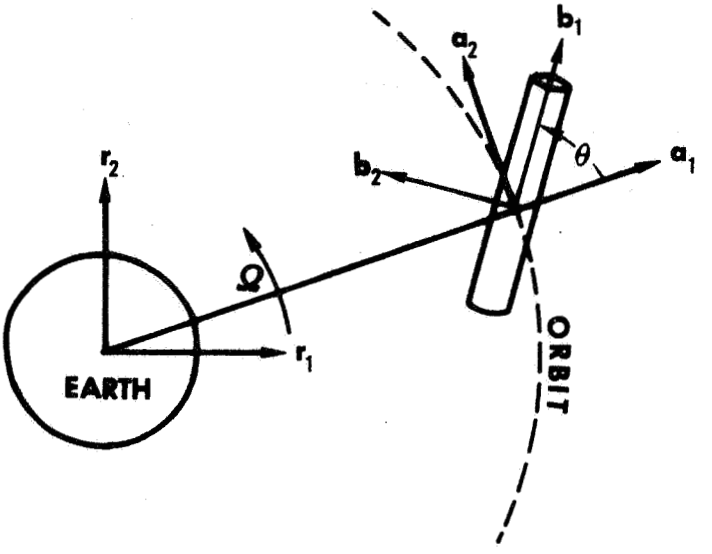

Fig. 1-1. Satellite Orbital and Attitude Reference Frames.

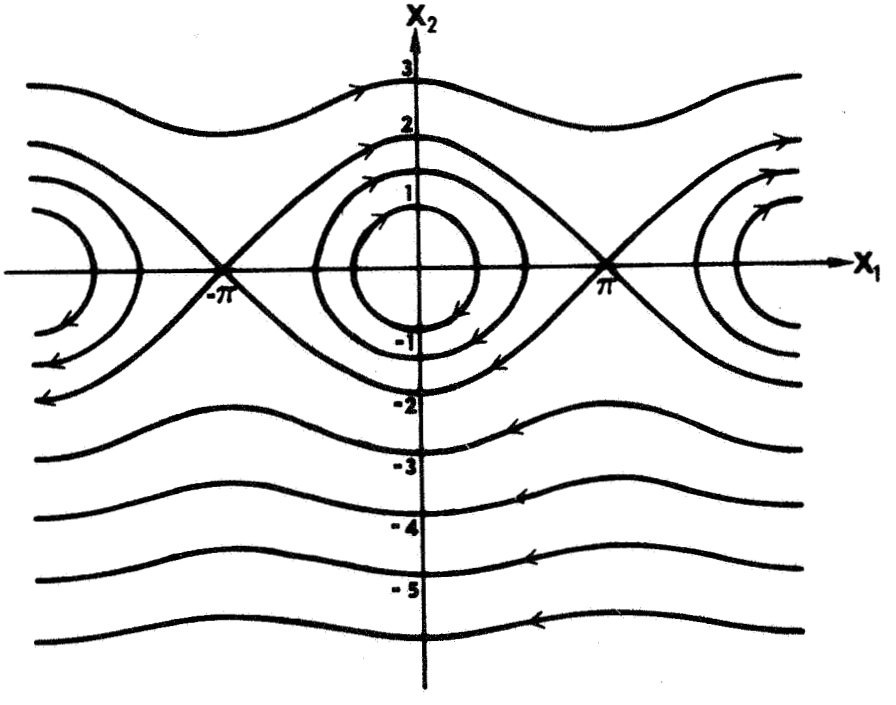

Fig. 1-2. O-System of Trajectories.

fuel consumption, minimizing the performance criterion

$$J = \int_0^T \frac{|M|}{6I_3K_3\Omega^2}\,dt$$

corresponds to using the least possible fuel to perform the desired maneuver of zeroing the error and error rate. Inasmuch as the satellite is to be earth pointing whenever passing over certain sections of the globe, errors and error rates should never accumulate to the point that they could not be zeroed in half a satellite orbit. We shall completely solve this problem where T the prescribed nondimensional time for zeroing the error rate is at most π or $\pi/\sqrt{-3K_3}$ radians of orbit (e.g., $K_3 = -0.03$, 5 orbits allowable; $K_3 = -1/3$, 0.5 orbits allowable; $K_3 = -1$, $\sqrt{3}/6$ orbits allowable.) In the real problem of reorienting a satellite so that it is again earth-pointing, it is of little consequence how many summersaults the satellite has passed through in righting itself. Our objective therefore is to force the error rate $\dot{\theta}$ to zero and the error θ to $2K\pi$ (K is any positive or negative integer) within a prescribed time T while minimizing the fuel spent. But in the reduced equation $\frac{d^2x}{d\tau^2} + \sin x = u$, the dependent variable x is twice the error θ; consequently, our aim is to zero the error rate $\dot{x}$ while transfering $x(\tau)$ to one of the values $4K\pi$. By first solving the case where we require the error and thus $x(\tau)$ to be brought to the position zero with zero error rate, we will then easily construct the solution to the actual earth pointing satellite problem where the number of complete revolutions about the pitch axis is immaterial.

BEHAVIOR OF THE ADJOINT VARIABLES - Introducing an auxiliary state variable $x_o(t) = \int_0^t [u(\tau)]d\tau$ the problem may be restated as minimizing $x_o(T)$ while driving $(x_1(t),x_2(t))$ to $(x_1(t),x_2(t)) = (0,0)$. The Hamiltonian for the augmented system is given by

$$H_1(p,x,u) = p_1x_2 + p_2(u-\sin x_1) + p_o|u| \tag{1-13}$$

where the adjoint variables $p_1(t)$ and $p_2(t)$ satisfy the following differential equations:

$$\begin{aligned} \dot{p}_1(t) &= -\frac{\partial H}{\partial x_1} \\ \dot{p}_2(t) &= -\frac{\partial H}{\partial x_2} \end{aligned} \tag{1-14}$$

which yield

$$\begin{aligned} \dot{p}_1(t) &= p_2(t)\cos x_1 \\ \dot{p}_2(t) &= -p_1(t) \end{aligned} \tag{1-15}$$

and p_o the adjoint variable corresponding to the augmented criterion state variable is a non-positive constant. Eliminating $p_1(t)$ from equations (1-15), we obtain

$$\ddot{p}_2(t) + \cos x_1(t)p_2(t) = 0 \tag{1-16}$$

whose solution we are going to investigate.

THE NECESSARY CONDITIONS ON THE OPTIMAL CONTROL - The Maximum Principle of Pontryagin will now be used to derive the necessary conditions on

the optimal control. Theorem 6 of Ref. [1] for our minimum effort problem reads as follows:

THEOREM 1-1 Let $u(t)$, $t\epsilon[0,t]$, be an admissible control which transfers the state point (x_{10},x_{20}) to $(0,0)$ and let $x(t) = (x_1(t),x_2(t))$ be the corresponding trajectory, according to (1-3), so that $x(0) = (x_{10},x_{20})$ and $x(T) = (0,0)$ where time T is fixed. In order that $u(t)$ yield a solution of the given optimal control problem with fixed time it is necessary that there exists a nonzero continuous vector function $p(t) = (p_o(t),p_1(t),p_2(t))$ corresponding to $u(t)$ and $x(t)$ such that:

i) For all t, $t\epsilon[0,T]$, the function $H(p(t),x(t),u(t))$ of the variable u, $|u| \leq A$, attains its maximum M at the point $u = u(t)$:

$$H(p(t),x(t),u(t)) = M(p(t),x(t)) \tag{1-17}$$

ii) The function $p_o(t)$ is nonpositive which need only be verified at any point of the interval $[0,t]$ since p_o is constant.

$$p_o \leq 0 \tag{1-18}$$

Applying Theorem 1-1 to our Hamiltonian

$$H(p,x,u) = p_1x_2 + p_2(u-\sin x_1) + p_o|u| \tag{1-19}$$

relation (1-17) yields

$$u^*(t) = \begin{cases} +A & \text{if} \quad p_2(t) > -p_o \\ 0 & \text{if} \quad |p_2(t)| < -p_o \\ -A & \text{if} \quad p_2(t) < p_o \end{cases} \tag{1-20}$$

Inasmuch as $u^*(t)$ maximizes our Hamiltonian (1-19) if and only if it maximizes $H(p,x,u)/|p_o|$ (where $|p_o| \neq 0$), and because the adjoint variable $p_2(t)$ satisfies a homogeneous differential equation (1-16), we may without loss of generality consider p_o to be either minus one or zero. In the case where $p_o = -1$ we obtain the control law

$$u^*(t) = \begin{cases} +A & \text{if} \quad p_2(t) > +1 \\ 0 & \text{if} \quad |p_2(t)| < 1 \\ -A & \text{if} \quad p_2(t) < -1 \end{cases} \tag{1-21}$$

whereas the pathological case of $p_o = 0$ yields

$$u^*(t) = \begin{cases} +A & \text{if} \quad p_2(t) > 0 \\ \\ -A & \text{if} \quad p_2(t) < 0 \end{cases} \tag{1-22}$$

It should be noted that in the pathological case the Hamiltonian is maximized by a control $u^*(t)$ without regard for the performance criterion. This arises when so many constraints are imposed on the system that our admissible set of controls yields only one value for

our performance functional $J(u)$. In our minimum effort problem, specifying a time of mission T equal to the minimum settling of that initial state $(x_1(0),x_2(0))$ gives rise to the pathological case. That equations (1-22) are the relations for the minimum time solution is readily apparent.

SINGULAR CONTROLS - We now investigate the possibility that $p_2(t) \equiv 1$ over a finite time interval $[t_1,t_2]$. Should such behavior occur then Pontryagin's Maximum Principle, in particular relation (1-17) is of limited assistance in characterizing candidates $u(t)$ for the optimal control $u^*(t)$ over these intervals. Such controls are usually termed singular controls.

For the problem at hand

$$p_2(t) \equiv 1 \tag{1-23}$$

over the interval (t_1,t_2) if and only if

$$\dot{p}_2(t) = -p_1(t) = 0 \tag{1-24}$$

over this interval in which case $\dot{p}_1 \equiv 0$. But,

$$\dot{p}_1 = p_2 \cos x_1(t) \tag{1-25}$$

implies that $\cos x_1(t) \equiv 0$ over (t_1,t_2) which can only occur if $\dot{x}_1(t) = x_2(t) \equiv 0$ over (t_1,t_2) or from (1-3) and (1-25):

$$u(t) = \sin x_1(t) = +1 \quad \text{or} \quad -1 \tag{1-26}$$

This control strategy corresponds to holding the phase point at $(x_1(t),x_2(t)) = ((2K+1)\frac{\pi}{2},0)$, where K is some positive or negative integer, during this time interval and then proceeding to zero the error and error rate. Since the system is autonomous, nothing is gained by waiting at a point in state space for a more favorable time to zero a disturbance. In addition the expenditure of fuel to hold such a position precludes our admitting such controls to candidacy for an optimal control. One notes that the requirement that the adjoint $p_2 \equiv 1$ over a finite time interval is incompatible with the condition that the Hamiltonian H be non-negative for on such an interval

$$H = p_2\dot{x}_2 + p_1\dot{x}_1 - |u| = -|u| = -1$$

We conclude that we may restrict our considerations to candidates $u^*(t)$ as given in equation (1-21). That the pathological case also has no singular controls is shown in Almuzara's solution of the minimum time problem, Ref. [2].

TRAJECTORIES - From condition (1-17) we have seen that the optimal control can attain only the constant values A, 0, $-A$. Let us find the trajectories of the system (1-3) subject to these controls. By assuming u to be constant, we can integrate equations (1-3) to obtain

$$\frac{x_2^2}{2} = \cos x_1 + ux_1 + K \qquad (1\text{-}27)$$

with K being a constant of integration. Equation (1-27) can also be

written

$$x_2^2/2 - x_{2s}^2/2 = \cos x_1 - \cos x_{1s} + u(x_1 - x_{1s}) \qquad (1\text{-}28)$$

where (x_{1s}, x_{2s}) is a point on the trajectory.

DEFINITION 1-2: If $u = +A$, the solution curves of (1-27) given by

$$\frac{x_2^2}{2} = +Ax_1 + \cos x_1 + K \qquad (1\text{-}29)$$

cover the entire plane exactly once since $A > 1$. This system of trajectories will be called the P-system, its curves P- curves, and portions of its curves P-arcs. See Figure 1-3.

Likewise, if $u = -A$ the solution curves of (1-27) are

$$\frac{x_2^2}{2} = -Ax_1 + \cos x_1 + K \qquad (1\text{-}30)$$

and the family of curves will be called the N-system, its curves N-curves, and portions of its curves N-arcs.

Similarly the family of coast trajectories where $u = 0$ given by

$$\frac{x_2^2}{2} = \cos x_1 + K \qquad (1\text{-}31)$$

will be called the 0-system, its curves 0-curves, and portions of its curves 0-arcs. See Fig. 2. One notes that there is a direction associated with each trajectory plotted in x_1, x_2 space, namely, the direction in which the phase point (x_1, x_2) moves with increasing time. Since trajectories in the upper half plane $(x_2 > 0)$ have a direction

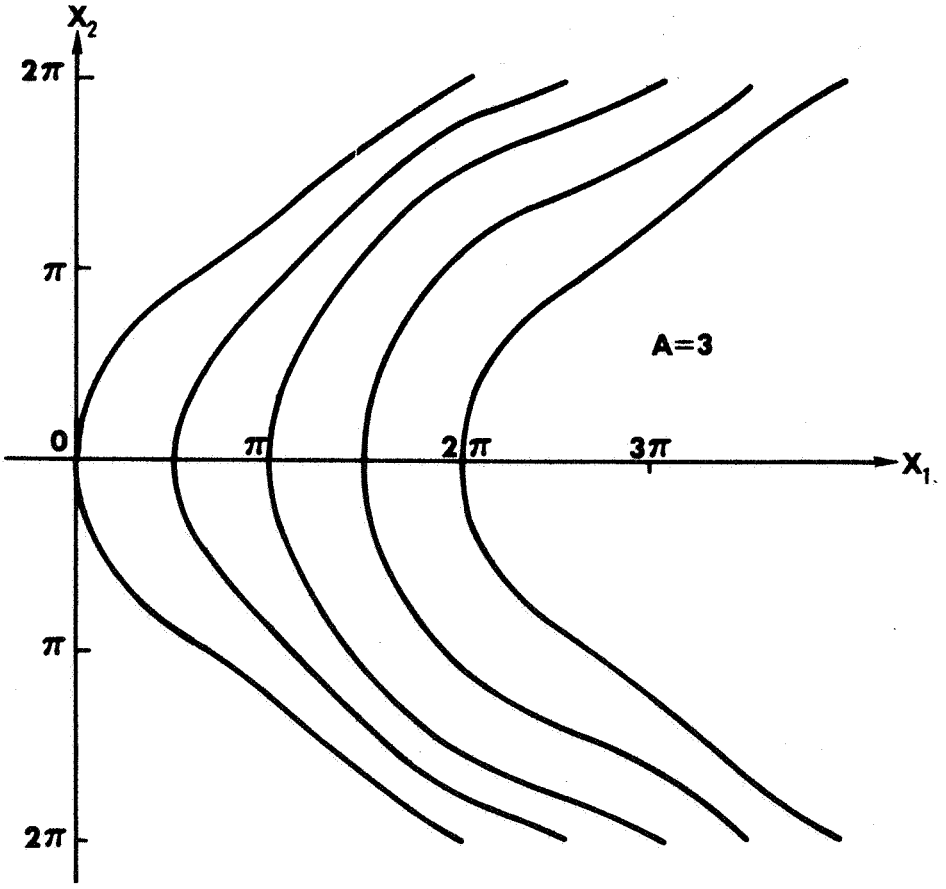

Fig. 1-3. P-System of Trajectories.

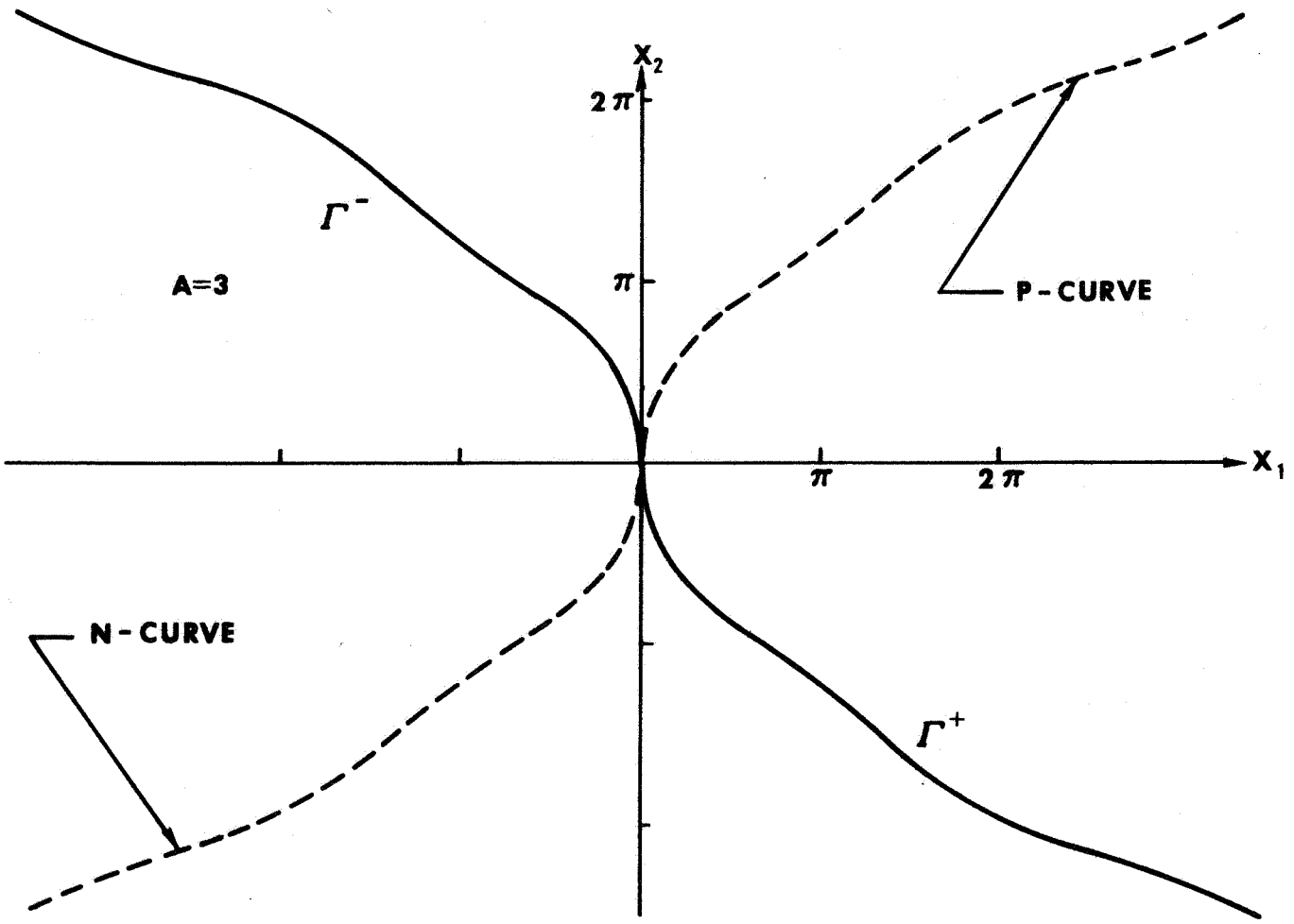

Fig. 1-4. Zero Trajectories Γ^+, Γ^-.

which indicates motion to the right of the phase point while just the opposite holds in the lower half plane.

DEFINITION 1-3: That portion of the $P(N)$ curve which passes through the origin of the x_1,x_2 plane and has an associated direction toward the origin will be called the zero trajectories and designated by Γ^+ (Γ^-) as in Fig. 1-4. Since the only 0-curve passing through the origin is the origin itself, any nontrivial trajectory to the origin meeting the necessary conditions for optimality of the Maximum Principle has as its final arc a portion of the zero trajectory.

DEFINITION 1-4 PSEUDOEXTREMAL: Any trajectory $(x_1(t),x_2(t))$ in the state space generated by a control $u^*(t)$ which meets all the requirements of the Pontryagin Maximum Principle will be designated a pseudo-extremal. The work pseudoextremal rather than extremal is used because as yet such trajectories are only candidates for optimal paths as they fulfill only the necessary conditions for optimality given by the Pontryagin Theorem. We do not as yet know that such solutions provide even a local minimum of the performance functional for neighboring trajectories; such solutions may not provide an extremum value. Moreover, a solution providing a local minimum may not provide a global minimum because our system is not linear.

To find the fuel optimal path, we may limit our considerations to pseudoextremals. Rather than compare the fuel consumption of pseudo-extremals directly to locate the optimal path, we instead compare their

times of solution. Then using Hamilton-Jacobi theory; namely, Corollary 3-1, we will deduce the fuel optimal path from the solution time comparisons.

To begin we develop two elementary lemmas exhibiting pseudoextremal properties. Although the lemmas concern properties well known in the literature, we include them for completeness and because their verification is immediate for our problem.

LEMMA 1-1 Along a pseudoextremal the Hamiltonian $H(p(t),x(t),u) = M(p(t),x(t))$ is constant.

PROOF Along those arcs for which the control u remains constant in value the time rate of change of the Hamiltonian is

$$\frac{dH}{dt} = \langle \nabla_p H, \dot{\bar{p}} \rangle + \langle \nabla_x H, \dot{\bar{x}} \rangle \tag{1-32}$$

But the adjoint equations satisfy

$$\dot{\bar{p}} = -\nabla_x H \tag{1-33}$$

and from the definition of $H = \langle \bar{p}, \dot{\bar{x}} \rangle$

$$\dot{\bar{x}} = \nabla_p H \tag{1-34}$$

Taking into account relations (1-33) and (1-34) we obtain

$$\frac{dH}{dt} = \langle \dot{\bar{x}}, \dot{\bar{p}} \rangle - \langle \dot{\bar{p}}, \dot{\bar{x}} \rangle = 0 \tag{1-35}$$

or H remains constant along those arcs where the control u remains constant.

We now consider the change in the Hamiltonian across a switching point along a pseudoextremal. Let t_s be the time of switching. Then the change ΔH is given by

$$\begin{aligned}\Delta H = {} & p_1(t_s^+)x_2(t_s^+) - p_2(t_s^+)\sin x_1(t_s^+) + u(t_s^+)p_2(t_s^+) - |u(t_s^+)| \\ & -\{p_1(t_s^-)x_2(t_s^-) - p_2(t_s^-)\sin x_1(t_s^-) + u(t_s^-)p_2(t_s^-) - |u(t_s^-)|\}\end{aligned} \tag{1-36}$$

where

$$x(t_s^-) = \lim_{\substack{t \to t_s \\ t < t_s}} x(t)$$

and

$$x(t_s^+) = \lim_{\substack{t \to t_s \\ t > t_s}} x(t)$$

From Pontryagin's Theorem we know $p_1(t)$ and $p_2(t)$ to be continuous. The state variables are also continuous since they are governed by differential equations with bounded control inputs. Therefore we have

$$\begin{aligned} x_1(t_s^-) &= x_1(t_s^+) \qquad p_1(t_s^-) = p_1(t_s^+) \\ x_2(t_s^-) &= x_2(t_s^+) \qquad p_2(t_s^-) = p_2(t_s^+) = p_2(t_s) \end{aligned} \tag{1-37}$$

and

$$\Delta H = p_2(t_s)[u(t_s^+)-u(t_s^-)]-(|u(t_s^+)|-|u(t_s^-)|) \qquad (1\text{-}38)$$

From relations (1-21), the fact that $p_2(t)$ is continuous, and that the absolute value of $p_2(t)$ can equal one only at isolated points $t\epsilon[0,T]$, the only possible switchings are from 0 to $\pm A$ or $\pm A$ to 0 except in the pathological minimum time case where the control may switch directly from +A to -A or -A to +A. Consideration of each sequence in turn reveals that

$$\Delta H = 0 \qquad (1\text{-}39)$$

across a switching on a pseudoextremal as asserted.

LEMMA 1-2 Along any speudoextremal passing through the point $(x_1,x_2) = (0,0)$ the Hamiltonian H is a nonnegative constant.

PROOF That H is constant along a pseudoextremal is the result of the previous lemma. Evaluating the Hamiltonian H at the origin of state space we see

$$H\Big|_{(x_1,x_2)=(0,0)} = p_2u + |u| \qquad (1\text{-}40)$$

which together with relation (1-21) yields

$$H(0,0) = 0 \qquad (1\text{-}41)$$

if absolute value of p_2 at origin is less than one. If the absolute value of p_2 at origin is greater than one then

$$H(0,0) > 0 \qquad (1\text{-}42)$$

Pontryagin has proven H to be a non-negative constant for generalized boundary conditions of autonomous systems, Ref. [1].

CHAPTER II

BACKWARDS TIME FORMULATION

Since our aim is to drive the phase point $(x_1(t),x_2(t))$ to the particular end state $(0,0)$ within a prescribed time, it will be advantageous to reverse the sense of time so that the state $(0,0)$ becomes the initial state. Both our system equation (1-1) and adjoint equation (1-16) are reversible over the interval (t_1,t_2) provided the solution curves possess no conjugate points on (t_1,t_2). Assuming such is the case one can rewrite the state (x_1,x_2) trajectories and their corresponding adjoint solutions (p_1,p_2) as functions of the backward time variable τ. To distinguish between forward and backward time solutions let

$$\begin{aligned} \tau &= T-t \\ y_o(\tau) &= x_o(t) \\ y_1(\tau) &= x_1(t) \\ y_2(\tau) &= x_2(t) \\ \lambda_1(\tau) &= p_1(t) \\ \lambda_2(\tau) &= p_2(t) \end{aligned} \tag{2-1}$$

Letting $'$ denote differentiation with respect to τ $\left(' = \frac{d}{d\tau} = -\frac{d}{dt}\right)$ the augmented system equations become

$$\begin{aligned} y_o'(\tau) &= -|u| \\ y_1'(\tau) &= -y_2(\tau) \\ y_2'(\tau) &= \sin y_1(\tau)-u \end{aligned} \tag{2-2}$$

with initial conditions:

$$\begin{aligned} y_o(0) &= x_o(T) \\ y_1(0) &= x_1(T) \\ y_2(0) &= x_2(T) \end{aligned} \tag{2-3}$$

The backward time Hamiltonian

$$H_B = -\lambda_1(\tau)y_2(\tau) + \lambda_2(\tau)(\sin y_1(\tau) - u) - \lambda_o|u| \tag{2-4}$$

is just the negative of the forward time Hamiltonian. Consequently, maximizing the forward Hamiltonian at each point $(\bar{x},\bar{p},u)$ with respect to the control variable u is equivalent to minimizing the backward time Hamiltonian H_B. For the non pathological case where λ_o may be taken to be -1, the control law generating pseudoextremals is

$$u = \begin{cases} A & \text{for} \quad \lambda_2(\tau) > 1 \\ 0 & \text{for} \quad |\lambda_2(\tau)| < 1 \\ -A & \text{for} \quad \lambda_2(\tau) < -1 \end{cases} \tag{2-5}$$

Again $\lambda_2(\tau)$ satisfies the linear differential equation with time varying coefficients

$$\lambda_2''(\tau) + \lambda_2(\tau)\cos y_1(\tau) = 0 \tag{2-6}$$

as

$$\lambda_1'(\tau) = -\frac{\partial H_B}{\partial y_1} = -\lambda_2(\tau)\cos y_1(\tau)$$
$$\lambda_2'(\tau) = -\frac{\partial H_B}{\partial y_2} = \lambda_1(\tau) \qquad (2\text{-}7)$$

BOUNDARY OF THE T - CONTROLLABLE REGION

DEFINITION 2-1: A point (x_1,x_2) is T - controllable if there exists an admissible control u which drives the initial state (x_1,x_2) to $(0,0)$ within the prescribed time T. The locus of all such points will be called the T - controllable region. See Fig. 2-1.

DEFINITION 2-2: A T-minimum time isochrone is the locus of all initial states (x_1,x_2) for which the minimum time in which any admissible control can transfer the state to $(0,0)$ is exactly T.

Almuzara (Ref. [2]) has shown that the minimum time solution for zeroing any initial disturbance can always be achieved in at most two switchings. For those initial states where the minimum time is at most π, the minimum time solution is achieved with only one switching. Before deriving this fact, we state a comparison theorem, Ref. [3] of which we make good use.

THEOREM 2-1 - Suppose $\varphi(t)$ is a real solution on (t_o,t_f) of

$$\ddot{p}_2 + g_1(t)p_2 = 0 \qquad (2\text{-}8)$$

and $\psi(t)$ is a real solution on (t_o,t_f) of

$$\ddot{\tilde{p}}_2 + g_2(t)\tilde{p}_2 = 0 \qquad (2\text{-}9)$$

where $g_1(t)$ and $g_2(t)$ are continuous on (t_o,t_f). Let $g_2(t) > g_1(t)$ on (t_o,t_f). If t_1 and t_2 are successive zeros of $\varphi(t)$ on (t_o,t_f) then $\psi(t)$ must vanish at some point of (t_1,t_2).

We remark that the comparison theorem remains valid for $g_2(t) \geq g_1(t)$ on (t_o,t_f) so long as strict equality holds only at isolated points on the interval (t_o,t_f). We now apply theorem 2-1 to the following differential equations

$$\ddot{p}_2 + \cos x_1(t) p_2 = 0 \qquad (2\text{-}10)$$

$$\ddot{\tilde{p}}_2 + 1\, \tilde{p}_2 = 0 \qquad (2\text{-}11)$$

to obtain the result that a non-zero solution of equation (2-10) can have at most one zero in any interval of time less than π units long. Identifying $\cos x_1(t)$ with $g_1(t)$ and the constant 1 with $g_2(t)$, in order for a nonzero solution of (2-10) to have zeros at t_1 and t_2, it is necessary that any solution $\tilde{p}_2$ of (2-11) have a zero within the interval (t_1,t_2). But the zeros of any solution to (2-11) are separated by π. Therefore should the interval (t_1,t_2) be less than π units in length, one could always construct a solution to (2-11) having no zero on that interval and thereby contradict the comparison theorem. Thus we have proved the following:

THEOREM 2-2 - The zeros of the adjoint variable $p_2(t)$ solving equation 2-10 are separated by at least π units in time.

COROLLARY 2-1 - Any initial state on a T-minimum time isochrone where T is less than π can be zeroed with one switching.

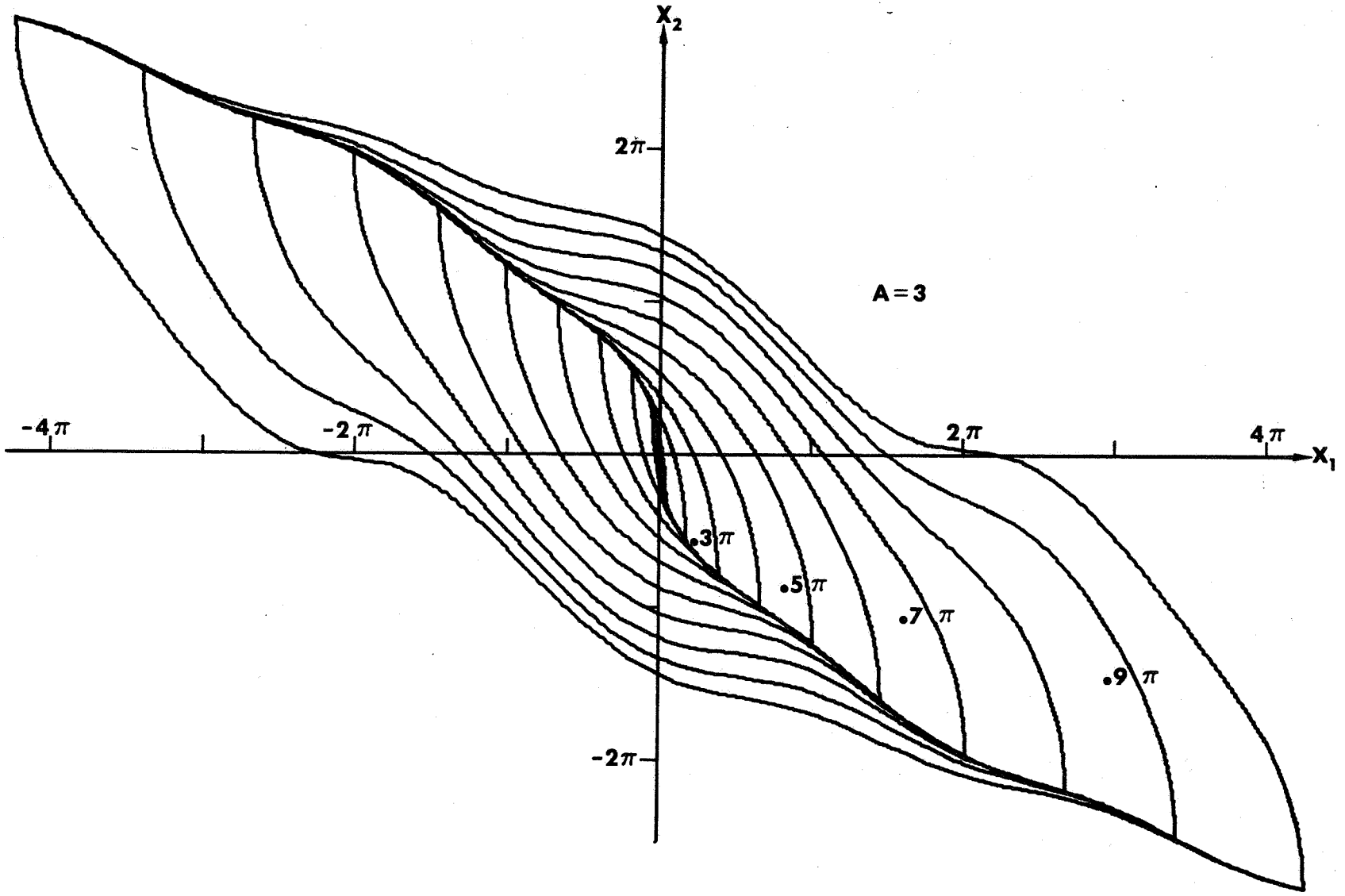

Fig. 2-1. Growth of the T-Controllable Region with Increasing T.

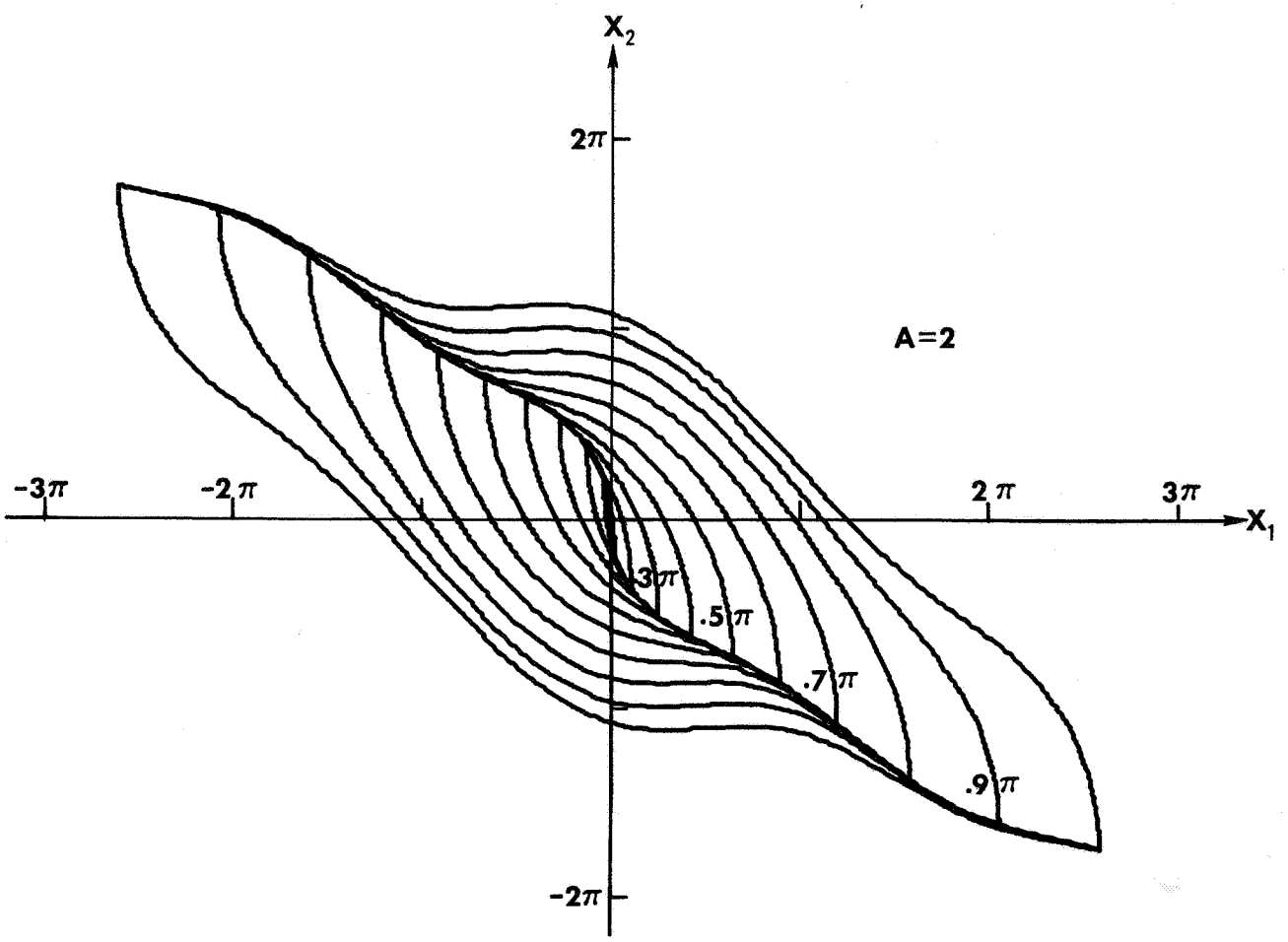

Fig. 2-2. Behavior of T-Minimum Time Isochrones (Growth of T-Controllable Region) with Increasing T.

PROOF: Almuzara, Ref. [2] has shown that a switching of a minimum time control can only occur at the zeros of the function $p_2(t)$. Application of theorem 2-2 completes the proof.

We now give a complete characterization of T - minimum time isochrone. Firstly, the T - minimum time isochrone is the boundary of the T - controllable region. Secondly, each point (x_1,x_2) of the T - minimum isochrone with $T < \pi$ can be generated by integrating equations (2-2) from initial condition (0,0) for R seconds with control $u(\tau) = +A(-A)$ and continuing the integration for T-R seconds with control $u(\tau) = -A(A)$. Hence, each value of the parameter R taken from the interval (0,T) maps into two points (x_1,x_2) of the T - minimum time isochrone; namely, one for $u(\tau)$ initially +A and one for $u(\tau)$ initially -A. See Fig. 2-2 illustrating T - minimum time isochrones.

POSSIBLE SWITCHING SEQUENCES

By limiting the normalized time of mission T to a value less than π (which corresponds to a limit of $\pi/\sqrt{-3K_3}$ radians of orbit of the satellite of half an orbit for our chosen value of $K_3 = -1/3$) we already have seen that initial disturbances coincident with the boundary of the T - controllable region can only be zeroed by the control sequence +A, -A or else by the sequence -A, A. We now investigate other possible switching sequences which satisfy the Maximum Principle while zeroing the initial disturbance within the allowable time T with minimum fuel expenditure. For any initial

disturbance which is an interior point of the T- controllable region p_o may always be chosen to be equal to minus one. With the continuity of the adjoint $p_2(t)$ assured by the Maximum Principle we easily obtain from equation (1-21) the fact that the control may switch only from a value 0 to +A or -A or from +A or -A to 0. That the control law given by (1-21) does not specify the value of the control at those points in time for which $|p_2(t)| = 1$ is of little consequence as we have already seen that we may limit our consideration to those controls $u(t)$ for which $|p_2(t)| = 1$ only at a finite number of isolated points. Choosing any admissible value for the control $u(t)$ at these points will leave the pseudoextremal and fuel cost unchanged. In specifying possible switching sequences we revert to the backward time formulation. Inasmuch as the state would remain at the origin if the control $u = 0$ were used, the backward time switching sequence begins with the control being initially +A or -A. We shall derive results only for those sequences beginning with the control at +A since identical logic yields analogous results for those sequences beginning with -A. The optimal pseudoextremal for zeroing state (x_{10},x_{20}) within time T must necessarily consist of some combination of p, 0, and N-arcs. In order to reduce the number of possible control sequences to be considered for generating this optimal pseudo-extremal, we shall always limit the allowed time of solution T to be at most π. In the proofs of certain preliminary theorems, however, we shall find it necessary to further restrict the maximum permissible times of solution T to be less than $\pi/2 + \text{arcsinh } 1 \ (\approx 0.78\pi)$. This

additional restriction occurs only in theorems related to consideration of pseudoextremals containing an N-arc. Alghough these proofs are accomplished for this smaller time limit $\pi/2$ + arcsinh 1, the method of proof suggests the conclusions to be valid for times larger than $\pi/2$ + arcsinh 1 - perhaps even as large as π. In order that we be aware of exactly where our conclusions are guaranteed valid for π and where just for $\pi/2$ + arcsinh 1, we extend proofs to be valid for T as large as π whenever possible and otherwise spellout clearly that a particular result has only been proved for times T up to $\pi/2$ + arcsinh 1. In so doing we obtain rigorously complete results for the lower time limitation and rigorously near complete results for the π time limit, with an indication that the complete picture may hold for times as large as π as well. First we consider a sequence of the type +A,0,-A,0,... and seek a limit for the number of such switchings which can occur within our prescribed time T. In order for such a sequence to meet the necessary conditions for optimality the backwards time adjoint function $\lambda_2(t)$ must behave as shown in Figure 2-3 where τ_i is the time of the i-th switching. That τ_3 is always greater than $\pi/2$ + arcsinh 1 $\approx$ 2.46 is the subject of the following theorem.

THEOREM 2-3 - If at time τ_1, $\lambda_2(\tau_1) \geq 1$ and the backward time state variables are zero $(y_1(\tau_1) = y_2(\tau_1)=0)$ then for any admissible control $u(\tau)$ such that $\lambda_2(\tau_2) < -1$ and $\lambda_2(\tau_f) = -1$ where $\tau_1 < \tau_2 < \tau_f$ the interval $\tau_f-\tau_1$ exceeds $\pi/2$ + arcsinh 1. The proof is achieved by examining the minimum time solution of an auxiliary problem having $\lambda_1(\tau)$ and $\lambda_2(\tau)$ in addition to $y_1(\tau)$ and $y_2(\tau)$ as state variables.

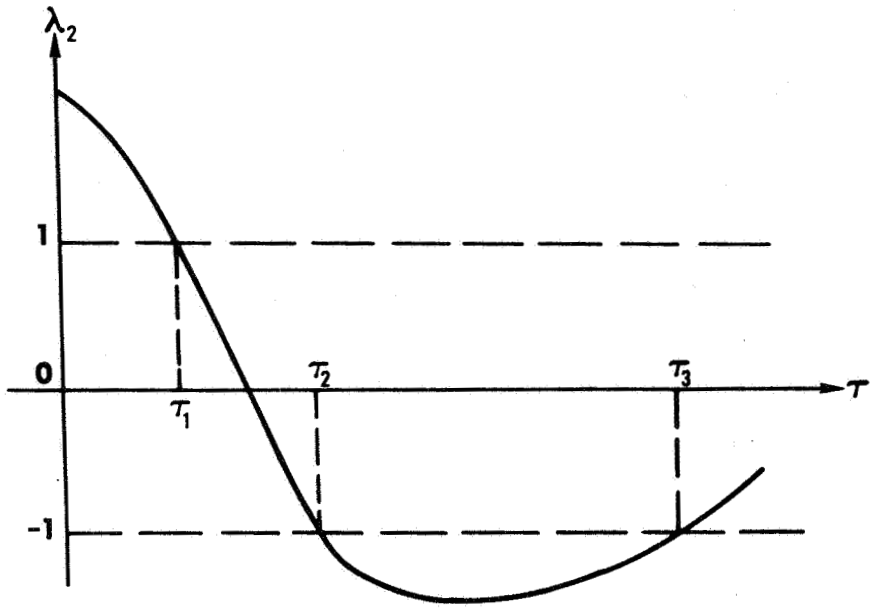

Fig. 2-3. Behavior of Adjoint $\lambda_2(\tau)$ in a Switching Sequence $+A,0,-A,0,\ldots$

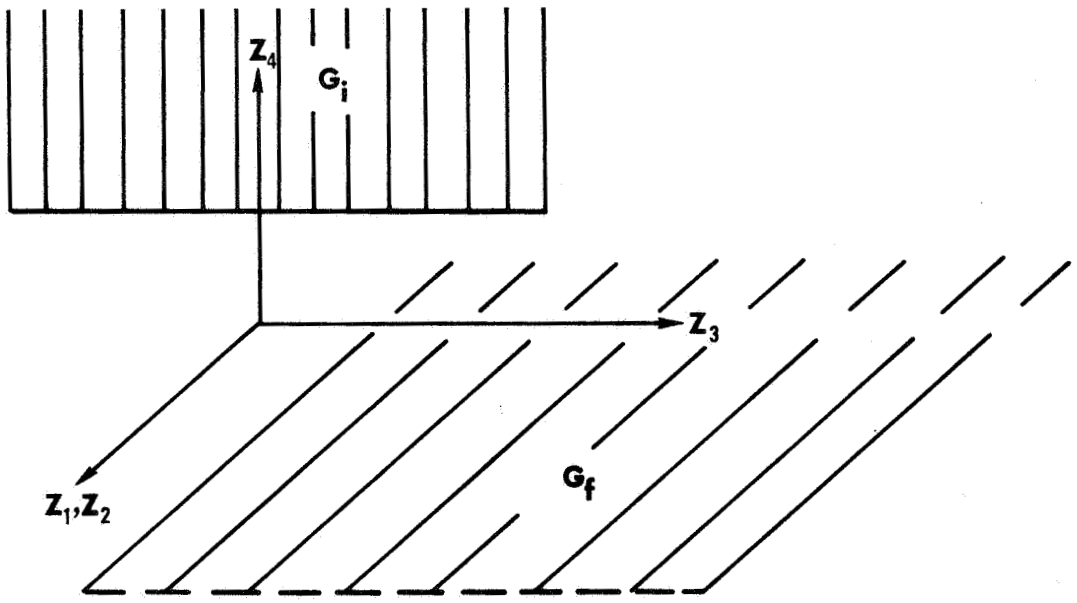

Fig. 2-4. Auxiliary Problem to Minimize the Time in Going from G_i to G_f.

The original system and adjoint equations are:

$$\begin{aligned} y_1(\tau) &= -y_2(\tau) \\ y_2(\tau) &= \sin y_1(\tau) - u \\ \lambda_1(\tau) &= -\lambda_2(\tau)\cos y_1(\tau) \\ \lambda_2(\tau) &= \lambda_1(\tau) \end{aligned} \tag{2-12}$$

We now let $z_i(\tau)$ denote the state variables of our auxiliary problem defined by

$$\begin{aligned} z_1(\tau) &= y_1(\tau) \\ z_2(\tau) &= y_2(\tau) \\ z_3(\tau) &= \lambda_1(\tau) \\ z_4(\tau) &= \lambda_2(\tau) \end{aligned} \tag{2-13}$$

and system equations

$$\begin{aligned} z_1'(\tau) &= -z_2(\tau) \\ z_2'(\tau) &= \sin z_1(\tau) - u \\ z_3'(\tau) &= -z_4(\tau)\cos z_1(\tau) \\ z_4'(\tau) &= z_3(\tau) \end{aligned} \tag{2-14}$$

and consider the problem of a minimum time transfer of the system from the initial region G_i (see Fig. 2-5) defined by

$$\begin{aligned} z_1 &= 0 \\ z_2 &= 0 \\ z_3 &\text{ free} \\ z_4 &\geq 1 \end{aligned} \tag{2-15}$$

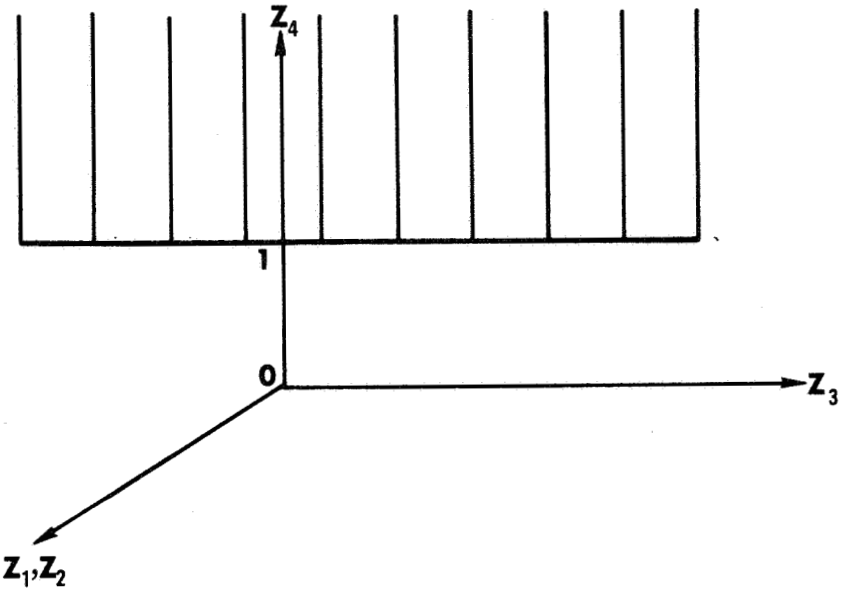

Fig. 2-5. Initial Region G_i of the Auxiliary Problem.

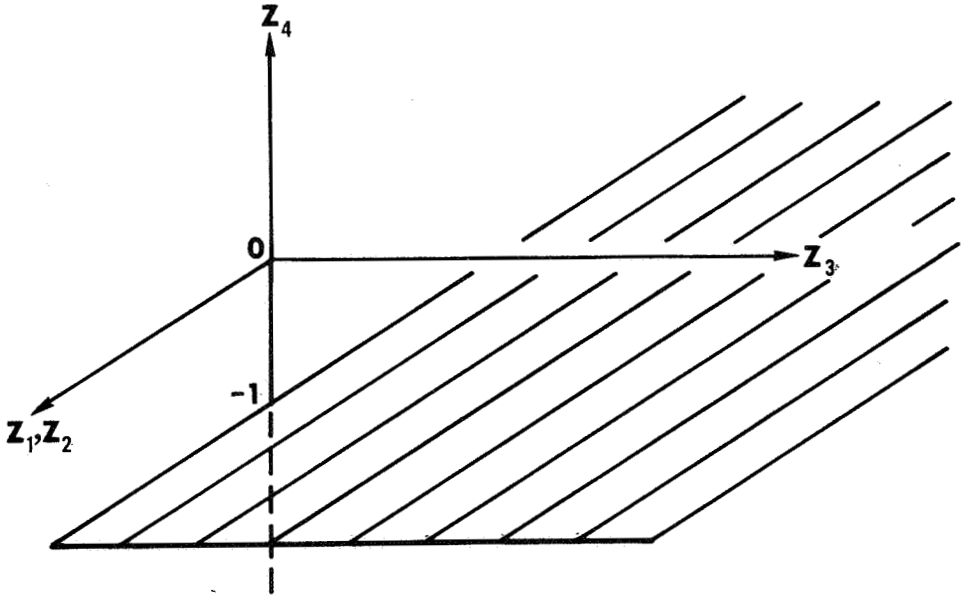

Fig. 2-6. Target Region G_f of the Auxiliary Problem.

to the target region G_f (see Fig. 2-6) defined by

$$\begin{aligned} &z_1(\tau_f) \quad \text{free} \\ &z_2(\tau_f) \quad \text{free} \\ &z_3(\tau_f) \geq 0 \\ &z_4(\tau_f) = -1 \,. \end{aligned} \tag{2-16}$$

In the auxiliary problem the system dynamics are described by four first order differential equations (2-14) whereas the original system dynamics had only two first order differential equations (2-2). Furthermore, the criterion of the auxiliary problem is time optimality, not fuel optimality. We note that the region G_i corresponds to the first part of the hypothesis of our theorem. Region G_f is just the second part of the hypothesis once we recognize that the requirement $\lambda_2(\tau_2) < -1$ can be replaced by requiring $\lambda_2'(\tau_f)$ to be ≥ 0 i.e., $z_3(\tau_f) \geq 0$. See Fig. 2-7, 2-8. This replacement includes all trajectories where the adjoint dips below minus one but also introduces additional trajectories which do not cross the plane $\lambda_2(\tau) = -1$ but are tangent to it as illustrated in Fig. 2-8. Thus the case $z_3(\tau_f) = 0$ may introduce extraneous trajectories which do not correspond to three switching points. Nevertheless, should the minimum time of solution exceed $\pi/2$ + arcsinh 1 for the G_1-G_f boundary region problem it would exceed $\pi/2$ + arcsinh 1 for the actual problem of interest which is more restrictive in that paths which do not dip below $z_3 = -1$ are excluded. Let

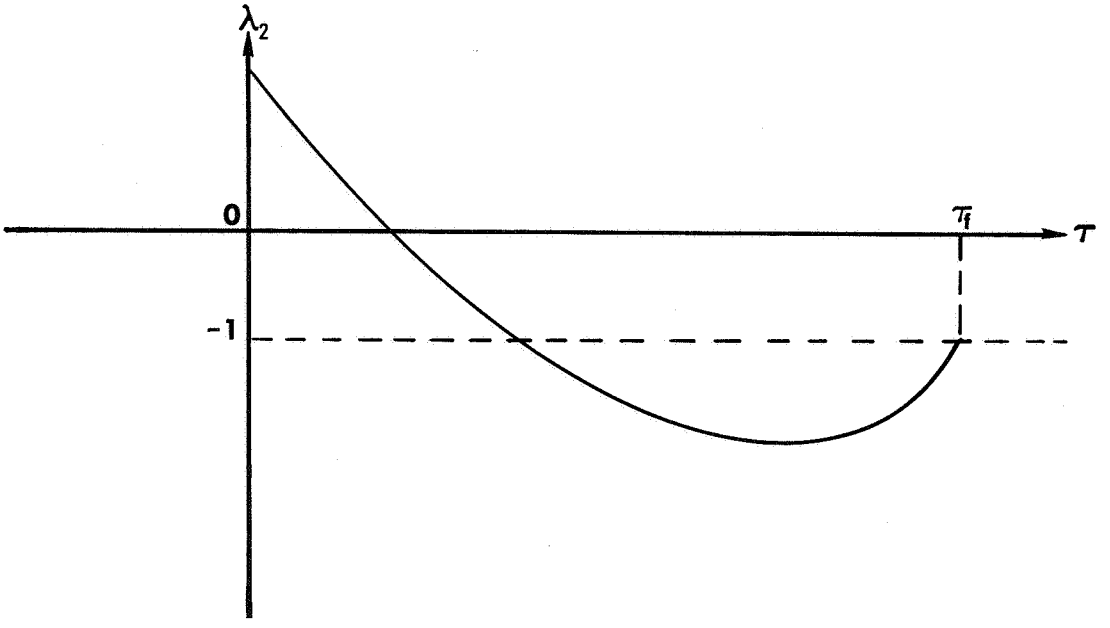

Fig. 2-7. Replacement of $\lambda_2(\tau_2) < -1$ by $\lambda_2'(\tau_f) \geq 0$.

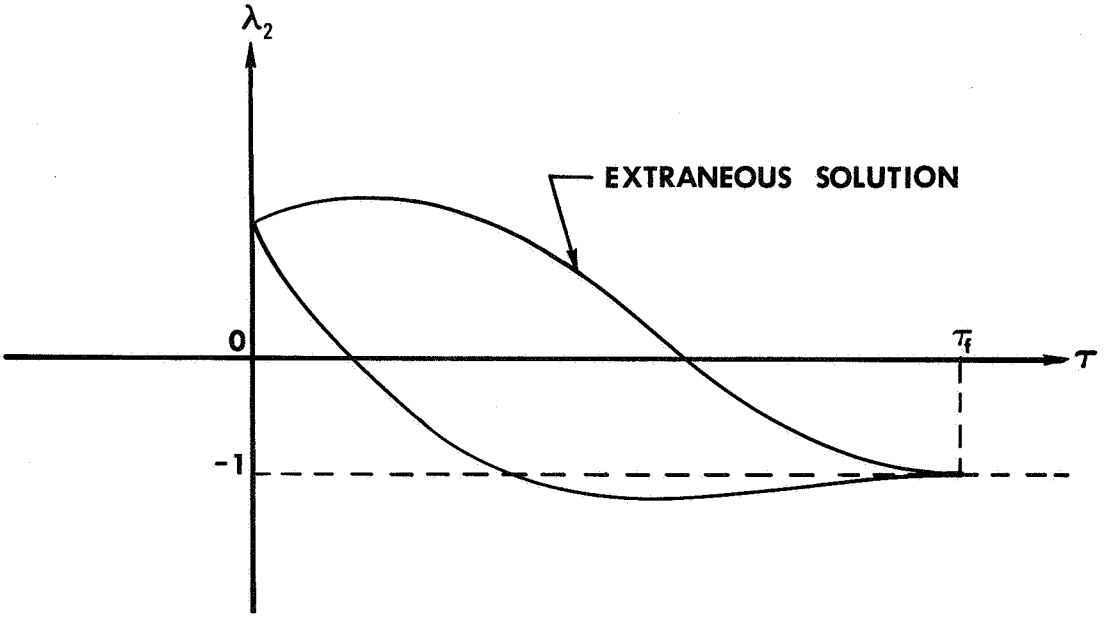

Fig. 2-8. Extraneous Solutions Introduced Via Replacement of $\lambda_2(\tau_2) < -1$ by $\lambda_2'(\tau_f) \geq 0$.

$$\hat{H} = -\psi_1 z_2 + \psi_2(\sin z_1 - u) - \psi_3 z_4 \cos z_1 + \psi_4 z_3 - 1 \tag{2-17}$$

define the new Hamiltonian for the auxiliary problem with backward time adjoint variables ψ_i satisfying the equations:

$$\psi_1' = -\frac{\partial \hat{H}}{\partial z_1} = -\psi_2 \cos z_1 - \psi_3 z_4 \sin z_1 \tag{2-18}$$

$$\psi_2' = -\frac{\partial \hat{H}}{\partial z_2} = \psi_1 \tag{2-19}$$

$$\psi_3' = -\frac{\partial \hat{H}}{\partial z_3} = -\psi_4 \tag{2-20}$$

$$\psi_4' = -\frac{\partial \hat{H}}{\partial z_4} = -\psi_3 \cos z_1 \tag{2-21}$$

The backward time Hamiltonian is minimized by the control law:

$$u = \begin{cases} +A \quad \text{for} \quad \psi_2 > 0 \\ \\ -A \quad \text{for} \quad \psi_2 < 0 \end{cases} \tag{2-22}$$

and by any admissible value of the control input $u(\tau)$ on the time set τ for which $\psi_2(\tau) = 0$. For the time optimal solution the adjoint vector $\bar{\psi}(\tau_f)$ at the moment of time $\tau = \tau_f$, where τ_f is the minimum time of solution, must be orthogonal to some hyperplane B which is a bracket for the set G_f as in Ref. [4]. Furthermore, the adjoint vector at time τ_f must be directed toward that side of the hyperplane B where the set G_f lies. The same transversality conditions must be met at the other endpoint $\tau = 0$ for some hyperplane B bracketing the set G_i except that the adjoint vector is now directed away from that

side of the hyperplane where the set G_i lies. By considering all bracketing hyperplanes we find that the requirement that the adjoint vector $\bar{\psi}(0)$ be orthogonal to some hyperplane B bracketing the set G_i and that the adjoint point out from that side of B where the region G_i lies, lead to the results

$$\begin{aligned} &\psi_1(\tau_i) && \text{unknown} \\ &\psi_2(\tau_i) && \text{unknown} \\ &\psi_3(\tau_i) = 0 \\ &\psi_4(\tau_i) \leq 0 \end{aligned} \tag{2-23}$$

The component $\psi_3(\tau_i)$ is zero because the state vector component $z_3(\tau_i)$ is free. The initial conditions for the adjoint components $\psi_1(\tau)$ and $\psi_2(\tau)$ are unknown as these components of the state vector $\bar{z}(\tau)$ are fixed at the left boundary. That $\psi_4(\tau_i)$ must be non positive can best be seen be viewing the planar initial manifold G_i from an end view as shown in Fig. 2-9. Consideration of all bracketing hyperplanes is equivalent to considering all θ satisfying

$$0 \leq \theta \leq \pi \tag{2-24}$$

in which case

$$\psi_4(\tau_i) \leq 0 \tag{2-25}$$

Since analogous transversality conditions must hold at the right boundary, i.e., at time τ_f the minimum time of solution, we again consider all bracketing hyperplanes B for the region G_f and require that $\bar{\psi}(\tau_f)$ be an inwardly directed normal for some hyperplane B.

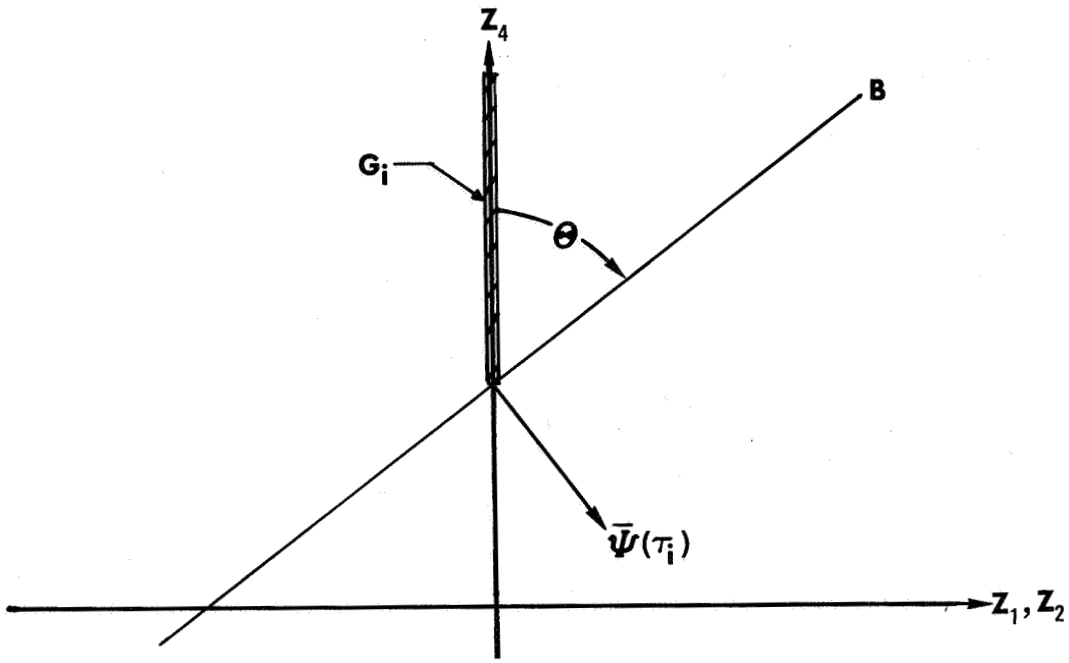

Fig. 2-9. Bracketing Hyperplane With Normal $\bar{\psi}$ to Region G_i.

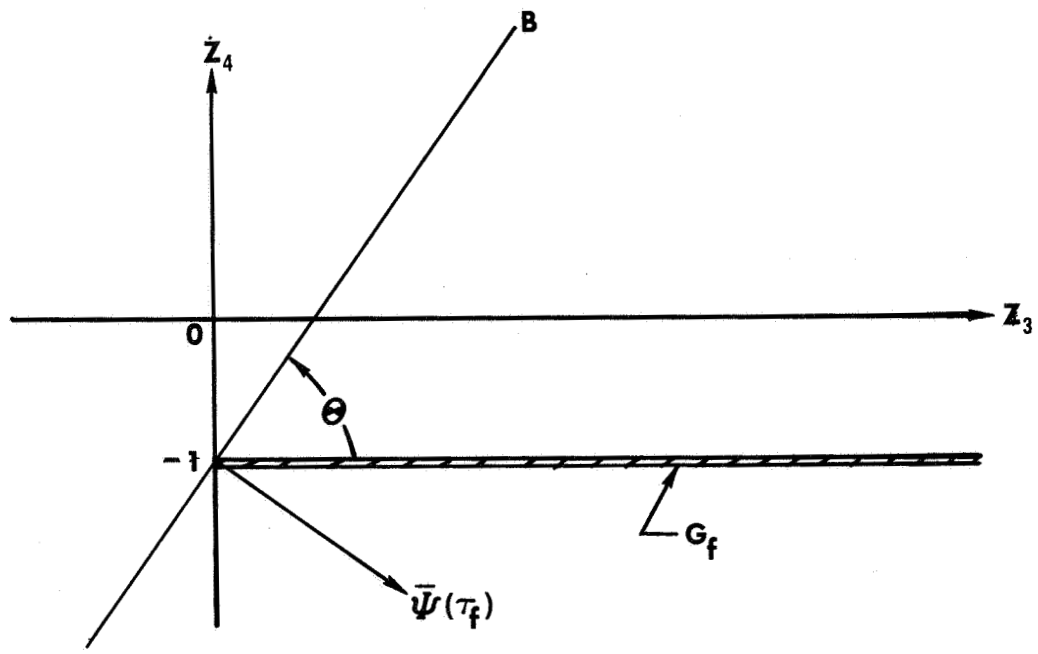

Fig. 2-10. Bracketing Hyperplane With Normal $\bar{\psi}$ to Region G_f.

The right end conditions for the adjoint vector $\bar{\psi}(\tau)$ are

$$\begin{aligned} \psi_1(\tau_f) &= 0 \\ \psi_2(\tau_f) &= 0 \\ \psi_3(\tau_f) &\geq 0 \\ \psi_4(\tau_f) &\quad \text{unknown} \end{aligned} \tag{2-26}$$

The components ψ_1 and ψ_2 vanish at time τ_f since these components of the state vector $\bar{z}$ are free. $\psi_4(\tau_f)$ is unknown as $z_4(\tau_f)$ is completely specified to be minus one. That $\psi_3(\tau_f)$ must be non-negative is readily seen by examining an end view of the planar target manifold G_f as shown in Fig. 2-10 and recalling the adjoint $\bar{\psi}(\tau_f)$ must now be an inwardly directed normal for some bracketing hyperplane. From equations (2-20) and (2-21) we have

$$\psi_3''(\tau) + \psi_3(\tau)\cos z_1(\tau) = 0 \tag{2-27}$$

where

$$\psi_3(\tau_i) = 0 \tag{2-28}$$

$$\psi_3(\tau_f) \geq 0 \tag{2-29}$$

in order to meet the transversality conditions. We now will demonstrate that in the last relation (2-23) the adjoint component $\psi_4(\tau_i)$ must be strictly less than zero in order that our problem possess a time optimal solution. Suppose $\psi_4(\tau_i) = 0$. Then since $\psi_3(\tau_i) = 0$ equations (2-20) and (2-21) yield

$$\psi_3(\tau) \equiv 0 \quad \tau > \tau_i \tag{2-30}$$

$$\psi_4(\tau) \equiv 0 \tag{2-31}$$

For any finite time interval $[\tau_i, \tau_f]$ the transversality conditions $\psi_1(\tau_f)$ and $\psi_2(\tau_f)$ together with the result $\psi_3(\tau) \equiv 0$ and equations (2-18) and (2-19) force that

$$\psi_1(\tau) \equiv 0 \quad \text{all} \quad \tau\epsilon[\tau_i, \tau_f] \tag{2-32}$$

$$\psi_2(\tau) \equiv 0 \tag{2-33}$$

as well. Therefore, the only solution to the adjoint equations satisfying the transversality relations and the requirement that $\psi_4(\tau_i) = 0$ is the trivial solution $\overline{\psi}(\tau) \equiv \overline{0}$. However, Pontryagin's Maximum Principle, and in particular theorem 2 of reference [1] guarantees that the adjoint solution corresponding to the optimal time solutions be nonzero. Hence, assuming the existence of the time optimal solution of a trajectory from region G_i to region G_j, the adjoint component ψ_4 must not be zero at the initial time and we have the result that

$$\psi_4(\tau_i) < 0 \tag{2-34}$$

Thus we are guaranteed a nontrivial solution to (2-27). Should the equality hold in the transversality relation (2-29) then application of theorem 2-2 to this solution of equation (2-27) yields the result

$$\tau_f - \tau_i \geq \pi \tag{2-35}$$

But in the event that the transversality relation at the right hand end is indeed

$$\psi_3(\tau_f) > 0 \tag{2-36}$$

we can no longer guarantee the validity of inequality (2-25). However, relation (2-36) implies upon examination of Fig. 2-10 that

$$z_3(\tau_f) = 0 \tag{2-37}$$

With the aid of this additional boundary condition on the state variable we now seek a lower bound on the minimum time of solution of the less restrictive problem

$$\dot{z}_4 = z_3 \tag{2-38}$$

$$\dot{z}_3 = -\tilde{u}z_4 \tag{2-39}$$

meeting boundary conditions

$$\begin{aligned} z_4(\tau_f) &= -1 & z_4(\tau_i) &\geq 1 \\ \dot{z}_4(\tau_f) &= z_3(\tau_f) = 0 & z_3(\tau_i) &\text{ free} \end{aligned} \tag{2-40}$$

where the control variable satisfies

$$|\tilde{u}| \leq 1 \tag{2-41}$$

as we have replaced $\cos z_1(\tau)$ by the control function $\tilde{u}$. Since now we consider $\tilde{u}(\cos z_1(t))$ to be an arbitrary piecewise boundary function of time no longer restricted by the plant dynamics formally described through z_1 and z_2, the minimum time of solution for this less

restrictive problem is a lower bound for the minimum time of solution of our auxiliary problem of interest. The solution to this problem is more readily seen if we revise the sense of time i.e., return to the forward time formulation. Then the problem is to drive the plant

$$\dot{x}_4(t) = -x_3(t) \tag{2-42}$$

$$\dot{x}_3(t) = x_4(t)\tilde{u} \tag{2-43}$$

from the position $x_4 = -1$ with zero velocity to the position $x_4 = +1$. The optimum policy as derived in Appendix B is to provide maximum acceleration all the way i.e., maximize $\ddot{x}_4 = -\tilde{u}x_4$ yielding control law:

$$\begin{aligned} \tilde{u} &= -1 \quad x_4 > 0 \\ \tilde{u} &= +1 \quad x_4 < 0 \end{aligned} \tag{2-44}$$

If t_c designates the time x_4 crosses into the positive half plane then the solution is given by

$$x_4(t) = -\cos(t-t_i) \qquad t_i \leq t \leq t_c \tag{2-45}$$

$$x_4(t) = \sinh(t-t_c) \qquad t_c \leq t \leq t_f \tag{2-46}$$

and the time of solution is

$$t_f = \frac{\pi}{2} + \operatorname{arcsinh} 1 \tag{2-47}$$

which completes the proof of theorem 2-3. The backward and forward time optimal solutions are illustrated in Figs. 2-11 and 2-12.

A straight forward modification of the proof of theorem 2-3 yields the result:

COROLLARY 2-2 - If at time τ_1, $\lambda_2(\tau_1) = 1$ and $\lambda_1(\tau_1) \geq 0$ and at time τ_f, $\lambda_2(\tau_f) \leq -1$ then the interval $\tau_f - \tau_1$ is greater than $\pi/2$ + arcsinh 1. See Fig. 2-13.

From theorem 2-3 we conclude that a P-0-N-0 sequence of arcs on a pseudoextremal could not occur in time $\pi/2$ + arcsinh 1. That an 0-P-0-N sequence can not occur within this time limit also is the conclusion of corollary 2-2. Therefore, the only pseudoextremals we need consider containing an N-arc is the P-0-N (or N-0-P) pseudoextremal, provided that time T permitted for zeroing the state is less than $\pi/2$ + arcsinh 1.

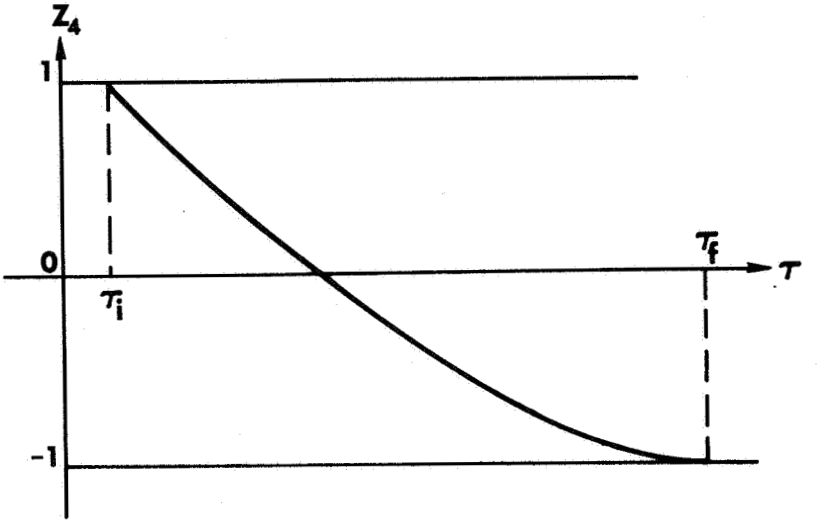

Fig. 2-11. Backward Time-Optimal Solution of the Reduced Auxiliary Problem.

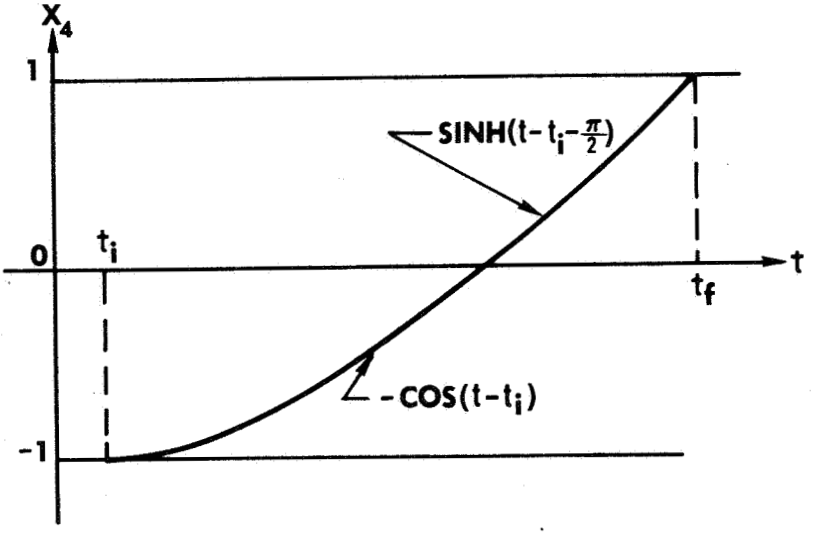

Fig. 2-12. Forward Time-Optimal Solution of the Reduced Auxiliary Problem.

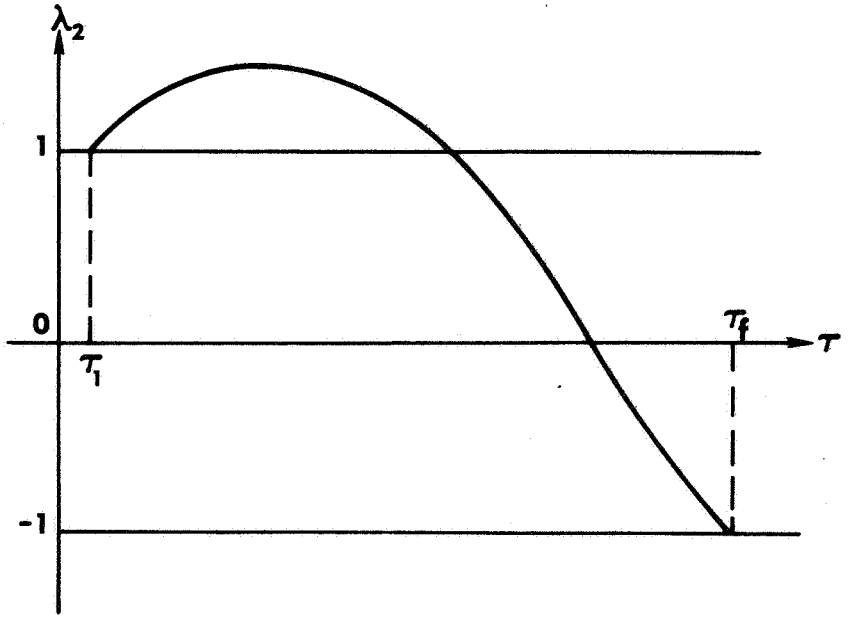

Fig. 2-13. Corollary 2-2 $\tau_f - \tau_1 > \frac{\pi}{2} + \text{arcsinh } 1$.

CHAPTER III

TRAJECTORIES IN BACKWARD TIME

We begin by considering the backward time pseudoextremals emanating from the origin for which the Hamiltonian H_B is zero. Again we consider only those extremals with the control initially $+A$ for identical reasoning yields analogous results for the case $-A$. In the backward time formulation the subscript s denotes the value of the state and adjoint variables at the first switching which occurs on the zero trajectory. The two succeeding switchings which may occur within time π are denoted by the subscripts r and q. For the case where the Hamiltonian

$$H_B = -\lambda_1(\tau)y_2(\tau) + \lambda_2(\tau)(\sin y_1(\tau) - u) + |u| = 0 \qquad (3\text{-}1)$$

the adjoint variables at the first switching have values

$$\lambda_{2s} = 1 \qquad (3\text{-}2)$$

$$\lambda_{1s} = \frac{\lambda_{2s}\sin y_{1s}}{y_{2s}} = \frac{\sin y_{1s}}{y_{2s}} \qquad (3\text{-}3)$$

The adjoint variable $\lambda_2(\tau)$ in Appendix C is shown to satisfy the following relation along an O-arc which does not cross the y_1 axis

$$\lambda_2(\tau) = y_2(\tau)\left[\frac{1}{y_{2s}} + H_B \int_{y_{1s}}^{y_1(\tau)} \frac{d\sigma}{-(2(\cos\sigma - \cos y_{1s}) + y_{2s}^2))^{3/2}}\right] \qquad (3\text{-}4)$$

where the point (y_{1s}, y_{2s}) is the starting point of the arc for $\tau = \tau_s$. Thus along this portion of the pseudoextremals under consideration

$$\lambda_2(\tau) = \frac{y_2(\tau)}{y_{2s}} \tag{3-5}$$

The second switching r occurs when

$$|\lambda_2(\tau_r)| = 1 \tag{3-6}$$

for the smallest τ_r greater than τ_s. A switching from 0 to +A occurs if

$$y_{2r} = y_{2s} \tag{3-7}$$

whereas a switching from 0 to -A occurs if

$$y_{2r} = -y_{2s} \tag{3-8}$$

Examination of the equation of an 0-curve

$$y_2^2 - 2\cos y_1 = y_{2s}^2 - 2\cos y_{1s} \triangleq 2K_1 \tag{3-9}$$

with the constant K_1 defined by equation (3-9) yields two classes of curves. For $K_1 > 1$ the curve defined by the first switching remains entirely below the y_1 axis for y_2 initially < 0. The second switching is therefore from 0 to +A. Applying (3-7) and (3-9) we find that

$$\cos y_{1r} = \cos y_{1s} \tag{3-10}$$

The locus of all points (y_{1r}, y_{2r}) satisfying conditions (3-7) and

(3-9) in the smallest time τ_r: $\tau_r > \tau_s$ is therefore a reflection of an arc of the zero trajectory about the line $y_1 = \pi$.

Letting C denote the y_1 coordinate of the intersection of the zero trajectory and the 0-curve corresponding to $K_1 = 1$ we have from (1-27)

$$\frac{y_{2c}^2}{2} - 0 = \cos c - \cos 0 + A(c-0) \tag{3-11}$$

$$\frac{y_{2c}^2}{2} - 0 = \cos c - \cos \pi \tag{3-12}$$

from which

$$c = \frac{2}{A} \tag{3-13}$$

Should the first switching of an $H_B = 0$ pseudoextremal occur for $\frac{2}{A} < y_{1s} < \pi$ then the second switching is from 0 to +A and occurs on the reflection of the zero trajectory about the line $y_1 = \pi$ as illustrated by Fig. 3-1.

In the case where $K_1 < 1$ the 0-curves form closed paths about the origin. Along such paths $(y_{1s} < \frac{2}{A})$ condition (3-6) is met for the first time at the point

$$(y_{1r}, y_{2r}) = (y_{1s}, -y_{2s}) \tag{3-14}$$

which represents a reflection of the zero trajectory about the y_1 axis. These points correspond to switching from 0 to -A.

We now note that for the first switching to have taken place $\lambda_2(\tau)$ had to cross the line $\lambda_2(\tau) \equiv 1$ from above and hence $\lambda_2'(\tau) \leq 0$

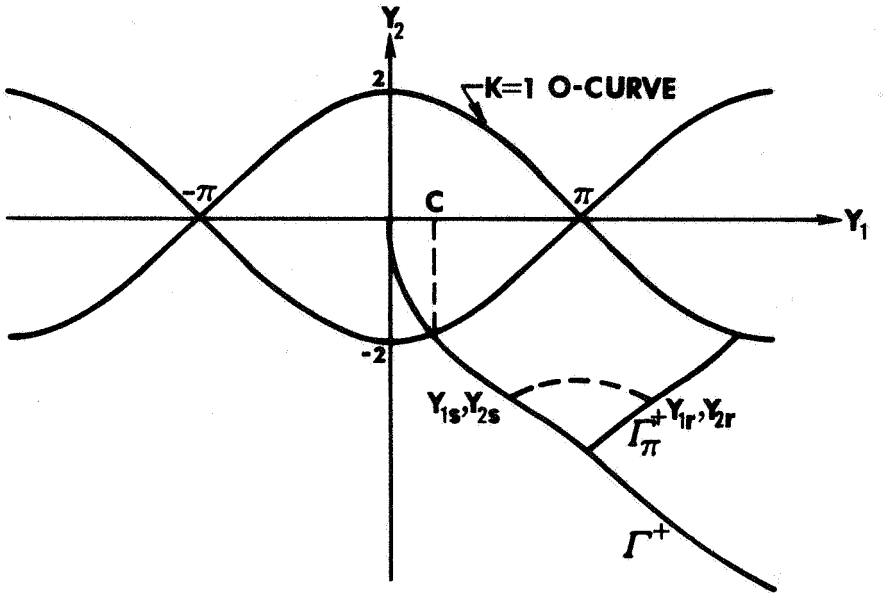

Fig. 3-1. Γ_{π}^{+} Locus Second Switching 0 to +A of an $H_B = 0$ Pseudoextremal.

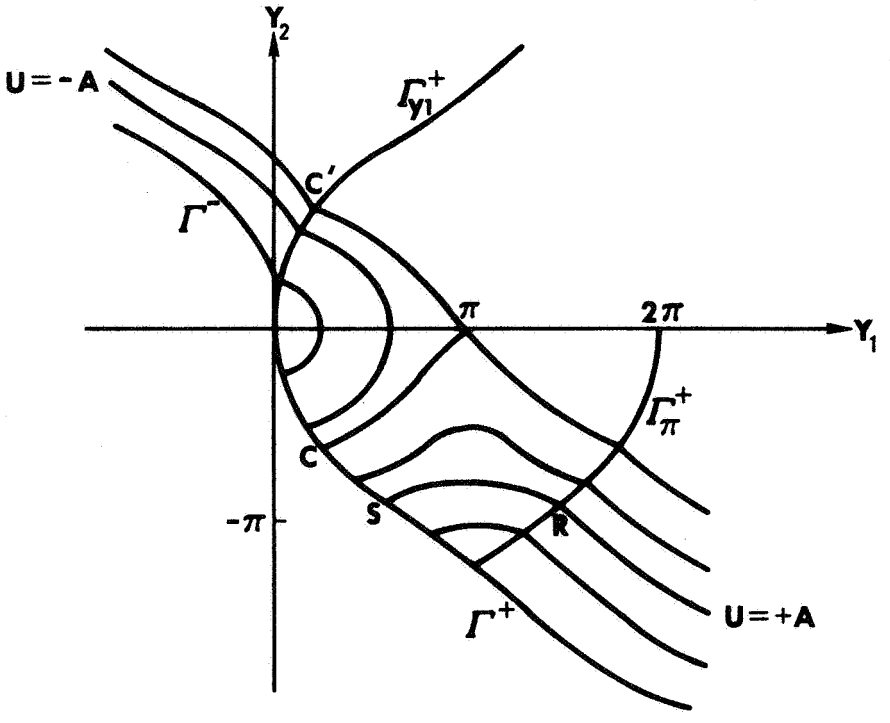

Fig. 3-2. $H_B = 0$ Pseudoextremals.

as seen in Fig. 3-3. Condition (3-3) leads to the requirement that

$$\sin y_{1s} \geq 0 \tag{3-15}$$

which rules out the possibility of any $H_B = 0$ pseudoextremals having a first switching y_{1s} on the interval $(\pi, 2\pi)$.

The complete system of $H_B = 0$ pseudoextremals for $y_{1s} < 2\pi$ is shown in Fig. 3-2.

These pseudoextremals whose Hamiltonian is zero are of particular interest. If we relax the time specified for reaching a given state (y_1, y_2) lying on such a pseudoextremal (i.e., relax the specified time to zero the disturbance (x_1, x_2) in the forward time formulation) we may achieve no reduction in fuel costs.

To demonstrate that such is the case we utilize the following result of Joseph C. Dunn first published in reference [5]:

THEOREM 3-1 For a compact set of admissible control inputs the canonical characteristic differential equations of Hamilton-Jacobi exist on a region, R, if and only if the pseudoextremals of the Maximum Principle are described by a unique system of differential equations. Furthermore, if this unique system of differential equations exists, then it necessarily coincides with the canonical characteristic equations.

As in the classical calculus of variations (see Ref. [6]) we may now introduce a best performance or minimum cost function

$$V(y_1, y_2, \tau_f) = \max_{u \in \bar{U}} \int_0^{\tau_f} -|u(\tau)|\, d\tau \tag{3-16}$$

where $\bar{U}(y_1, y_2)$ is the set of all admissible controls which transfer

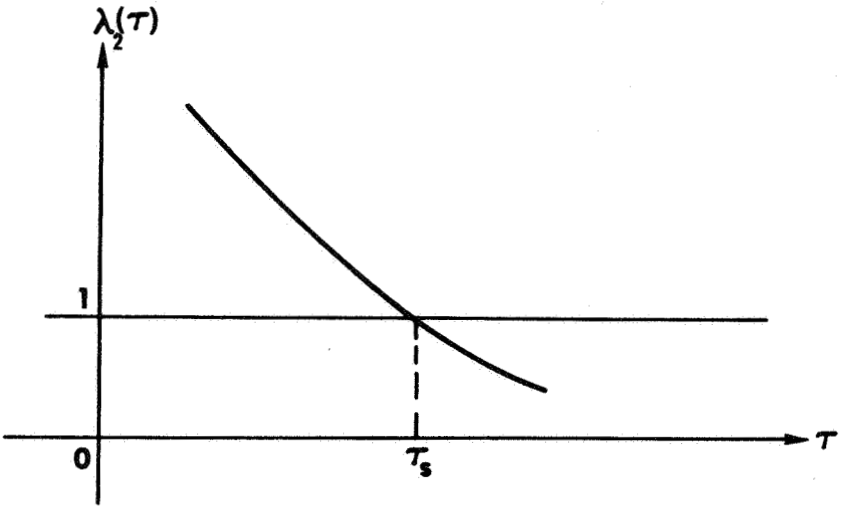

Fig. 3-3. Behavior of Adjoint $\lambda_2(\tau)$ at First Backward Time Switching τ_s.

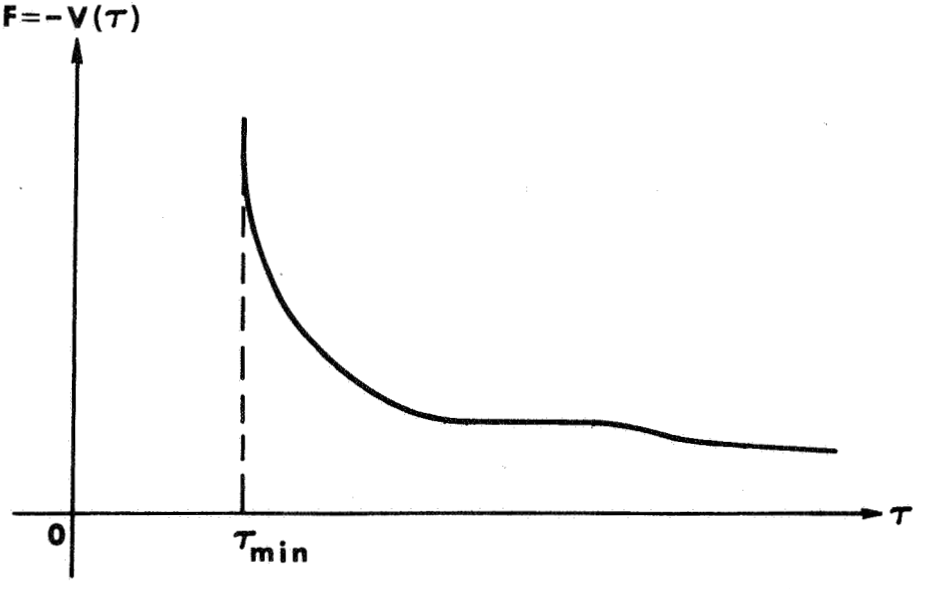

Fig. 3-4. Fuel Expenditure F Versus Allowed Time of Solution T_f.

the state from $(0,0)$ to (y_1,y_2) within time τ_f. Then in that region R of the cartesian product space $y_1 \times y_2 \times \lambda_1 \times \lambda_2 \times \tau$ where the pseudoextremals of the maximum principle are described by a unique system of differential equations; namely, wherever $|\lambda_2(\tau)| \neq 1$ we have (see Ref. [7]) the following:

$$\frac{\partial V(y_1,y_2,\tau)}{\partial \tau} + H_B^o(\lambda_1,\lambda_2,y_1,y_2) = 0 \tag{3-17}$$

where

$$H_B^o = \sup_{u \in \bar{U}} H_B(\lambda_1,\lambda_2,y_1,y_2,u) \tag{3-18}$$

and

$$\frac{\partial V}{\partial y_i}(y_1,y_2,\tau) = \lambda_i(\tau) \tag{3-19}$$

as a direct consequence of theorem 3-1.

Therefore along the $H_B = 0$ extremals excepting switching points we find that

$$\frac{\partial V}{\partial \tau}(y_1,y_2,\tau) = 0 \tag{3-20}$$

and differential changes in the time constraint do not lead to any reduction in fuel expenditure.

If we plot the minimum fuel cost F versus the time constraint T for a particular initial state (x_1,x_2) lying in the region spanned by these pseudoextremals one expects to find flat portions at least locally corresponding to a range of τ for which equation (3-18) holds. See Fig. 3-4.

As we shall see in the synthesis of the optimal control law for the range of τ where (3-20) holds for our particular initial state (x_1,x_2), the phase point arrives at the origin at a fixed time and then waits there with control zero until the time constraint is met.

Since

$$H_B \leq 0 \tag{3-21}$$

along any pseudoextremal through the origin $(0,0)$ for a fixed end point in backward time $(y_1(\tau_f),y_2(\tau_f))$

$$-\partial V(y_1,y_2,\tau)/\partial\tau \leq 0 \tag{3-22}$$

whenever the derivative exists.

As one would expect the fuel cost $-V(\tau)$ versus backward time τ curve for a fixed end point must be monotonically decreasing. In the forward time formulation the fact that no fuel is expended holding the phase point at the final state $(0,0)$ means that such minimum fuel cost versus time curves must be monotonic.

We are now in position to assert the following corollary:

COROLLARY 3-1 Any pseudoextremal possessing a non-zero Hamiltonian which zeros the state (x_{10},x_{20}) in time t_f where t_f is strictly less than the prescribed time of mission T_f is not fuel optimal for the prescribed time T_f.

Thus the phenomenon of waiting at the origin i.e., meeting the time constraint "too early" is fuel optimal only for pseudoextremals along which the Hamiltonian vanishes.

Corollary 3-1 is a direct consequence of the theorem due to Dunn. Suppose such a pseudoextremal were optimal. Then by relaxing the exact time of zeroing the state (x_{10},x_{20}) from t_f to T_f, Dunn's theorem predicts a reduction in fuel consumption; i.e., another path would consume less fuel for the maximum time of mission T_f thereby contradicting the optimality of such a pseudoextremal.

Up to now we have not worried about the fact that for those points τ where $|\lambda_2(\tau)| = 1$ (i.e., at switching points) relations (3-17), (3-18), and (3-19) are not defined inasmuch as the canonical differential equations of Hamilton-Jacobi do not exist unless the pseudoextremals of the Maximum Principle are defined by a unique system of differential equations. But we have already seen that singular controls are not optimal. The system of differential equations of the Maximum Principle is unique except for the isolated points on the time axis where $|\lambda_2(\tau)| = 1$. With the aid of this fact, Corollary 3-1 remains valid whether or not we are at a switching point at the moment of consideration. If at such a point τ_s we can always wait an arbitrarily small time until time $\tau_s-\delta\tau$ at which time relations (3-17), (3-18), and (3-19) are defined. From this new point $\tau_s-\delta\tau$ we insist that for the time remaining, the path must be fuel optimal for time $\tau_s-\delta\tau$ if the original path were fuel optimal for a time τ_s. This is merely a restatement of Bellman's Principle of Optimality. From this new point we may reapply the arguments of Corollary 3-1 to substantiate our claim that Corollary 3-1 is valid even when (3-17), (3-18), and (3-19) are not definable.

Whenever we limit the time of mission such that

$$\tau_f \leq \pi \tag{3-23}$$

then there is a unique $H_B = 0$ pseudoextremal passing through any state (y_1,y_2) reachable within time τ_f by such extremals. Otherwise, for larger τ_f two types of multiplicity can occur. In Fig. 3-5, the state (y_1,y_2) can be reached by the path OBCDEFH generated by the control sequence A, 0, -A, 0, A, 0 which is an $H_B = 0$ pseudoextremal. Another candidate is path OGH generated by the control sequence A, 0. The other type is the path OD'E generated by the sequence -A, 0. Both multiplicities are eliminated by limiting the time τ_f so that at most two switchings can occur. It should be clear that the path OBCDEFH requires less fuel than OGH and therefore one $H_B = 0$ pseudoextremal may not be the optimal path once the time constraint is relaxed. Almuzara Ref. [2] has shown the zero trajectories Γ^+,Γ^- to be time optimal and thus OG could only be fuel optimal in the pathological case. Clearly path OBCDEFG uses less fuel.

Having previously demonstrated that the second switching of P-0-N type $H_B = 0$ pseudoextremals occurs on the reflected zero trajectory $\Gamma^+_{y_1}$ we now will show:

LEMMA 3-1a The second switching (0-N corner) of any P-0-N pseudoextremal with nonvanishing Hamiltonian occurs below the curve $\Gamma^+_{y_1}$.

PROOF: Along that portion of an 0-arc below the y_1 axis the adjoint $\lambda_2(\tau)$ satisfies

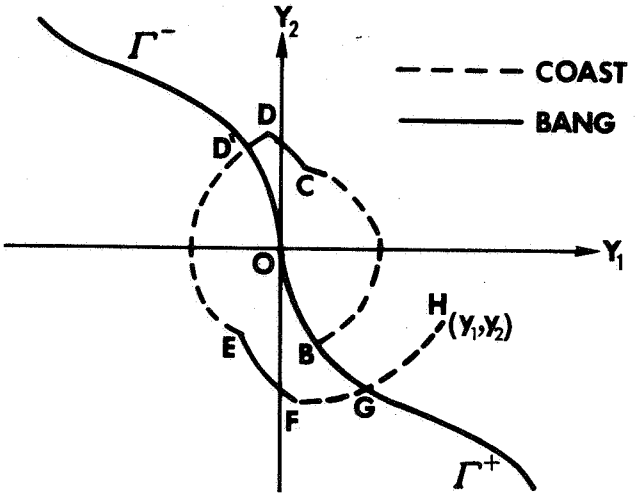

Fig. 3-5. Nonuniqueness of $H_B = 0$ Pseudoextremals Through a State (y_1, y_2).

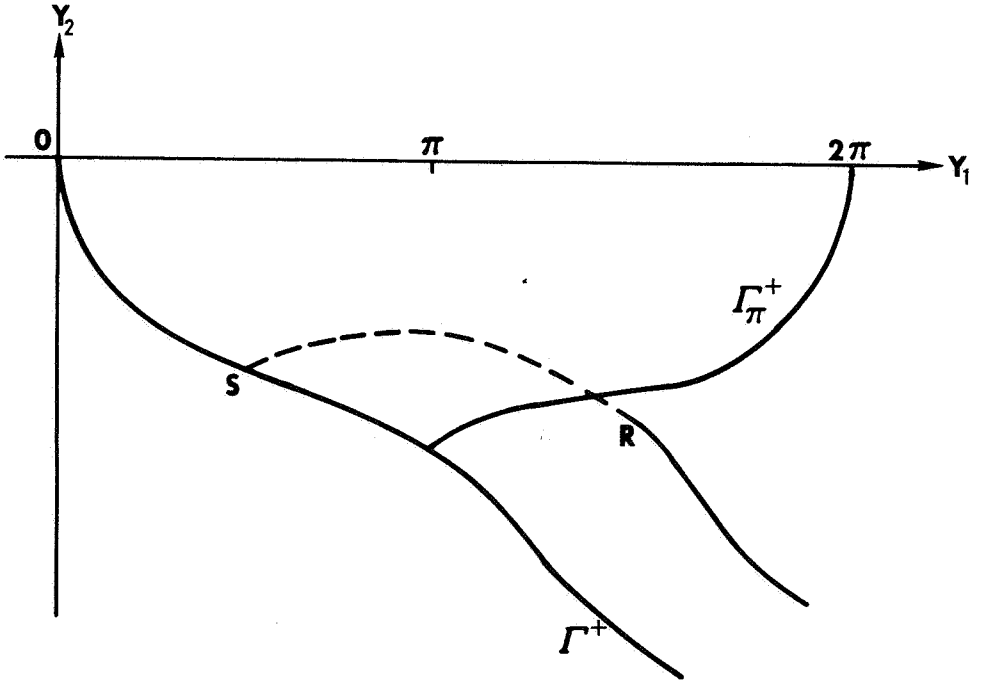

Fig. 3-6. Second Switchings of P-0-P··· Pseudoextremals. In a P-0-P··· the second switching R lies below the curve Γ_π^+.

$$\lambda_2(\tau) = y_2(\tau)\left[\frac{1}{y_{2s}} + H_B \int_{y_{1s}}^{y_1(\tau)} - \frac{d\sigma}{[2(\cos\sigma-\cos y_{1s})+y_{2s}^2]^{3/2}}\right] \qquad (3\text{-}24)$$

whereas on that portion of an 0-arc above the y_1 axis, $\lambda_2(\tau)$ satisfies

$$\lambda_2(\tau) = y_2(\tau)\left[\frac{1}{y_{2s}} + H_B \left\{ \int_{y_{1s}}^{y_{1m}} \left[\frac{-1}{[2(\cos\sigma-\cos y_{1s})+y_{2s}^2]^{3/2}} + \frac{1}{[2\sin y_{1m}(y_{1m}-\sigma)]^{3/2}}\right] d\sigma + \frac{1}{[2\sin^3 y_{1m}(y_{1m}-y_{1s})]^{1/2}} \right.\right.$$

$$\left.\left. + \int_{y_1(\tau)}^{y_{1m}} \left[\frac{-1}{[2(\cos\sigma-\cos y_{1s})+y_{2s}^2]^{3/2}} + \frac{1}{[2\sin y_{1m}(y_{1m}-\sigma)]^{3/2}}\right] d\sigma \right.\right.$$

$$\left.\left. + \frac{1}{[2\sin^3 y_{1m}(y_{1m}-y_1(\tau))]^{1/2}} \right\}\right] \qquad (3\text{-}25)$$

where y_{1m} denotes the y_1 coordinate of the path at the crossing of the y_1 axis. The derivation of (3-25) is given in Appendix D.

Let $\hat{\lambda}_2(\tau)$ denote the adjoint corresponding to an $H_B = 0$ pseudo-extremal and $\lambda_2(\tau)$ the value of the adjoint along that portion of an $H_B \neq 0$ pseudoextremal which coincides with the $H_B = 0$ pseudoextremal up to the second switch point. Then on an 0-arc below the y_1 axis

$$\lambda_2(\tau)-\hat{\lambda}_2(\tau) = y_2(\tau)H_B \int_{y_{1s}}^{y_1(\tau)} \frac{d\sigma}{-[2(\cos\sigma-\cos y_{1s})+y_{2s}^2]^{3/2}} < 0 \qquad (3\text{-}26)$$

and on an 0-arc above the y_1 axis

$$\lambda_2(\tau)-\hat{\lambda}_2(\tau) = y_2(\tau)H_B \left\{ \int_{y_{1s}}^{y_{1m}} \left[\frac{-1}{[2(\cos\sigma-\cos y_{1s})+y_{2s}^2]^{3/2}} + \right.\right.$$

$$\left.\left. + \frac{1}{[2\sin y_{1m}(y_{1m}-\sigma)]^{3/2}} \right] d\sigma + \frac{1}{[2\sin^3 y_{1m}(y_{1m}-y_{1s})]^{1/2}} \right.$$

$$\left. + \int_{y_1(\tau)}^{y_{1m}} \left[\frac{-1}{[2(\cos\sigma-\cos y_{1s})+y_{2s}^2]^{3/2}} + \frac{1}{[2\sin y_{1m}(y_{1m}-\sigma)]^{3/2}} \right] d\sigma + \right. \tag{3-27}$$

$$\left. + \frac{1}{[2\sin^3 y_{1m}(y_{1m}-y_1(\tau)]^{1/2}} \right.$$

That $\lambda_2(\tau)-\hat{\lambda}_2(\tau)$ is infact less than zero above the y_1 axis as well, is yet to be determined from equation (3-27). From (3-26) up to the point $M(y_{1m},y_{2m})$, where the pseudoextremal crosses the y_1 axis, the quantity $\lambda_2(\tau)-\hat{\lambda}_2(\tau)$ remains negative. Suppose that $\lambda_2(\tau)-\hat{\lambda}_2(\tau)$ where not negative above the y_1 axis. Then from the continuity of both $\lambda_2(\tau)$ and $\hat{\lambda}_2(\tau)$ there must be some τ_c for which

$$\lambda_2(\tau_c) = \hat{\lambda}_2(\tau_c) \tag{3-28}$$

or from (3-27)

$$\frac{1}{[2\sin y_{1m}(y_{1m}-y_{1s})]^{3/2}} + \int_{y_{1s}}^{y_{1m}} \left[\frac{-1}{[2(\cos\sigma-\cos y_{1m})]^{3/2}} + \right.$$

$$\left. + \frac{1}{[2\sin y_{1m}(y_{1m}-)]^{3/2}} \right] d\sigma \quad =$$

$$= \frac{1}{[2\sin y_{1m}(y_{1m}-y_1(\tau_c))} + \int_{y_1(\tau_c)}^{y_{1m}} \left[\frac{-1}{[2(\cos\sigma-\cos y_{1m})]^{3/2}} + \right.$$

$$\left. + \frac{1}{[2\sin y_{1m}(y_{1m}-)]^{3/2}} \right] d\sigma \qquad (3\text{-}29)$$

Considering the left hand side of equation (3-29) to be a function of y_{1s} say $G(y_{1s})$ where y_{1m} is now fixed, equation (3-29) becomes simply

$$G(y_{1s}) = G(y_1(\tau_c)) \qquad (3\text{-}30)$$

But $G(y_1)$ for $y_1 \neq y_{1m}$ is a monotonic function of y_1 inasmuch as

$$\frac{dG(y_1)}{dy_1} = \frac{1}{[2(\cos y_1-\cos y_{1m})]^{3/2}} = \frac{1}{|y_2(\tau)|^3} > 0 \qquad (3\text{-}31)$$

and hence equation (3-29) can only hold if

$$y_{1s} = y_1(\tau_c) \qquad (3\text{-}32)$$

This means the first time $\lambda_2(\tau)$ could again equal $\hat{\lambda}_2(\tau)$ is when the phase point reaches $\Gamma^+_{y_1}$ in which case a switching would occur on $\Gamma^+_{y_1}$. On the other hand should (3-32) not be valid, then (3-28) also does not hold in which case

$$\lambda_2(\tau) - \hat{\lambda}_2(\tau) < 0 \qquad (3\text{-}33)$$

remains valid on that portion of an 0-arc above the y_1 axis and continues to hold past the time of crossing the curve $\Gamma^+_{y_1}$. In

either case (3-26) or (3-33)

$$\lambda_2(\tau) < \hat{\lambda}_2(\tau) \tag{3-34}$$

along that portion where the two pseudoextremal state trajectories coincide. Since on $\Gamma^+_{y_1}$

$$\hat{\lambda}_2(\tau) = -1 \tag{3-35}$$

by continuity of $\lambda_2(\tau)$ a switching from 0 to -A must have occurred on or below $\Gamma^+_{y_1}$.

In like manner we seek the result:

LEMMA 3-1b. The second switching (0-P corner) of any P-0-P pseudo-extremal must occur below the curve Γ^+_π the reflected zero trajectory about the line $y_1 = \pi$. (See Fig. 3-6).

PROOF: From (3-24) we have at the second switching

$$1 = \lambda_{2r} = y_{2r}\left[\frac{1}{y_{2s}} + H_B \int_{y_{1s}}^{y_{1r}} \frac{d\sigma}{-[2(\cos\sigma - \cos y_{1s}) + y_{2s}^2]^{3/2}}\right] \tag{3-36}$$

or since $H_B \leq 0$

$$\frac{1}{y_{2r}} \geq \frac{1}{y_{2s}} \tag{3-37}$$

Since both y_{2r} and y_{2s} are negative

$$y_{2r}^2 \geq y_{2s}^2 \tag{3-38}$$

But

$$y_{2r}^2 - y_{2s}^2 = 2(\cos y_{1r} - \cos y_{1s}) \tag{3-39}$$

and therefore

$$\cos y_{1r} > \cos y_{1s} \tag{3-40}$$

or for

$$0 < x_{1s} < \pi \qquad x_{1r} > \pi \tag{3-41}$$

and the second switching is indeed below Γ_{π}^{+}. See Fig. 3-6.

DEFINITION 3-1: A T-Bang-Coast Isochrone is the locus of all initial states (x_1,x_2) which can be zeroed in exactly time T by the control sequence 0, +A. See Fig. 3-7.

Whereas any point on a T-bang-coast isochrone may be reached from the origin by a P-0 type backward time trajectory, such a path is not necessarily the fuel optimal path for that particular time T. When these paths are fuel optimal is the topic of the following theorem.

THEOREM 3-2: If $T \leq \pi$ then the fuel optimal path for zeroing any state lying on the T-bang-coast isochrone within T units of time is a P-0 trajectory.

Thus once the state point $(x_1(t),x_2(t))$ and the time-to-go T have values such that the state point lies upon the T-bang-coast isochrone, the state point merely "rides" the T-bang-coast isochrone to the origin.

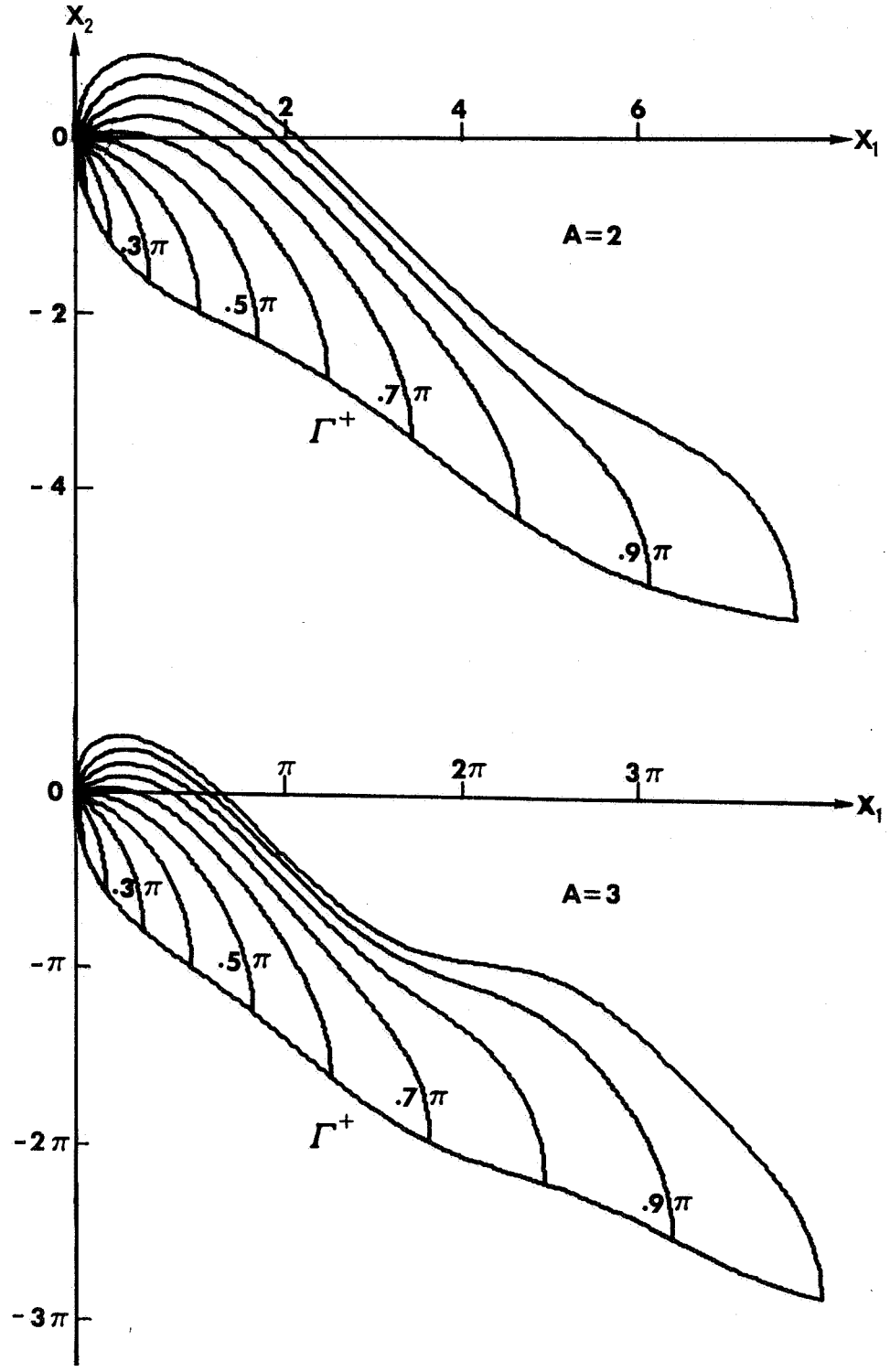

Fig. 3-7. Behavior of T-Bang-Coast Isochrones as T Changes.

The proof of theorem 3-2 proceeds by direct elimination of other candidate pseudoextremals.

Candidate 1 is a P-O-N trajectory with first switch point (y_{1s}, y_{2s}) such that $y_{1s} < C$. See Figs. 3-8 and 3-1.

We desire to show that path O, S_2, Q_2 (P-O type trajectory generating the T-bang-coast isochrone) uses less fuel than the O, S_1, R_1 Q_2 path consisting of a P-O-N type trajectory. First we note that this P-O-N trajectory uses less time than the P-O trajectory. By the definition of T-bang-coast isochrone the P-O trajectories O, S_1, R_1, Q_1 and O, S_2, Q_2 both require time T.

Denoting the time required to traverse a particular arc path by $\tau(\cdot)$ we have

$$\tau(R_1, Q_2, Q_1) < \tau(R_1, Q_1) \tag{3-42}$$

This result follows from the fact that

$$d\tau = \frac{dy_1}{y_1'} = -\frac{dy_1}{y_2} \tag{3-43}$$

and therefore

$$\tau(R_1, Q_2, Q_1) = \int_{Q_1}^{R_1} \frac{d\xi}{\bar{y}_2(\xi)} \tag{3-44}$$

$$\tau(R_1, Q_1) = \int_{Q_1}^{R_1} \frac{d\xi}{\hat{y}_2(\xi)} \tag{3-45}$$

Since

$$\hat{y}_2(\xi) < \bar{y}_2(\xi) \quad \forall \xi: \; Q_1 < \xi < R_1 \tag{3-46}$$

i.e., the path R_1,Q_2,Q_1 lies entirely above the path R_1,Q_1 and relation (3-42) is valid. From (3-42) it follows

$$\tau(0,S_1,R_1,Q_2) < \tau(0,S_1,R_1,Q_2,Q_1) < \tau(0,S_1,R_1,Q_1) = \\ = \tau(0,S_2,Q_2) = T \tag{3-47}$$

Furthermore since any T-bang-coast isochrone for $T < \pi$ lies below the curve $\Gamma^{+}_{y_1}$, the P-0-N trajectory $0\text{-}S_1\text{-}R_1\text{-}Q_2$ could only result from a pseudoextremal possessing a nonzero Hamiltonian as required by lemma 3-1. Taking into account that

$$\tau(0,S_1,R_1,Q_2) < T \tag{3-48}$$

and applying Corollary 3-1 eliminates such a P-0-N extremal from consideration as a fuel optimal path.

Candidate 2 is a P-0-N trajectory with first switch point (y_{1s},y_{2s}) such that $y_{1s} \geq C$. See Fig. 3-9.

Clearly the P-0 path $(0,S_1,Q)$ uses less fuel than the P-0-N path $(0,S,R,Q)$ for the latter expends additional fuel along arc $S_1\text{-}S$ and arc R-Q.

Candidate 3 is any trajectory consisting of P arcs alternating with 0 arcs (P-0-P-0-P-...) as in Fig. 3-10.

By definition of T-bang-coast isochrone the arc $0,S_1,P$ requires T units of time. Furthermore,

$$\tau(0,S,R,Q,P) > \tau(0,S_1,P) = T \tag{3-49}$$

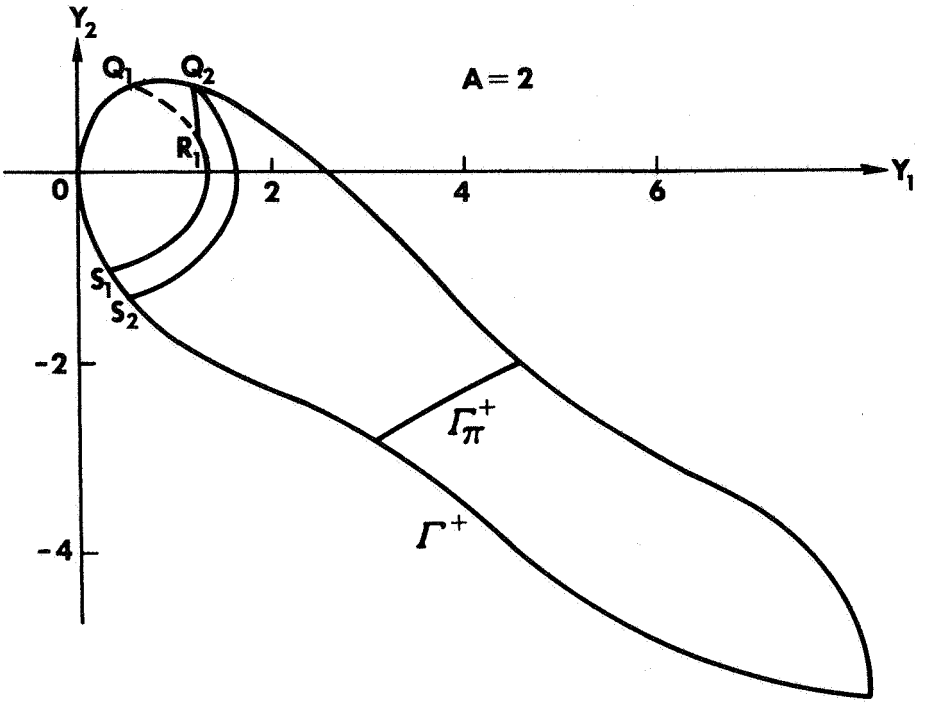

Fig. 3-8. Candidate 1 P-O-N Type Trajectory $(0, S_1, R, Q_2)$.

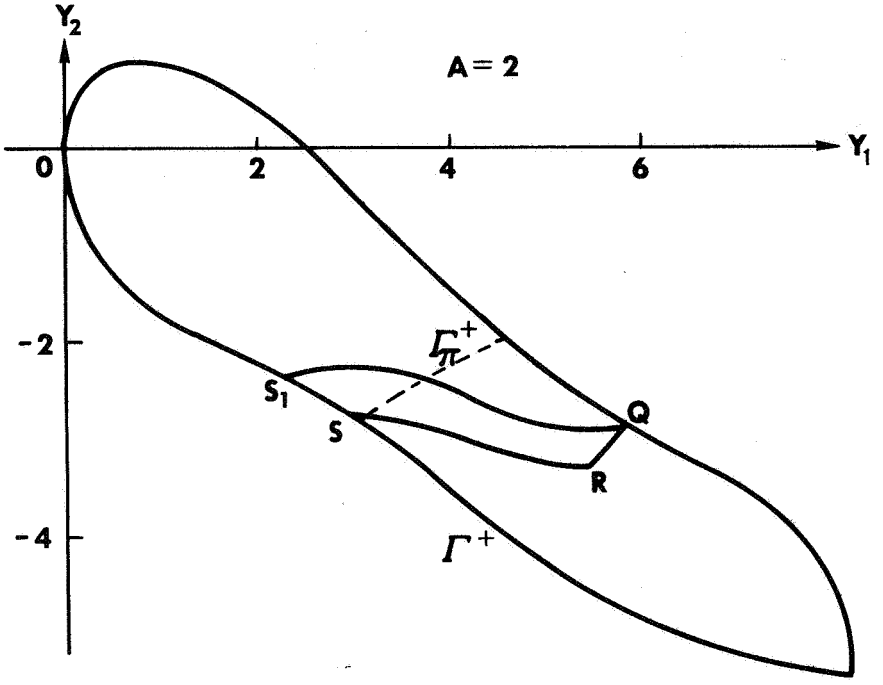

Fig. 3-9. Candidate 2 P-O-P Type Trajectory $(0, S, R, Q)$.

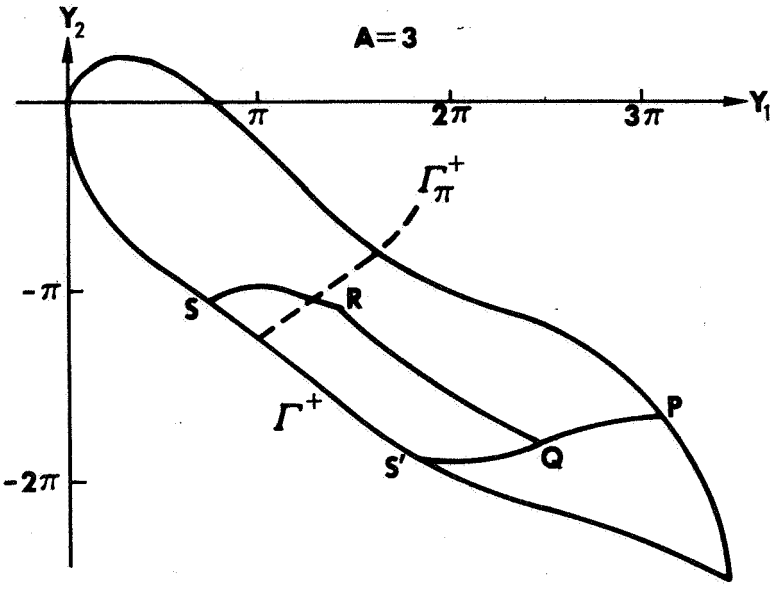

Fig. 3-10. Candidate 3 P-O-P-O... Type Trajectory (O,S,R,Q,P).

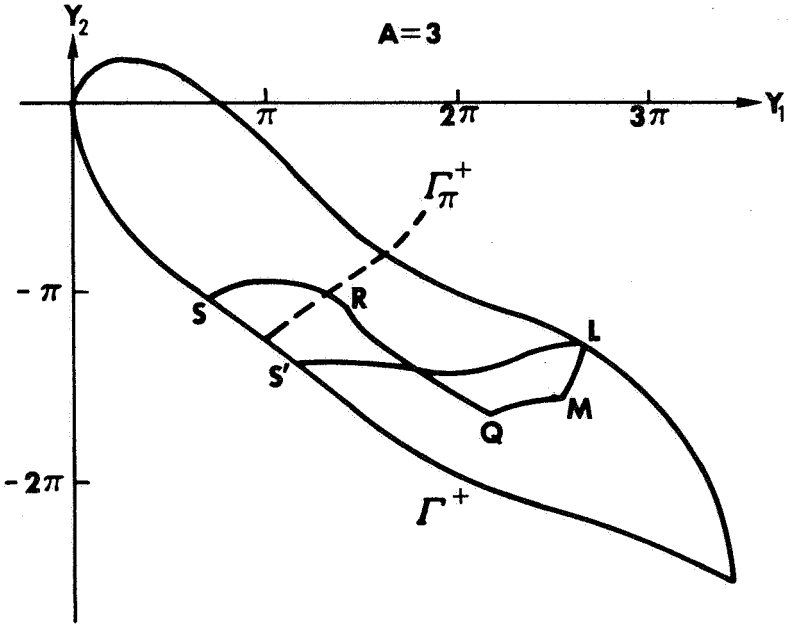

Fig. 3-11. Candidate 4 P-O-P-O-N Type Trajectory (O,S,R,Q,M,L)

via the argument of (3-43). Such trajectories are eliminated due to their failure to meet the time constraint.

Candidate 4 is the P-0-P-0-N trajectory shown in Fig. 3-11.

A P-0-P-0-N trajectory can always be found such that

$$\tau(0,S,R,Q,M,L) = \tau(0,S_1,L) = T \tag{3-50}$$

If furthermore

$$\tau(S,S_1) > \tau(R,Q) + \tau(M,L) \tag{3-51}$$

then this P-0-P-0-N trajectory would use less fuel than the P-0 trajectory $0,S',L$. In order for such a P-0-P-0-N trajectory to be optimal the adjoint variable $\lambda_2(\tau)$ would have to behave as shown in Fig. 3-12. But employing the conclusion or corollary 2-3 we have

$$\tau(R,Q,M) > \frac{\pi}{2} + \text{arcsinh } 1 \tag{3-52}$$

Furthermore, from lemma 3-1 the second switching of such a pseudo-extremal (y_{1r},y_{y2}) is such that

$$y_{1r} > \pi \tag{3-53}$$

If $\tau(0,\pi)$ denotes the minimum time to drive the state point from the origin to the line $y_1 = \pi$ then certainly

$$\tau(0,S,R,Q,M) > \frac{\pi}{2} + \text{arcsinh } 1 + \tau(0,\pi) \tag{3-54}$$

But

$$\tau(0,\pi) = \int_0^{\pi} \frac{d\sigma}{[2(\cos\sigma - 1 + A\sigma)]^{1/2}} \tag{3-55}$$

If we restrict the magnitude of A such that

$$\tau(0,\pi) > \frac{\pi}{2} - \text{arcsinh } 1 \tag{3-56}$$

or equivalently $A < A_{max}$ where A_{max} satisfies

$$\int_0^{\pi} \frac{d\sigma}{[2(\cos\sigma - 1 + A_{max}\sigma)]^{1/2}} = \frac{\pi}{2} - \text{arcsinh } 1 \tag{3-57}$$

then

$$\tau(0,S,R,Q,M) > \pi \tag{3-58}$$

and such a pseudoextremal can not occur for our solution where T_f is restricted to be less than π. Relation (3-57) is no restriction at all in the solution of the actual earth pointing satellite problem for the control bound A could still be about 13.6 times the maximum gravitational torque (see eq. 1-32) as can be verified by evaluating (3-57). The design parameter A, as indicated in Chapter V, should probably lie between 1.2 and 5.0 to achieve efficient zeroing of disturbances without undue control torque requirements.

All possible pseudoextremal candidates other than the P-0 extremals which generate the T-bang-coast isochrone have now been eliminated from being fuel optimal. The existence of an optimal solution together with Pontryagin's Maximum Principle completes the argument that these P-0 pseudoextremals are indeed the optimal trajectories as asserted by the theorem 3-1.

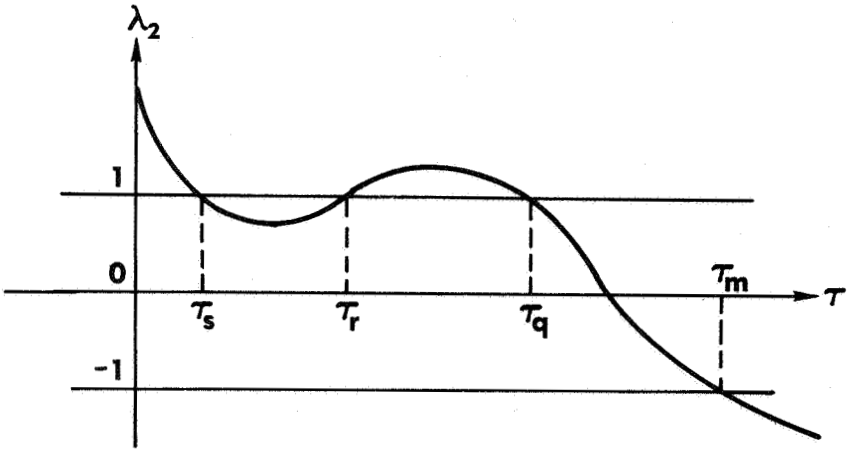

Fig. 3-12. Adjoint λ_2 Behavior Corresponding to Candidate 4.

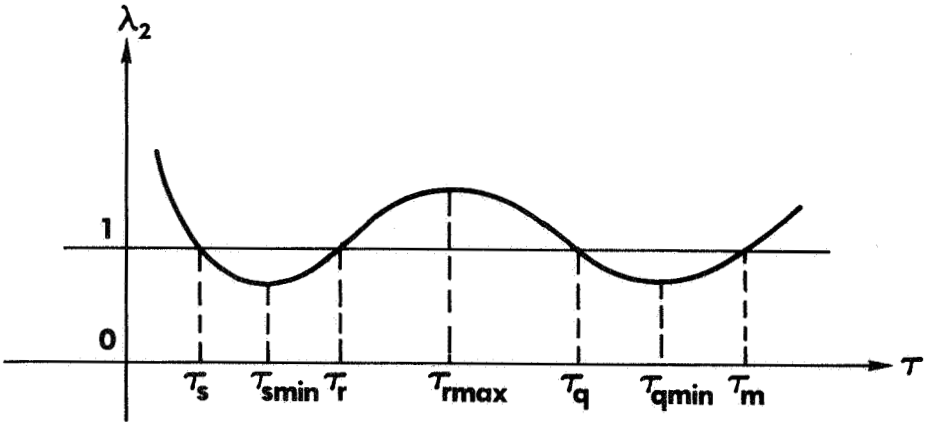

Fig. 3-13. Adjoint λ_2 Behavior Generating a P-0-P-0-P... Pseudoextremal.

CONTROL LAW FOR REGION BOUNDED BY T-BANG-COAST ISOCHRONE AND T-MINIMUM TIME ISOCHRONE

In the analysis of theorem 3-2 one fact should have become clear. In order for any state beyond the T-bang-coast isochrone to reach the origin within time T its path must necessarily contain an N-arc. Now the reason for our preoccupation in Chapter II with limiting the fixed times of mission T_f to be less than $\frac{\pi}{2}$ + arcsinh 1 becomes clear. Such states must have as pseudoextremals a P-0-N trajectory. A P-0-P-0-N... or P-0-N-0... type can not occur within the time limit $\frac{\pi}{2}$ + arcsinh 1 via corollary 2-2. Therefore for a state outside the T-bang-coast isochrone at time-to-go T where $T \leq \frac{\pi}{2}$ + arcsinh 1 the control is $u(t) = -A$. See Fig. 3-13.

This region of Fig. 3-14a for which the optimal control is $-A$ is a time dependent region. Its isochrone boundaries are the T-minimum-time isochrone and the T-bang-coast isochrone which are time varying curves as their names suggest. Given an initial disturbance (x_{10},x_{20}) to be zeroed within time T_f lying outside the T_f-bang-coast isochrone, we now seek the trajectory traced by the phase point. If t denotes the time that has lapsed since we began zeroing the disturbance, then the time remaining for completing the solution i.e., time-to-go T is given by

$$T = T_f - t \tag{3-59}$$

Referring to Figs. 3-14a,b,c,d so long as the state $(x_1(t),x_2(t))$ belongs to the region bounded by the T-minimum-time and T-bang-coast

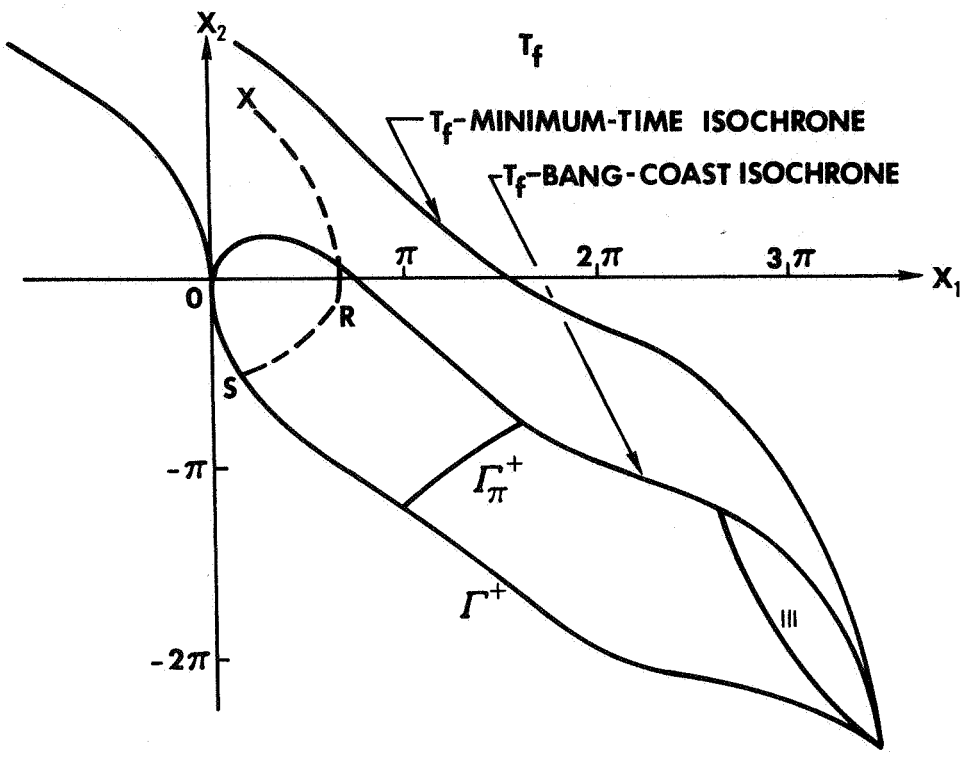

Fig. 3-14a. Optimal P-0-N Path for Zeroing State X within Time T_f (OSRX). Dashed portion is yet to be traversed. Solid portion is that already traversed.

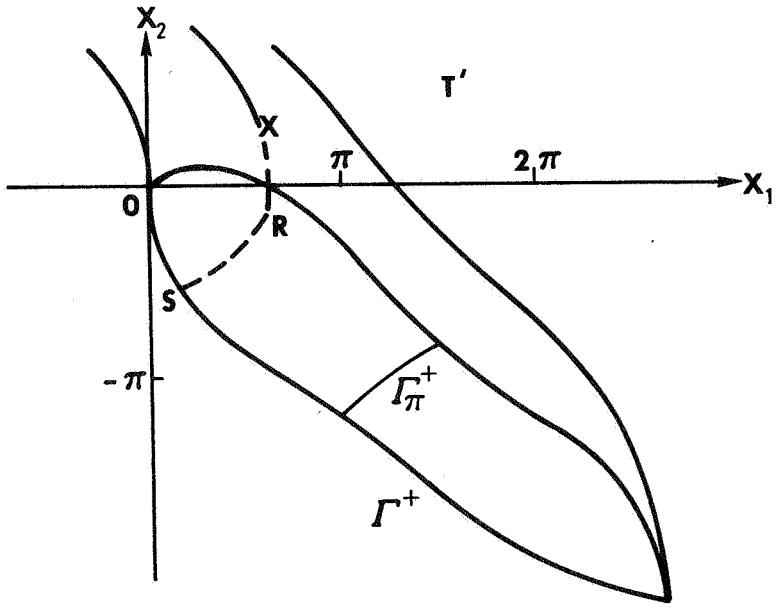

Fig. 3-14b. State X is still within the time-varying u = -A control region.

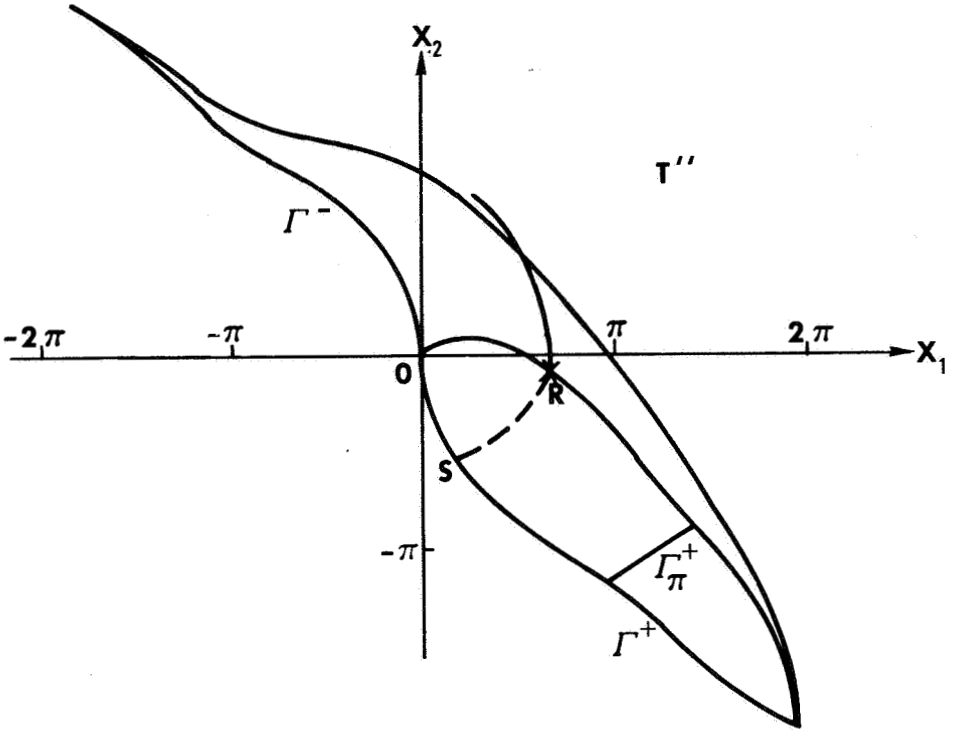

Fig. 3-14c. State X intercepts the shrinking bang-coast isochrone and control switches to zero.

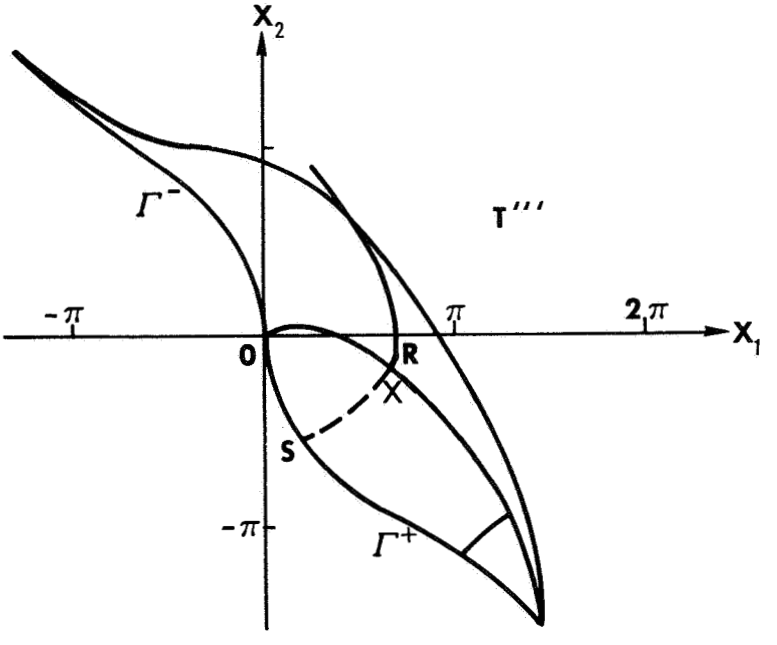

Fig. 3-14d. State X 'rides' the shrinking bang-coast isochrone to Γ^+.

isochrones the control remains $u(t) = -A$. As the phase point proceeds along an N-arc toward the boundary of the $u = -A$ region; namely, the T-bang-coast isochrone, this boundary is itself shrinking toward the origin. The control remains $u(t) = -A$ until the phase point (x_1,x_2) intercepts the T''-bang-coast isochrone at time-to-go $T'' < T$ from which time on the solution is given by theorem 3-2, i.e., the phase point rides the shrinking bang-coast isochrone to the origin. We write for future reference:

OPTIMAL CONTROL LAW 3-1. Any state (x_1,x_2) residing within the region bounded by the T-minimum-time isochrone and the T-bang-coast isochrone at time-to-go T has control $u(t)$ equal minus A.

CONTROL LAW FOR REGION BOUNDED BY T-BANG-COAST ISOCHRONE AND ZERO TRAJECTORY

Theorem 3-2 provides the optimal control law whenever the time-to-go T is such that the state $(x_1(t),x_2(t))$ belongs to the T-bang-coast isochrone. We now seek the minimum effort optimal trajectories and control law for those initial disturbances $(x_1(t_o),x_2(t_o))$ belonging to the region bounded by the T_f-bang-coast isochrone and the zero trajectory where T_f is the maximum time allowed for zeroing the disturbance.

By limiting the allowable time T_f to be at most π units it is sufficient to consider only trajectories consisting of alternating P and 0-arcs. That this is the case can be seen by merely reconstructing the arguments of the proof of theorem 3-1.

Before delving into the precise structure of such P-0-P-0··· pseudoextremals we develop some preliminary lemmas.

LEMMA 3-2 Along any pseudoextremal consisting of alternate P and 0-arcs (P-0-P-0···) the adjoint variable is always positive up to the last 0-P or P-0 corner of the sequence.

PROOF: Along a P-arc the adjoint variable $\lambda_2(\tau)$ is always greater than or equal to one and therefore surely positive. Along an 0-arc $\lambda_2(\tau)$ is given by

$$\lambda_2(\tau) = y_2(\tau)\left[\frac{1}{y_{2s}} + H_B \int_{y_{1s}}^{y_1(\tau)} \frac{-d\sigma}{[2(\cos\sigma-\cos y_{1s})+y_{2s}^2]^{3/2}}\right] \quad (3\text{-}60)$$

where the subscript s now denotes the values of the variable at the first switching i.e., P-0 corner in backward time. Should $\lambda_2(\tau)$ become negative then the term in brackets in equation (3-60) must be positive at that time. Letting τ_N denote the first time $\lambda_2(\tau)$ vanishes we have

$$\frac{1}{y_{2s}} + H_B \int_{y_{1s}}^{y_1(\tau_n)} \frac{d\sigma}{-[2(\cos\sigma-\cos y_{1s})+y_{2s}^2]^{3/2}} = 0 \quad (3\text{-}61)$$

Thereafter the bracketted term is monotonically increasing and therefore for some $\tau > \tau_N$

$$\lambda_2(\tau) < -1 \quad (3\text{-}62)$$

since $y_2(\tau)$ along an 0-arc of a P-0-P sequence must be negative and bounded away from zero. But then the pseudoextremal would consist of an N-arc. This contradicts the fact that we are dealing with a

P-0-P-0··· type extremal and thus until the final P-0 corner $\lambda_2(\tau)$ must be positive and nonzero.

LEMMA 3-3 In a P-0-P-0-P-0 pseudoextremal the fourth switching (second 0-P corner) occurs to the right of the line $y_1 = 3\pi$.

PROOF: For such a pseudoextremal the associated adjoint must behave as shown in Fig. 3-13. Here we have used lemma 3-2 guaranteeing $\lambda_2(\tau)$ to be positive. Between the switching points S and R the adjoint function $\lambda_2(\tau)$ achieves a relative minimum as it also does between the switching points Q and M.

At these relative minimum of $\lambda_2(\tau)$ two relations hold:

$$\text{i)} \quad \lambda_2'(\tau_{min}) = 0 \tag{3-63}$$

$$\text{ii)} \quad \lambda_2''(\tau_{min}) > 0 \tag{3-64}$$

Recalling that

$$\lambda_2'(\tau) = \lambda_1(\tau) \tag{3-65}$$

and expression (3-1) for the backward time Hamiltonian H_B we obtain

$$H_B = \lambda_2(\tau_{min}) \sin y_1(\tau_{min}) \tag{3-66}$$

Furthermore, from (3-54) and (2-6)

$$\lambda_2''(\tau_{min}) = -\lambda_2(\tau_{min}) \cos y_1(\tau_{min}) > 0 \tag{3-67}$$

Now from lemma 3-2

$$\lambda_2(\tau_{min}) > 0 \tag{3-68}$$

and therefore at these relative minima we have from (3-56) and (3-67)

$$\text{i)} \quad \sin y_1(\tau_{min}) \leq 0 \tag{3-69}$$

$$\text{ii)} \quad \cos y_1(\tau_{min}) < 0 \tag{3-70}$$

Therefore the smallest value of $y_1(\tau_{smin})$ must lie in the half open interval given by

$$\pi \leq y_1(\tau_{smin}) < \frac{3\pi}{2} \tag{3-71}$$

At the relative maximum of $\lambda_2(\tau)$ the condition

$$\lambda_2''(\tau_{max}) < 0 \tag{3-72}$$

leads to the requirement

$$\cos y_1(\tau_{max}) > 0 \tag{3-73}$$

Therefore the smallest value of $y_1(\tau_{rmax})$ such that $y_1(\tau_{rmax}) > y_1(\tau_{smax})$ lies on the open interval

$$\frac{3\pi}{2} < y_1(\tau_{rmax}) < 2\pi + \frac{\pi}{2} \tag{3-74}$$

Reapplying relations (3-69) and (3-70) and the requirement that

$$y_1(\tau_{qmin}) > y_1(\tau_{rmax}) \tag{3-75}$$

we obtain the result that

$$3\pi \leq y_1(\tau_{qmin}) < 3\pi + \frac{\pi}{2} \tag{3-76}$$

Now since

$$y_1(\tau_m) > y_1(\tau_{q\min}) \tag{3-77}$$

we have the desired result

$$y_1(\tau_m) > 3\pi \tag{3-78}$$

as asserted by lemma 3-3.

Thus whenever the T-controllable region lies entirely between the lines $x_1 = -3\pi$ and $x_1 = +3\pi$ we may limit our consideration of P-0-P-0... sequences to those candidates having at most three switchings.

We now embark upon a method to order these P-0-P-0 type pseudo-extremals so that we may derive the switching curves. Consider the zero trajectory Γ^+ and a parallel P-curve to the right of Γ^+ as shown in Fig. 3-15. The first switch point (P-0 corner) on Γ^+ is denoted by the point S whereas the second switch point (0-P corner) lying on the given fixed P-curve is denoted by the point R. A third switching (P-0 corner) should it occur will also lie on the given P-curve and be labeled point Q.

The first switch point S is allowed to vary or move down along the zero trajectory Γ^+. We seek the effect of such variation upon the position of the third switch point Q which is constrained to remain on the given P-curve. The result we are seeking, as given in the next theorem and illustrated in Fig. 3-15, is that as S moves down to S', Q moves up to Q'. Furthermore, if the points S and R characterize an actual pseudoextremal, then the function mapping the points S into the points Q is piecewise continuous. If in

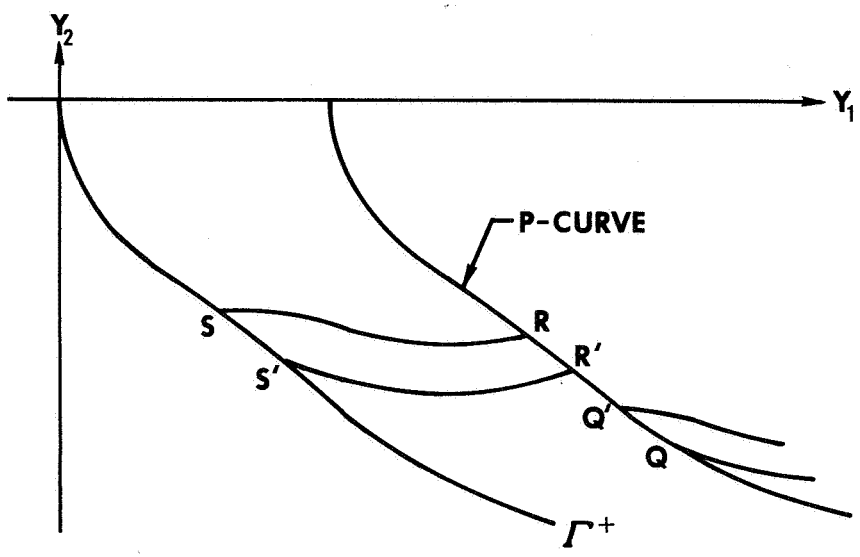

Fig. 3-15. Switching Points S, R, Q of the P-0-P-0 Trajectories of Theorem 3-3.

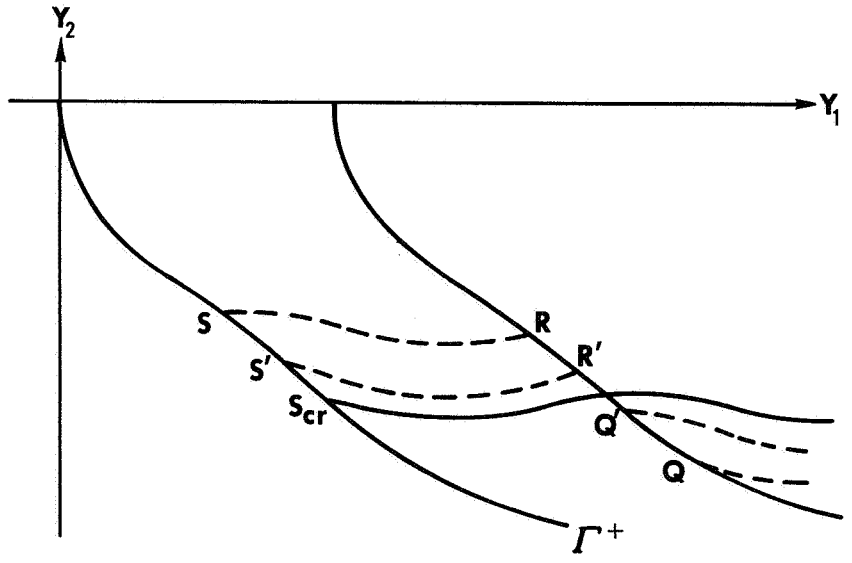

Fig. 3-16. Sandwiching of P-0-P-0 Type Trajectories about the Degenerate Trajectory at S_{cr} in which the Points R_{cr} and Q_{cr} Coincide.

addition Q remains in the region under consideration; namely,

$$y_{1q} \leq 3\pi \tag{3-79}$$

the mapping is continuous.

Restated in the form of a theorem we have:

THEOREM 3-3 If point S on Γ^+ and point R on a fixed P-curve are first and second switch points of some P-0-P-0... pseudoextremal, then the mapping M_1 of the y_1 coordinates of the points S onto the y_1 coordinates of the points Q is a monotonically decreasing function.

This theorem means that the P-0-P-0 pseudoextremals are "sandwiched" between the second and third switch points. The point Q approaches the point R until the second and third switch points coincide. See Fig. 3-16. The behavior of the adjoint variable λ_2 corresponds to the coincidence of points R and Q is shown in Fig. 3-19 where the curve is tangent to the switching line $\lambda_2(\tau) \equiv 1$.

To facilitate the proof of theorem 3-3 we will need the preliminary result of lemma 3-4.

LEMMA 3-4 If point S on Γ^+ and point R on a fixed P-curve are first and second switch points of some P-0-P pseudoextremal, then the mapping H_B is a monotonically decreasing function.

We shall return to the proof of this lemma but first let us complete the proof of theorem 3-3.

PROOF OF THEOREM 3-3 Given y_{1s} and y_{1q} as the y_1 coordinates of the first and third switch points of a P-0-P-0... pseudoextremal and $\hat{y}_{1s}$ and $\hat{y}_{1q}$ the corresponding abscissas of another P-0-P-0

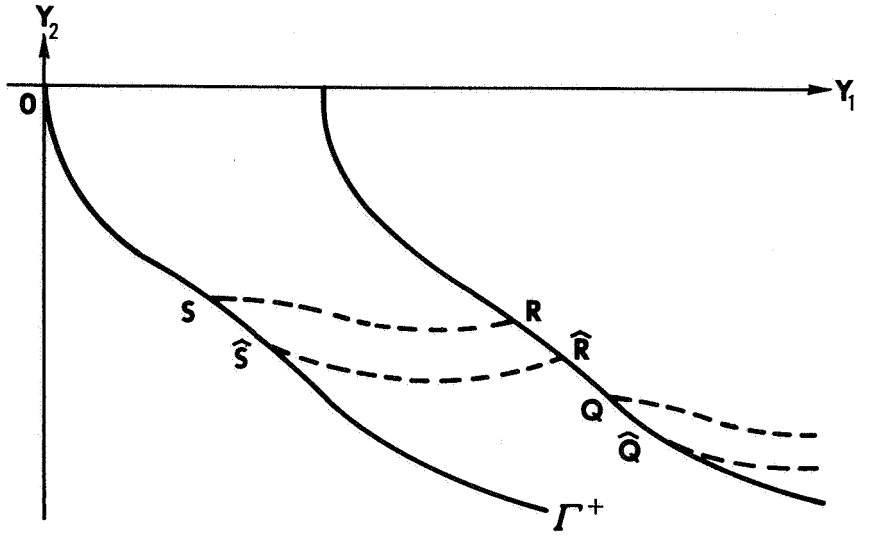

Fig. 3-17. Capped and uncapped trajectories coincide for $\hat{Y}_{1r} \leq Y_1 \leq Y_{1q}$. If path OSRQ is a pseudoextremal, path $O\hat{S}\hat{R}\hat{Q}$ is not.

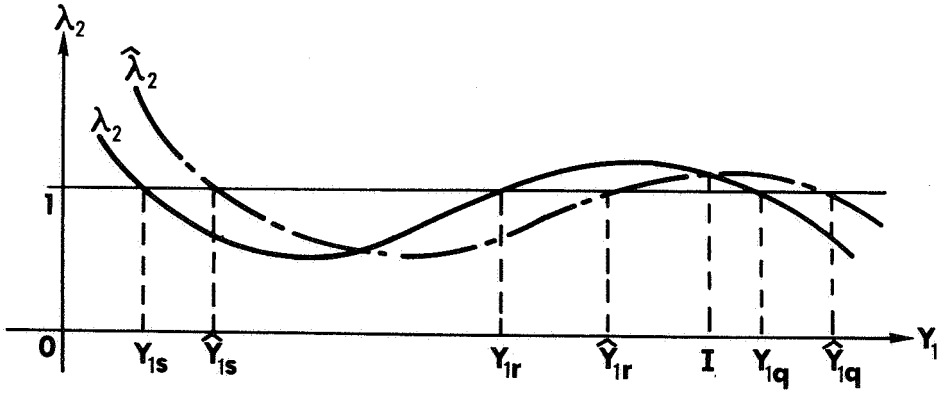

Fig. 3-18. Behavior of λ_2 and $\hat{\lambda}_2$ If Y_{1q} Were Greater Than Y_{1q}. If λ_2 corresponds to the pseudoextremal solution $\hat{\lambda}_2$ does not.

pseudoextremal of theorem 3-3, we must show that

$$\hat{y}_{1s} > y_{1s} \Rightarrow \hat{y}_{1q} < y_{1q} \tag{3-80}$$

Suppose to the contrary $\hat{y}_{1q} \geq y_{1q}$. For

$$\hat{y}_{1r} \leq y_1 \leq y_{1q} \tag{3-81}$$

both pseudoextremals coincide. See Fig. 3-17. Now consider the behavior of the adjoint variables $\lambda_2(y_1)$ and $\hat{\lambda}_2(y_1)$ corresponding to such pseudoextremals as functions of the variable y_1. See Fig. 3-18. In order that $\hat{y}_{1q} \geq y_{1q}$ it is necessary that the adjoints have equal values

$$\lambda_2(I) = \hat{\lambda}_2(I) \tag{3-82}$$

for some $y_1 = I$ on the interval

$$\hat{y}_{1r} \leq I \leq y_{1q} \tag{3-83}$$

Evaluating the Hamiltonians H_B and $\hat{H}_B$ at $y_1 = I$ and noting that $y_2(I) = \hat{y}_2(I)$ we find

$$\begin{aligned} H_B - \hat{H}_B &= -(\lambda_1(I)-\hat{\lambda}_1(I))y_2(I) + (\lambda_2(I)-\hat{\lambda}_2(I)) \cdot \\ &\quad \cdot(\sin I - u) + |u| - |u| \\ &= -y_2(I)(\lambda_1(I)-\hat{\lambda}_1(I)) \end{aligned} \tag{3-84}$$

But

$$y_2^2 \frac{d\lambda_2}{dy_1} = y_2^2 \frac{d\lambda_2}{d\tau} \frac{d\tau}{dx_1} = y_2^2 \lambda_1 \left(\frac{1}{-y_2}\right) = -y_2\lambda_1 \tag{3-85}$$

Therefore

$$H_B - \hat{H}_B = y_2^2 \left(\frac{d\lambda_2}{dy_1} - \frac{d\hat{\lambda}_2}{dy_1}\right)\Bigg|_{y_1=I} \leq 0 \tag{3-86}$$

where the last inequality follows from Fig. 3-18. Thus $\hat{H}_B \geq H_B$ which is a contradiction of lemma 3-4. The proof of theorem 3-3 is complete once we verify lemma 3-4.

PROOF OF LEMMA 3-4: Given the points S on Γ^+ and R on a fixed P-curve (See Fig. 3-17 or 3-16) to be first and second switching points for some P-O-P pseudoextremal, we first must express the Hamiltonian H_B in terms of the points S and R. Next we must find the variation in H_B; namely, δH_B as the points S and R move to S' and R' of Fig. 3-15.

From appendix C we have the expression for the adjoint $\lambda_2(y_1)$ along the O-arc from y_{1s} to y_{1r}:

$$\lambda_2(y_1) = y_2\left[\frac{\lambda_{2s}}{y_{2s}} + H_B \int_{y_{1s}}^{y_1} \frac{1}{y_2^3(\sigma)}\, d\sigma\right] \tag{3-87}$$

where $y_2(\sigma)$ denotes the coast trajectory through the point S and is explicitly

$$y_2(\sigma) = -[2(\cos\sigma - \cos y_{1s}) + y_{2s}^2]^{1/2} \tag{3-88}$$

Since S and R are switch points

$$\lambda_2(y_{1s}) \triangleq \lambda_{2s} = 1 \tag{3-89}$$

$$\lambda_2(y_{1r}) \triangleq \lambda_{2r} = 1 \tag{3-90}$$

and equation (3-87) evaluated at R becomes

$$1 = y_{2r}\left[\frac{1}{y_{2s}} + H_B \int_{y_{1s}}^{y_{1r}} \frac{1}{y_2^3(\sigma)}\, d\sigma\right] \tag{3-91}$$

from which

$$H_B = \frac{\frac{1}{y_{2r}} - \frac{1}{y_{2s}}}{\int_{y_{1s}}^{y_{1r}} \frac{1}{y_2^3(\sigma)}\, d\sigma} \tag{3-92}$$

We now seek the first order variation δH_B of the backward time Hamiltonian created by a variation δS of the first switching point S. We require that $S' = S + \delta S$ remain on Γ^+. Thus

$$\frac{y_{2s}'^2}{2} = \frac{y_{2s}^2}{2} + \cos y_{1s} - \cos y_{1s}' + A(y_{1s} - y_{1s}') \tag{3-93}$$

or for first order variations

$$y_{2s}\delta y_{2s} = (A - \sin y_{1s})\delta y_{1s} \tag{3-94}$$

Also we require that the second switch point R remain on the given P-curve. This means that

$$\frac{y'^2_{2r}}{2} = \frac{y^2_{2r}}{2} + \cos y_{1r} - \cos y'_{1r} + A(y_{1r}-y'_{1r}) \tag{3-95}$$

or as before the first order variations satisfy

$$y_{2r}\delta y_{2r} = (A-\sin y_{1r})\delta y_{1r} \tag{3-96}$$

We now look for some relation between δy_{1r} and δy_{1s}. The points S and R are on an 0-arc and thus

$$\frac{y^2_{2r}}{2} = \frac{y^2_{2s}}{2} + \cos y_{1r} - \cos y_{1s} \tag{3-97}$$

or

$$y_{2r}\delta y_{2r} = y_{2s}\delta y_{2s} - \sin y_{1r}\delta y_{1r} + \sin y_{1s}\delta y_{1s} \tag{3-98}$$

Using (3-94), (3-96) to eliminate δy_{2r} and δy_{2s} from (3-98) we obtain the desired relationship

$$\delta y_{1r} = \delta y_{1s} \tag{3-99}$$

so that the given P-curve and zero trajectory Γ^+ are in fact parallel. We now are in a position to compute the variation δH_B taken as prescribed by lemma 3-4. From (3-92)

$$H_B = \left\{\delta\left(\frac{1}{y_{2r}} - \frac{1}{y_{2s}}\right)\int_{y_{1s}}^{y_{1r}} \frac{1}{y_2^3(\sigma)}\, d\sigma - \left[\delta\left(\int_{y_{1s}}^{y_{1r}} \frac{1}{y_2^3(\sigma)}\right)d\sigma\right]\cdot \right.$$

$$\left.\cdot\left(\frac{1}{y_{2r}} - \frac{1}{y_{2s}}\right)\right\}\Big/\left(\int_{y_{1s}}^{y_{1r}} \frac{1}{y_2^3(\sigma)}\, d\sigma\right)^2 \tag{3-100}$$

or using (3-92)

$$\delta H_B = \frac{\delta\left(\frac{1}{y_{2r}} - \frac{1}{y_{2s}}\right) - H_B\delta\left(\int_{y_{1s}}^{y_{1r}} \frac{1}{y_2^3(\sigma)}\, d\sigma\right)}{\int_{y_{1s}}^{y_{1r}} \frac{1}{y_2^3(\sigma)}\, d\sigma} \tag{3-101}$$

But

$$\delta\left(\frac{1}{y_{2r}} - \frac{1}{y_{2s}}\right) = -\frac{1}{y_{2r}^2}\frac{(\sin y_{1r} - A)}{(-y_{2r})}\delta y_{1r} + \frac{1}{y_{2s}^2}\frac{(\sin y_{1s} - A)}{(-y_{2s})}\delta y_{1s} \tag{3-102}$$

or using (3-99)

$$\delta\left(\frac{1}{y_{2r}} - \frac{1}{y_{2s}}\right) = \left[\frac{(\sin y_{1r} - A)}{y_{2r}^3} - \frac{(\sin y_{1s} - A)}{y_{2s}^3}\right]\delta y_{1s} \tag{3-103}$$

Also we have

$$\delta\left(\int_{y_{1s}}^{y_{1r}} \frac{1}{y_2^3(\sigma)}\, d\sigma\right) = \frac{1}{y_{2r}^3}\delta y_{1r} - \frac{1}{y_{2s}^3}\delta y_{1s} + \int_{y_{1s}}^{y_{1r}} \delta\left(\frac{1}{y_2^3(\sigma)}\right) d\sigma \tag{3-104}$$

Using (3-88) we find that

$$\delta y_2(\sigma) = \frac{[2\sin y_{1s}\delta y_{1s} + 2y_{2s}\delta y_{2s}]}{2y_2(\sigma)} \tag{3-105}$$

or with the aid of (3-94)

$$\delta y_2(\sigma) = \frac{A\delta y_{1s}}{y_2(\sigma)} \tag{3-106}$$

and (3-104) can be rewritten as

$$\delta\left(\int_{y_{1s}}^{y_{1r}} \frac{1}{y_2^3(\sigma)}\, d\sigma \right) = \left[\frac{1}{y_{2r}^3} - \frac{1}{y_{2s}^3} - 3A \int_{y_{1s}}^{y_{1r}} \frac{1}{y_2^5(\sigma)}\, d\sigma \right] \delta y_{1s} \tag{3-107}$$

Putting these results together (i.e., combining (3-101), (3-103), and (3-107)) we finally obtain the variation in H_B due to the variation δS as prescribed by lemma 3-4.

$$\delta H_B = \left[\frac{(-H_B + \sin y_{1r} - A)}{y_{2r}^3} - \frac{(-H_B + \sin y_{1s} - A)}{y_{2s}^3} + \right.$$
$$\left. + 3H_B A \int_{y_{1s}}^{y_{1r}} \frac{1}{y_2^5(\sigma)}\, d\sigma \right] \frac{\delta y_{1s}}{\int_{y_{1s}}^{y_{1r}} \frac{1}{y_2^3(\sigma)}\, d\sigma} \tag{3-108}$$

This may be rewritten by using (3-1) as

$$\delta H_B = \left[\frac{\lambda_{1r}}{y_{2r}^2} - \frac{\lambda_{1s}}{y_{2s}^2} + A\left(\frac{1}{y_{2s}^3} - \frac{1}{y_{2r}^3} + 3H_B \cdot \right.\right.$$
$$\left.\left. \cdot \int_{y_{1s}}^{y_{1r}} \frac{1}{y_2^5(\sigma)}\, d\sigma \right) \right] \frac{\delta y_{1s}}{\int_{y_{1s}}^{y_{1r}} \frac{1}{y_2^3(\sigma)}\, d\sigma} \tag{3-109}$$

Since the integral of the denominator is always negative as y_2 is negative, our goal is to show the term in brackets to be positive

along P-O-P pseudoextremals. If this is true then

$$\delta H_B < 0 \tag{3-110}$$

for the restricted variations of lemma 3-4; namely, for

$$\delta y_{1s} > 0 \tag{3-111}$$

To determine the sign of the bracketed term of (3-109) is yet an awesome task. If we first note that

$$\int_{y_{1s}}^{y_{1r}} \lambda_2 \frac{d}{d\sigma}\left(\frac{1}{3y_2^3(\sigma)}\right)d\sigma = \int_{y_{1s}}^{y_{1r}} \frac{\lambda_2 \sin\sigma}{y_2^5(\sigma)}\, d\sigma \tag{3-112}$$

and using (3-1) and the fact that we are integrating along an O-arc we have

$$\int_{y_{1s}}^{y_{1r}} \frac{\lambda_2 \sin\sigma}{y_2^5(\sigma)}\, d\sigma = \int_{y_{1s}}^{y_{1r}} \frac{H_B + \lambda_1 y_2}{y_2^5(\sigma)}\, d\sigma \tag{3-113}$$

Now integrating by parts the left hand side of (3-112)

$$\int_{y_{1s}}^{y_{1r}} \frac{\lambda_2 \sin\sigma}{y_2^5(\sigma)}\, d\sigma = \frac{\lambda_2(\sigma)}{3y_2^3(\sigma)}\Bigg|_{y_{1s}}^{y_{1r}} - \int_{y_{1s}}^{y_{1r}} \frac{1}{3y_2^3(\sigma)} \frac{\lambda_1}{(-y_2(\sigma))}\, d\sigma \tag{3-114}$$

$$= \frac{1}{3}\left[\frac{1}{y_{2r}^3} - \frac{1}{y_{2s}^3} + \int_{y_{1s}}^{y_{1r}} \frac{\lambda_1 y_2}{y_2^5}\, d\sigma\right] \tag{3-115}$$

By now combining (3-113) and (3-115) we get finally

$$\frac{1}{y_{2s}^3} - \frac{1}{y_{2r}^3} + 3H_B \int_{y_{1s}}^{y_{1r}} \frac{d\sigma}{y_2^5(\sigma)} = -2 \int_{y_{1s}}^{y_{1r}} \frac{\lambda_1 y_2}{y_2^5} \, d\sigma \qquad (3\text{-}116)$$

Now the bracketed term of (3-109) may be somewhat simplified to

$$[3\text{-}109] = \frac{\lambda_{1r}}{y_{2r}^2} - \frac{\lambda_{1s}}{y_{2s}^2} - 2A \int_{y_{1s}}^{y_{1r}} \frac{\lambda_1 y_2}{y_2^5(\sigma)} \, d\sigma = \frac{\lambda_{1r}}{y_{2r}^2} + F(y_{1r}) \qquad (3\text{-}117)$$

where (3-117) defines the term $F(y_{1r})$, which is a function of the second switch point (y_{1r}, y_{2r}). Now the term λ_{1r}/y_{2r}^2 is always non negative since R is an 0-P corner. It is sufficient to show (see Appendix E) that

$$F(y_{1r}) > 0 \qquad (3\text{-}118)$$

to guarantee that the bracketed term of (3-109) be positive. And therefore,

$$\delta H_B < 0 \quad \text{for} \quad \delta y_{1s} > 0 \qquad (3\text{-}119)$$

which is what we set out to prove. With lemma 3-4 now verified, the proof of theorem 3-3 is also complete.

The purpose of this rather tedious development has been to structure the pseudoextremals via theorem 3-3 so that we can construct the locus of third switching curves of a P-0-P-0 pseudoextremal. Finally, we then hope to construct the complete fuel-optimal time-varying feedback control law by exhibiting all the switching curves. With this aim in sight, we find the following corollary of theorem 3-3 to be of pertinence.

COROLLARY 3-2 If point S on Γ^+ and point R on a fixed P-curve are first and second switch points of some P-0-P-0$\cdots$ pseudoextremal, then the mapping τ of the y_1 coordinates of the points Q into the interval $[0,\pi]$ via the backward time of the third switching is a monotonically increasing function.

The proof is apparent from Fig. 3-15. Theorem 3-3 has structured the pseudoextremals as shown by the figure. If $\tau(\cdot)$ denotes the time required to zero the point $(\cdot)$ along the unprimed trajectory 0-S-R-Q and $\tau'(\cdot)$ the time along the primed trajectory, then

$$\tau'(Q') < \tau(Q') \tag{3-120}$$

as the primed trajectory lies below the unprimed. But also

$$\tau(Q) = \tau(Q') + \text{time from Q to Q'} \tag{3-121}$$

and so

$$\tau'(Q') < \tau(Q) \tag{3-122}$$

as asserted by the corollary. Furthermore, we note that the mapping τ is continuous. The mapping of the points Q into the points S can be seen to be continuous in the development of theorem 3-3. Since the mapping τ can be written as a continuous function of the points S, R and Q; namely,

$$\tau(Q) = \int_0^{y_{1s}} \frac{d\sigma}{[2(\cos\sigma - 1 + A\sigma)]^{1/2}} + \int_{y_{1s}}^{y_{1r}} \frac{d\sigma}{[y_{2s}^2 + 2(\cos\sigma - \cos y_{1s})]^{1/2}} + \int_{y_{1r}}^{y_{1q}} \frac{d\sigma}{-y_2(\sigma)} \tag{3-123}$$

and since S (and hence R also via (3-97)) depend continuously on Q, the mapping τ is continuous. This result holds equally well for any set of third switch points Q and is not restricted to only those points Q on a fixed P-curve. Therefore the locus of the third switching points Q for a particular time τ_Q of switching is a continuous curve in state space and a surface in the cartesian product space $y_1 \times y_2 \times \tau$.

CONSTRUCTION OF THE THIRD SWITCHING ISOCHRONE FOR P-O-P-O TRAJECTORIES

From Fig. 3-15 we note that for a pseudoextremal solution the third switching Q must occur after the second switching R, i.e.,

$$x_{1q} \geq x_{1r} \tag{3-124}$$

For every P-curve of 3-16 there is one point for which Q = R

$$x_{1q} = x_{1r} \tag{3-125}$$

corresponding to an adjoint λ_2 behavior of Fig. 3-19. The locus of these points in state space for varying P - curves forms a boundary limiting the region for which an O-P corner can occur. In Fig. 3-19 we have the behavior of the adjoint $\lambda_2(\tau)$ at one such Q = R point. For a second switching to occur to the right of this point (an O-P corner) the adjoint $\hat{\lambda}_2(\tau)$ would have to lie below $\lambda_2(\tau)$ in which case as seen in Fig. 3-19, the O-P corner would not occur. Fig. 3-20 illustrates this boundary beyond which an O-P corner does not occur for our region of investigation $-3\pi \leq x_1 \leq 3\pi$. See (3-76) and Fig. 3-19

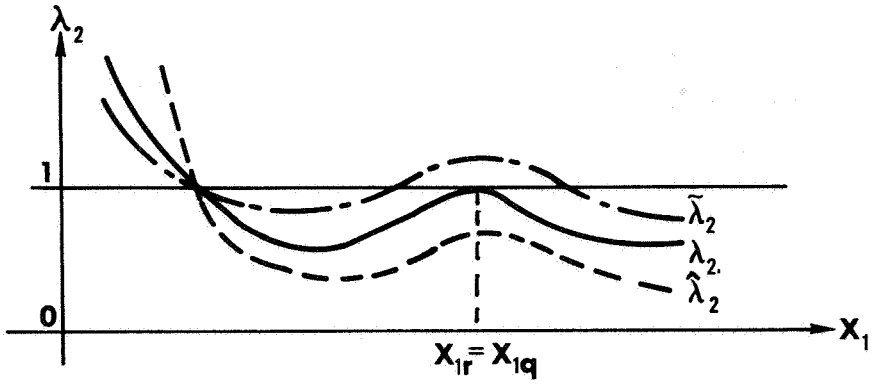

Fig. 3-19. Behavior of Adjoint $\lambda_2(\tau)$ Generating Boundary of O-P Corner Region at which Switchings R and Q Coincide.

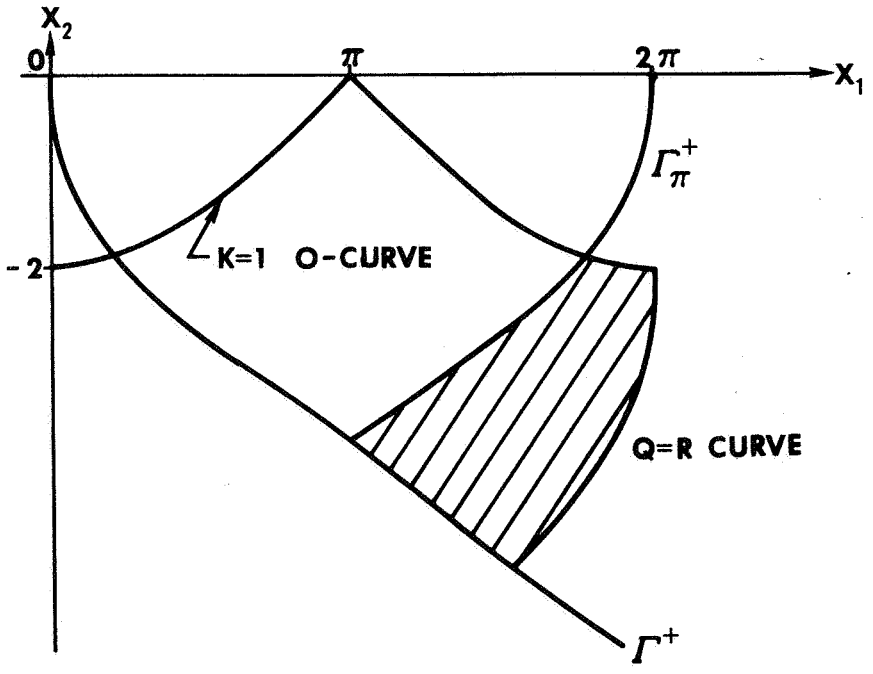

Fig. 3-20. O-P Corner Region Bounded on Right by Q=R Curve.

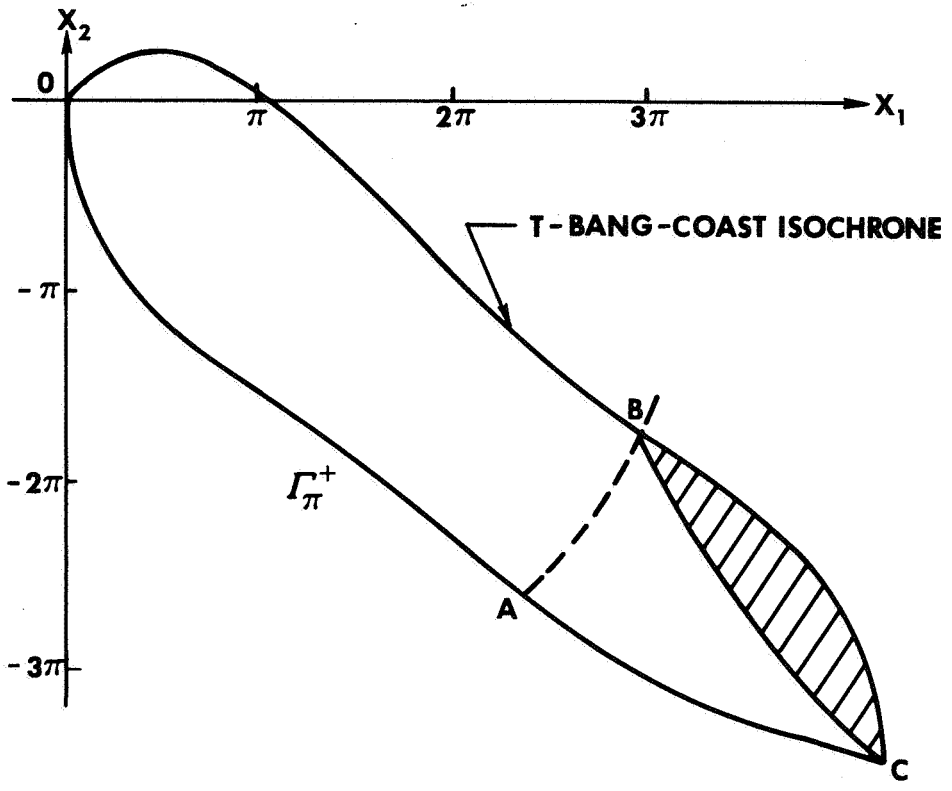

Fig. 3-21. T-Third-Switch Isochrone BC Partitioning Region Within T-Bang-Coast Isochrone. Curve AB is the Q=R Curve of Fig. 3-20.

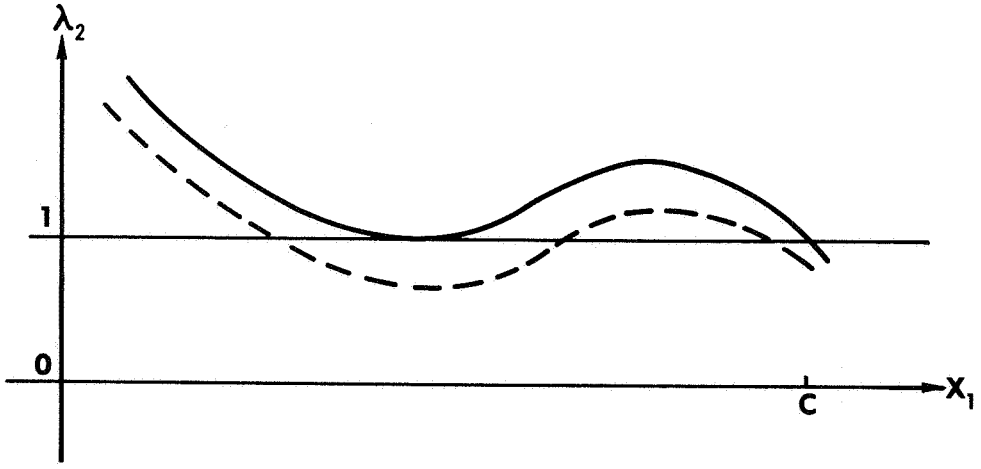

Fig. 3-22. Limiting Behavior of Adjoint λ_2 Generating a Third Switching at the Point C on Γ^+.

for verification. With T the time remaining to reach the origin specified, we anticipate the result that the locus of those third switching points that occur exactly at backward time T (the T-third-switch isochrone) partitions the region bounded by the T-bang-coast isochrone and the zero trajectory Γ^+. In Fig. 3-21 point B, the intersection of the third switching locus and the T-bang-coast isochrone, lies on the time invariant $Q = R$ curve of Fig. 3-20 and corresponds to the limiting adjoint behavior of Fig. 3-19. Point C of the Fig. 3-21 which is the intersection of the third switching curve and the zero trajectory Γ^+ must represent both a three switch (P-0-P-0) trajectory and a P trajectory coincident with Γ^+ up to the point C. The behavior of the adjoint λ_2 corresponding to a pseudoextremal for this point C is given in Fig. 3-22. At long last we are ready to construct the time-varying fuel-optimal control law for our nonlinear system. As an application of theorem 3-3 and the above we now have

OPTIMAL CONTROL LAW 3-2. Any state (x_1,x_2) residing within the region bounded by the T-bang-coast isochrone and the T-third-switch isochrone at time-to-go T has control $u(t)$ equal zero.

PROOF: By lemma 3-3 and theorem 3-2 we are dealing with a P-0-P-0 trajectory or a portion thereof. The control is therefore either 0 or +A for a state within the region of consideration at time-to-go T. If the control is zero no further consideration is needed. Suppose on the contrary it were +A. Then the pseudoextremal would have to be of type P-0-P. From Fig. 3-23 where path OSRQ is that pseudoextremal for a point Q initially upon the T-third switch isochrone, the only

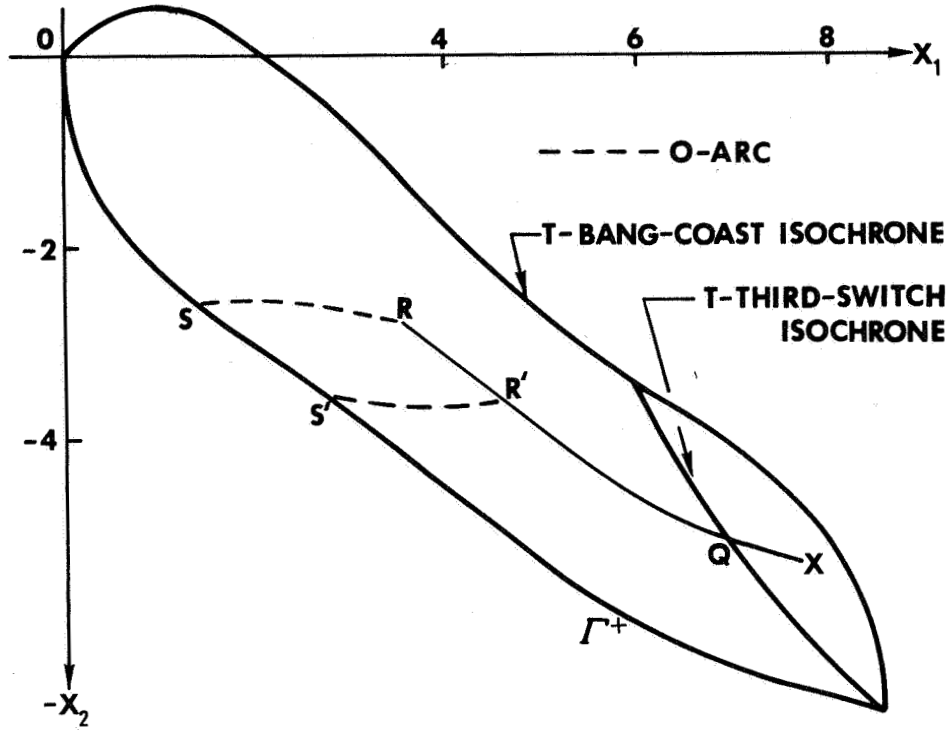

Fig. 3-23. Pseudoextremal Path (OSRQ) for Zeroing State Q Belonging to the T-Third-Switch Isochrone at Time-to-go T. The P-O-P path OS' R'X is not a pseudoextremal.

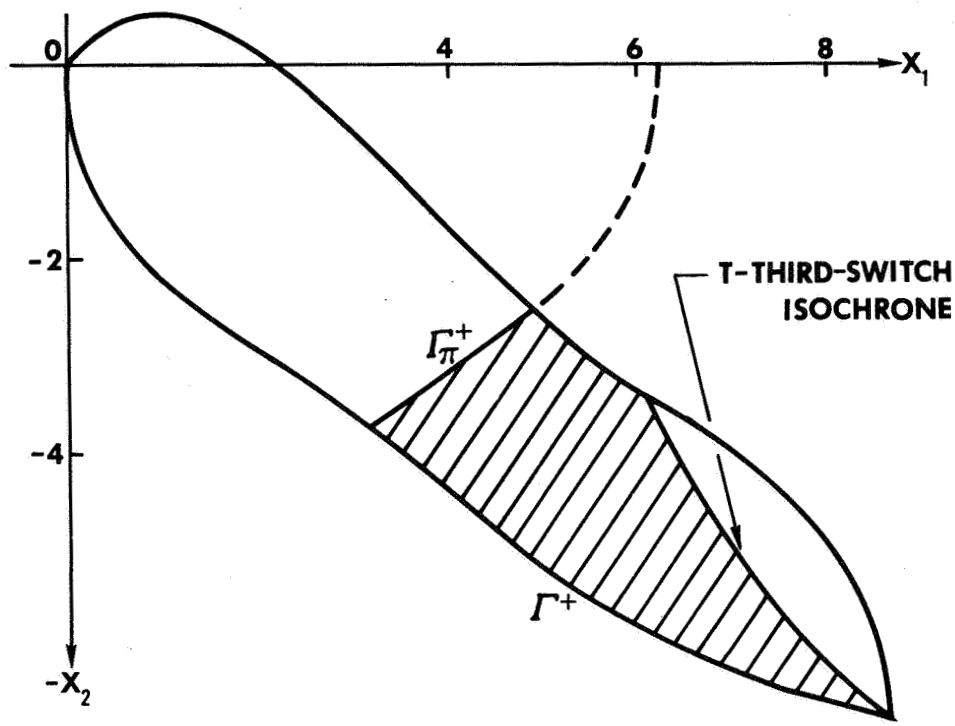

Fig. 3-24. Region (Shaded) of Optimal Control Law 3-3 Having Control u = +A.

way a P-O-P extremal for the point x can meet the time constraint is via a path OS'R'X. But this is impossible in that it would contradict theorem 3-3 as illustrated by Fig. 3-15. To be in agreement with theorem 3-3 path OS'R'X of Fig. 3-23 would have had a P-O corner between R' and Q.

We now illustrate the trajectory traced by the phase point $(x_1(t),x_2(t))$ for an initial disturbance (x_{10},x_{20}) belonging to the region bounded by the T_f-third-switch isochrone and the T_f-bang-coast isochrone, where T_f is the time allowed for zeroing the disturbance. With t denoting the time that has lapsed since we began zeroing the disturbance, the time-to-go T satisfies

$$T = T_f - t \tag{3-126}$$

Referring to Fig. 3-25, as long as the state $(x_1(t),x_2(t))$ belongs to the region bounded by the T-third switch and T-bang-coast isochrones the control remains $u(t) = 0$. As the phase point proceeds along an O-arc toward the boundary of this region, the boundaries themselves are shrinking toward the origin. The control remains $u(t) = 0$ until the phase point (x_1,x_2) intercepts the T'-third-switch isochrone at which time the control switches to $u(t') = +A$. The phase point continues along this P-arc until colliding with the shrinking bang-coast isochrone at time-to-go T'''. At T''' the control switches again to zero and the phase point 'rides' the shrinking T-bang-coast isochrone to the origin by following an O-arc to Γ^+ and then the P-curve to the origin. Note the $u = 0$ region of Fig. 3-6 disappears when the

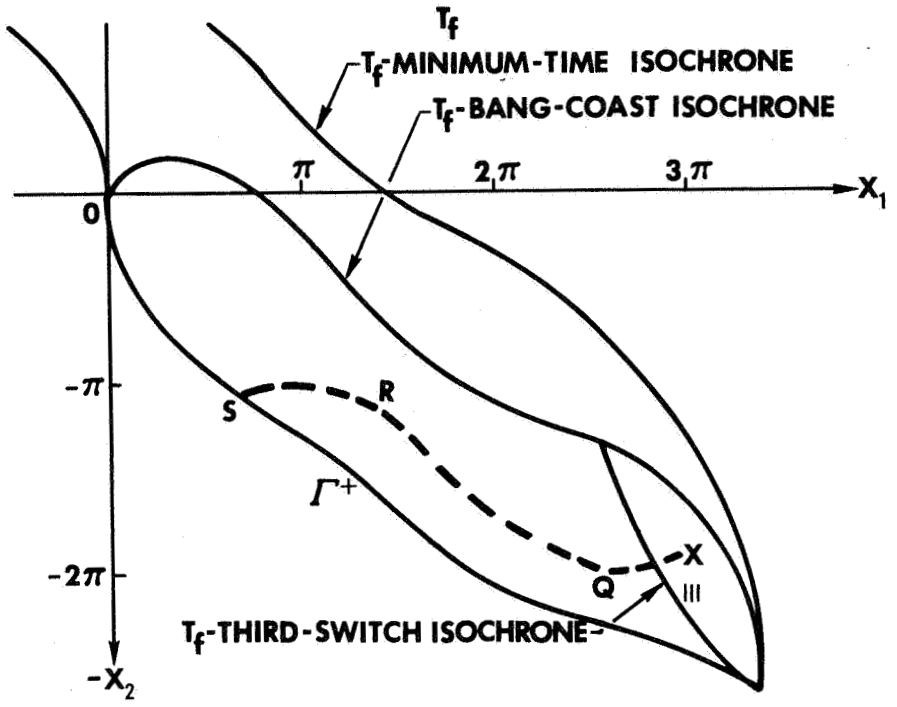

Fig. 3-25a. Optimal P-0-P-0 Paths for Zeroing State X Within Time T_f. The dashed portion is yet to be traversed while the solid arc is that alreacy traversed.

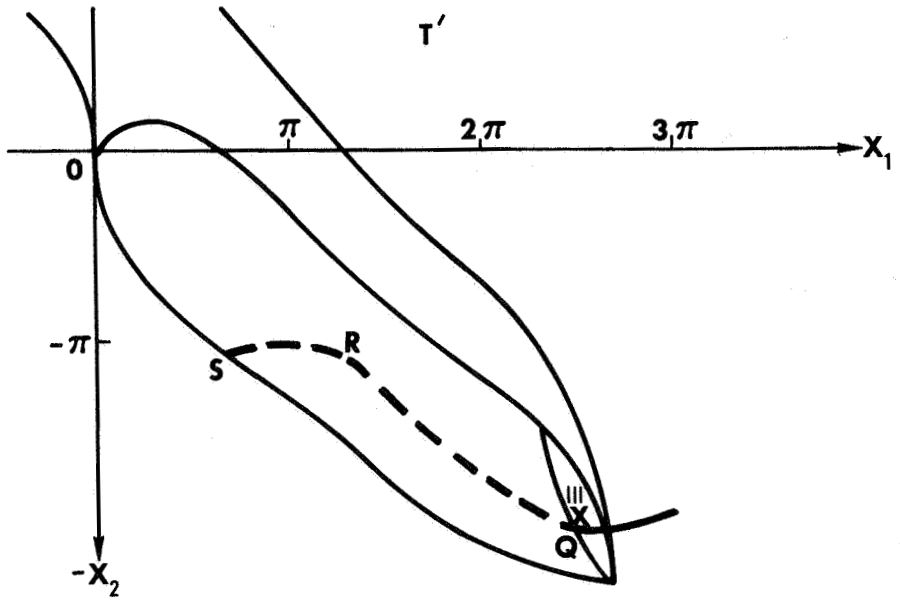

Fig. 3-25b. State X intercepts boundary of u = 0 control region; namely, T'-third-switch isochrone at time-to-to T' and control switches to +A.

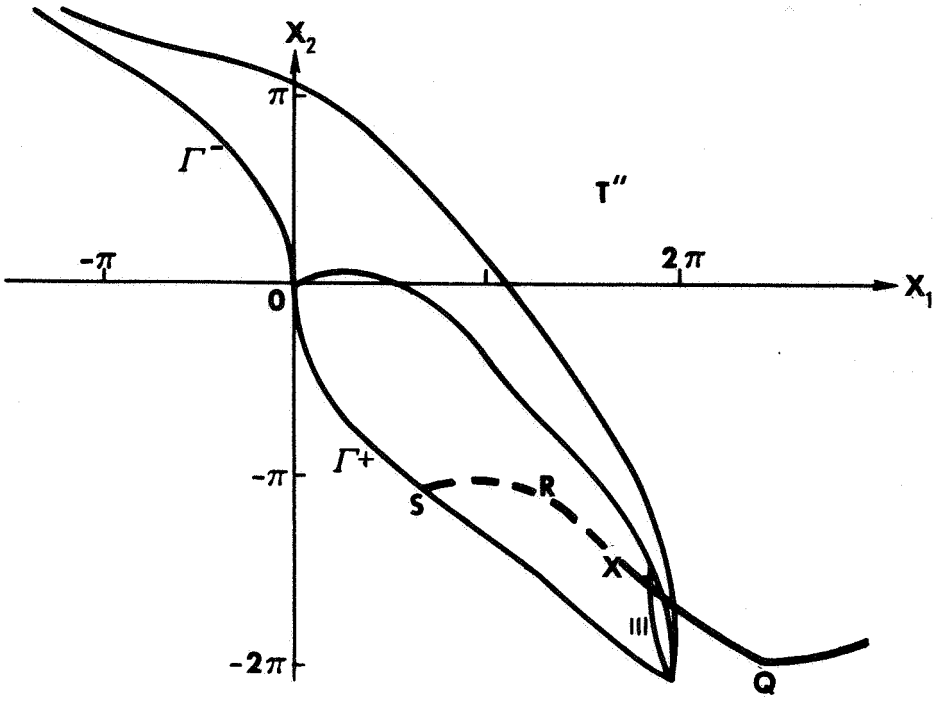

Fig. 3-25c. State X continues along P-curve until colliding with shrinking bang-coast isochrone.

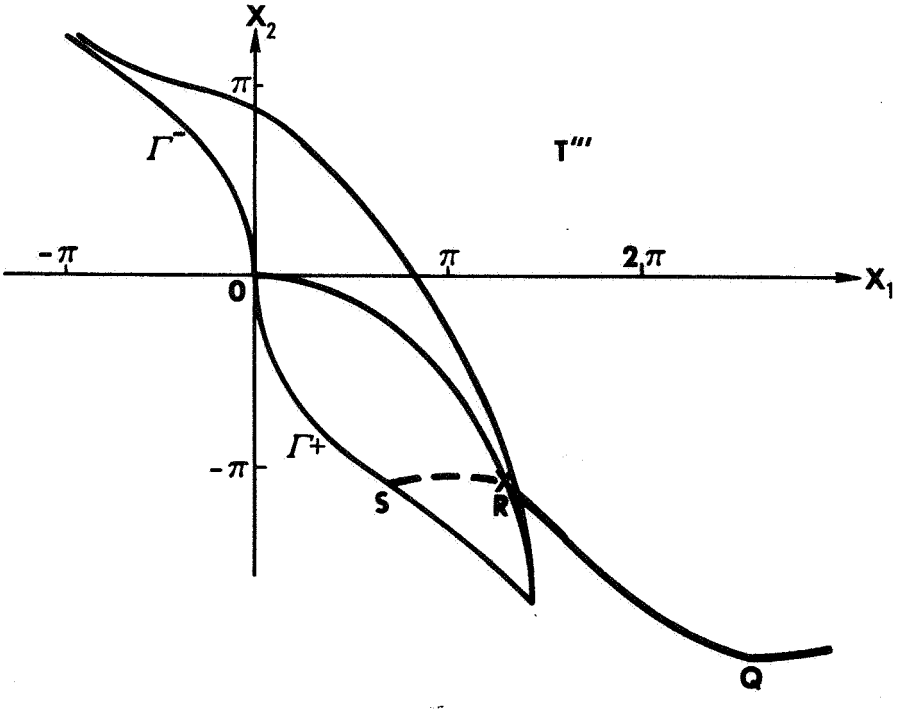

Fig. 3-25d. State X meets shrinking bang-coast isochrone at time-to-go T‴′ and control switches to zero.

time-to-go becomes so short that the T-controllable region lies between $x_1 = \pm 3\pi/2$. We now are ready to attack the region bounded by the T-third-switch line, T-bang-coast isochrone, reflected zero trajectory Γ_π^+, and zero trajectory Γ^+. See Fig. 3-24.

OPTIMAL CONTROL LAW 3-3. Any state residing within the region bounded by T-third-switch isochrone, T-bang-coast isochrone, Γ_π^+, and Γ^+ at time-to-go T has optimal control $u(t) = +A$.

PROOF: We need only show that

$$u(T) \neq 0 \tag{3-127}$$

for this region at time-to-go T. Suppose $u(t)$ were zero for some state X residing in this region at time-to-go T. Then the state would have either a P-0 or P-0-P-0 pseudoextremal as its optimal path for being zeroed within time T. But a P-0 trajectory arrives too early by definition of T-bang-coast isochrone. See Fig. 3-27. Furthermore, it is not an $H_B = 0$ pseudoextremal (see Fig. 3-2) and by corollary 3-1 cannot be optimal. Likewise a P-0-P-0 pseudoextremal OSRQX as shown in Fig. 3-27 would arrive early and cannot be optimal. To demonstrate that this is the case requires additional effort. To begin we assert analogous to corollary 3-2 the following:

COROLLARY 3-3. If the set of points Q along some portion of an 0-arc represent third switching points for some P-0-P-0 pseudoextremal, then the mapping τ of the x_1 coordinates of the points Q into the reals via the backward time of the third switching is a monotonically increasing function.

Thus along each such 0-arc we may associate a unique time of third switching. See Fig. 3-26. Corollary 3-3 is verified by first noting that as the time-to-go T decreases the third switching point Q moves continuously up a given P-curve as seen in (3-122) and (3-123). Because each such P-curve intersects the said 0-arc in exactly one point, only one value of the time of third switching is associated with any point Q of the P-arc – i.e., the mapping τ is a function. To demonstrate that the function $\tau(\cdot)$ is monotonic consider the points X of Fig. 3-27 belonging to that portion of an 0-curve bounded by the T-third-switch and T-bang-coast isochrones which are to be zeroed in exactly time T. From control law 3-2 each such X has a third switching Q somewhere on this arc. Now X_1 switches at Q_1 and X_2 at Q_2. Assuming we must meet the time constraint T_f exactly (i.e., we are not on an $H_B = 0$ pseudoextremal) then the mapping of the points X of that portion of the 0-arc between X_1 and X_2 into that portion between Q_2 and Q_1 via the third switching point Q is one to one and onto. For if this were not true, distinct states X_a and X_b on an 0-arc would both have the same third switching point Q_a along pseudoextremals requiring exactly time T_f to reach the origin. But since X_a spends less time than X_b in reaching point Q two different third switching times $\tau(Q)$ must be associated with a single point – contradicting the fact that such a mapping $\tau(\cdot)$ is a function.

With the aid of Fig. 3-27 and the fact that the mapping of the points X into the points Q is monotonic and continuous we complete the verification of corollary 3-3. Letting $\tau(X_i, Q_i)$ denote the time

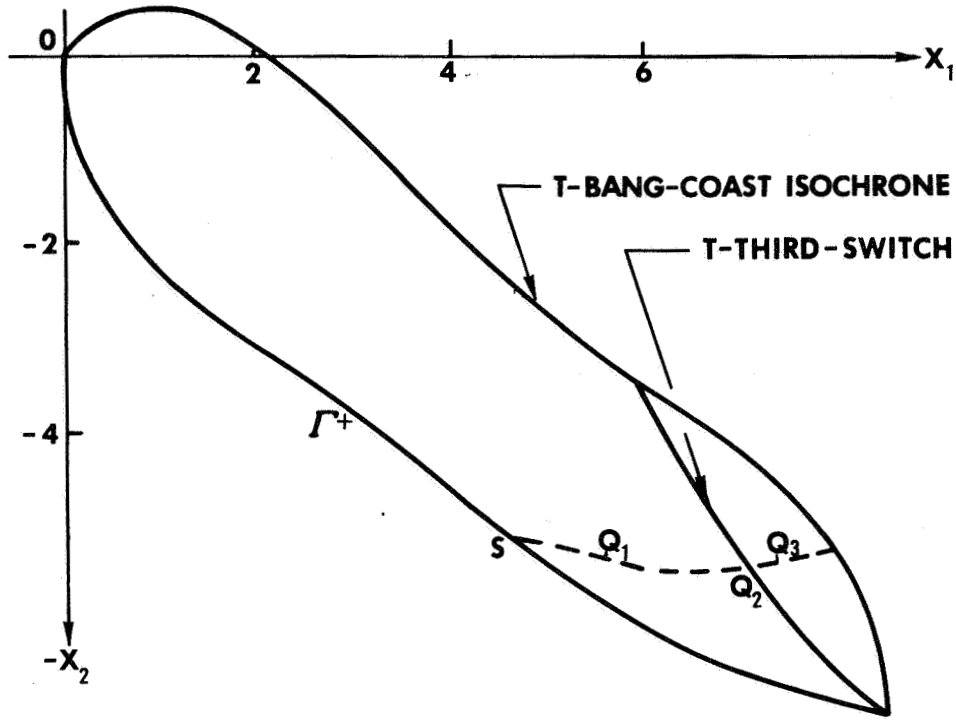

Fig. 3-26. Illustration 1 of Corollary 3-3. The mapping $\tau(Q)$ of the third switch points Q belonging to the same 0-curve of a P-0-P-0 pseudoextremal is monotonic. $\tau(Q_1) < \tau(Q_2) < \tau(Q_s)$.

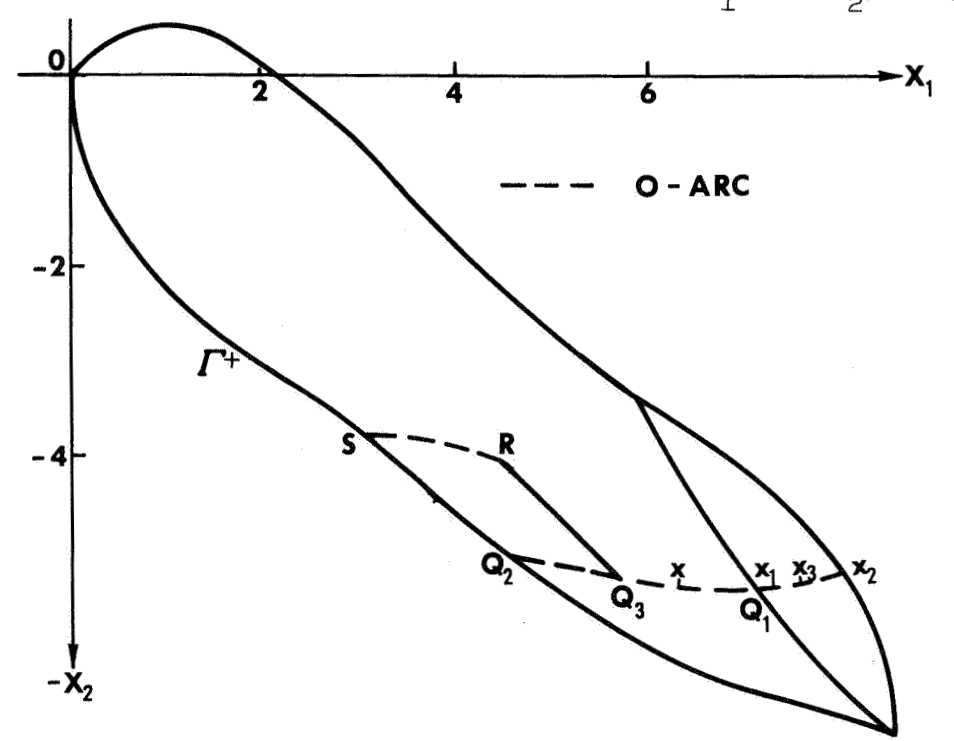

Fig. 3-27. Illustration 2 of Corollary 3-3. The mapping of the x_1x_2 of an 0-arc into the Q_2Q_1 portion via the third switch point of a pseudoextremal is one to one and onto.

spent as state X_i moves to its third switch point Q_i and $\tau(Q_i)$ denote the time of the third switching we have for each X_i

$$\tau(Q_i) + \tau(X_i,Q_i) = T_f \tag{3-128}$$

But the time $\tau(X_i,Q_i)$ for state X_i to coast to switch point Q_i along a pseudoextremal is a monotonic decreasing function of the abscissa of the point Q_i because the distance between the points X and Q along the 0-arc as a function of the abscissa of the point Q is monotonic as seen in Fig. 3-27. Therefore $\tau(Q_i)$ is monotonically increasing as asserted.

Using corollary 3-3 we can now eliminate any P-0-P-0 pseudoextremal from consideration and thereby complete the proof of optimal control law 3-3. From Fig. 3-27 any P-0-P-0 pseudoextremal switching at Q_3 with starting point $X < X_1$, must arrive too early. Furthermore, it can not be an $H_B = 0$ pseudoextremal because theorem 3-3 and lemma 3-4 guarantee that the third switching point of such a pseudoextremal must be below that third switch point of any third switching locus belonging to the same given P-curve. Such a trajectory can not be optimal and therefore optimal control law 3-3 is established.

We now illustrate the P-0-P trajectory traced by the phase point $(x_1(t),x_2(t))$ for an initial disturbance (x_{10},x_{20}) belonging to the region bounded by the T_f-third-switch and T_f-bang-coast isochrones and the fixed curves Γ^+ and Γ_π^+. The time specified for zeroing the initial disturbance (x_{10},x_{20}) is T_f. Referring to Fig. 3-28a,b, c,d as long as the state $(x_1(t),x_2(t))$ belongs to the region bounded by the T-third-switch and T-bang-coast isochrones and the

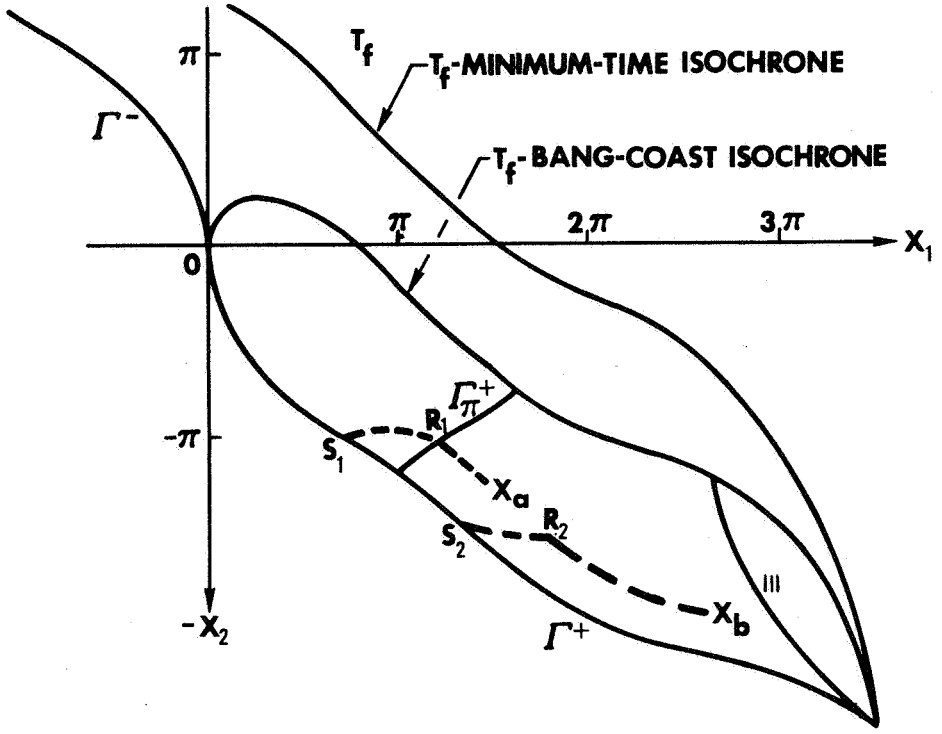

Fig. 3-28a. Optimal P-0-P Trajectories. Path $0,S_1,R_1,X_a$ zeros state X_a early but nonetheless optimally. The dashed portion is yet to be traversed while the solid arc is that already traversed.

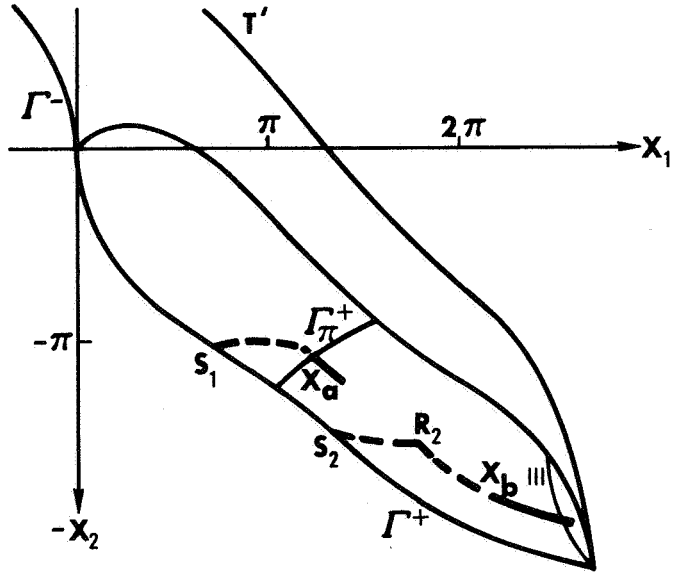

Fig. 3-28b. State X_a reaches curve Γ_π^+ ahead of the shrinking bang-coast isochrone and control switches to zero.

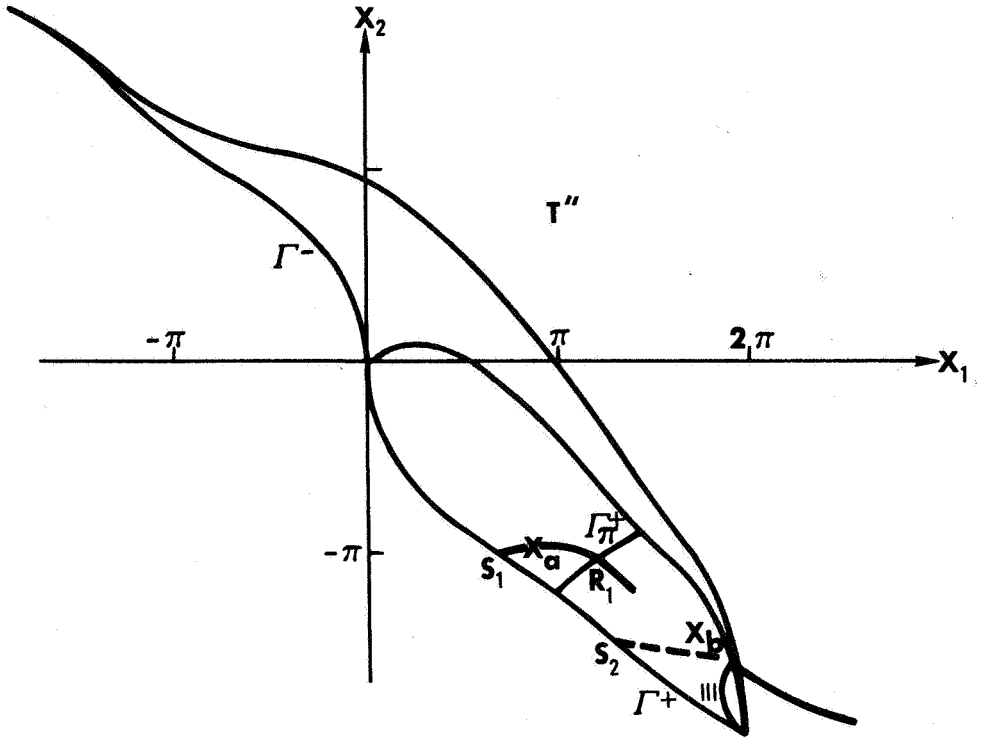

Fig. 3-28c. State X_b collides with the shrinking bang-coast isochrone before meeting Γ_π^+ and control switches to zero.

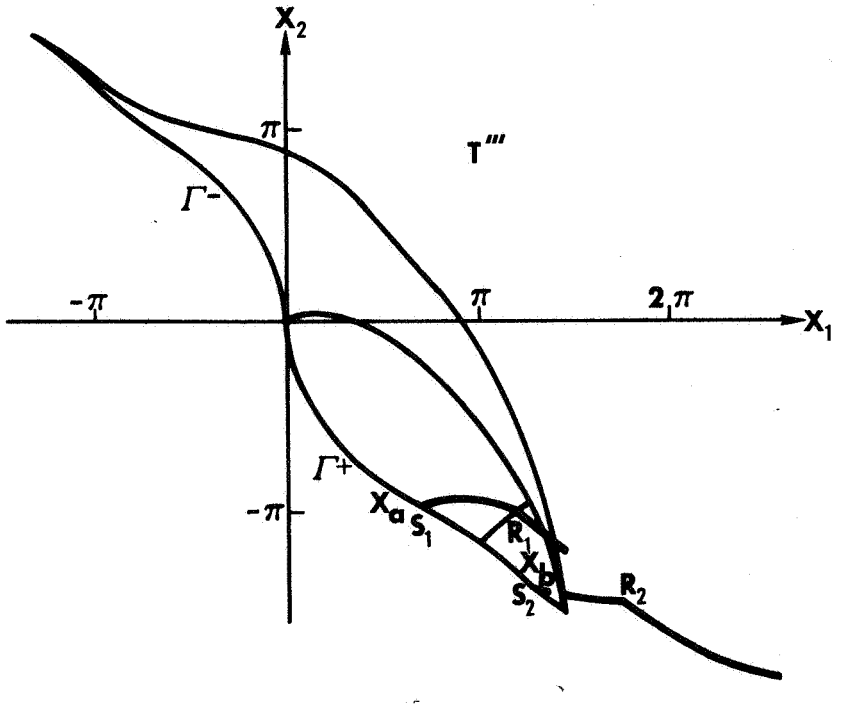

Fig. 3-28d. State X_a arrives early at origin; state X_b rides shrinking bang-coast isochrone to arrive at time T_f.

curves Γ^+ and Γ_π^+ (T is the time-to-go) the control remains $u(t) = +A$. The phase point proceeds along a P-arc toward the boundary of this region until either meeting the fixed line Γ_π^+ or colliding with the shrinking T-bang-coast isochrone. The first case illustrated by the point $\mathbf{X}_a$ in Fig. 3-28 corresponds to an $H_B = 0$ pseudoextremal. The phase point $\mathbf{X}_a$ is always ahead of the shrinking bang-coast isochrone and arrives at the origin early. In the second case the initial disturbance was too far from the Γ_π^+ switch line to reach that line before being intercepted by the shrinking bang-coast isochrone. Here X_b proceeds with control $u(t) = A$ until time-to-go T'' at which time the control switches to zero. Thereafter the phase point 'rides' the shrinking bang-coast isochrone to the origin.

We conclude our development with the fuel optimal feedback control law for the remaining shaded region of Fig. 3-29a.

OPTIMAL CONTROL LAW 3-4. Any state residing within the region bounded by the T-bang-coast isochrone, Γ_π^+ and Γ^+ at time-to-go T has optimal control $u(t) = 0$.

PROOF: That no P-0-P$\cdots$ trajectories may occur within this region was deduced in lemma 3-1b. We need only consider the possibility of a P-0-N trajectory, i.e., the control being $u(t) = -A$ within this region. But any point within this region can be zeroed within time T by a P-0 trajectory because of the definition of the T-bang-coast isochrone. Inasmuch as a P-0-N trajectory would zero a state faster than a P-0 trajectory, such a path must arrive too early. Furthermore,

for $T \leq \pi$ the bang-coast isochrone lies below the curve $\Gamma^{+}_{y_1}$ (reflection of the zero trajectory about the y_1 or x_1 axis). From Fig. 3-2 such pseudoextremals are not $H_B = 0$ extremals. Corollary 3-1 prohibits these P-0-N... paths from being optimal because they do not meet the time constraint exactly.

We now illustrate the P-0 trajectory traced by the phase point $(x_1(t),x_2(t))$ for an initial disturbance (x_{10},x_{20}) belonging to the region bounded by the time dependent T_f-bang-coast isochrone and the fixed Γ^{+}_{π} and Γ^{+} curves associated with optimal control law 3-4. Referring to Figs. 3-29a,b,c,d as long as the state belongs to the region just described the control remains $u(t) = 0$. But the phase point always will belong to this region until reaching the zero trajectory Γ^{+} at which point the control switches to $+A$. All states lying upon the T_f-bang-coast isochrone, such as state X_a, ride the shrinking bang-coast isochrone to the origin. Other states such as X_b and X_c are within the T_f-bang-coast isochrone initially. Since they follow P-0 trajectories they arrive at the zero trajectory ahead of the shrinking isochrone. There the control switches to $+A$ and the phase points continue along the zero trajectory arriving at the origin in a time less than T_f.

By assemblying optimal control laws (3-1), (3-2), (3-3), and (3-4) we now have the complete time varying feedback control law for any state within the T_f-controllable region. The only restrictions we have had to impose are

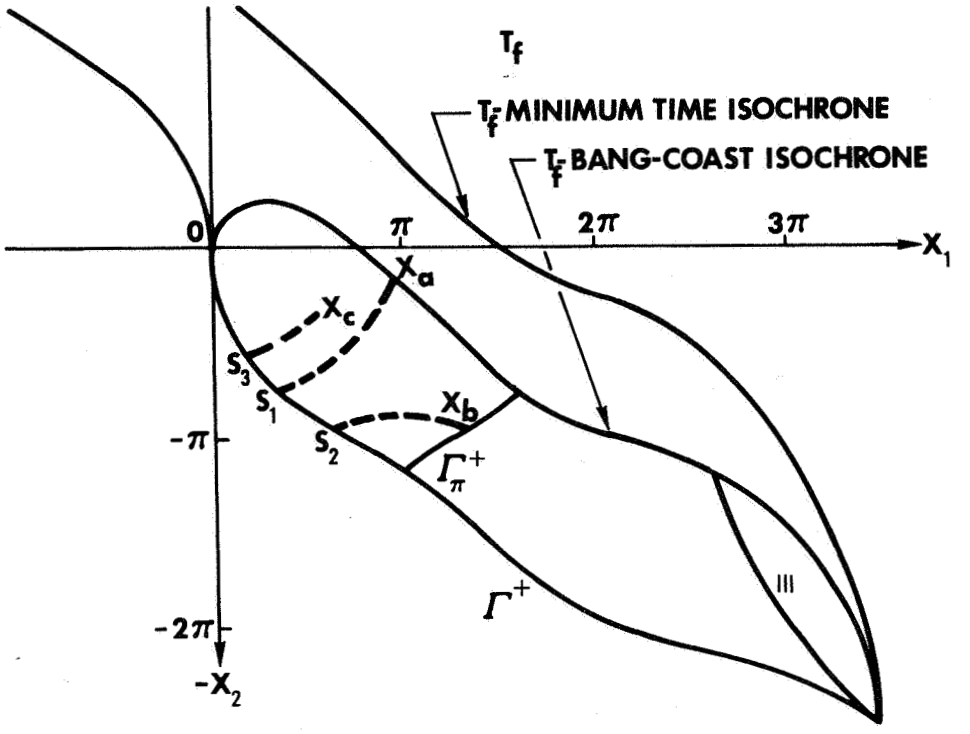

Fig. 3-29a. Optimal P-O Trajectories. Paths O,S_1,X_a; O,S_2X_b; O,S_3,X_c are all optimal for a specified time of solution T_f.

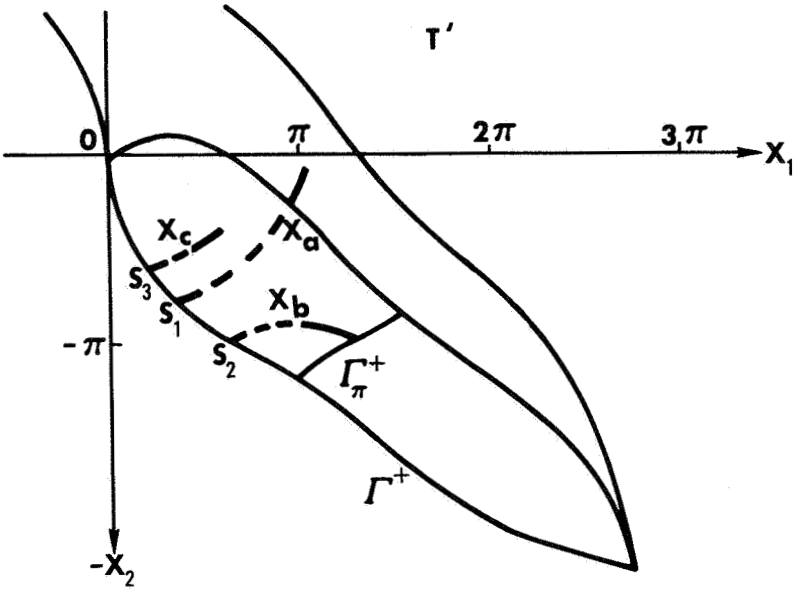

Fig. 3-29b. All states initially within this region follow O-arcs to Γ^+.

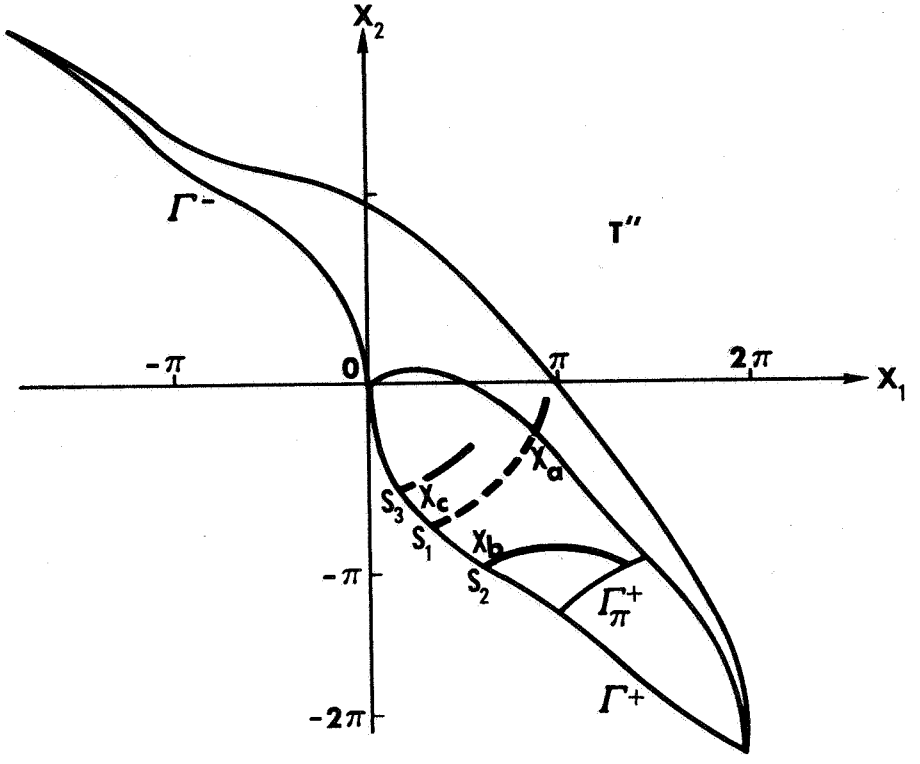

Fig. 3-29c. Both X_b and X_c will arrive at origin early whereas X_a 'rides' shrinking bang-coast isochrone to arrive on schedule.

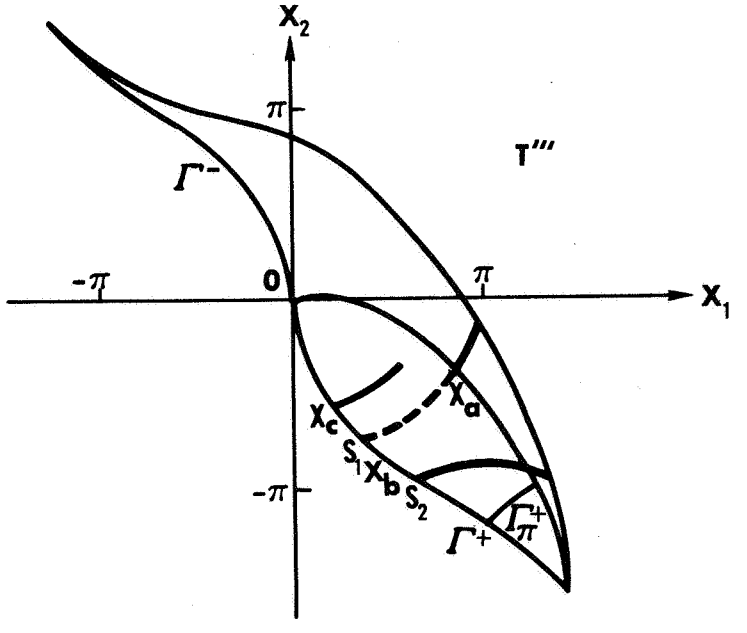

Fig. 3-29d. X_c reaches Γ^+; X_b moves along Γ^+; X_a will arrive at 0 in precisely time T_f.

$$1)\quad T_f \leq \frac{\pi}{2} + \text{arcsinh } 1 \tag{3-129}$$

and that the T_f-controllable region be limited by

$$2)\quad -3\pi \leq x_1 \leq 3\pi \tag{3-130}$$

The complete control law is shown in Fig. 3-30.

Restriction (3-129) was imposed in order to limit any pseudoextremal candidates having both P and N-arcs to merely a P-0-N trajectory. We note that in the proof of theorem 2-2 we have a lower bound on the time T_f for which a longer sequence P-0-N-0$\cdots$ or 0-P-0-N$\cdots$ could occur if it were in fact a pseudoextremal. Because $\pi/2$ + arcsinh 1 is a lower bound we might well expect the results to hold equally well for times as large as π. No pseudoextremals were found using digital computer simulations to contradict this expectation. The lower bound of $\pi/2$ + arcsinh 1 is certainly too strong a bound inasmuch as it arose from the consideration of a minimum time of solution — a time limit which was lowered still further via the introduction of a reduced broader problem in appendix B. No alternate proof was found which would raise this power bound even though the infinium of times for which a P-0-N-0 pseudoextremal could occur probably is at least π.

Restriction (3-130) enabled us to limit our consideration of P-0-P-0$\cdots$ pseudoextremals to a sequence P-0-P-0 or a truncation thereof. If one now recalls the actual earth pointing satellite problem wherein the x_1 coordinate is driven to some integral multiple of 4π, the desirability of being able to zero the initial state $(2\pi,0)$ becomes

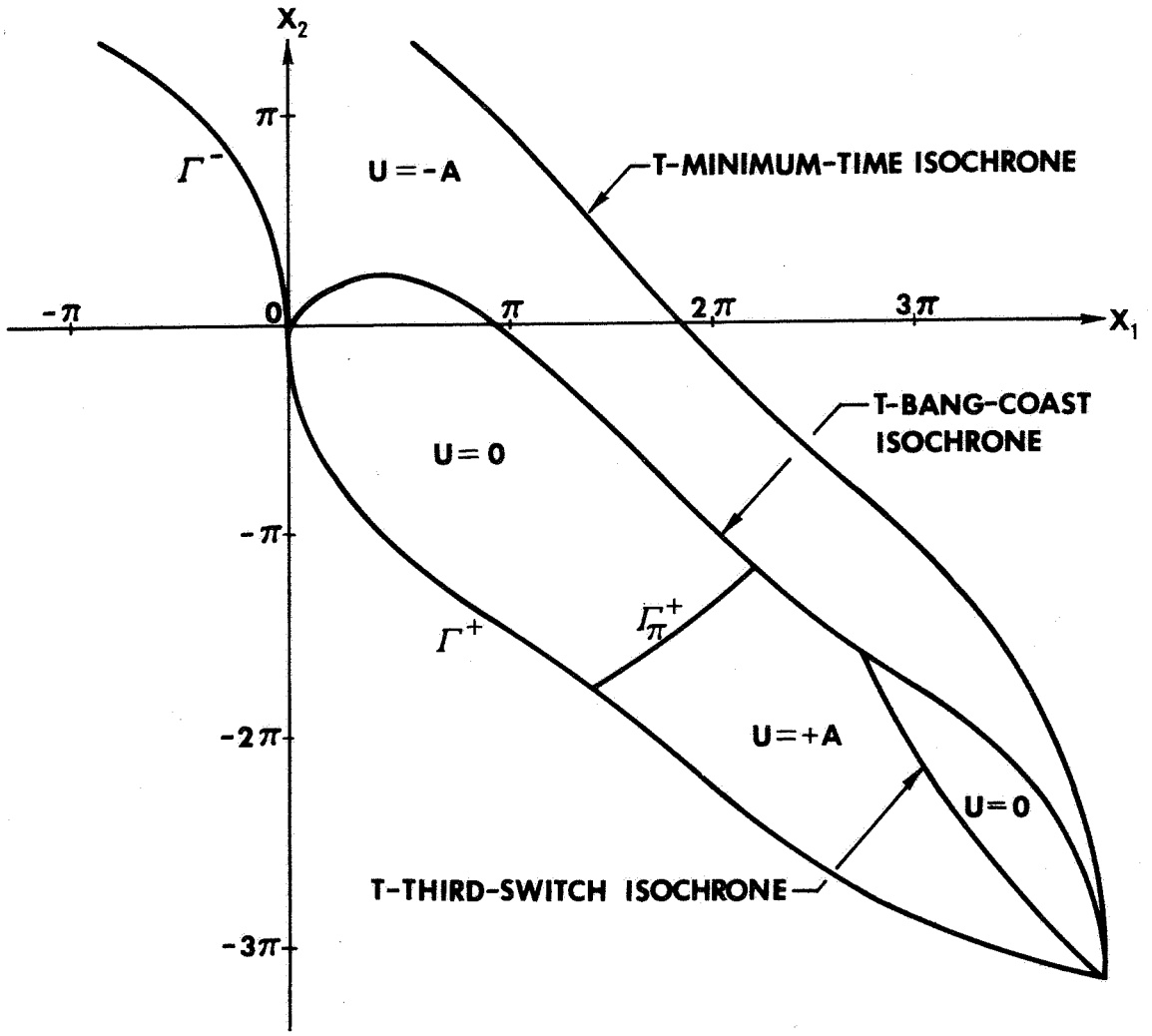

Fig. 3-30. Fuel Optimal Feedback Control Law for the Instant $t = T_f - T$.

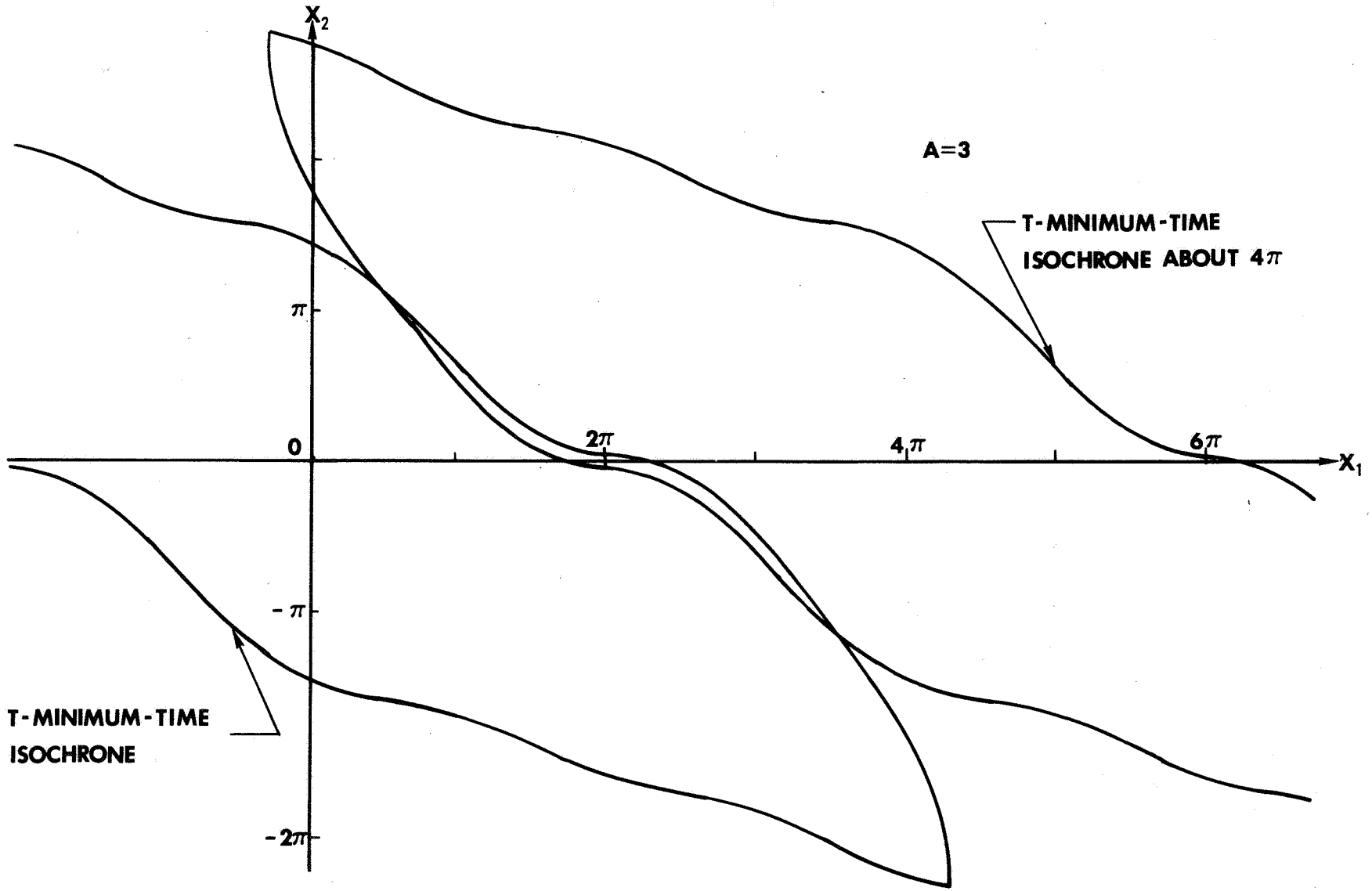

Fig. 3-31. Union to the T-controllable Regions about the Points $(4k\pi,0)$. Since $(2\pi,0)$ belongs to the T-controllable region about $(0,0)$ the union is simply connected.

apparent. For if this state $(2\pi,0)$ is within the T_f-controllable region, the T_f-controllable region about $(4\pi,0)$ will overlap the T_f-controllable region about $(0,0)$. The union of all such T-controllable regions about the points $4k\pi$ on the x_1 axis will then form a simply connected region. We therefore can control any pitch angle within time T_f provided the pitch velocity is not excessive; i.e., x_2 lies within the envelop of these T_f-controllable regions. See Fig. 3-31. Unfortunately the requirement that the T_f-controllable region lie between the lines $x_1 = \pm 3\pi$ (3-130) excludes the point $(2\pi,0)$ from the T_f-controllable-region. Should we adhere to (3-130) then there would be holes of uncontrollability within the union of such T_f-controllable-regions corresponding to states we are unable to drive to $(4k\pi,0)$ within time T_f. In Chapter IV we abandon restriction (3-130) and admit P-0-P-0$\cdots$ sequences with more than three switchings. In so doing we will also leave our theorem-proof type format and generate these more complex switching surfaces on the digital computer always taking advantage of the structure already developed in this chapter.

CHAPTER IV

In this chapter we remove the requirement that the T-controllable region always be bounded by the lines $x_1 = -3\pi$ and $x_1 = +3\pi$ to which we adhered throughout chapter III. In so doing we no longer may exploit lemma 3-3 to limit our consideration of P-0-P-0-... pseudo-extremals to those with at most three switchings. In fact, as we shall see, for a control bound $A = 3$ and time of mission $T_f = \pi$, we may have as many as five switchings on such a pseudoextremal. Thus the control law for the region bounded by the T-bang-coast isochrone and zero trajectory becomes much more complex than before. We content ourselves with the generation of the switching curves by a computer program which exploits the structure of theorem 3-3.

As before we consider only those backward time pseudoextremals beginning with a P-arc since identical reasoning yields analogous results for those pseudoextremals having control initially -A. Furthermore, we now relax the time T_f allowed for solution from $\pi/2 + \text{arcsinh } 1$ to π.

Whenever we still limit the maximum time of solution to $\pi/2 + \text{arcsinh } 1$, the control law for the region bounded by the upper T-minimum time isochrone and the T-bang-coast isochrone remains unchanged; namely $u(t) = -A$. However, we shall assume that this control law remains valid for times T as large as π. No contradictions were found while generating P-0-N pseudoextremals on the digital computer. Furthermore, as already discussed, the time restriction $\pi/2 + \text{arcsinh } 1$ for

excluding the occurrence of P-O-N-P pseudoextremals was too strong. Optimal control law 3-1 certainly remains valid for times T greater than $\pi/2 + \text{arcsinh } 1$ and most likely even for times T larger than π. Theorem 3-2 continues also to provide the optimal control for those states belonging to the T-bang-coast isochrone, namely $u(t) = 0$, provided the control magnitude A satisfy equation (3-57). Our task then is to determine the new feedback control law for the region bounded by the T-bang-coast isochrone and the zero trajectory Γ^+. If we first relax the previous constraint on the T-controllable region to the constraint

$$-3\pi-\pi/2 < y_1 \leq 3\pi+\pi/2 \qquad (4\text{-}1)$$

obvious extension of lemma 3-3 yields the result that an alternating P-O type pseudoextremal has at most four switchings. The optimal control law for times large enough to permit the T-controllable region to extend beyond the line $y_1 = 3\pi$ yet not beyond the line $y_1 = 3\pi+\pi/2$ is given in Fig. 4-1. Whereas before the T-third-switch isochrone extended from the T-bang-coast isochrone all the way to the zero trajectory Γ^+ and thereby partitioned the region within the T-bang-coast isochrone, the T-third-switch isochrone (III) now only extends to the point B of Fig. 4-1. If we define a T-fourth-switch isochrone to be the locus of fourth switchings of a P-O-P-O-P pseudoextremal which occur exactly in backward time T, then the T-fourth-switch isochrone joins the T-third-switch isochrone (III) at B and links back to the

T-bang-coast isochrone as shown in Fig. 4-1. It is these isochrones end to end that now isolate one section of the region within the T-bang-coast isochrone. For this section we have:

OPTIMAL CONTROL LAW 4-1. If a state $(x_1(t),x_2(t))$ resides at time-to-go T within the region bounded by the T-third and T-fourth-switch isochrones and the T-bang-coast isochrone the optimal control is $u(t) = 0$.

As in chapter III, the point A must simultaneously represent both a second and third switching since it belongs to the T-bang-coast isochrone and the T-third-switch isochrone. In Fig. 3-19 the limiting behavior of the adjoint λ_2 for such a point was illustrated. Furthermore, the $Q = R$ curve, which is the locus of points at which the second and third switchings coincide, is a fixed curve in state space beyond which an 0-P corner did not occur. In Fig. 4-1 as throughout this chapter we give the $Q = R$ curve the more suggestive name L_{32} to indicate the limiting case where the third and second switchings of a P-0-P pseudoextremal coincide. As the time-to-go T decreases, the T-bang-coast isochrone shrinks and the point A, which is the intersection of the T-third-switch and T-bang-coast isochrones moves along the curve L_{32}.

For $-3\pi \leq x_1 \leq +3\pi$ the second switchings of a P-0-P type pseudoextremal were limited to a region bounded by Γ_π^+, $Q = R$ curve, and the zero trajectory as shown in Fig. 3-20. For $x_1 > 3\pi$ a second such region emerges consisting of second switch points of some P-0-P

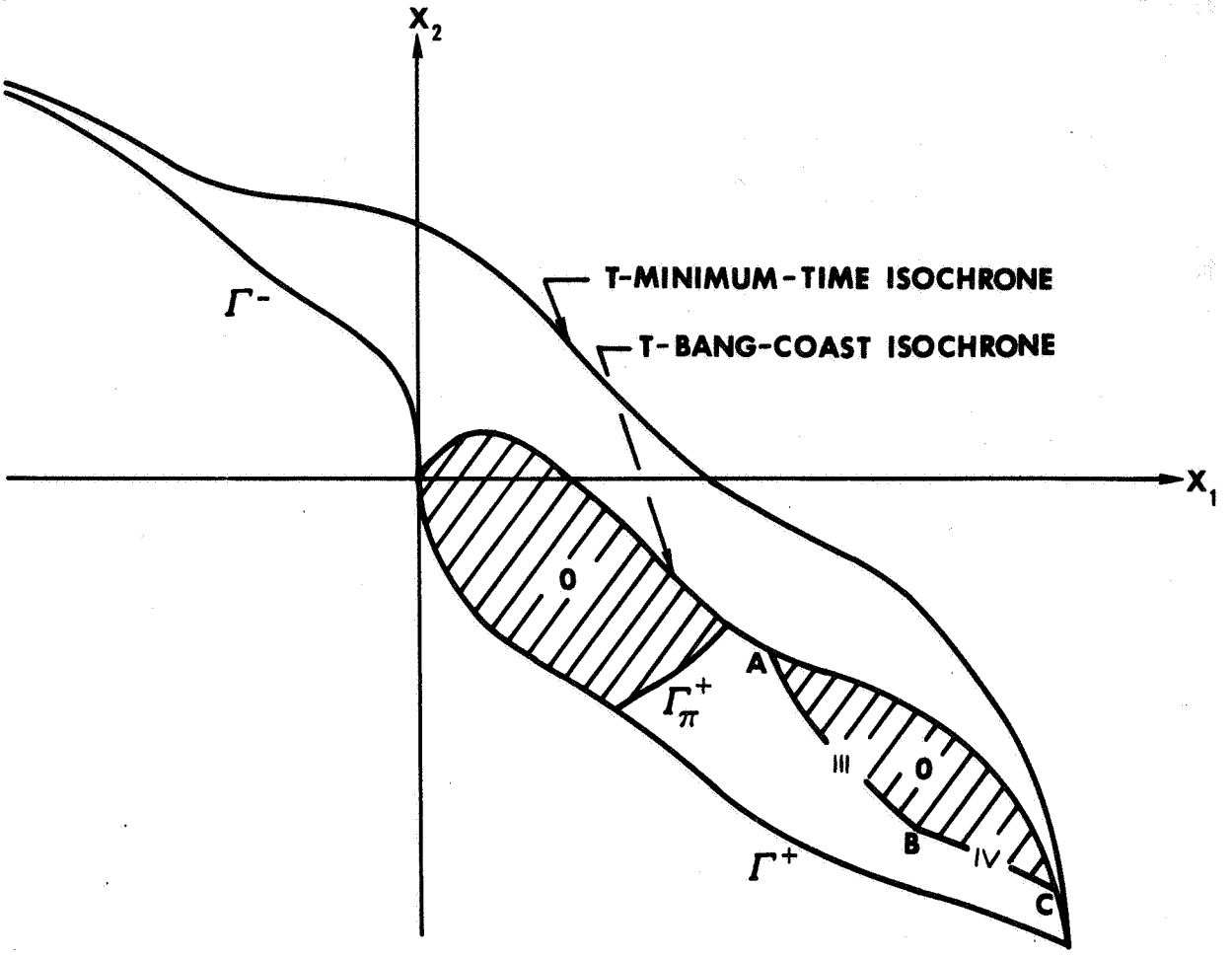

Fig. 4-1. Emergence of T-Fourth-Switch Isochrone. Shaded regions have optimal control $u = \pm 0$. The T-Third-Switch Isochrone no longer extends to Γ^+.

pseudoextremals. See Fig. 4-2. The boundaries of this region are labeled $L_{4\to 2}$ and L_{32} for reasons yet to be developed.

The notation L_{ij} $(i=j+1)$ designates the locus of phase points (x_1,x_2) where for some P-0-P pseudoextremal the i-th and j-th switchings coincide. The integer i represents the highest numbered switching under consideration. At L_{ij} the adjoint λ_2 equals the switching value +1 and is in addition at a relative minimum or maximum. Since the adjoint λ_2 fails to cross the switch line $\lambda_2 = 1$ at a point on L_{ij}, the i-th and j-th switchings do not occur in the limit. In any neighborhood of L_{ij} the i-th and j-th switchings are present.

The notation $L_{i\to j}$ $(i=j+2)$ designate the locus of points (x_1,x_2) in state space for which an i-th switch P-0-P-... pseudoextremal degenerates into a j-th switch P-0-P type pseudoextremal. At $L_{i\to j}$ the adjoint λ_2 again equals the switching value +1, but λ_2 is no longer at a relative maximum or minimum on $L_{i\to j}$. Instead a relative maximum or minimum with $\lambda_2 = 1$ occurred prior to the j-th switching and eliminated two switchings as in Fig. 4-3.

The behavior of the adjoint $\hat{\lambda}_2$ corresponding to a P-0-P pseudoextremal with second switching on the boundary $L_{4\to 2}$ is given in Fig. 4-3. The adjoint $\hat{\lambda}_2$ is really a limiting case of that λ_2 behavior shown in dashed lines. The point of tangency T corresponds to either two switchings or in the limit zero switchings. At R then in the limiting case a four switch P-0-P-0-P pseudoextremal degenerates into a two switch P-0-P pseudoextremal. The locus of all such points where the second and fourth switchings coincide we designate $L_{4\to 2}$ in accordance with our previous notation.

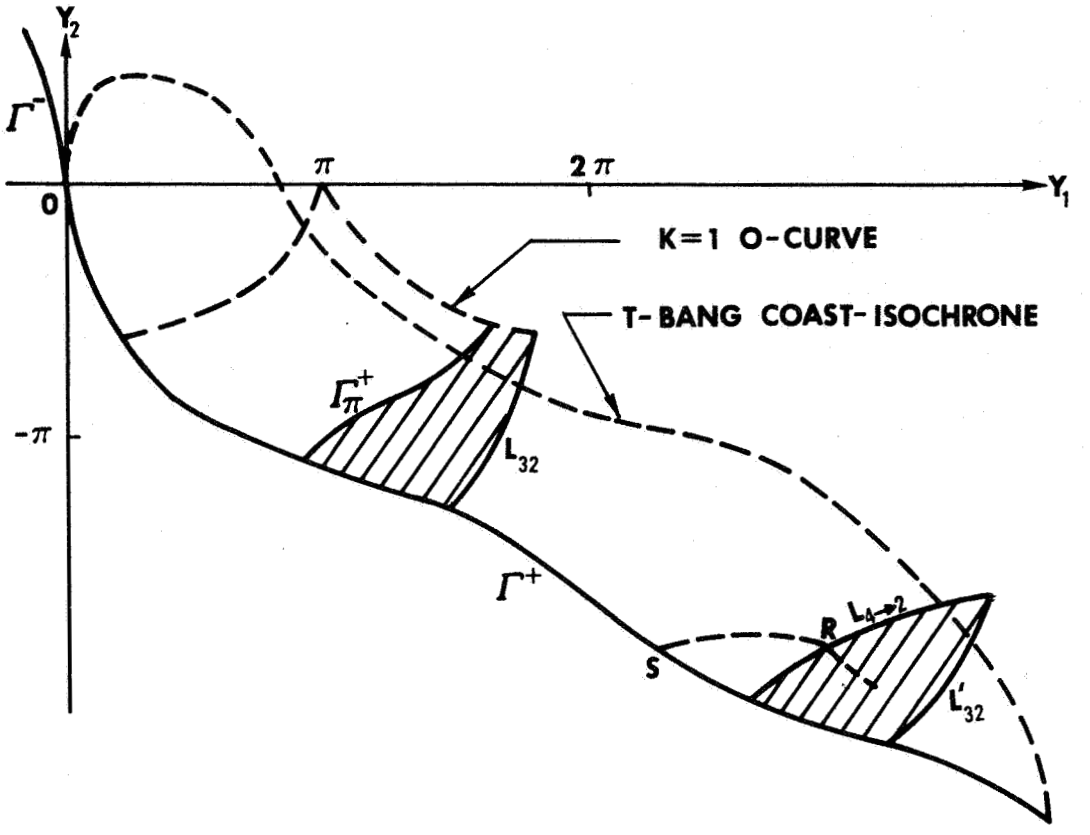

Fig. 4-2. Upper and Lower Regions of Second Switchings of a P-0-P Pseudoextremal. The boundaries of these 0-P corner regions are time invariant.

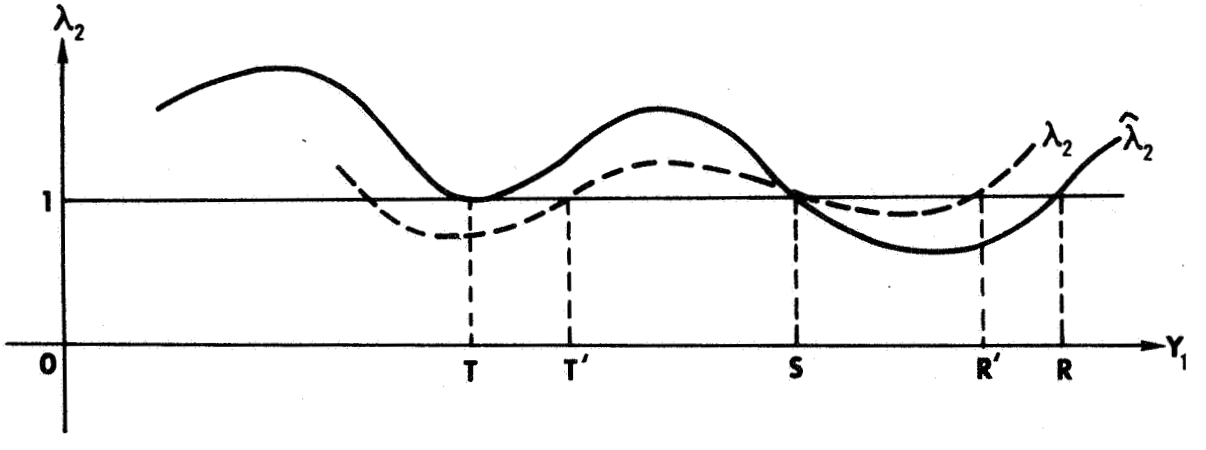

Fig. 4-3. Adjoint $\hat{\lambda}_2$ Generating a Second Switching R at the $L_{4\to 2}$ Boundary. The corresponding trajectory is given in Fig. 4-4.

That the line $L_{4\to 2}$ must be the boundary of our second switch region is deduced by the following argument. Suppose a second switching R' could occur along the path OSR of Fig. 4-2 for R' < R. Then the adjoint λ_2 generating such a switching would have to be as shown in Fig. 4-3. It could not cross the $\hat{\lambda}_2$ curve between T and S by reasoning analogous to the proof of theorem 3-3. Consequently an earlier switching from 0 to +A would have occurred contradicting the assumption that R' is the first 0-P corner.

The furthermost boundary L'_{32} of this lower first 0-P corner region is the locus of those points for which the second and third switchings coincide. The prime distinguishes this curve from the previous L_{32} boundary of the upper first 0-P corner region. Just as the line L_{32} was a boundary beyond which the second switching R (first 0-P corner) could not occur for $x_1 \leq 3\pi$ (see 3-130), the line L'_{32} is a boundary beyond which the first 0-P corner can not occur for $x_1 \leq 5\pi$. The verification proceeds identically as that in the earlier result. The adjoint λ_2 generating such a P-0-P pseudoextremal in which the second and third switchings coincide is shown in Fig. 4-4.

The method used to generate the $L_{4\to 2}$ line on the computer is suggested by Fig. 4-3. We integrate the backward time system equations (2-2) and adjoint equations (2-7) using control law (2-5) from some particular initial conditions until an 0-P corner occurs. The initial conditions are suggested by (3-71) and Fig. 4-3; namely,

$$\pi \leq y_{10} \leq 3\pi/2 \tag{4-2}$$

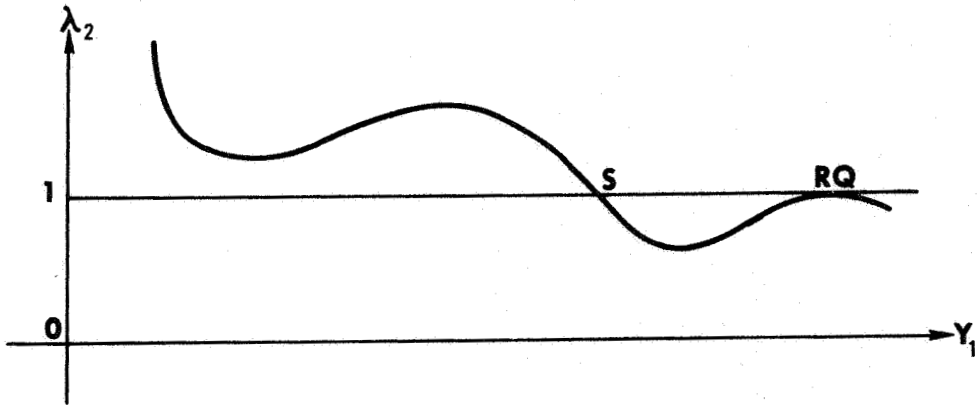

Fig. 4-4. Adjoint λ_2 Generating a Second Switching R at the L_{32} Boundary of the Lower First O-P Corner Region.

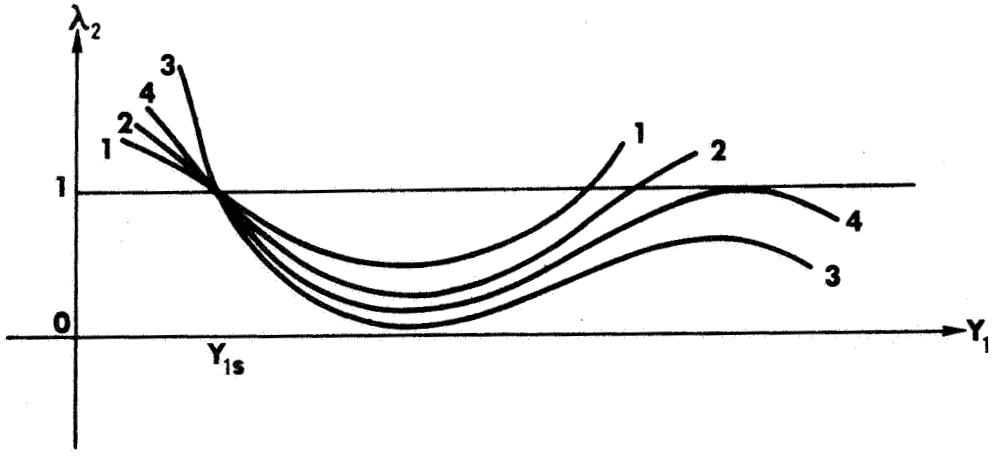

Fig. 4-5. Procedure for Adjusting λ_{1s} to Generate the Curve L_{32}.

$$y_{20} = -(\cos y_{10} - 1 + A y_{10})^{1/2} \tag{4-3}$$

$$\lambda_{20} = 1 \tag{4-4}$$

$$\lambda_{10} = 0 \tag{4-5}$$

The far boundary L'_{32} is generated by integration of the system and adjoint equations from the initial conditions as given on the switching from the zero trajectory Γ^+ i.e., at S. Thus

$$y_{2s} = -(\cos y_{1s} - 1 + A y_{1s})^{1/2} \tag{4-6}$$

$$\lambda_{2s} = 1 \tag{4-7}$$

$$\lambda_{1s} = \text{negative constant to be adjusted} \tag{4-8}$$

$$y_{1s_o} \leq y_{1s} \leq 3\pi + \pi/2 \tag{4-9}$$

where y_{1s_o} is the smallest value of y_{1s} for which a second switching (0-P corner) occurred in the previous scheme for generating $L_{4\to 2}$. The scheme for obtaining L'_{32} then is to be given an arbitrary switch point S, and to integrate along the 0-arc until an 0-P corner occurs. After the 0-P corner is found, λ_{1s} is reset so that

$$\lambda_{1s}(\text{new}) < \lambda_{1s}(\text{old}) \tag{4-10}$$

and we integrate again until either λ_2 exceeds one or a relative

maximum occurs. If the condition

$$\lambda_2 > 1 \tag{4-11}$$

occurs first, we continue the scheme. If a relative maximum occurs first, we back up and readjust λ_{1s} to converge on the limiting case. The procedure is illustrated by Fig. 4-5. Referring to Fig. 4-6 we have already seen that the point A moves with the shrinking T-bang-coast isochrone along L_{32} as the time-to-go becomes less. Likewise the point C of Fig. 4-6 designating the intersection of the T-bang-coast and T-fourth switch isochrones must represent the degeneration of a four switch pseudoextremal into a two switch pseudoextremal. Such points as C must belong to $L_{4\to 2}$. As the time-to-go decreases, the point C moves along $L_{4\to 2}$ toward Γ^+ with the shrinking bang-coast isochrone as seen in Fig. 4-6.

The point B designating the junction of the T-third and T-fourth switching isochrones similarly follows the curve L_{43} down to the zero trajectory Γ^+ as the time-to-go decreases. The adjoint behavior corresponding to the coincidence of the third and fourth switchings is given in Fig. 4-7. From chapter III, for T sufficiently small the T-third switching locus rejoins the zero trajectory Γ^+ and there can be no fourth switching, i.e., the T-fourth switching isochrone disappears. Thus when B reaches Γ^+, C simultaneously reaches Γ^+ and is coincident with B in order that the T-fourth switching isochrone vanish. Therefore the curves L_{43} and $L_{4\to 2}$ intersect the zero trajectory at a common point G as shown in Fig. 4-6.

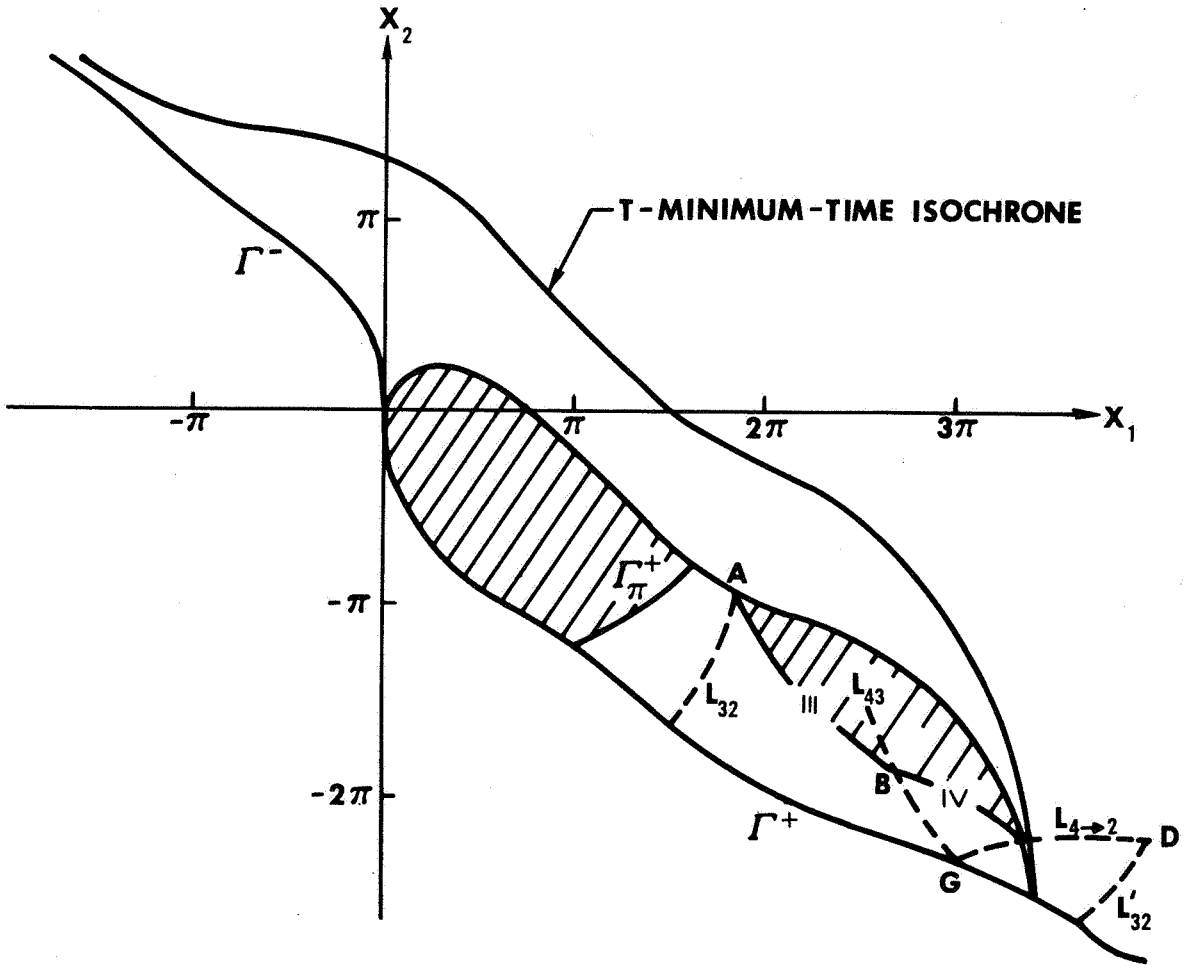

Fig. 4-6. Fixed Lines L_{43} and $L_{4\to 2}$ – the Paths Traced by the Endpoints to the T-Fourth Switch Isochrone as the Time-to-go Decreases. The shaded regions have optimal control u = 0. Lines L_{43} and $L_{4\to 2}$ meet at G on Γ^+.

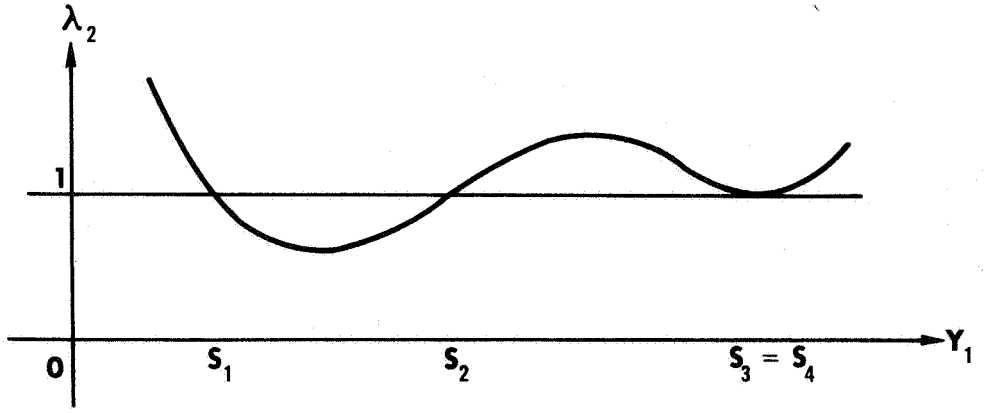

Fig. 4-7. Adjoint Behavior Generating a Point on the L_{43} Curve for which the Third and Fourth Switchings Coincide.

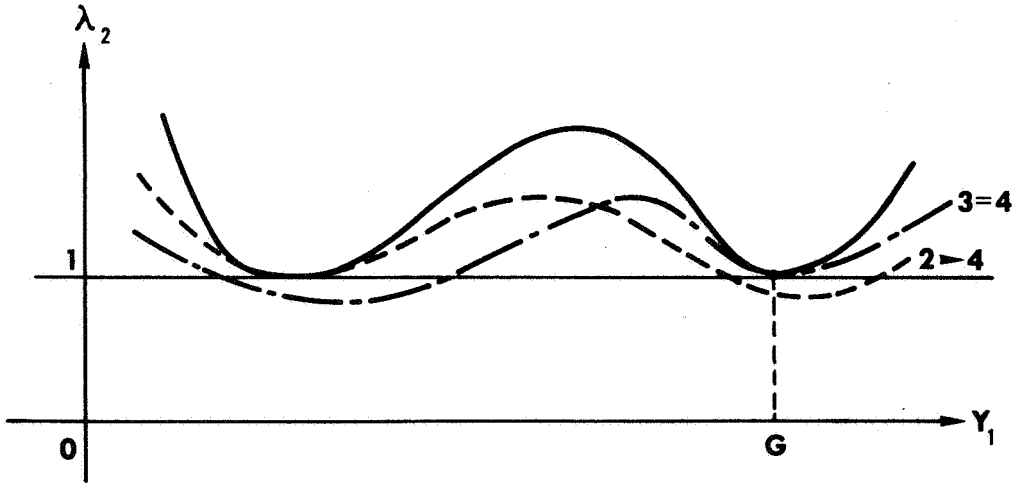

Fig. 4-8. Special Adjoint Solution Corresponding to an O-P Corner at the Point G. Four switchings degenerate into two via the first tangency; the four switching coincides with the third at the second tangency.

At this special point not only must the third switching be coincident with the second (L_{32}) but also four switchings must degenerate to two ($L_{4\to 2}$). The special adjoint solution corresponding to this behavior is given by Fig. 4-8.

We now illustrate a typical P-0-P-0-P trajectory resulting from our extended region of control by Figs. 4-9a,b,c. Only a state initially within the $u(t) = +A$ region, i.e., the unshaded region within the T-bang-coast isochrone of Fig. 4-9a may experience four switchings. Such a state X continues on a P-arc until meeting the oncoming T-fourth-switch isochrone at which point a P-0 corner occurs. The state now is within the $u = 0$ control region and continues with control zero until reaching the boundary of the shrinking T-third-switch isochrone. The state then reenters the $u = +A$ region and continues on a P-arc until it intersects the shrinking T-bang-coast isochrone at which time control switches to zero and the state rides the shrinking bang-coast isochrone to the origin. The final portions of the trajectory as well as the behavior of the control regions during these portions were previously illustrated in Fig. 3-25.

If we now relax T_f still further so that now the T_f- controllable region includes the point of intersection of the line L'_{32} and zero trajectory Γ^+, a third $u = 0$ control region emerges as shown in Fig. 4-10a. Now the time is sufficiently long for the lower P-0-P trajectories — those having 0-P corners in the lower 0-P corner region — to have a third switching. Using a prime to distinguish these third switchings from those of the upper region we have:

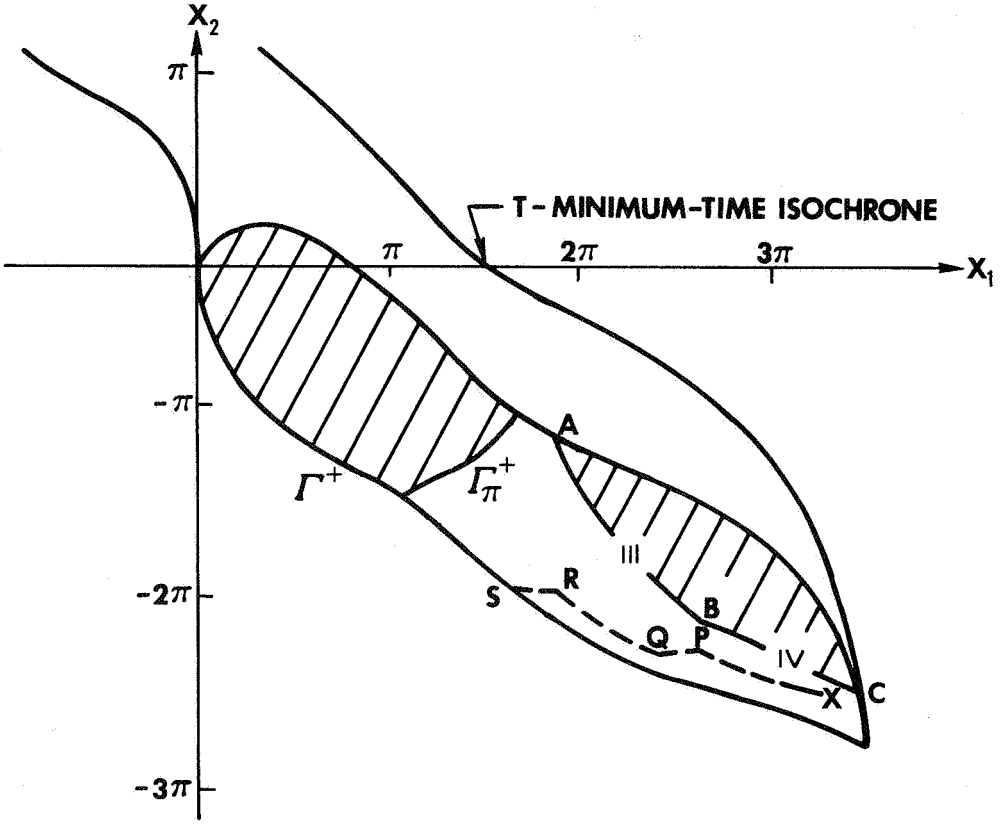

Fig. 4-9a. Four Switch P-O-P-O-P Trajectory of Optimal Control Law 4-1. Dashed path is yet to be traversed whereas solid path is that already traversed.

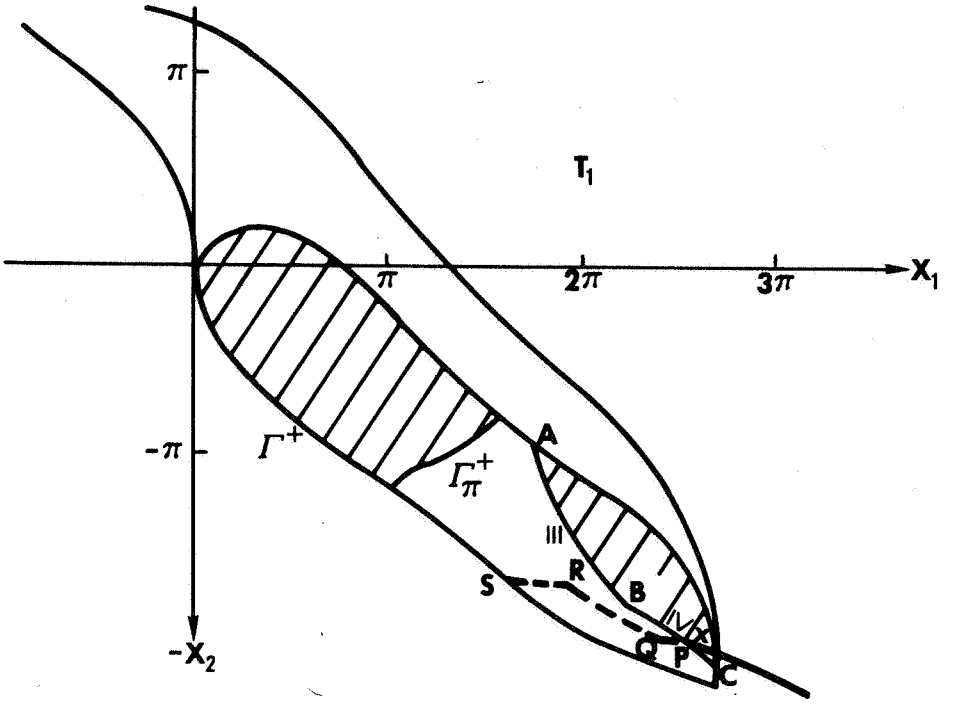

Fig. 4-9b. State X collides with oncoming T-fourth-switch isochrone (IV) at P and control switches to zero.

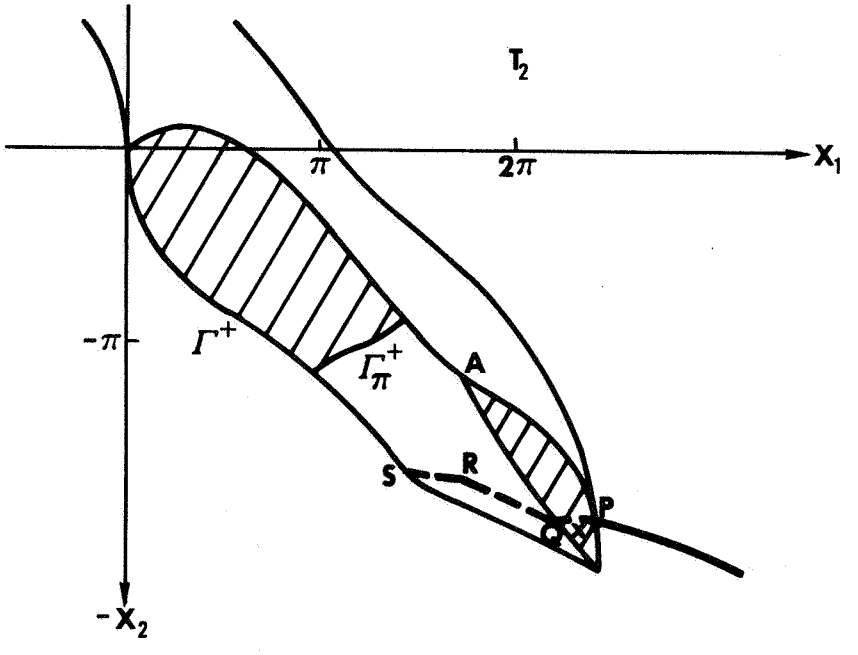

Fig. 4-9c. State X is coasting within the region of optimal control law 3-2.

OPTIMAL CONTROL LAW 4-2. Any state $(x_1(t),x_2(t))$ residing at time-to-go T within the region bounded by the T-third-switch isochrone and the T-bang-coast isochrone has optimal control $u(t) = 0$.

The optimal trajectory for a state X belonging to this region at time-to-go T is illustrated by Figs. 4-10a,b,c. State X proceeds along an 0-arc until catching the shrinking T-third-switching boundary at time T_1. The control then switches to +A. The state continues along a P-arc until it collides with the shrinking bang-coast isochrone at time T_2 at which time the control switches to zero. Thereafter the state merely rides the shrinking isochrone to the region.

THE OCCURRENCE OF THE FIFTH SWITCHING

In order that a switching occur at the point D, where the fixed lines L'_{32} and $L_{4\to 2}$ intersect, the second, third, and fourth switchings of a P-0-P type pseudoextremal must simultaneously occur. (See Figs. 4-6, 4-10a.) As the fourth, third, and second switching points of nearby P-0-P type pseudoextremals approach D, the associated P-0-P-0-P, P-0-P-0, and P-0-P pseudoextremals degenenate to a P-0 pseudoextremal. The adjoint behavior generating such a degenerate pseudoextremal is given in Fig. 4-11.

In addition to the lines L_{32} and $L_{4\to 2}$ radiating from the point D, the analagous lines $L_{5\to 3}$ and L_{54} also emanate from that point. The line $L_{5\to 3}$, representing the locus of those switch points for which a P-0-P-0-P-0 or five switch trajectory degenerates into a P-0-P-0 or three switch trajectory, is shown in Fig. 4-14. The line

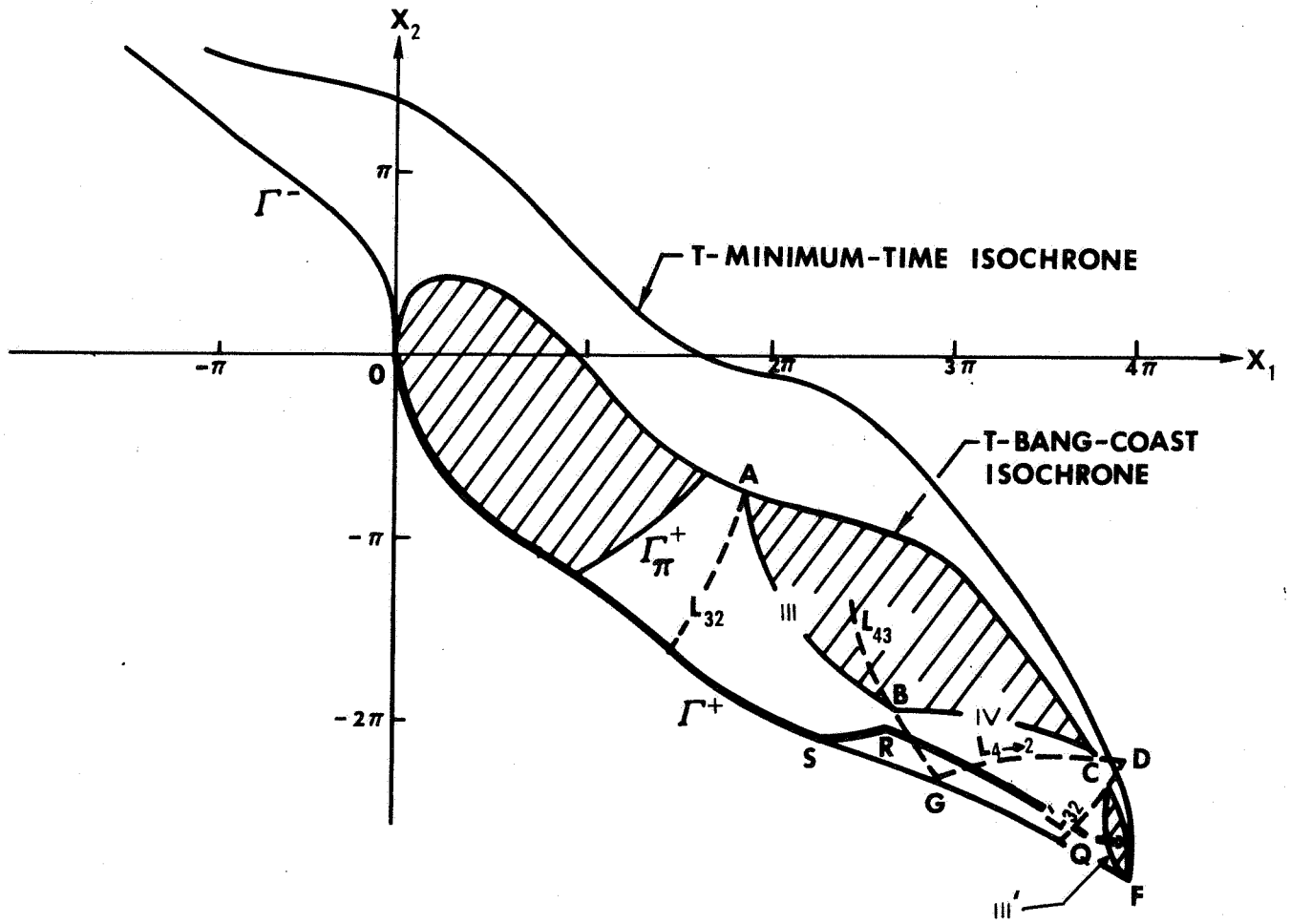

Fig. 4-10a. Emergence of a Disjoined u = 0 Control Region Bounded by the T-Bang-Coast Isochrone and T-Third-Switch Isochrone (III'). State X follows the P-0-P-0 trajectories 0SRQX to the origin. All shaded areas have optimal control u(t) = 0.

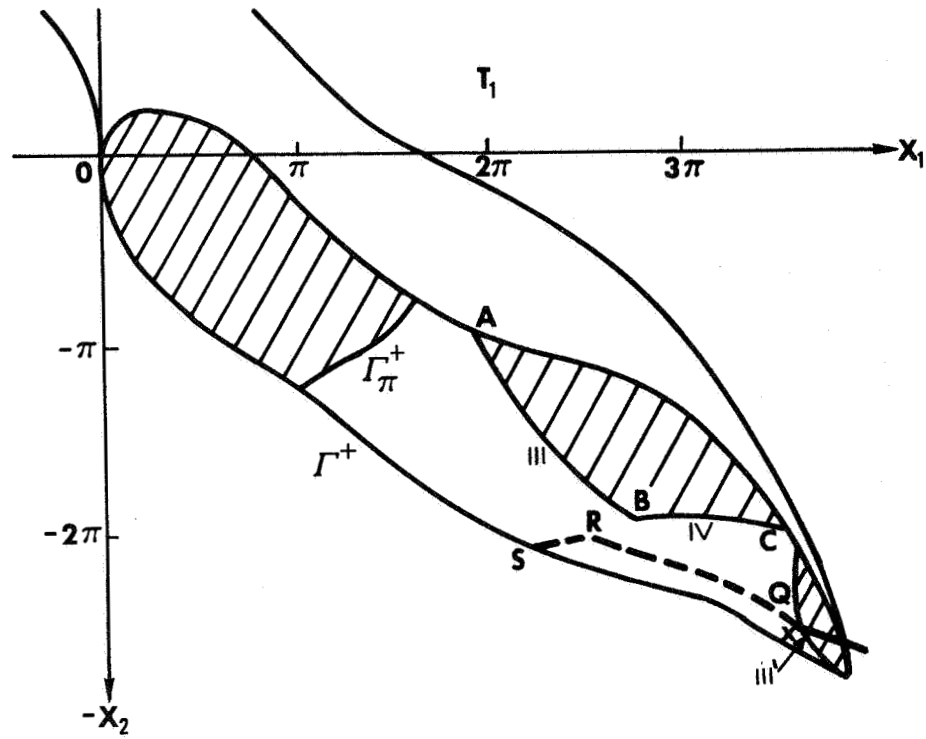

Fig. 4-10b. At time-to-go T_1 state X catches the shrinking T_1-third-switching isochrone (III') and control switches to +A.

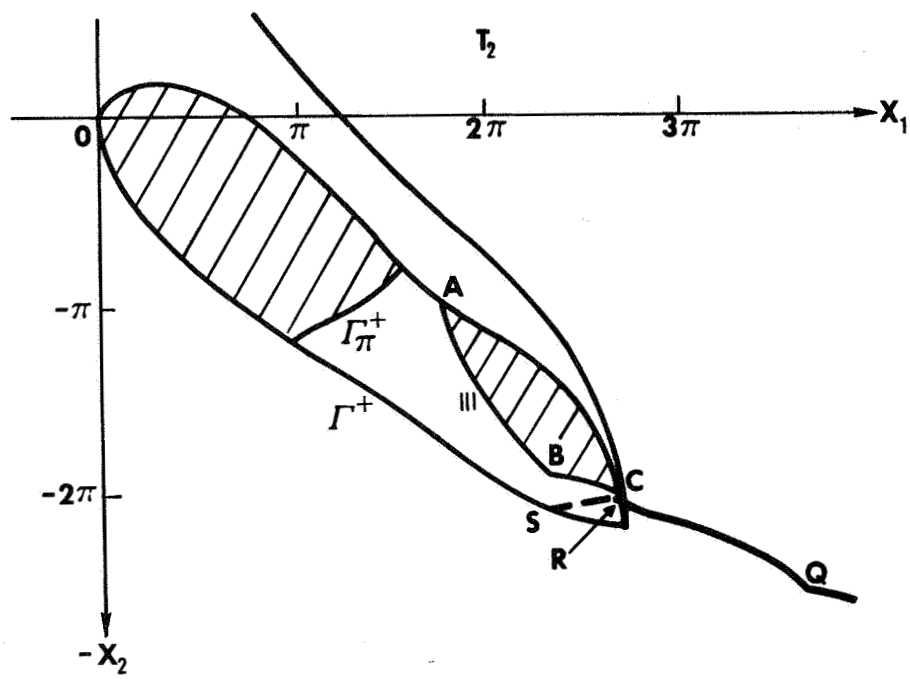

Fig. 4-10c. State X collides with shrinking bang-coast isochrone at R at time-to-go T_2 and thereafter 'rides' that shrinking isochrone to the origin.

$L_{5\to 3}$ is generated by merely extending the pseudoextremals generating $L_{4\to 2}$ up to the next switching point. The corresponding limiting adjoint λ_2 is shown in Fig. 4-12. As the relative maximum of λ_2 (M_1 in Fig. 4-12) approaches the value $\lambda_2 = 1$, the corresponding switching points of L_{54} approach D. On L_{54} (Fig. 4-14) where the fourth and fifth switch points coincide, the adjoint λ_2 behaves as in Fig. 4-13. As the relative minimum of λ_2 (M_2 in Fig. 4-13) approaches the value $\lambda_2 = 1$, the locus L_{54} approaches the point D. Then in an arbitrarily small neighborhood of D there are switchpoints representing a second, third, fourth, or even fifth switching for some pseudoextremals consisting of alternating P and 0-arcs.

From Fig. 4-11 the point D corresponds to the second relative maximum of λ_2. Reasoning as in lemma 3-3 yields the result that the x_1 coordinate of the point D-x_{1D} satisfies

$$3\pi + \pi/2 < x_{1D} < 4\pi \qquad (4\text{-}12)$$

It is only when the time-to-go T becomes so large that the point D belongs to the region bounded by the T-bang-coast isochrone and zero trajectory that a fifth switching occurs. In such a case the lower two $u = 0$ control regions rejoin to form a single region bounded by the T-bang-coast, T-third switch, T-fourth switch, T-fifth switch, and T-third' switch isochrones as shown in Fig. 4-14. For this region we have:

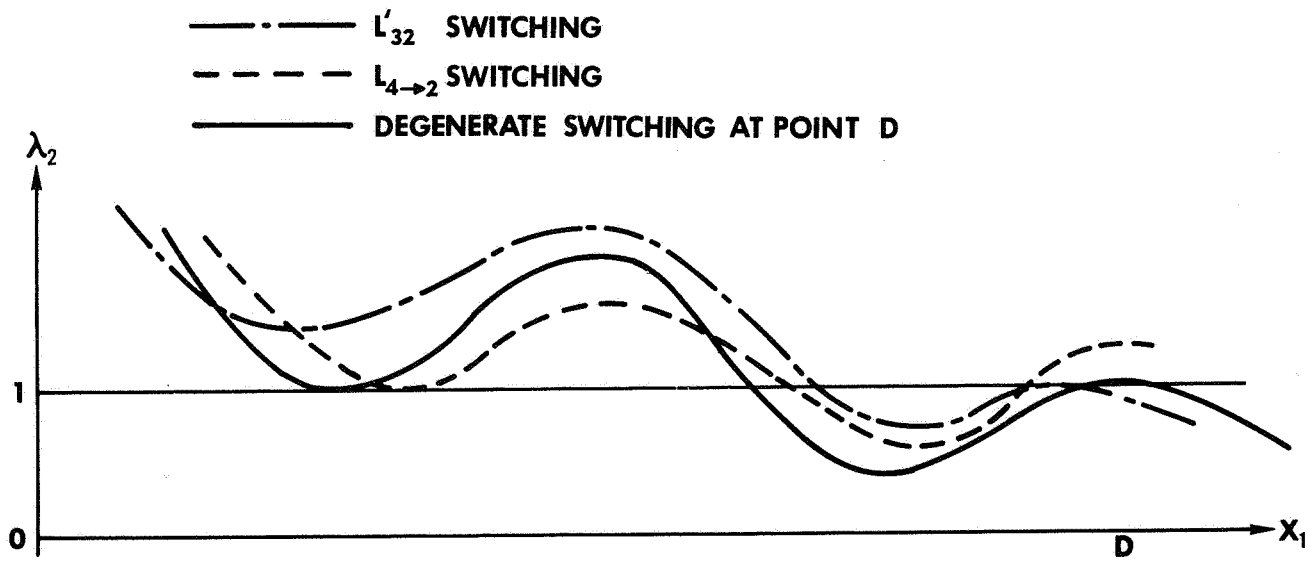

Fig. 4-11. Limiting Adjoint Behavior Corresponding to the Switching Point D - the Intersection of the Fixed Lines L'_{32} and $L_{4\to 2}$.

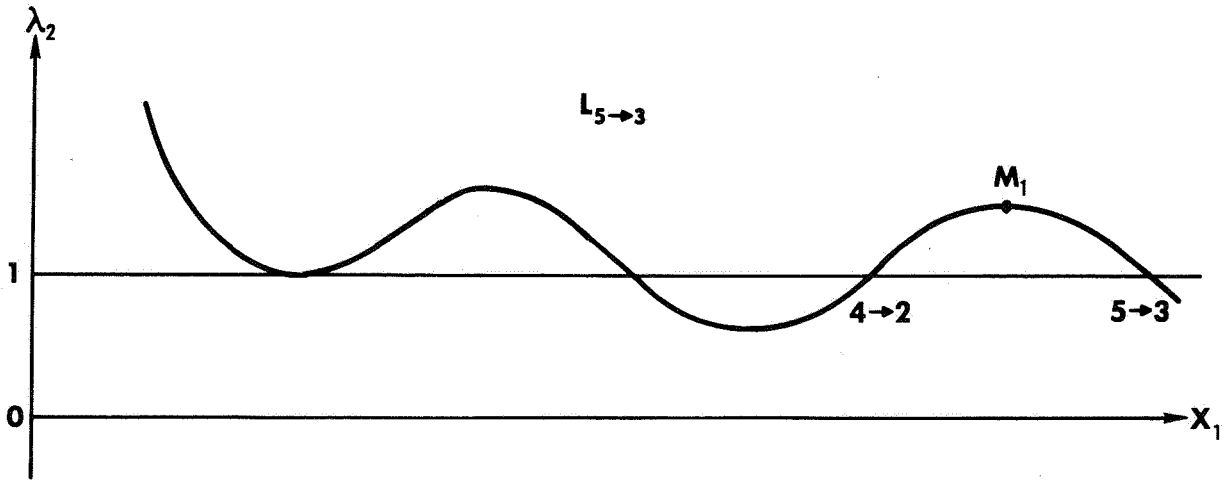

Fig. 4-12. Adjoint Behavior for Five Switchings Degenerating into Three Switchings on the Fixed Line $L_{5\to3}$.

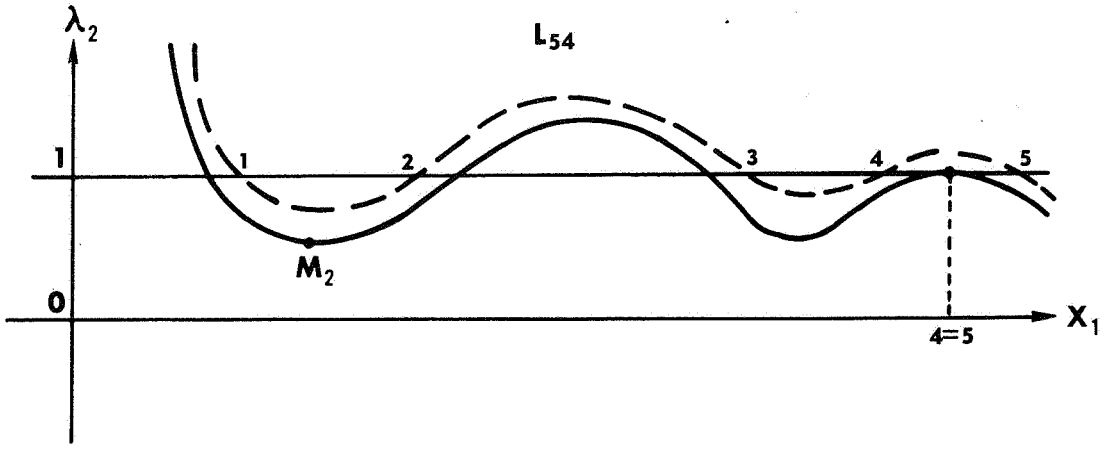

Fig. 4-13. Adjoint Behavior for Coincidence of the Fourth and Fifth and Fifth Switchings on the Fixed Line L_{54}.

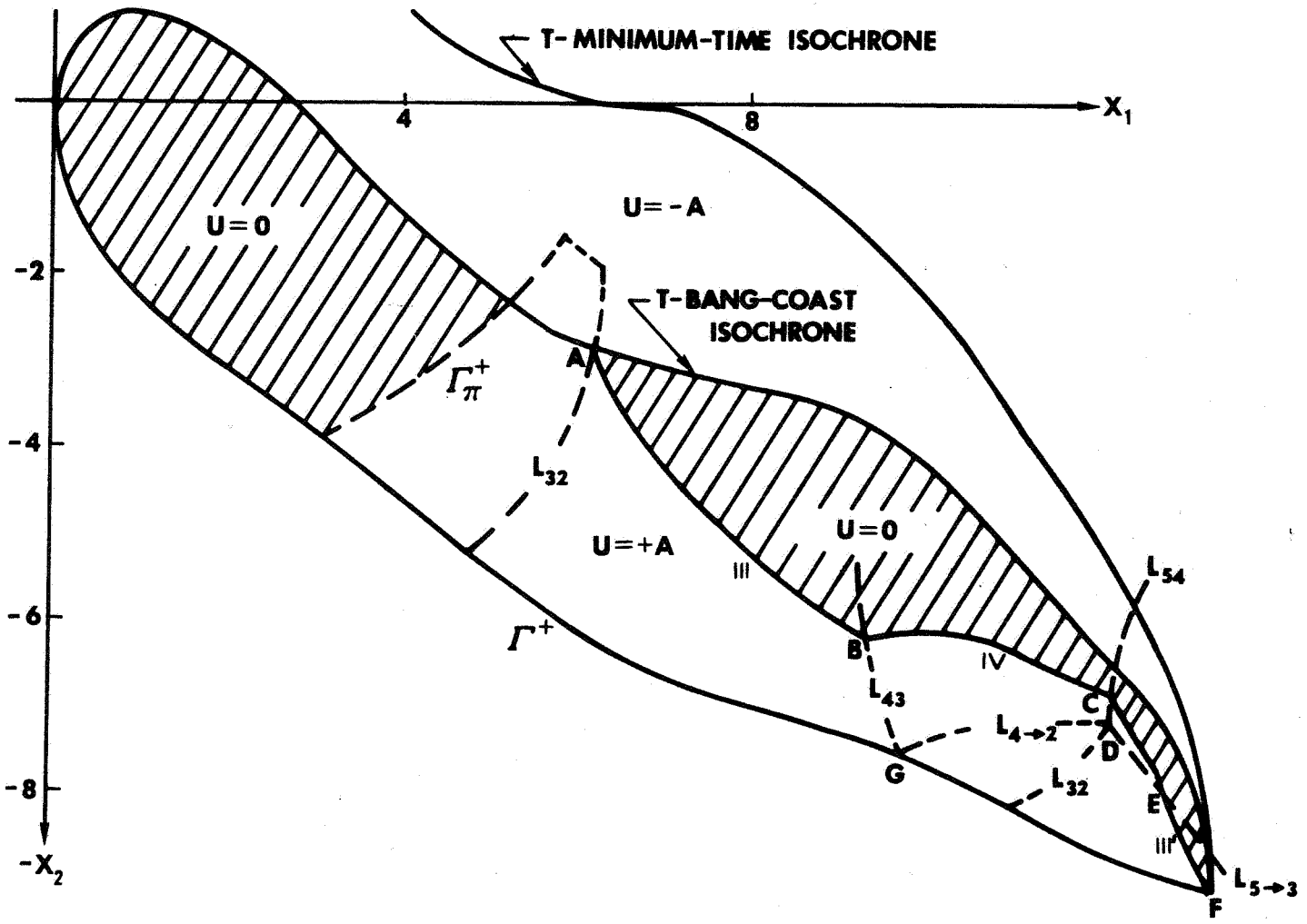

Fig. 4-14. Reunion of the Lower u = 0 Control Regions and Optimal Control Law 4-3. When the T-bang-coast isochrone is beyond the point D, a fifth switching may occur; the T-fifth-switch isochrone is now a boundary of the control region.

OPTIMAL CONTROL LAW 4-3. Any state $(x_1(t),x_2(t))$ belonging at time-to-go T to the region bounded by the T-bang-coast, T-third switch, T-fourth switch, T-fifth switch, and T-third' switch isochrones has optimal control $u(x_1(t),x_2(t)) = 0$.

States initially belonging to this region have as optimal paths either a three switch P-0-P-0 trajectory or a five switch P-0-P-0-P-0 trajectory. Any state within this region moves along an 0-arc until reaching the time dependent boundary of the region at which time a switching occurs. Those states which meet the third switch isochrone boundary (arcs AB and EF of Fig. 4-15) will be zeroed by a P-0-P-0 path. Crossing this boundary the control switches to +A and the phase point continues along a P-arc until meeting the shrinking T-bang-coast isochrone. Thereafter the phase point coasts along an 0-arc over to Γ^+ and follows that P-curve to the origin. The upper trajectory of Fig. 4-15 illustrates the case where the phase point intersects the boundary at the T-fifth switch isochrone. The state then moves along a P-arc until meeting the oncoming T-fourth switch isochrone at which time it re-enters the $u = 0$ control region. By now the lower $u = 0$ control region of Fig. 4-15 has shrunk considerably and possibly split into two regions as in Fig. 4-10a depending upon the time remaining. The phase point then continues along an 0-curve until catching the moving third-switch isochrone boundary. The motion thereafter has already been described by Fig. 3-25.

No state belonging to the region of control law 4-3 can intersect the boundary of this region at the fourth switch isochrone. The fourth-

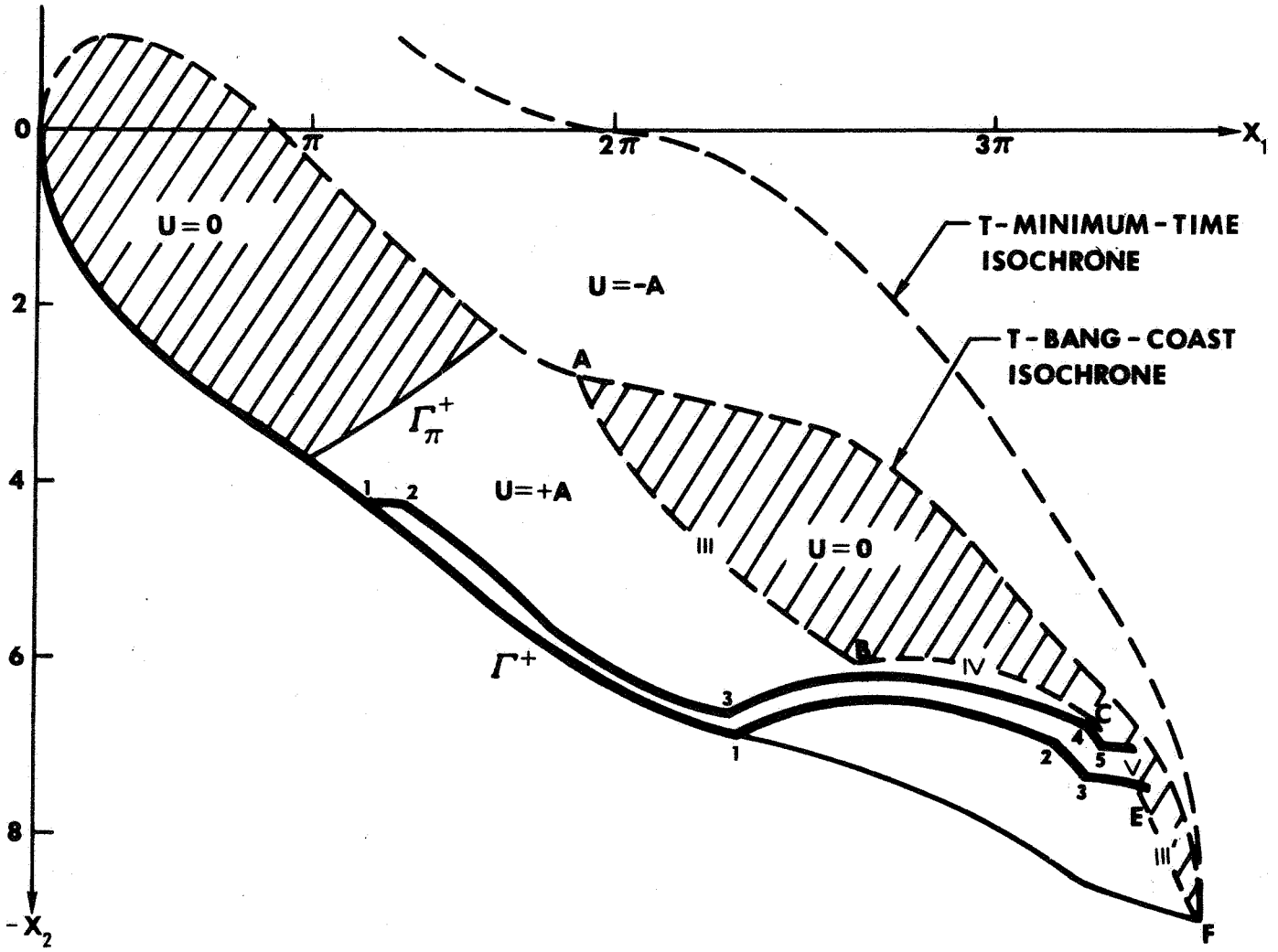

Fig. 4-15. Optimal P-0-P and P-0-P-0-P Trajectories Associated with Optimal Control Law 4-3. Initial states nearest D have five switch trajectories. Nearby three switch trajectories are optimal.

switch isochrone is moving to the left faster than the phase point is moving along the 0-arc.

Extending the result of lemma 3-3 we find that at most five switchings may occur in a P-0-P type pseudoextremal whenever x_1 is restricted to the cylinder

$$-5\pi \leq x_1 \leq 5\pi \tag{4-13}$$

If we adhere to the maximum time restriction

$$T < \frac{\pi}{2} + \text{arcsinh } 1 \tag{4-14}$$

we have completely characterized the fuel optimal, time varying feedback control law provided that the T-controllable region satisfies (4-13). Moreover the T-controllable region may now satisfy restrictions (4-13) and (4-14) and still include the phase point $(2\pi,0)$. To do this would require the control magnitude A to be sufficiently large so that

$$2\int_0^{\pi} \frac{d\sigma}{|x_2(\sigma)|} = 2\int_0^{\pi} \frac{d\sigma}{[2(\cos\sigma-1)+2A\sigma]^{1/2}} \leq \frac{\pi}{2} + \text{arcsinh } 1 \tag{4-15}$$

or evaluating numerically condition (4-15)

$$A \geq 4.57 \tag{4-16}$$

Rather than insist that A be at least 4.57 times the maximum gravitational torque, we shall replace (4-14) by

$$T \leq \pi \tag{4-17}$$

in order that even smaller control torques will be sufficient to guarantee that the phase point $(2\pi,0)$ belong to the T-controllable region. Our characterization of the fuel optimal feedback control law is now complete provided Optimal Control law 3-1 continues to hold for all T satisfying (4-17). All indications tend to substantiate the claim that indeed Optimal Control law 3-1 remains valid for such T.

Instead of driving the state to the origin $(0,0)$, we now seek the optimal control law for driving the state to $(4\pi,0)$ with minimum fuel expenditure. Because both the state and adjoint variables are governed by differential equations (1-3) and (1-15) that are invariant under the translation

$$\hat{x}_1 = x_1 + 4k\pi \qquad k \text{ integer} \tag{4-18}$$

or in backward time formulation

$$\hat{y}_1 = y_1 + 4k\pi \tag{4-19}$$

the fuel optimal switching surface for driving the state to $(4k\pi,0)$ is just the switching surface already derived translated $4k\pi$ units in the $x_1(y_1)$ direction. Inasmuch as the state $(2\pi,0)$ is within the T-controllable region centered about $(0,0)$, the T-controllable region centered about $(4\pi,0)$ will overlap that centered about $(0,0)$ to form a simply connected region. The union of all such T-controllable regions will contain no holes of uncontrollable states; the feedback

control law is given for all values of the pitch coordinate. The only restriction is that the pitch velocity x_2 must lie within the envelope of these T-controllable regions.

From equation (1-10) the pitch error rate satisfies

$$\dot{\theta} = \frac{\sqrt{-3K_3}}{2} \Omega x_2 \tag{4-20}$$

where K_3 is an inertial parameter of the satellite and Ω the orbital angular velocity. From Fig. 4-16, for the control magnitude $A = +3$ and time of mission π, any state having velocity x_2 less than approximately π can always be controlled. Our control law can zero any actual pitch error rate $\dot{\theta}$

$$\dot{\theta} \leq \frac{\sqrt{-3K_3}}{2} \Omega\pi \tag{4-21}$$

within normalized time $T = \pi$ or real time t_f

$$t_f = \frac{\pi}{\sqrt{-3K_3}\Omega} \tag{4-22}$$

for the parameter $A = +3$. By increasing the magnitude of control torque A even greater error rates could always be zeroed while realigning the earth-pointing satellite within the same fixed time t_f.

Just as in equation (3-14) we may introduce a minimum cost function

$$V_k(x_1,x_2,T) = \min_{u \epsilon \bar{u}_k} \left\{ \int_0^T |u(t)|\,dt \right\} \tag{4-23}$$

where $\bar{u}_k$ is the set of all admissible controls which transfer the state from (x_1,x_2) to $(4k\pi,0)$ within time T. As before, k is

an integer. Such a function is certainly continuous in all its arguments. One would therefore expect that time dependent curves partition the state space into segments within which it is more economical to drive the state to the included point $(4k\pi,0)$ than any other such multiple of 4π. Such curves are defined by the following:

DEFINITION 4-1. The $T^{\underline{k}}$ indifference curve is the set of all states (x_1,x_2) such that

$$v_k(x_1,x_2,T) = v_{k+1}(x_1,x_2,T) \tag{4-24}$$

Any state lying on such a curve may be driven to $(4k\pi,0)$ or $(4(k+1)\pi,0)$ with equal fuel economy. Such indifference curves are shown in Figs. 4-16, 4-17, and 4-18 displaying the complete feedback optimal control law for the actual earth-pointing satellite problem. From symmetry arguments the point $(4k\pi+2\pi,0)$ will always belong to such a curve provided T is sufficiently large to allow such a point to be controlled. As the time-to-go becomes less each such indifference curve splits into two segments due to the enlargening hole developing in the T-controllable region. These two curves gradually shrink and finally vanish when the time T is so short that the T-controllable regions centered along the x_1 axis at multiples of $4k\pi$ no longer overlap as in Fig. 4-18.

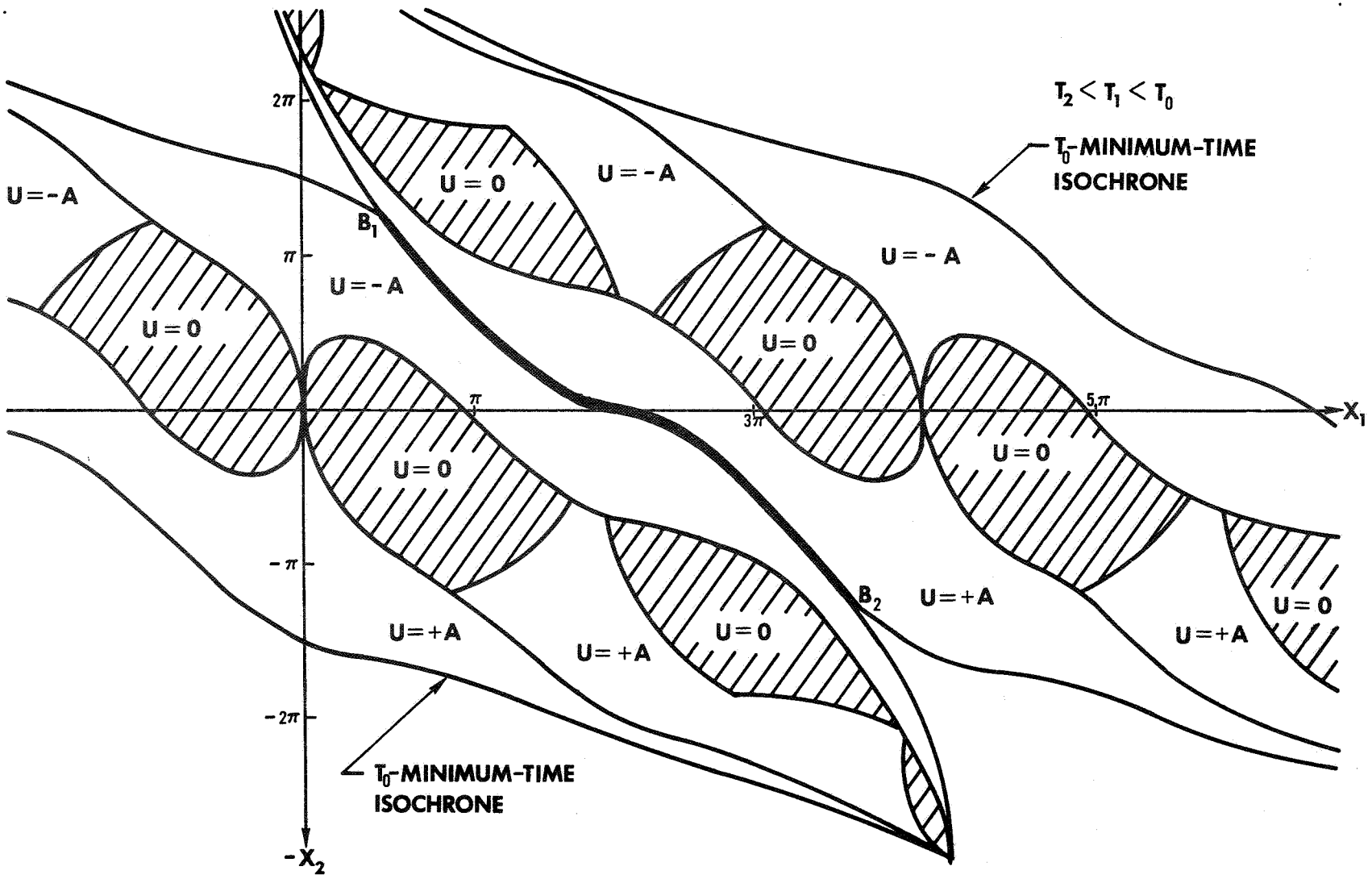

Fig. 4-16. T^k-Indifference Curve (B_1B_2) as A Continuous Curve.

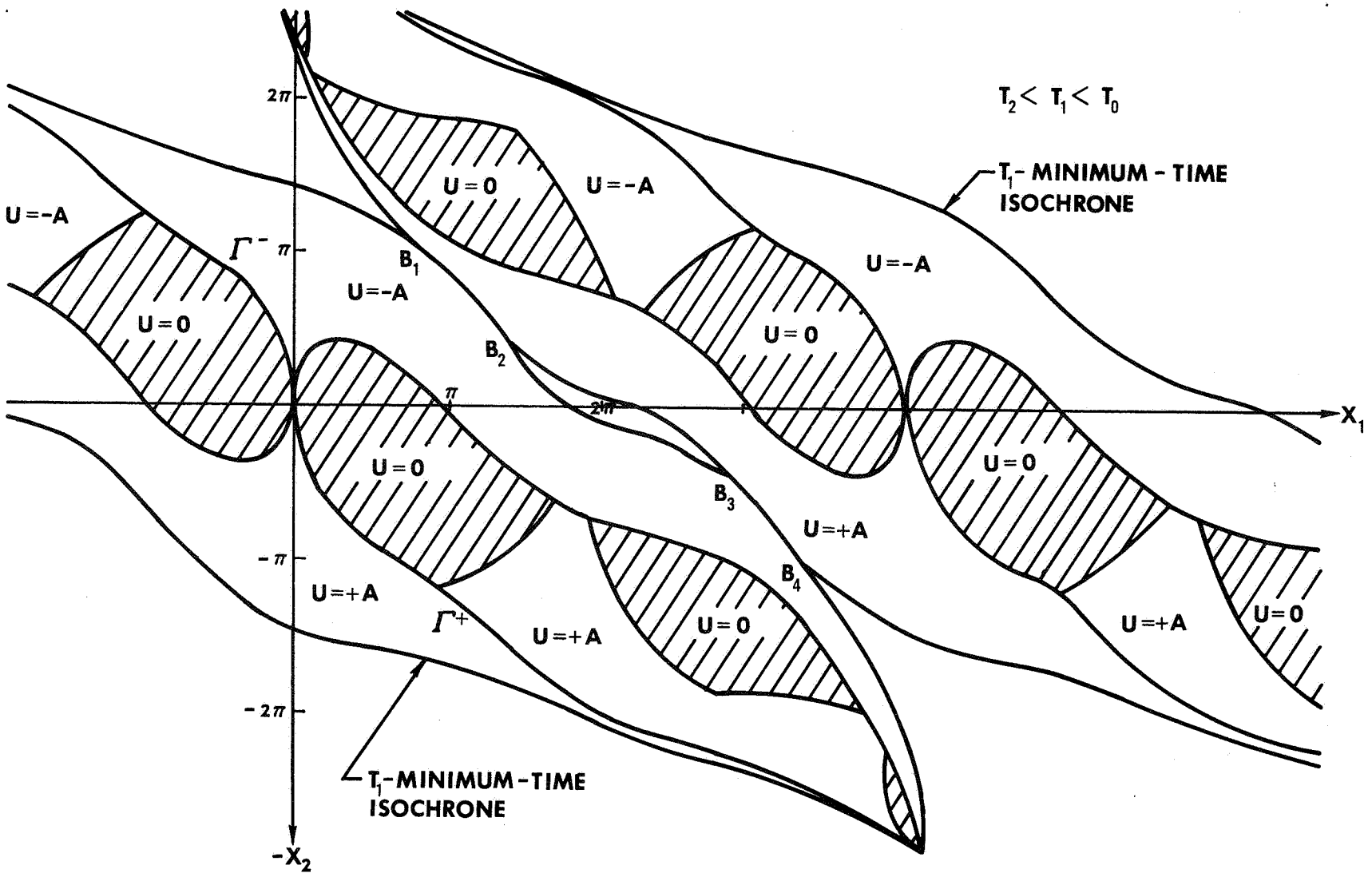

Fig. 4-17. Splitting of T^k-Indifference Curve into Two Arcs (B_1B_2,B_3B_4).

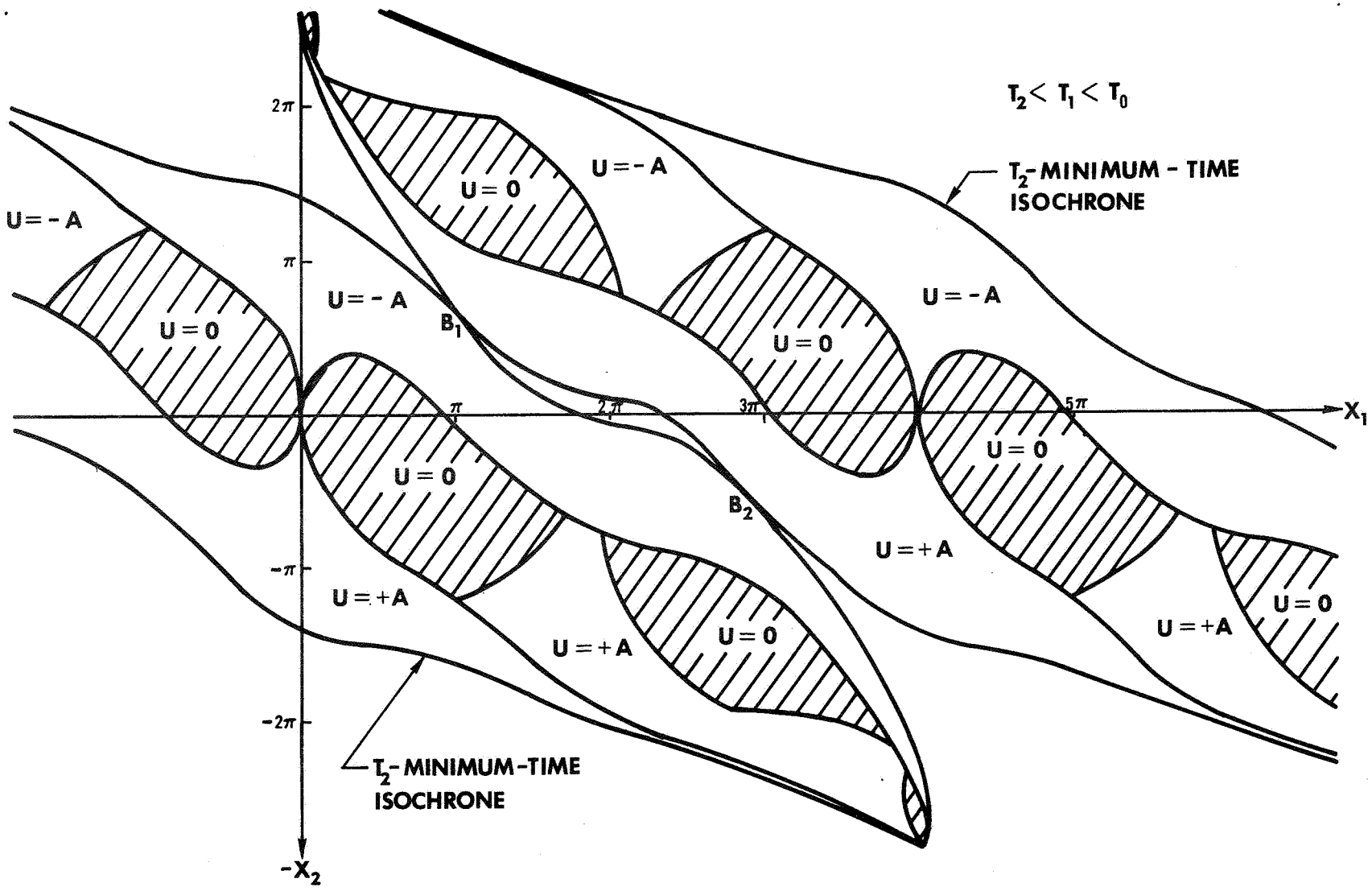

Fig. 4-18. Degeneration of T^k-Indifference Curves into Two Points (B_1, B_2).

CHAPTER V

COMPARISON OF THE LINEAR AND NONLINEAR OPTIMAL CONTROL PROBLEMS

Due to the technical difficulties encountered in the nonlinear analysis of optimization problems, wherever an equation such as (1-1) appears, one frequently linearizes the equation and considers only small motions of the system. At times one may even apply the results of such analysis to motions that are by no means small with the expectation of obtaining reasonable conclusions for the nonlinear regime. The results of both the linear and nonlinear plants are presented to indicate how far one may extend the results of the linear analysis into the nonlinear region and still obtain good performance estimates.

The linearized plant dynamics are governed by

$$\ddot{x}(t) + x(t) = u \qquad |u| \leq A \tag{5-1}$$

Again we seek an admission control $u(t)$ which transfers the state from some known initial state $(x_1(t_o), x_2(t_o))$ to the terminal state $(x_1(t_f), x_2(t_f)) = (0,0)$ within a specified time $T = t_f - t_o$. The solution of this problem is contained in Ref. [9].

The main differences encountered in the two problems are

i) Whereas the optimal control in either case is of type bang-coast-bang, the linear optimal control $u(t)$ is a periodic function of time with period π. An optimal path consists of alternating P and N-arcs separated always by an O-arc or a truncation of such a

path should the time T be less than a complete period π. In contrast the nonlinear optimal control is not periodic. Furthermore, optimal control sequences of type P-0-P-... where P (or N)-arcs alternate with 0-arcs are present.

ii) The number of switchings may be quite different. For $T \leq \pi$ the linear problem has at most two switchings. The maximum number of switchings that can occur for solution time $T \leq \pi$ along an optimal path for the nonlinear problem depends upon the magnitude of the control bound A. For A equal 2 at most three switchings could occur as a P-0-P-0 (N-0-N-0) path is the longest sequence. In chapter IV, it has been shown that for A equal 3 an optimal sequence could have five switchings. As A increases without bound one expects the maximum number of switchings occurring for solution time π to also grow without bound. In the limiting case the problem reduces to the $1/s^2$ plant:

$$\ddot{x}(t) = u \qquad |u| \leq A \tag{5-2}$$

which may have an unbounded number of switchings along singular arcs, which arise for appropriate initial conditions as seen in Ref. [9].

iii) There may be big differences in the fuel required to zero an initial disturbance within time T. In figures (5-1) to (5-5) the fuel cost is plotted as a function of the initial state variable x_{10}, for different values of the other state variable x_{20}. The permitted time for the maneuver is $T = .75\pi$ and the control bound $A = 3$.

This value of T corresponds to allowing $3/8$ of an orbit to realign a satellite having the inertial parameter $K_3 = -1/3$. Furthermore, such a value is representative of the times we have been considering; namely, times T less than π. Also the time T is sufficiently large to allow zeroing of large disturbances so that we obtain good contrast of the linear and nonlinear results.

The control bound of $A = 3$ was selected to enable the zeroing of the disturbance $(2\pi,0)$ within time π and thereby remove the "holes" of the controllable region discussed in chapter IV. With this bound on the control, any pitch error may be zeroed provided the pitch error rate lies within the envelope of the T-controllable regions. The larger the control bound A the less fuel required to zero a given initial disturbance within time T. Increasing the bound A on available control torque u, while lowering fuel consumption, is not without penalty. The larger weight requirement necessary to provide larger control torques may significantly alter the satellite configuration (inertial parameters) in addition to imposing rather severe restrictions on the weight of useful payload. The fuel savings in zeroing the states of interest of large A values is not sufficient to justify the extra hardware. Furthermore, as presented later, the magnitude of errors in fuel expenditure of a discrete time suboptimal feedback control law increases as the control bound A increases. The value $A = 3$ where the available control torque is three times the maximum gravitational torque is a good compromise. Efficient zeroing of disturbances of interest is achieved without undue control torque requirements.

The fuel cost curves are given only for negative values of x_{20} inasmuch as a reflection of that curve about the fuel axis gives the fuel cost curve for the corresponding positive x_{20} value. In general for a fixed value of x_{20} there are zones for which the linear plant exhibits greater fuel economy and zones for which the nonlinear plant is more efficient. If $x_{20} < 0$, the nonlinear appears the more economical when $x_{10} > 0$ and less economical for $x_{10} < 0$. The greatest discrepancy between the optimal fuel prediction of the linearized model and the actual optimal fuel requirement of the nonlinear system occurs for those values of x_{10} lying near either the linear or nonlinear T-minimum-time isochrone. Here a severe fuel penalty is paid to meet the time constraint and the corresponding fuel cost curve rises much more rapidly than the other fuel cost curve.

In Fig. 5-6, the importance of allowing as much time as is reasonable to complete the earth-pointing maneuver to avoid such extravagant fuel expenditures is further emphasized. As the time T approaches the minimum settling time for the initial state (x_{10},x_{20}), the slope $\frac{\partial F}{\partial T}$ of the fuel versus time curve becomes infinite. If

$$F = -V(x_{10},x_{20},T) \tag{5-3}$$

then the Hamilton-Jacobi partial differential equation (3-17)

$$\frac{\partial F}{\partial T} + H = 0 \tag{5-4}$$

indicates that the Hamiltonian H becomes unbounded as the fuel optimal solution degenerates into the minimum time solution.

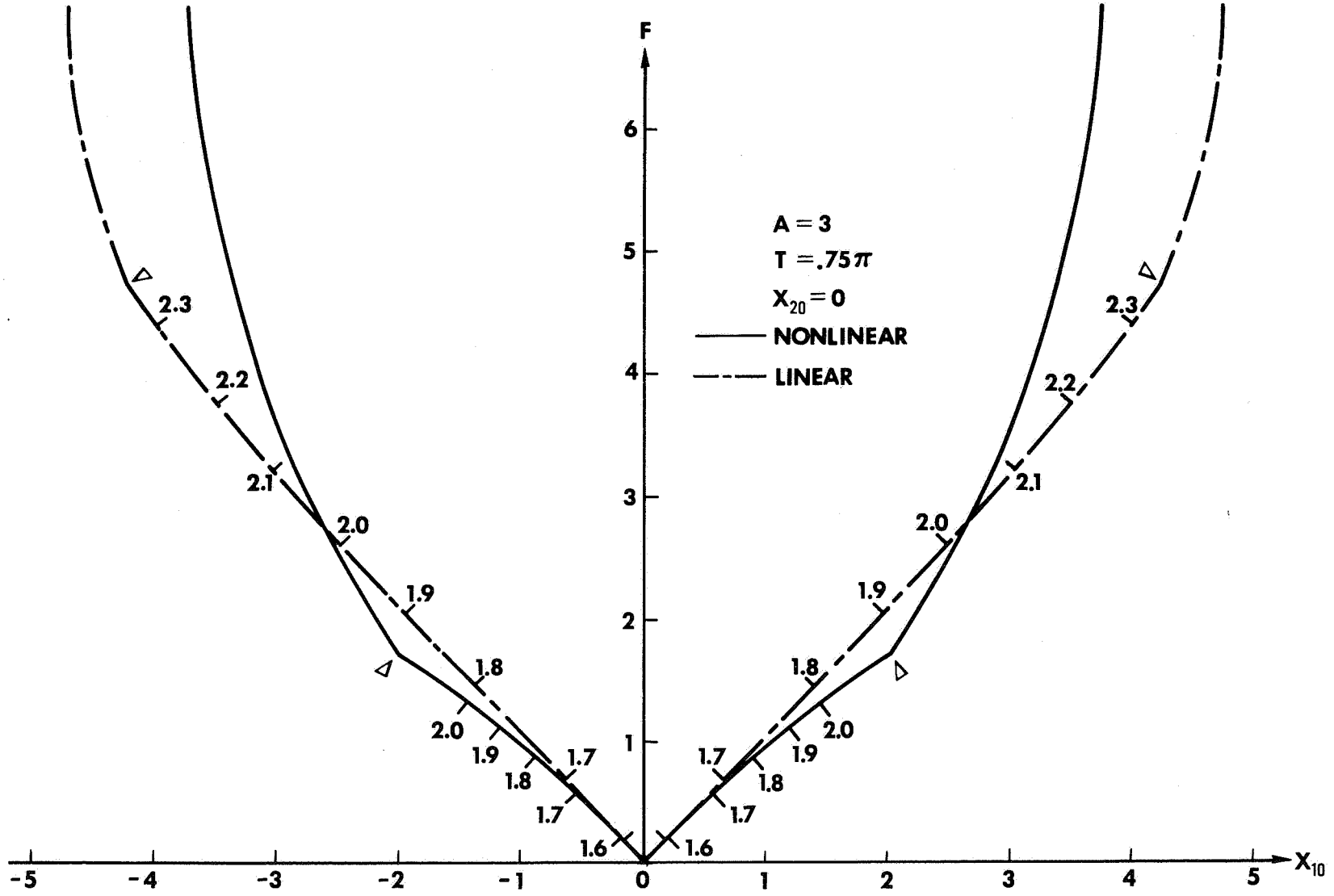

Fig. 5-1. Fuel Cost Linear and Nonlinear Solutions Versus x_{10} for $x_{20} = 0$, A = 3, and T = .75π. The points between the corners (△) arrive early at origin at the times demarked along the curve.

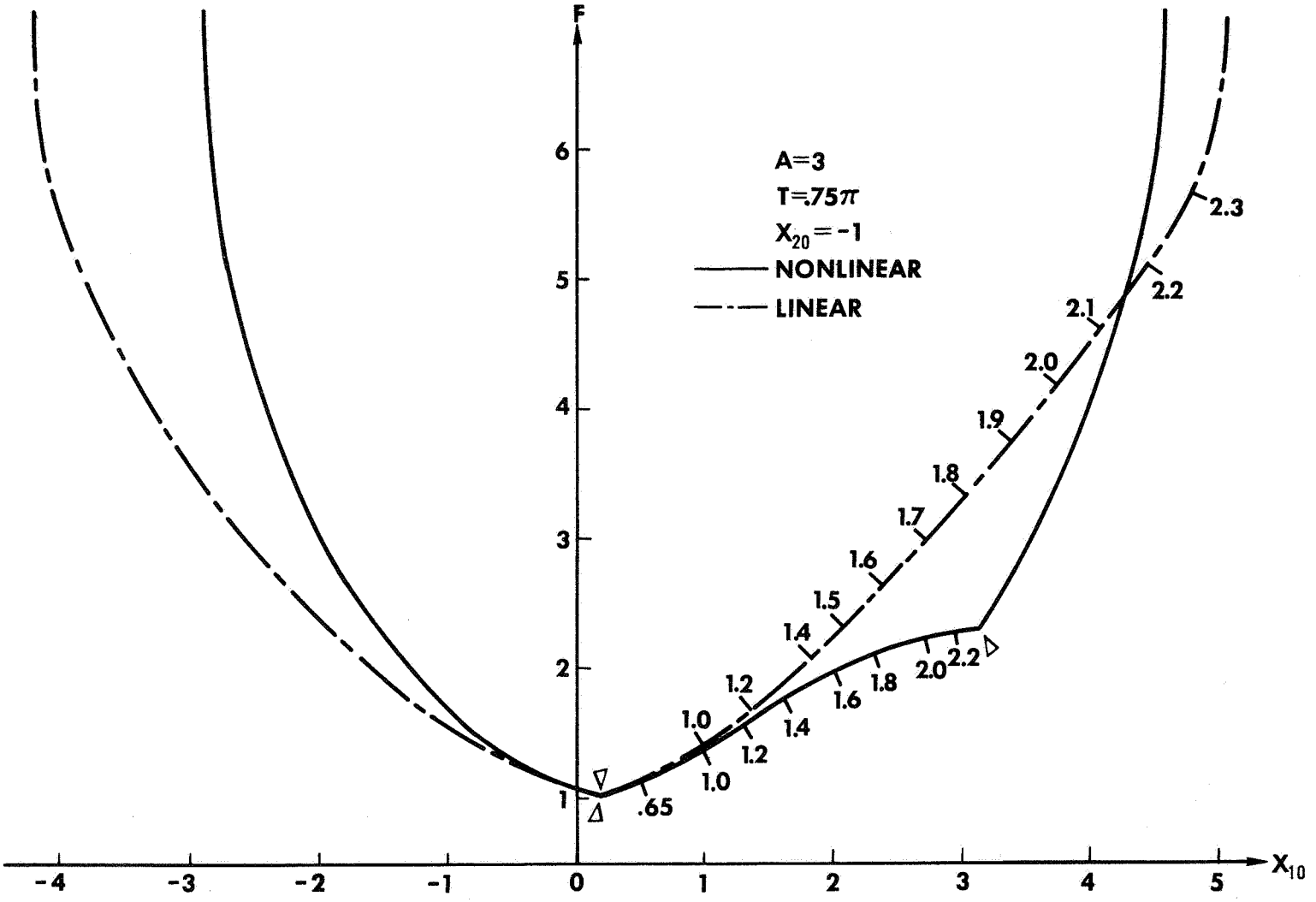

Fig. 5-2. Fuel Cost Linear and Nonlinear Solutions Versus x_{10} for x_{20} = -1, A = 3, and T = .75π. The points between the corners (△) arrive early at origin at the times demarked along the curve.

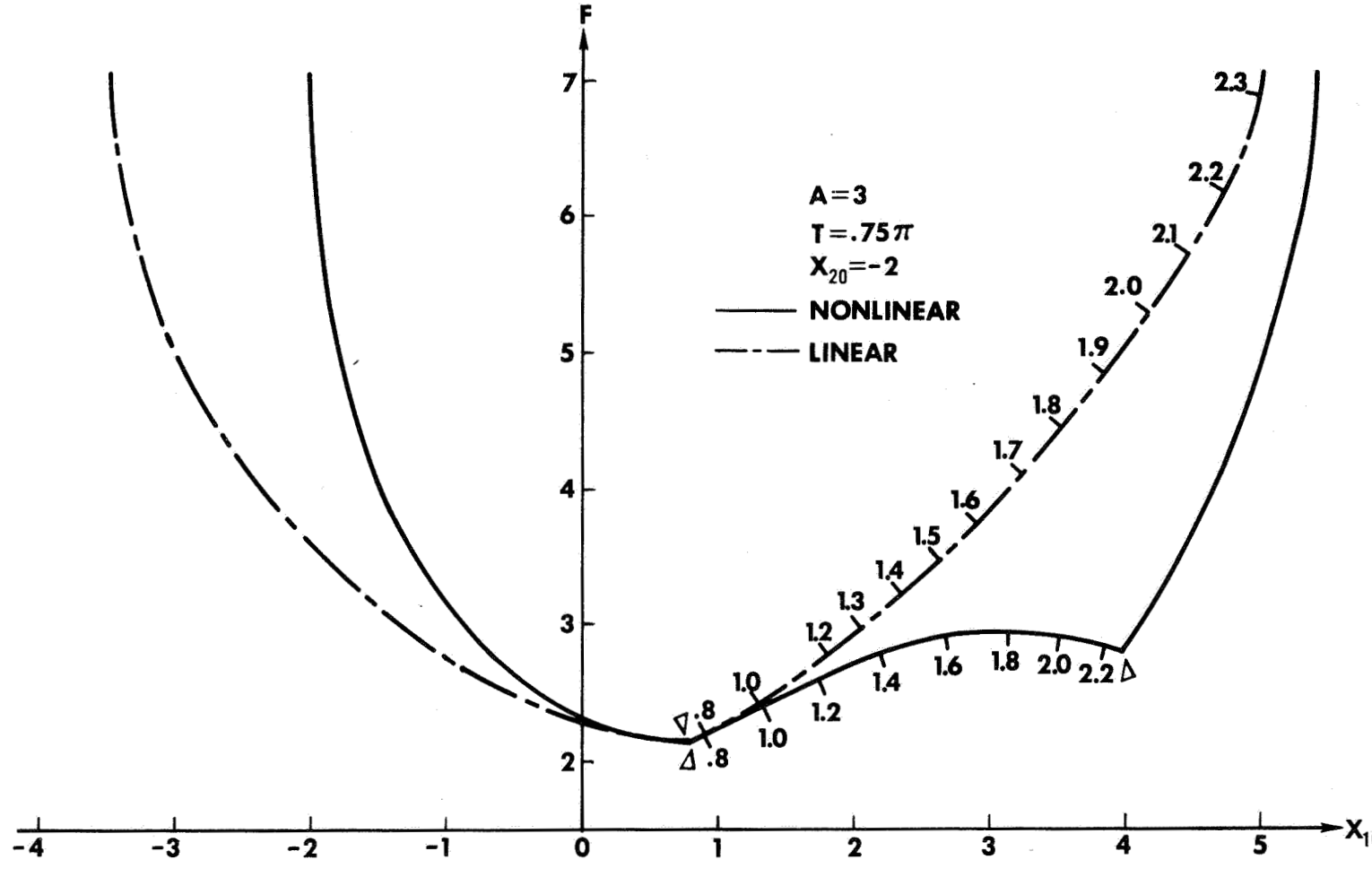

Fig. 5-3. Fuel Cost Linear and Nonlinear Solutions Versus x_{10} for x_{20} = -2, A = 3, and T = .75π. The points between the corners (△) arrive early at origin at the times demarked along the curve.

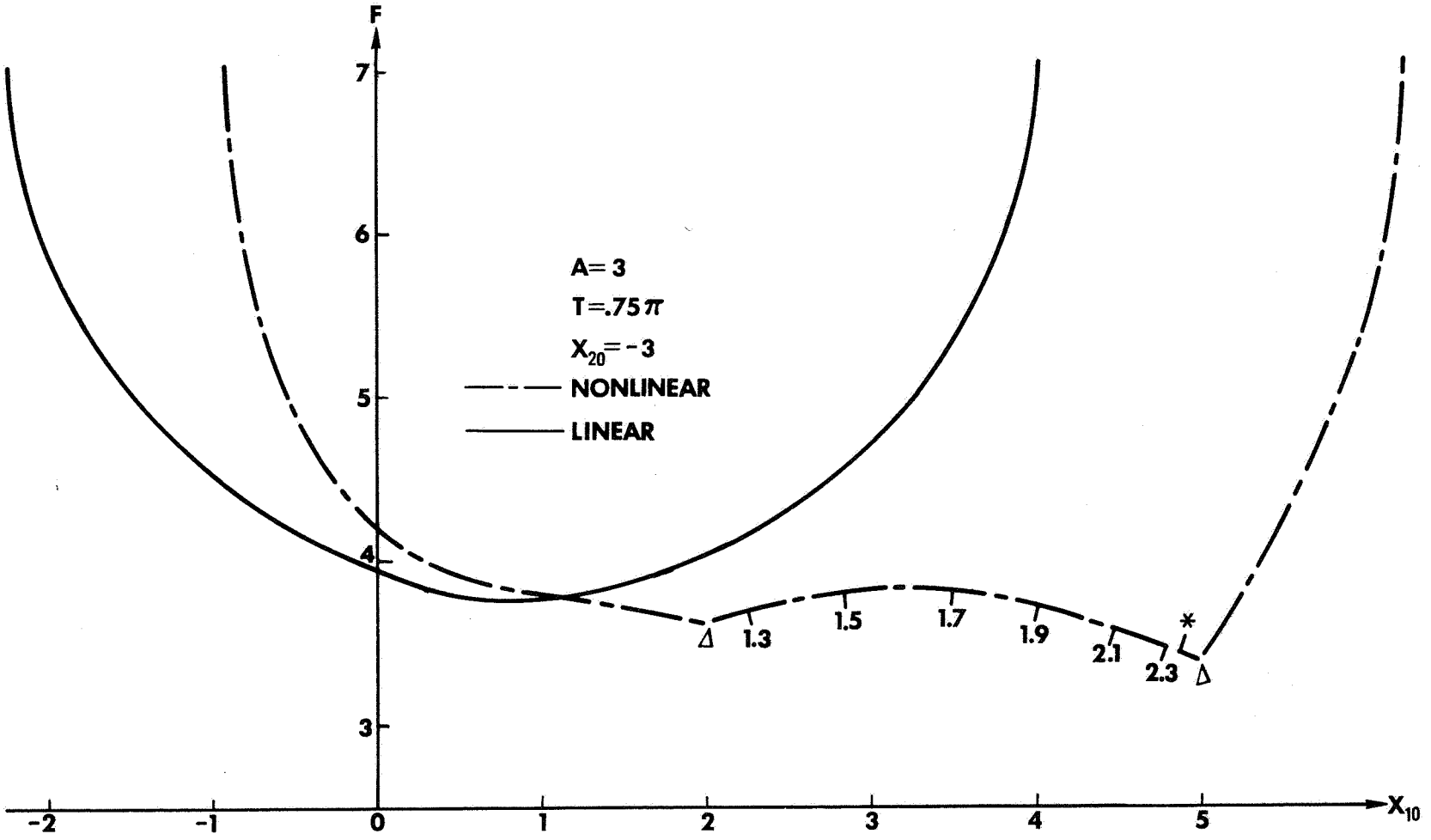

Fig. 5-4. Fuel Cost Linear and Nonlinear Solutions Versus x_{10} for x_{20} = -3, A =3, and T = .75π. Now only those points between the left corner and the point * arrive at origin in times less than T as shown.

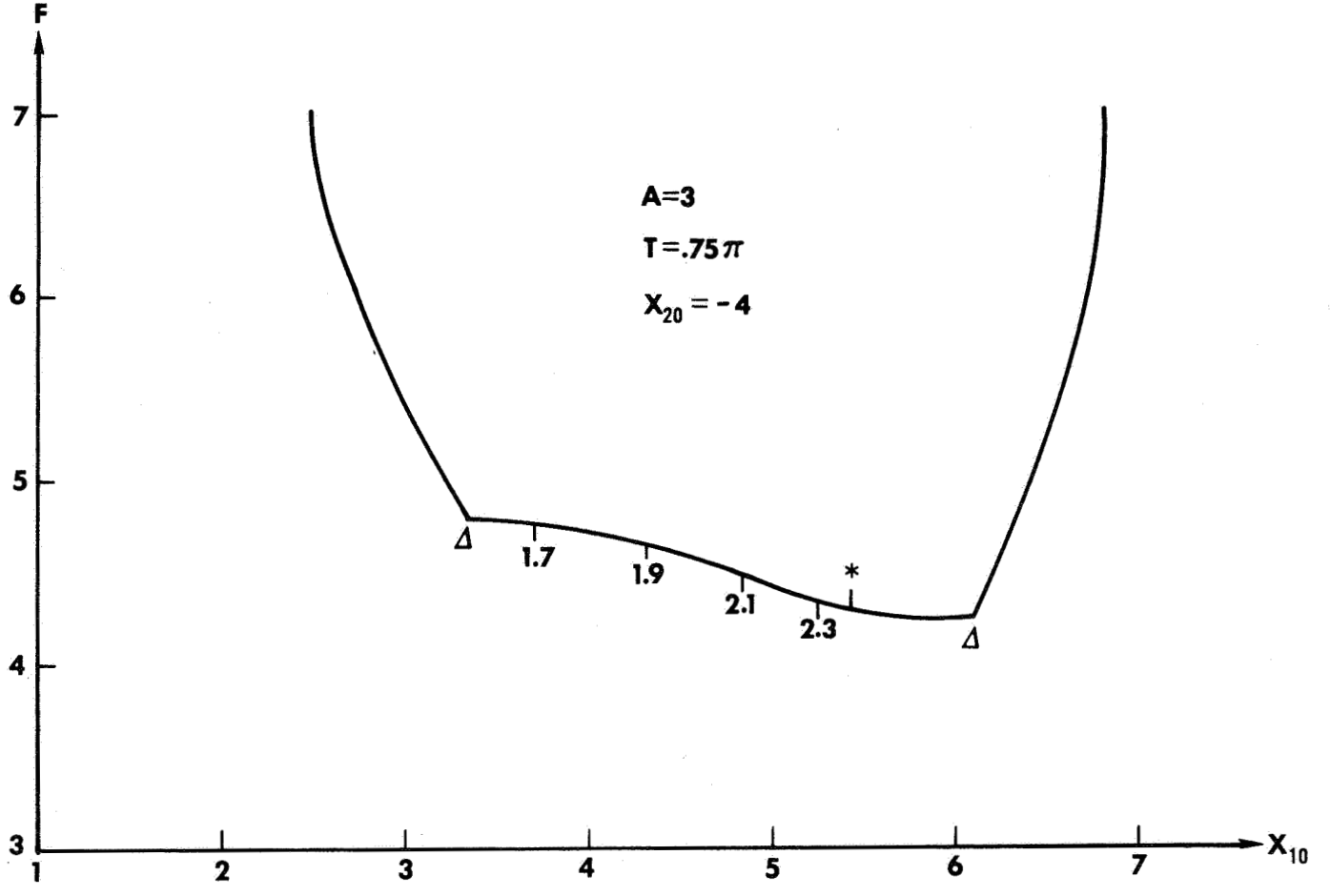

Fig. 5-5. Fuel Cost of Nonlinear Solution Versus x_{10} for x_{20} = -4, A = 3, and T = .75π. Points between left corner Δ and the point * arrive at origin in times less than T as shown. No state with x_{20} = -4 can be zeroed within time T by the linear plant.

At those points for which a switching occurs at time T, the slope is discontinuous. To the left or right of such a corner the solution to the Hamilton-Jacobi canonical equations exists and the slope is well defined and continuous. In the example with $(x_{10},x_{20}) = (-2,2)$ shown in Fig. 5-6 the Hamiltonian is zero to the right of the corner, and no reduction in fuel expenditure is achieved by relaxing the time constraint over the interval shown.

As one would expect, the results of the linear and nonlinear analysis are less and less similar as the absolute value of x_{20} increases. Finally, as shown in Fig. 5-5, no state with $x_{20} = -4$ can be zeroed within the specified time $T = .75\pi$ by the linear solution. However, there is a surprisingly large region for which the linear solution predicts the optimal performance of the nonlinear system with good accuracy. For the region

$$\begin{aligned} -1 < x_{10} < +1 \\ -2 < x_{20} < +2 \end{aligned} \tag{5-5}$$

the greatest error is about 12.5% for the case $A = 3$ and $T = .75\pi$. For most of the region there is much closer agreement. In terms of the actual pitch error θ and error rate $\dot{\theta}$ of the satellite region (5-5) is

$$\begin{aligned} -.5 < \theta < +.5 \\ -\sqrt{-3K_3}\,\Omega < \dot{\theta} < +\sqrt{-3K_3}\,\Omega \end{aligned} \tag{5-6}$$

where Ω is the angular frequency of the satellite orbit.

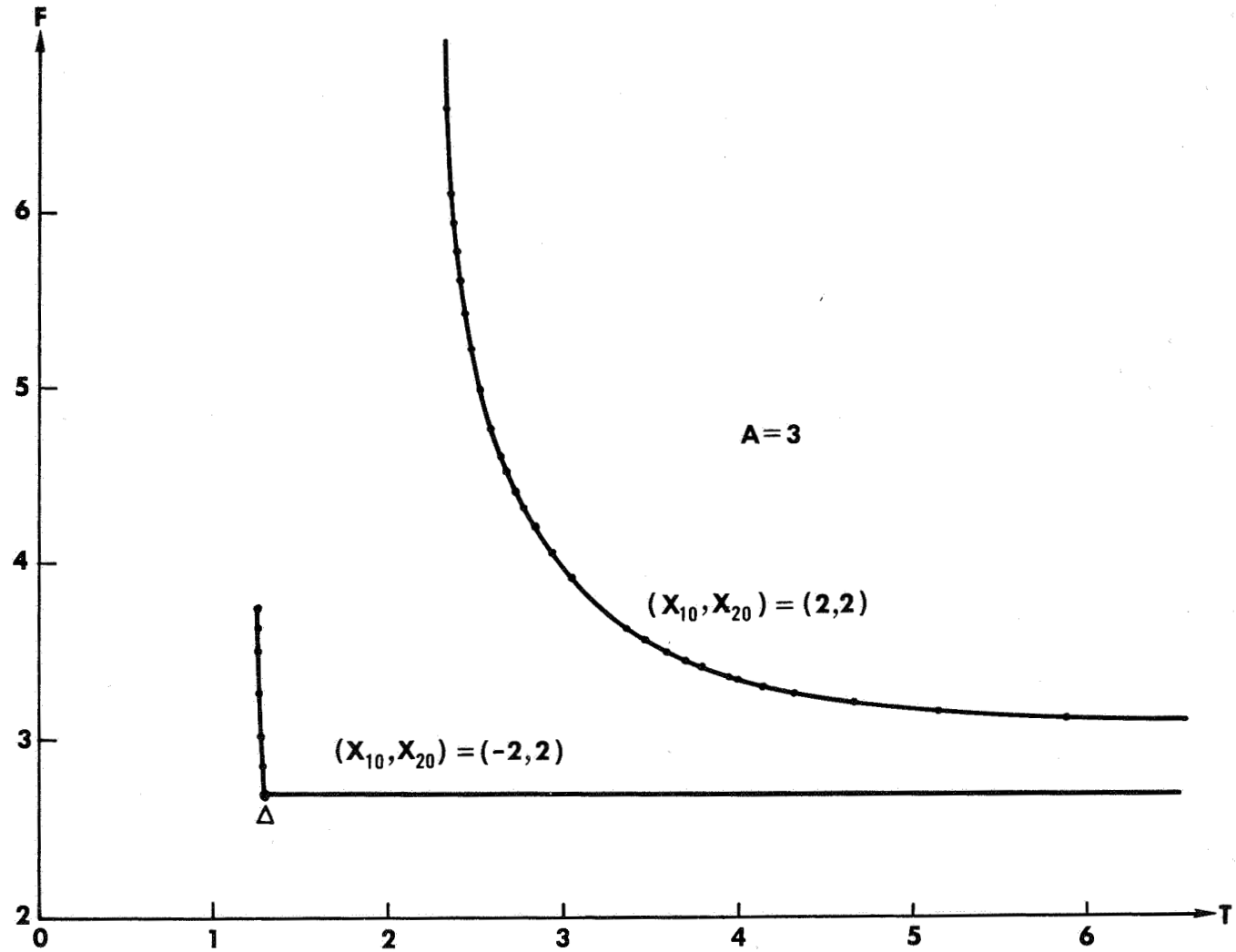

Fig. 5-6. Fuel Cost Versus Allowable Time of Solution for the Initial Disturbances $(x_{10},x_{20}) = (2,2)$; $(-2,2)$. A discontinuity in the slope $\partial F/\partial T = H_B$ appears in the $(2,-2)$ curve due to a switching at Δ. To the left of P-O-N paths are optimal. To the right $H_B = 0$ pseudoextremals which arrive early are optimal.

FUEL COSTS CURVES AND HAMILTON-JACOBI THEORY

The fuel cost curves are intimately connected to the Hamilton-Jacobi theory as seen in the discussion following theorem 3-1. The slope $\frac{\partial F}{\partial x_{10}}$ of these curves is equal to the value of the adjoint variable λ_1 at the point (x_{10},x_{20}) corresponding to the optimal pseudoextremal for zeroing the state (x_{10},x_{20}) within time T. This slope becomes vertical at the end points as the adjoint variables become infinite and the fuel optimal solution degenerates into the minimum time solution.

Corners where the slope is discontinuous appear in both the linear and nonlinear fuel cost curves. For the linear case one corner appears at the intersection of the horizontal line x_{20} = fixed constant and the zero trajectories:

$$x_{20} = +\sqrt{A^2-(x_{10}+A)^2} \quad \text{for} \quad -2A \leq x_{10} \leq 0 \tag{5-7}$$

$$x_{20} = -\sqrt{A^2-(x_{10}-A)^2} \quad \text{for} \quad 0 \leq x_{10} \leq 2A \tag{5-8}$$

which are the final semicircular arcs of the switching locus for the Bushaw problem (Ref. [10]). For $|x_{20}| > A$ the corner disappears in the linear solution curve.

More pronounced are the corners in the nonlinear fuel cost curves. The first corner x_{1cr} is at the intersection of the horizontal line x_{20} = present constant and the zero trajectory Γ^+. For those states immediately to the right of x_{1cr} the optimal paths are either P-O-P

or P-0 pseudoextremals depending upon whether or not the intersection occurred at a value $x_{1cr} > \pi$. The subscript cr denotes the value at the corner. In terms of x_{20} then we have a P-0-P trajectory for

$$x_{20} < -\sqrt{2(\cos \pi - 1 + A\pi)} \tag{5-9}$$

and a P-0 trajectory for

$$x_{20} > -\sqrt{2(\cos \pi - 1 + A\pi)} \tag{5-10}$$

Immediately to the left of the corner $(x_{10} < x_{1cr})$ the optimal pseudo-extremals for time $T = .75\pi$ are of type N-0-P.

The second corner is at the intersection of the given horizontal line x_{20} = constant and the T-bang-coast isochrone where T here has the value $.75\pi$. For points immediately to the left $(x_{10} < x_{1cr})$ of this corner the optimal pseudoextremal is either a P-0-P or P-0 path depending upon whether the corner lies to the right of Γ_{π}^{+}. The optimal pseudoextremals for those x(t) which have $x_1 > x_{1cr}$ are P-0-N trajectories.

Since such a corner represents a switching, theorem 3-1 does not guarantee the existence of a solution to the canonical characteristic differential equations. Inasmuch as the slope has a discontinuity of the first kind at this corner we expect no solution to (3-19), i.e., to

$$\frac{\partial F}{\partial x_{10}}(x_{10}, x_{20}, t) = -\lambda_1(t) \tag{5-11}$$

where $F = -v(x_{10}, x_{20}, t)$ is the optimal fuel cost. However, we may

still associate the slope immediately to the left or right of this corner with the value of the adjoint λ_1 at the corner for the appropriate pseudoextremal. The slope to the right is given the value of the adjoint λ_1 for a P-O-N pseudoextremal having a switching from 0 to -A at the corner. From equation (3-4) along an O-arc

$$\lambda_2 = x_2(\lambda_{2s}+H_B \int_{x_{1s}}^{x_1} -[2(\cos\sigma-\cos x_{1s})+x_{2s}^2]^{-3/2}d\sigma) \qquad (5\text{-}12)$$

where the subscript s now denotes values at the switching from the zero trajectory.

If (x_{1cr},x_{2cr}) denote the coordinates of such a corner then the Hamiltonian of such a P-O-N pseudoextremal is given by

$$H_B = \frac{\left(\frac{-1}{x_{2cr}} - \frac{1}{x_{2s}}\right)}{\int_{x_{1s}}^{x_{1cr}} -[2(\cos\sigma-\cos x_{1s})+x_{2s}^2]^{-3/2}d\sigma} \qquad (5\text{-}13)$$

where we have made use of the fact that $\lambda_2 = -1$ in equation (5-12). Since (x_{1s},x_{2s}) and $(x_{1cr},-x_{2cr})$ belong to the same O-curve

$$\frac{x_{2s}^2}{2} - \cos x_{1s} = \frac{x_{2cr}^2}{2} - \cos x_{1cr} \qquad (5\text{-}14)$$

But (x_{1s},x_{2s}) is a point on the zero trajectory Γ^+ or

$$\frac{x_{2s}^2}{2} - \cos x_{1s} = Ax_{1s} - 1 \qquad (5\text{-}15)$$

Combining (5-14) and (5-15) we obtain

$$x_{1s} = \left(\frac{x_{2cr}^2}{2} - x_{1cr} + 1\right)/A \qquad (5\text{-}16)$$

with which x_{2s} may be determined from (5-15). Since at a switch point

$$H_B = -\lambda_1 x_2 + \lambda_2 \sin x_1 \tag{5-17}$$

we obtain

$$\lambda_{1cr} = -\frac{H_B + \lambda_2 \sin x_{1r}}{x_{2cr}} \tag{5-18}$$

The slope to the right of x_{1cr} is obtained by combining equation (5-11) and (5-18) to get

$$\frac{\partial F}{\partial x_{10}} = -\lambda_1 = \frac{H_B + \sin x_{1cr}}{x_{2cr}} \tag{5-19}$$

where H_B is given by (5-13).

In the case of a P-0-P pseudoextremal being optimal for $x_{10} < x_{1cr}$ we make use of the fact that $\lambda_2 = +1$ in equation (5-12) to obtain the Hamiltonian

$$H_B = \frac{\left(\frac{1}{x_{2cr}} - \frac{1}{x_{2s}}\right)}{\int_{x_{1s}}^{x_{1cr}} -[2(\cos\sigma - \cos x_{1s}) + x_{2s}^2]^{-3/2} d\sigma} \tag{5-20}$$

and that

$$\frac{\partial F}{\partial x_{10}} = -\lambda_{1cr} = \frac{H_B - \sin x_{1cr}}{x_{2cr}} \tag{5-21}$$

Should (x_{1cr}, x_{2cr}) lie above Γ_π^+ then for $x_{10} < x_{1cr}$ a P-0 pseudoextremal is optimal. In this case the Hamiltonian is zero and the slope is obtained from (5-12) and (5-18)

$$\frac{\partial F}{\partial x_{10}} = -\lambda_{1cr} = -\frac{\lambda_{2cr} \sin x_{1cr}}{x_{2cr}} \qquad (5\text{-}22)$$

The adjoint value λ_{2cr} is no longer at a switching but is obtained from (5-12) with the Hamiltonian being zero.

$$\lambda_{2cr} = \frac{x_{2cr}}{x_{2s}} \qquad (5\text{-}23)$$

from which

$$\frac{\partial F}{\partial x_{10}} = -\frac{\sin x_{1cr}}{x_{2cr}} \qquad (5\text{-}24)$$

SYNTHESIS OF A SUBOPTIMAL CONTROL LAW

To implement the fuel-optimal, time-varying, feedback control law would require such complex switching strategy as to be hardly feasible. Nevertheless, the optimal study does indicate how an efficient suboptimal control law may be designed. Furthermore, the study provides a yardstick by which to gauge the effectiveness of any suboptimal proposal.

The simplified suboptimal control scheme eliminates all switching loci found between the T-bang-coast isochrone and zero trajectory. The only switching curves in the state plane for the suboptimal proposal are the fixed zero trajectories and the time dependent T-bang-coast isochrones. Thus suboptimal paths have at most two switchings and are either P-O-N (N-O-P) or P-O (N-O) trajectories. The two strategies are identical except for those states which at time-to-go T belong to the region below Γ_{π}^{+} bounded by the T-bang-coast isocrhone and zero

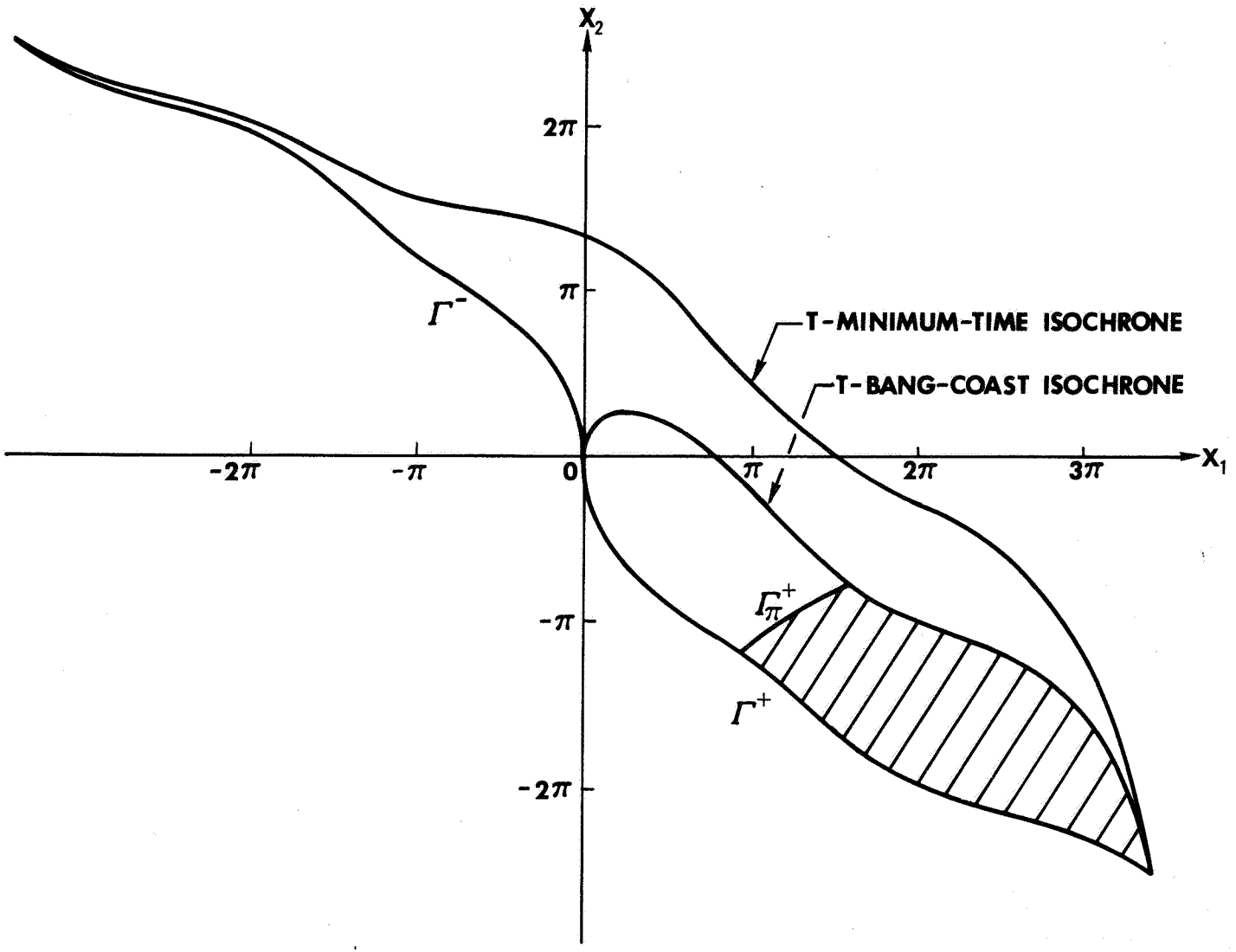

Fig. 5-7. Region for Which Suboptimal and Optimal Control Laws Differ.

trajectory Γ^+ (see Fig. 5-7). For this region a slight fuel penalty is paid in return for a simplified switching strategy. Initial disturbances are also zeroed slightly faster than the prescribed mission time T.

Because the suboptimal path is infact an optimal path for a smaller prescribed time T', the difference between the fuel consumptions of the two laws increases as the prescribed time of mission $T > T'$ grows longer. For our selected control bound of $A = 3$, the maximum penalty suffered by the simplified control law is 3.6% which occurs at the maximum allowable time of mission $T = \pi$. For most initial disturbances (including other x_2 values) the penalty is less than 1%. In fact for time of mission $T = .75\pi$, the maximum fuel penalty for any initial disturbance is down to 1% as shown in Fig. 5-8.

The suboptimal control scheme thus far proposed requires implementation of the T-bang-coast isochrones as the time-dependent second switching locus. These switching curves are approximated by 2n-1 degree Hermit polynomials which match the coordinates and slope of the isochrone at n points. For $T \leq .7\pi$ the T-bang-coast isochrones are closely approximated by fifth degree polynomials. (See Fig. 5-9.) But for $T > .7\pi$, seventh degree polynomials are needed for an accurate representation of the T-bang-coast isochrones. (See Fig. 5-10.) In Figs. 5-9, and 5-10 the slopes and coordinates which determine the matching Hermite polynomial are indicated. The slope at (0,0) was not matched exactly but instead was adjusted to give better overall agreement between the approximating polynomial and the isochrone. The

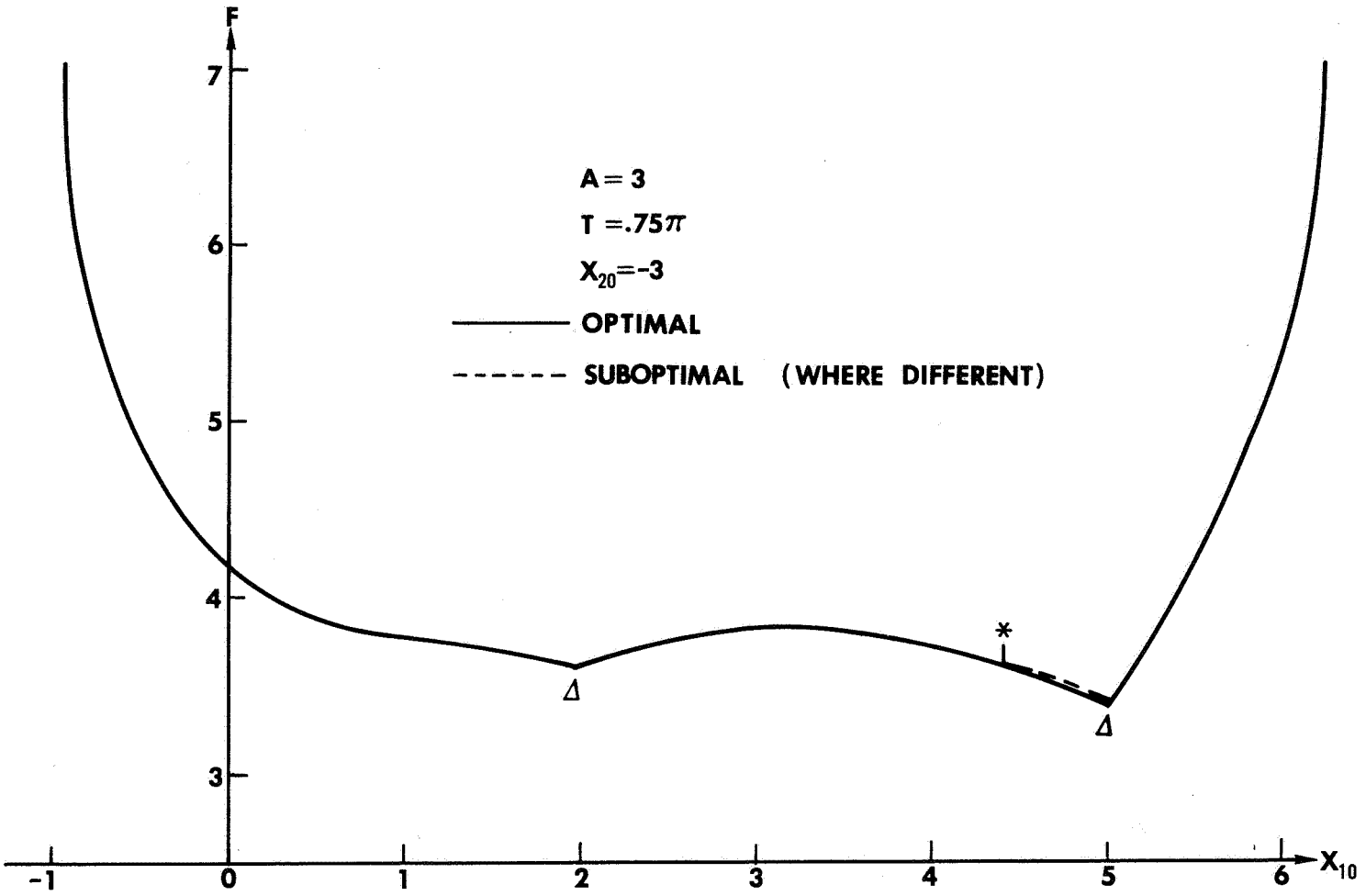

Fig. 5-8. Fuel Costs of Suboptimal and Optimal Solutions Versus x_{10} for x_{20} = -3, A = 3, and T = .75π.

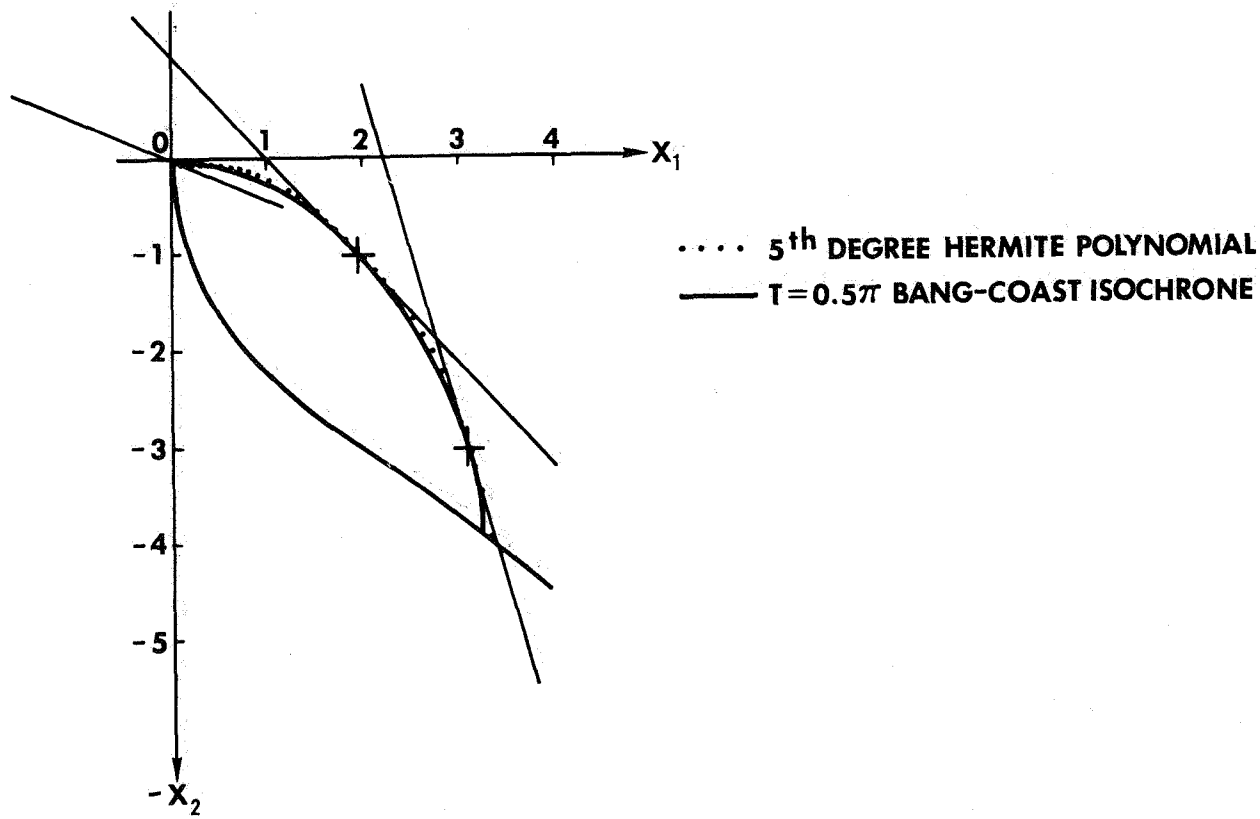

Fig. 5-9. Fifth Degree Hermite Polynomial Approximation to T-Bang-Coast Isochrone for A = 3, T = .5 π.

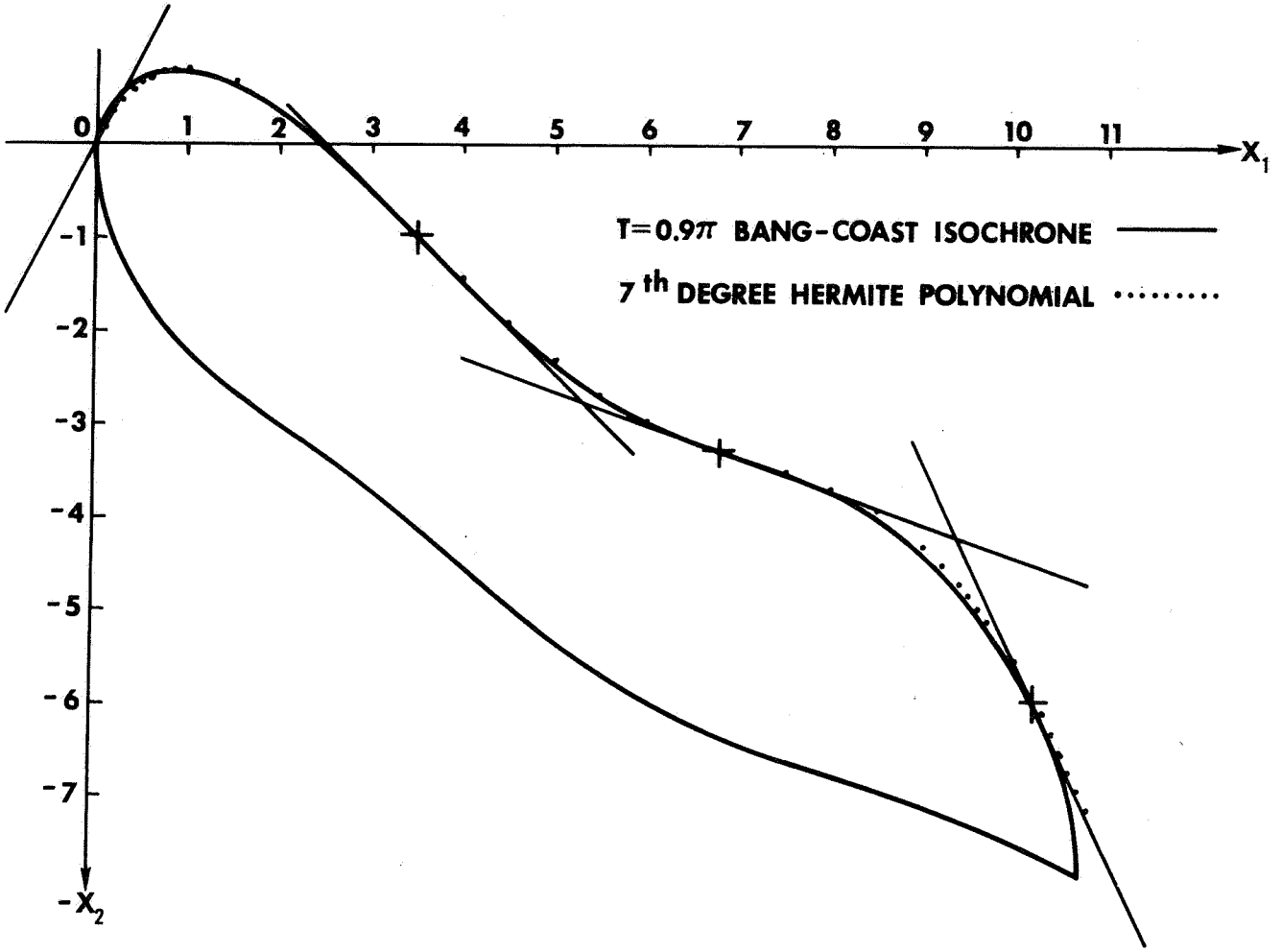

Fig. 5-10. Seventh Degree Hermite Polynomial Approximation to T-Bang-Coast Isochrone for A = 3, T = .9π.

approximation is seen to be so accurate that little additional fuel penalties would result from this refinement of the previous suboptimal proposal provided polynomials were stored for sufficient values of T.

The greatest source of error arises in the approximation of the continuous time-varying suboptimal feedback control law by a discrete time-varying feedback law. If one samples the state (x_1,x_2) only at those times for which a polynomial switching curve is stored, many polynomials may be required to reduce the fuel errors to an acceptable level. The greatest error results when a state (x_1,x_2) with $x_1 > 0$ and $x_2 < 0$ lies just outside the second switching locus at time T and thus continues with control $u = -A$ until the next sampling time at which it now is well within the $u = 0$ control region. In this event a double penalty is paid because upon reaching the final switching locus Γ^+, fuel must now be used to reduce the excessive velocity x_2 which resulted from the late switching at the T-bang-coast isochrone. For a sample time ΔT the maximum error is nearly $2A\Delta T$ where A is the control bound. In the most adverse circumstance for $A = 3$ an additional 1.88 units of fuel would be expended if ten polynomials were stored and the state only sampled at these ten values of time. Depending upon the state to be zeroed, anywhere from 20% to 80% excess fuel would be consumed. This maximum error, while rarely encountered for any given disturbance, could be proportionally reduced by storing more polynomials and accordingly reduce the sample time ΔT or preferably by increasing the sample rate without storing additional polynomials.

To take greater advantage of increased sampling rates for a fixed number of stored polynomials, the following scheme is proposed. Those sample points for which times a polynomial switching curve is stored are called major sample points. Let T_1 and T_2 denote the two largest times-to-go for which a polynomial is stored such that

$$T_2 < T_1 < T \tag{5-25}$$

where T is the time remaining for zeroing the state $x(t)$. The interval T_1-T_2 is subdivided into n equal segments thereby creating $n-1$ interior minor sampling points for which no switching polynomial is stored. The sampling points are ordered such that the 0-th occurs at the first major sampling time T_1 and the n-th at the second major sampling point T_2. The refined suboptimal control scheme is then illustrated in Fig. 5-11 for $n = 10$. At time-to-go T state (x_1,x_2) is assumed to be outside the T_1 switching polynomial. (If it were inside this polynomial the control would be zero and no further switching would occur until reaching the zero trajectory.) Letting the integer k $(0 \leq k \leq n)$ denote the sampling point we adopt the following control strategy:

i) If state $x(t)$ has crossed the T_2-switching polynomial at sample point k, switch control to zero at sample k.

Otherwise

ii) If state $x(t)$ has crossed the T_1-switching polynomial at sample point k where $k \leq \frac{n}{2}$

switch control to zero at sample 2k-1 unless overridden by control law (i) for any $k \leq n$.

In control law (ii) the time at which the T_1-switching polynomial is crossed is used to help determine the time of next switching. The effect of control law (ii) is to approximate intermediate switching curves for those times-to-go at which no switching polynomial is available.

For $k > n$ the process is repeated with the T_2 polynomial now taking the role of the T_1 polynomial and a T_3 $(T_3 < T_2)$ polynomial replacing the T_2 polynomial. This refinement in the suboptimal control realization will reduce the maximum error by nearly a factor of n.

By merely increasing the sample rate a proportional reduction in excess fuel expenditure has been achieved without increasing the number of switching polynomials required.

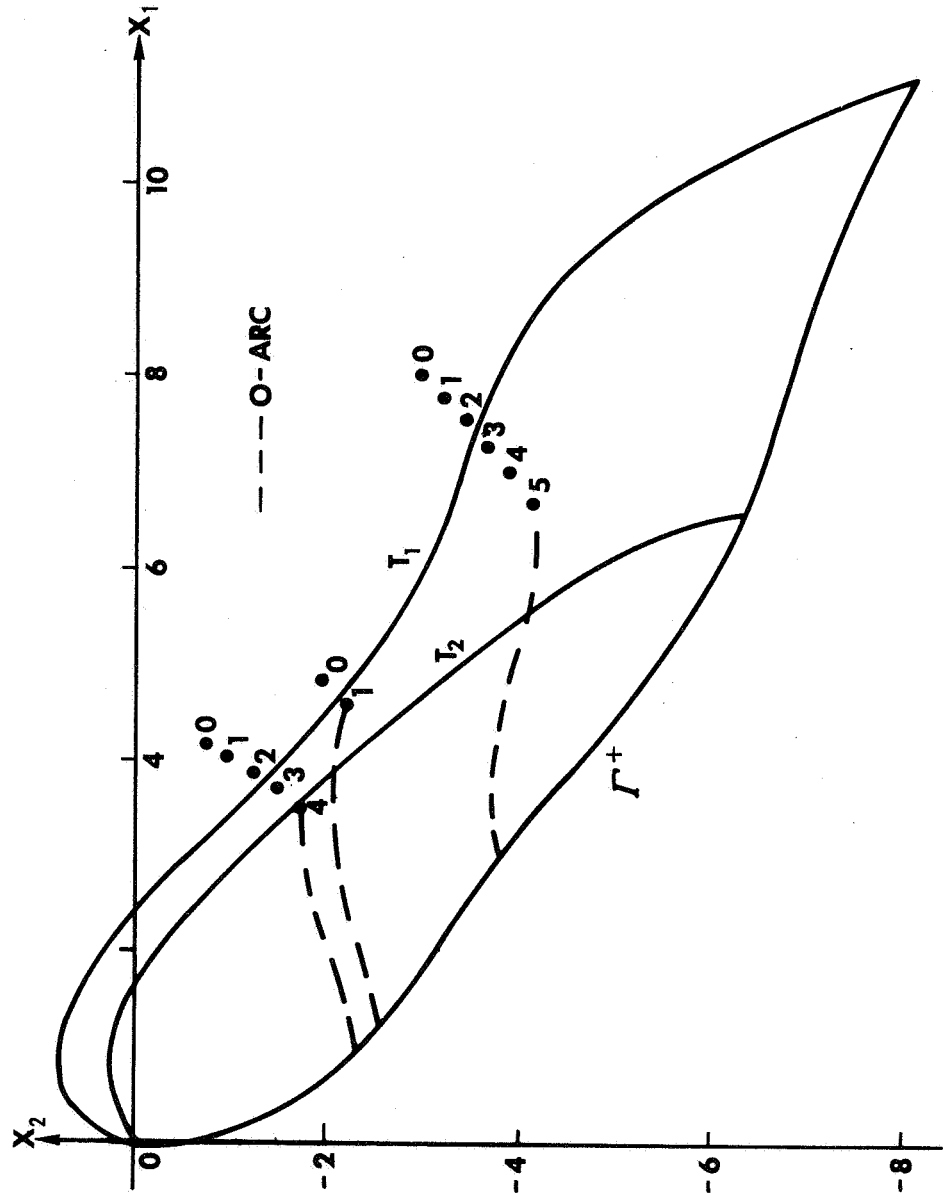

Fig. 5-11. Refined Suboptimal Control Law.

CONCLUSION

The problem of finding the minimum effort control for a particular satellite attitude motion, where the pitch motion may be described by the nonlinear differential equation

$$\ddot{x}(t) + \sin x(t) = u(t) \qquad |u| \leq A,\ A > 1$$

is the subject of this investigation. For reaction jet controllers, the minimum effort criterion corresponds to minimum fuel expenditure.

In chapter I, after formulation of the problem to be studied, the Maximum Principle of Pontryagin is used to obtain the necessary conditions on the control $u(t)$ in order that the resulting trajectory be fuel optimal. The trajectories meeting such conditions are termed pseudoextremals and are the candidates for the optimal paths. The optimal control is found to be of type "bang-coast-bang" in which the control is either zero or at a limiting value $\pm A$.

In chapter II, the backwards time formulation is presented and possible control sequences are enumerated. By restricting the time T to be always less than π, the minimum-time isochrone boundary of the controllable region is found to be generated by a single switch, bang-bang control sequence. Such a restriction seems appropriate for it corresponds to requiring the satellite to be reoriented within $\pi/\sqrt{-3K_3}$ radians of orbit or, for a satellite having inertial parameter $K_3 = -1/3$, within half an orbit. The consideration of an auxiliary problem shows that optimal control sequences of type $\pm A,\ 0,\ \mp A, \ldots$

are limited in length to the sequences $\pm A, 0, \mp A$ whenever the problem time T is less than $\pi/2 + \text{arcsinh } 1 \approx .78\pi$. An alternate proof raising this lower bound $.78\pi$ was not found. Nevertheless, the method of proof and all computer examples indicate that the result holds for times as large as π as well.

In chapter III, the backwards time adjoint variables $\lambda_1(\tau)$ and $\lambda_2(\tau)$ are found as functions of the state variables and initial conditions. A theorem of J.C. Dunn is used to relate the pseudoextremals of the Maximum Principle to the characteristic canonical equations of Hamilton-Jacobi. Only those pseudoextremals with vanishing Hamiltonian H may arrive at the origin in time t_f less than the prescribed time T and still be fuel optimal for time T. By limiting the T-controllable region to the cylinder

$$-3\pi \leq x_1 \leq +3\pi$$

the complete time varying fuel optimal control law is derived. The control law is time varying because the time remaining for zeroing the state vector is an essential parameter. The T-bang-coast isochrone and the curve Γ_π^+ form the second switching locus.

The restriction $-3\pi \leq x_1 \leq +3\pi$ is imposed in order to limit a control sequence of type $\pm A, 0, \pm A, 0, \ldots$ to a sequence of at most three switchings. The third switching locus is derived by ordering the corresponding P-0-P type pseudoextremals in a special manner.

In chapter IV this restriction is removed and longer control sequences of type $\pm A, 0, \pm A, 0, \ldots$ are allowed to occur. By exploiting

the structure of such pseudoextremals established in chapter III, the fourth, fifth, and a disjoined third switching loci are generated. Although the resultant optimal control law is presented only for the control bound $A = 3$, the same switching structure is present for any bound $A > 1$. Only the shape and size of the switching surfaces is changed. The value $A = 3$ is selected as providing efficient zeroing of anticipated disturbances without requiring unduly large controllers. The solution is then applied to the actual earth pointing satellite problem in which the pitch error is driven to some multiple of $2k\pi$ while zeroing the error rate. Time varying indifference curves then subdivide the state space into periodic segments within which all states are driven to the same end point. The chosen value $A = 3$ is sufficient to guarantee that any pitch error can be corrected within π radians of orbit provided the pitch error rate is sufficiently small.

In chapter V the linear problem is compared to the nonlinear and an indication given of the large region for which the linearized solution predicts the nonlinear system performance with good accuracy. An efficient suboptimal design is proposed and evaluated.

APPENDIX A

DERIVATION OF CONTROLLED SATELLITE ATTITUDE MOTION

THE INERTIAL TORQUE

For a rigid satellite B, the inertial torque about the mass center B^* is well known (See Ref. [8].) From Fig. 1-1, $\bar{b}_1$, $\bar{b}_2$, and $\bar{b}_3$ form a right-handed set of orthogonal unit vectors which are parallel to the principal axes I_1, I_2, and I_3 of inertia of B for B^*. The inertial torque of the satellite B about B^* is given by

$$\begin{aligned}\bar{T}_I = {} & [\omega_2\omega_3(I_2-I_3)-\dot{\omega}_1 I_1]\bar{b}_1 + \\ & + [\omega_3\omega_1(I_3-I_1)-\dot{\omega}_2 I_2]\bar{b}_2 + \\ & + [\omega_1\omega_2(I_1-I_2)-\dot{\omega}_3 I_3]\bar{b}_3\end{aligned} \tag{A-1}$$

where ω_i, $i=1,2,3$ are the measure numbers of the angular velocity of B in inertial reference frame R for the basis $\bar{b}_i$, $i=1,2,3$. The dot $(\cdot)$ denotes differentiation with respect to time.

For the particular motion under consideration in which $\bar{b}_3$ remains normal to the orbital plane, the angular velocity ω is given by

$$\begin{aligned}\omega_1 &\equiv 0 \\ \omega_2 &\equiv 0 \\ \omega_3 &= \Omega + \dot{\theta}\end{aligned} \tag{A-2}$$

where Ω is the angular velocity of reference frame A with respect to inertial frame R and θ is the pitch coordinate as defined in Fig. 1-1. For the given motion of a satellite in circular orbit, Ω is

a constant and the inertial torque $\bar{T}_I$ simplifies to the expression

$$\bar{T}_I = -I_3 \dot{\theta} \bar{b}_3 \tag{A-3}$$

THE GRAVITATIONAL TORQUE

The gravitational torque is given by

$$\bar{T}_G = -\frac{3GM}{R^3} \times \bar{I}_{a_1} \tag{A-4}$$

(see Ref. [8]) where $\bar{a}_1$ is a unit vector along the line of centers of the earth and satellite, $\bar{I}_{a_1}$ is the second moment of B relative to B* for $\bar{a}_1$, i.e.,

$$\bar{I}_{a_1} = \begin{pmatrix} I_1 & 0 & 0 \\ 0 & I_2 & 0 \\ 0 & 0 & I_3 \end{pmatrix} \begin{bmatrix} (\bar{a}_1 \cdot \bar{b}_1) \\ (\bar{a}_1 \cdot \bar{b}_2) \\ (\bar{a}_1 \cdot \bar{b}_3) \end{bmatrix} \tag{A-5}$$

where $(\bar{a}_i \cdot \bar{b}_j)$ denotes the innerproduct of the vectors $\bar{a}_i$ and $\bar{b}_j$. The universal gravitational constant is G; the mass of the earth is M; and the distance between the mass centers of the earth and satellite is R. For a circular orbit the gravitational and centrifugal forces balance

$$\frac{GM}{R^2} = \Omega^2 R \tag{A-6}$$

and relation (A-4) may be rewritten

$$\bar{T}_G = -3\Omega^2 \bar{a}_1 \times \bar{I}_{a_1} \tag{A-7}$$

But from Fig. 1-1

$$\bar{a}_1 = \bar{b}_1 \cos\theta - \bar{b}_2 \sin\theta \tag{A-8}$$

Using (A-5), (A-7), and (A-8) we obtain the expressions

$$\bar{T}_G = -3\Omega^2 \bar{a}_1 \times (I_1 \cos\theta\, \bar{b}_1 - I_2 \sin\theta\, \bar{b}_2 + 0\bar{b}_3) \tag{A-9}$$

$$= -3\Omega^2 (I_1 \sin\theta \cos\theta\, \bar{b}_3 - I_2 \sin\theta \cos\theta\, \bar{b}_3) \tag{A-10}$$

$$= -3\Omega^2 K_3 I_3 \sin\theta \cos\theta\, \bar{b}_3 \tag{A-11}$$

If the control torque is denoted by

$$\bar{T}_c = M\bar{b}_3 \tag{A-12}$$

the total active torque on the satellite $\bar{T}_A$ is given by

$$\bar{T}_A = \bar{T}_G + \bar{T}_c = (-3\Omega^2 K_3 I_3 \sin\theta \cos\theta + M)\bar{b}_3 \tag{A-13}$$

Since the velocity of the mass center of the satellite is independent of $\dot{\theta}$ the generalized active force F_θ satisfies

$$F_\theta = \bar{\omega}_{,\dot{\theta}} \cdot \bar{T}_A \triangleq \frac{\partial \bar{\omega}}{\partial \dot{\theta}} \cdot \bar{T}_A = \bar{b}_3 \cdot \bar{T}_A \tag{A-14}$$

and the generalized inertial force F^* satisfies

$$F^*_\theta = \bar{\omega}_{,\dot{\theta}} \cdot \bar{T}_I = \bar{b}_3 \cdot \bar{T}_I = -I_3 \ddot{\theta} \tag{A-15}$$

But

$$F^*_\theta + F_\theta = 0 \tag{A-16}$$

or with the aid of relations (A-13), (A-14), and (A-15)

$$I_3\ddot{\theta} + 3\Omega^2 K_3 I_3 \sin\theta \cos\theta = M \qquad \text{(A-17)}$$

and the equation (1-9) for the pitch motion is verified.

APPENDIX B

TIME OPTIMAL POLICY FOR THE REDUCED AUXILIARY PROBLEM OF THEOREM 2-3

Consider the system

$$\dot{x}_4 = x_3 \tag{B-1}$$

$$\dot{x}_3 + -\tilde{u}x_4 \tag{B-2}$$

where the control $\tilde{u}$ satisfies the constraint

$$|\tilde{u}(t)| \leq 1 \quad \forall t \tag{B-3}$$

The Hamiltonian is

$$H = x_3 p_4 - \tilde{u} x_4 p_3 - p_o \tag{B-4}$$

and corresponding adjoint differential equations are

$$\dot{p}_4 = -\frac{\partial H}{\partial x_4} = \tilde{u} p_3 \tag{B-5}$$

$$\dot{p}_3 = -\frac{\partial H}{\partial x_3} = -p_4 \tag{B-6}$$

Our objective is to drive the phase point (x_4, x_3) from the initial position (1, free) to the fixed final state $(-1,0)$ in minimum time. The Hamiltonian H is maximized by the control law

$$\tilde{u} = \begin{cases} -1 & x_4 p_3 > 0 \\ +1 & x_4 p_3 < 0 \\ \text{Indeterminate} & x_4 p_3 = 0 \end{cases} \tag{B-7}$$

We begin by eliminating the possibility of a singular control generating a pseudoextremal. Should $x_4 p_3 = 0$ over a finite time interval (t_1, t_2) then either

$$\text{i)} \quad p_3 \equiv 0 \quad \text{on} \quad (t_1, t_2) \tag{B-8}$$

$$\text{ii)} \quad x_4 \equiv 0 \quad \text{on} \quad (t_1, t_2) \tag{B-9}$$

Taking first case (i)

$$p_3 \equiv 0 \quad \text{on} \quad (t_1, t_2) \Rightarrow p_4 \equiv 0 \quad \text{on} \quad (t_1, t_2) \tag{B-10}$$

Because our adjoint equations are linear and homogeneous, the only continuous solution valid for all t and satisfying equation (B-10) on (t_1, t_2) is the trivial solution $p_4 \equiv p_3 \equiv 0 \ \forall t$. Such a trivial solution does not satisfy the necessary conditions of Pontryagin's theorem (Ref. [2]).

Analogous reasoning for case (ii) yields only the trivial solution $x_4 \equiv x_3 \equiv 0 \ \forall t$, a solution which fails to meet the requirements of our mission. Thus without loss of generality, we may limit the control to the values $+1$ and -1 seeking the time optimal solution.

The boundary conditions for this problem are

$$\begin{aligned} x_4(0) &= 1 \qquad & x_4(t_f) &= -1 \\ x_3(0) &\text{ free} \qquad & x_3(t_f) &= 0 \end{aligned} \tag{B-11}$$

and the transversality condition is

$$p_3(0) = 0 \tag{B-12}$$

Switchings occur only at zeros of $p_3(t)$ and $x_4(t)$ where p_3 and x_4 are governed by the differential equations

$$\ddot{p}_3(t) + \tilde{u}p_3(t) = 0 \tag{B-13}$$

$$\ddot{x}_4(t) + \tilde{u}x_4(t) = 0 \tag{B-14}$$

and $\tilde{u}$ is either 1 or -1. Letting $p_{3,-1}$ denote the solution to (B-13) for $\tilde{u}$ initially = -1 and $p_{3,+1}$ denote the solution for $\tilde{u}$ initially = +1 the only solutions to equation (B-13) meeting requirement (B-12) valid in some neighborhood of $t = 0$ up to the time of the first switching t_s are

$$p_{3,-1} = C_1 \sinh t \qquad t\epsilon[0,t_s] \tag{B-15}$$

$$p_{3,+1} = C_2 \sin t \qquad t\epsilon[0,t_s] \tag{B-16}$$

where C_1 and C_2 are constants of integration. These solutions remain pseudoextremals until either

$$\text{i)} \quad x_4(t_s) = 0 \quad t_s > 0 \tag{B-17}$$

or

$$\text{ii)} \quad p_3(t_s) = 0 \quad t_s > 0 \tag{B-18}$$

at which time a switching occurs. From (B-13) and (B-14) we see that both $p_3(t)$ and $x_4(t)$ solutions consist of alternating trignometric and hyperbolic arcs. We first consider all possible solutions

corresponding to $\tilde{u}$ being initially $+1$ which could yield an optimal time of solution less than π. After completing this task, we then consider those solutions for which $\tilde{u}$ is initially -1. Now $p_{3,+1}(t_s) = 0$ again for the first time at

$$t_s = \pi \tag{B-19}$$

Therefore assuming

$$x_4(t_s) = 0 \tag{B-20}$$

in a time t_s such that

$$t_s \leq \pi \tag{B-21}$$

The control remains constant $(+1)$ until

$$x_4(t) = 0 \tag{B-22}$$

at which time the first switching occurs. Up to the first switching t_s

$$x_{4,+1}(t) = \cos t + B_1 \sin t \quad t\epsilon[0,t_s] \tag{B-23}$$

at which time a switching occurs and the solutions $p_{3,+1}(t)$ and $x_{4,+1}(t)$ are extended by

$$p_{3,+1}(t) = C_1 \sin t_s \cosh(t-t_s) + C_1 \cos t_s \sinh(t-t_s) \tag{B-24}$$

$$x_{4,+1}(t) = D_1 \sinh(t-t_s) \qquad t\epsilon[t_s,t_r] \tag{B-25}$$

to the interval $[t_s,t_r]$ where t_r denotes the time of the second switching, i.e., the smallest $t_r > t_s$ such that either

$$p_{3,+1}(t_r) = 0 \tag{B-26}$$

or

$$x_{4,+1}(t_r) = 0 \tag{B-27}$$

But from (B-25) $x_{4,+1}(t)$ never again vanishes. Should a second switching occur, it could only have been induced by a zero of $p_{3,+1}(t)$ in which case

$$\sin t_s \cosh(t_r - t_s) + \cos t_s \sinh(t_r - t_s) = 0 \tag{B-28}$$

Since $\cosh(t_r - t_s)$ and $\sinh(t_r - t_s)$ are both positive, equation (B-27) implies that

$$t_s > \frac{\pi}{2} \tag{B-29}$$

But from equations (B-22) and (B-23)

$$\cos t_s + B_1 \sin t_s = 0 \tag{B-30}$$

Recalling also that $t_s < \pi$ we find that

$$B_1 > 0 \tag{B-31}$$

and that $x_{4,+1}(t)$ behaves as shown in Fig. B-1 up to the first switching. But such a solution can not be time optimal because clearly the solution beginning at point B of Fig. B-1 would use less time. We conclude that no solution beginning with control initially $+1$ and having two or more switchings can meet boundary conditions (B-11) and be time optimal, if the minimum time is to be less than π. Inasmuch

as $x_4(t)$ must be zero for some $t\epsilon(0,t_f)$ in order to satisfy (B-11), there must be at least one switching. A path containing but one switching is the only candidate remaining for which the optimal time of solution might be less than π. Differentiating equation (B-25) we get

$$x_{3,+1}(t) = \dot{x}_{4,+1}(t) = D_1\cosh(t-t_s) \quad t > t_s \tag{B-32}$$

which is never zero. We can not meet the terminal boundary condition $x_3(t_f) = 0$ with a path having only one switching which begins with the control initially $+1$. Hence there is no optimal path having control initially $+1$, if the minimum time for solution is indeed less than π. We now return to those solutions beginning with control initially -1 in anticipation of finding just such a solution.

Now from the expression (B-15) for $p_{3,-1}(t)$ valid up to the first switching, we see that the first switching can not be induced by a zero of $p_{3,-1}(t)$. Up to the first switching

$$x_{4,-1}(t) = A_2\cosh t + B_2\sinh t \quad t\epsilon[0,t_s] \tag{B-33}$$

Applying the initial boundary condition of (B-11)

$$x_{4,-1}(t) = \cosh t + B_2\sinh t \quad t\epsilon[0,t_s] \tag{B-34}$$

To meet the boundary conditions $x_4(t)$ must necessarily pass through zero at which time t_s the first switching occurs.

$$x_{4,-1}(t_s) = \cosh t_s + B_2\sinh t_s = 0 \tag{B-35}$$

from which B_2 may be evaluated

$$B_2 = - \frac{\cosh t_s}{\sinh t_s} \tag{B-36}$$

Extending the solution for $x_{4,-1}(t)$ beyond the first switching we obtain the expressions

$$x_{4,-1}(t) = D_2 \sin(t-t_s) \qquad t\epsilon[t_s,t_r] \tag{B-37}$$

$$x_{3,-1}(t) = \dot{x}_{4,-1}(t) = D_2 \cos(t-t_s) \qquad t\epsilon[t_s,t_r] \tag{B-38}$$

valid up to the time of second switching t_r. But from expression B(-34) and (B-36)

$$\begin{aligned} x_{3,-1}(t_s) &= \sinh t_s + \left(- \frac{\cosh t_s}{\sinh t_s} \right) \cosh t_s \\ &= - \frac{1}{\sinh(t_s)} \end{aligned} \tag{B-39}$$

from which we may evaluate the constant D_2 of equation (B-38). Therefore up to the second switching, $x_{4,-1}(t)$ is given by

$$x_{4,-1}(t) = - \frac{\sin(t-t_s)}{\sinh t_s} \qquad t\epsilon[t_s,t_r] \tag{B-40}$$

and

$$x_{3,-1}(t) = \dot{x}_{4,-1}(t) = - \frac{\cos(t-t_s)}{\sinh t_s} \qquad t\epsilon[t_s,t_r] \tag{B-41}$$

Such a solution meets the terminal boundary conditions (B-11) in time $\pi/2 + \text{arc sinh } 1$.

Now

$$x_{3,-1}(t_f) = 0 \Rightarrow \cos(t_f - t_s) = 0 \tag{B-42}$$

which first occurs for

$$t_f = t_s = \pi/2 \tag{B-43}$$

$$x_{4,-1}(t_f) = -1 \Rightarrow -\frac{\sin(t_f - t_s)}{\sinh t_s} = -1 \tag{B-44}$$

Substituting for t_f from (B-43) into equation (B-44) we find

$$\sinh t_s = 1 \tag{B-45}$$

which together with equation (B-43) yields

$$t_f = \operatorname{arcsinh} 1 + \pi/2 \approx .78\pi \tag{B-46}$$

as asserted. If we now demonstrate that any solution $x_{3,-1}(t)$ having more than one switching requires a time of solution greater than π, then the solution $x_{3,-1}(t)$ with one switching must be optimal, and the minimum time is infact $\pi/2 + \operatorname{arcsinh} 1$.

In order that the second switching occur in time $t_r < \pi$, it must be induced by a zero of $p_{3,-1}(t)$. A second switching induced by a zero of $x_{4,-1}(t)$ would occur at time $t_r = t_s + \pi$ from expression (B-37). The solution $p_{3,-1}(t)$ as given by (B-15) may be extended to the interval $[t_s, t_r]$ by

$$p_{3,-1}(t) = C_1 \sinh t_s \cos(t - t_s) + C_1 \cosh t_s \sin(t - t_s) \tag{B-47}$$

At the second switching then

$$\sinh t_s \cos(t_r - t_s) + \cosh t_s \sin(t_r - t_s) = 0 \qquad \text{(B-48)}$$

which can only occur for

$$t_r - t_s > \pi/2 \qquad \text{(B-49)}$$

We now demonstrate that such a two switching solution can not meet the terminal boundary conditions (B-11) within time π. Extending the solutions for $x_{4,-1}(t)$ and $x_{3,-1}(t)$ as given by equations (B-37) and (B-38) on to the interval $[t_r, t_f]$ we obtain

$$x_{4,-1}(t) = D_2 \sin(t_r - t_s)\cosh(t - t_r) + D_2 \cos(t_r - t_s)\sinh(t - t_r) \qquad \text{(B-50)}$$

$$x_{3,-1}(t) = + D_2 \sin(t_r - t_s)\sinh(t - t_r) + D_2 \cos(t_r - t_s)\cosh(t - t_r) \qquad \text{(B-51)}$$

In order that

$$x_{3,-1}(t_f) = 0 \qquad \text{(B-52)}$$

we must require rearranging (B-51) that

$$\cosh(t_f - t_r)\cos(t_r - t_s) + \sinh(t_f - t_r)\sin(t_r - t_s) = 0 \qquad \text{(B-53)}$$

The condition for the second switching (B-48) and equation (B-53) can simultaneously hold only if the determinate of the coefficients of $\cos(t_r - t_s)$ and $\sin(t_r - t_s)$ vanishes; namely,

$$\sinh t_s \sinh(t_f - t_r) - \cosh t_s \cosh(t_f - t_r) = 0 \qquad \text{(B-54)}$$

or

$$\cosh[(t_f - t_r) - t_s] = 0 \qquad \text{(B-55)}$$

which is impossible. Therefore a solution $x_{3,-1}(t)$ with two switchings within time π cannot satisfy the boundary conditions (B-11).

We now demonstrate that in order for three switchings to occur on an $x_{3,-1}(t)$ solution, the time of the third switching t_q must be greater than π. If this be true, then the solution given by (B-40) must be the minimum time solution because we finally have demonstrated that any other solution satisfying the maximum principle and meeting our boundary conditions (B-11) requires more time.

We already have ssen that the second switching must have been induced by a zero of $p_{3,-1}(t)$ in order that t_r be less than π. Therefore up to the third switching at time t_q we have

$$p_{3,-1}(t) = E_1 \sinh(t - t_r) \qquad t \epsilon [t_r, t_q] \qquad \text{(B-56)}$$

an expression which is never again zero. The third switching must be induced by a zero of $x_{4,-1}(t)$.

$$x_{4,-1}(t_q) = 0 \qquad \text{(B-57)}$$

But at the first switching

$$x_{4,-1}(t_s) = 0 \qquad \text{(B-58)}$$

therefore for some t_m such that

$$t_s < t_m < t_q \tag{B-59}$$

the derivative of $x_{4,-1}(t)$ must vanish.

$$\dot{x}_{4,-1}(t_m) = x_{3,-1}(t_m) = 0 \tag{B-60}$$

But requirement (B-60) is just equation (B-53) with t_f replaced by t_m. Reconstructing the same argument as before we obtain

$$\cosh[t_m - t_r - t_s] = 0 \tag{B-61}$$

which is impossible. Hence three switchings must require more time than π. The only solution satisfying the maximum principle and the boundary conditions (B-11) in time less than π is that $x_{4,-1}(t)$ solution having one switching. The minimum time for the problem must be $\pi/2$ + arcsinh 1.

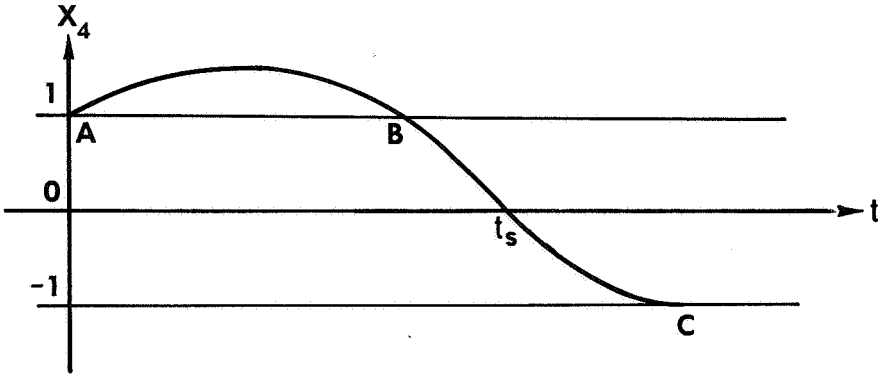

Fig. B-1. Solution BC Requires Less Time Than Solution ABC.

APPENDIX C

SOLUTION FOR THE ADJOINT VARIABLES

We now week to integrate the adjoint differential equations along a state trajectory in the backward time direction, i.e., integrate

$$\lambda_2''(\tau) + \cos y_1(\tau)\, \lambda_2(\tau) = 0 \tag{C-1}$$

along the path

$$y_1' = -y_2 \tag{C-2}$$

$$y_2' = \sin y_1 - u \tag{C-3}$$

where u is +A, -A, or 0. We note that

$$\frac{d\lambda_2}{d\tau} = \frac{d\lambda_2}{dy_1}\frac{dy_1}{d\tau} = -\frac{d\lambda_2}{dy_1}\, y_2 \tag{C-4}$$

$$\frac{d^2\lambda_2}{d\tau^2} = \frac{d\lambda_2^2}{dy_1^2}\, y_2^2 + \frac{d\lambda_2}{dy_1}\,[u-\sin y_1] \tag{C-5}$$

Substituting $\dfrac{d^2\lambda_2}{d\tau^2}$ into (C-1), we get

$$y_2^2 \frac{d\lambda_2^2}{dy_1^2} + [u-\sin y_1]\frac{d\lambda_2}{dy_1} + \lambda_2 \cos y_1 = 0 \tag{C-6}$$

If we consider only those trajectories which do not cross the y_1 axis (y_2 never zero) then

$$y_2^2 \frac{d\lambda_2^2}{dy_1^2} + 2[u-\sin y_1] \frac{d\lambda_2}{dy_1} + [\sin y_1 - u] \frac{d\lambda_2}{dy_1} + \lambda_2 \cos y_1 =$$

$$\frac{d}{dy_1} [y_2^2 \frac{d\lambda_2}{dy_1} + \lambda_2 \sin y_1 - u \lambda_2] = 0 \qquad (C-7)$$

Hence, integrating we get

$$y_2^2 \frac{d\lambda_2}{dy_1} + \lambda_2 \sin y_1 - u\lambda_2 = c_1 \qquad (C-8)$$

or

$$\frac{c_1}{y_2^2} = \frac{d\lambda_2}{dy_1} + \frac{(\sin \mathbf{y}_1 - u)\lambda_2}{y_2^2} = \frac{d\lambda_2}{dy_1} + \frac{\lambda_2}{y_2^2} \frac{dy_2}{d\tau} = \frac{d\lambda_2}{dy_1} - \frac{\lambda_2}{y_2} \frac{dy_2}{dy_1} \qquad (C-9)$$

thus

$$\frac{c_1}{y_2^3} = \frac{1}{y_2} \frac{d\lambda_2}{dy_1} - \frac{\lambda_2}{y_2^2} \frac{dy_2}{dy_1} = \frac{d}{dy_1} (\frac{\lambda_2}{y_2}) \qquad (C-10)$$

Integrating

$$\frac{\lambda_2}{y_2} = c_2 + c_1 \int_{y_{1s}}^{y_1} \frac{d(\sigma)}{y_2^3(\sigma)} \qquad (C-11)$$

then

$$\lambda_2 = y_2 \left[c_2 + c_1 \int_{y_{1s}}^{y_1} \frac{d\sigma}{y_2^3(\sigma)} \right] \qquad (C-12)$$

and

$$\lambda_1 = \lambda_2' = -\frac{c_1}{y_2} + (\sin y_1 - u)\left[c_2 + c_1 \int_{y_{1s}}^{y_1} \frac{d\sigma}{y_2^3(\sigma)}\right] \qquad (C\text{-}13)$$

From the initial condition $\tau = \tau_s$

$$\lambda_2(\tau_s) \triangleq \lambda_{2s} = 1 \qquad (C\text{-}14)$$

we get

$$c_2 = \frac{\lambda_{2s}}{y_{2s}} = \frac{1}{y_{2s}} \qquad (C\text{-}15)$$

and

$$\lambda_{1s} = -\frac{c_1}{y_{2s}} + (\sin y_{1s} - u)c_2 \qquad (C\text{-}16)$$

or

$$c_1 = -\lambda_{1s}\, y_{2s} + (\sin y_{1s} - u)\lambda_{2s} = H_B - |u| \qquad (C\text{-}17)$$

Therefore (C-13) becomes

$$\lambda_2 = y_2\left[\frac{\lambda_{2s}}{y_{2s}} + (H_B - |u|) \int_{y_{1s}}^{y_1} \frac{d\sigma}{y_2^3(\sigma)}\right] \qquad (C\text{-}18)$$

or along an 0-arc having last switching at (y_{1s}, y_{2s})

$$\lambda_2 = y_2\left[\frac{1}{y_{2s}} + H_B \int_{y_{1s}}^{y_1} \frac{d\sigma}{y_2^3(\sigma)}\right]$$

APPENDIX D

SOLUTION FOR THE ADJOINT VARIABLES WHEN EITHER THE INITIAL OR FINAL POINT IS ON THE y_1 AXIS

INITIAL POINT ON THE y_1 AXIS

We wish to integrate the differential equation

$$y_2^2 \frac{d\lambda^2}{dy_1^2} + (u-\sin y_1) \frac{d\lambda_2}{dy_1} + \lambda_2 \cos y_1 = 0 \qquad \text{(D-1)}$$

along a P,O, or N-arc starting from the singular point $M(y_{1m},0)$. Our previous expression for the adjoint variables as derived in Appendix C; namely (C-18), is invalid for this point $M(y_{1m},0)$. The term $\frac{\lambda_{2s}}{y_{2s}}$ becomes infinite for $y_{2s} \to 0$ as does the term $\int_{y_{1s}}^{y_1} \frac{d\sigma}{y_2^3(\sigma)}$ because of the integrand. Then repeating the development of Almuzara's Appendix B Ref. [2], we transform the integral in such a way that its principle part cancels the corresponding principle part of λ_{2s}/y_{2s}. As we proceed to the limit we obtain a finite expression for λ_2.

Near the singular point $M(x_{1m},0)$ we have the following series expansions:

$$\sin y_1 = \sin y_{1m} + \cos y_{1m}(y_1-y_{1m}) + o[(y_1-y_{1m})^2] \qquad \text{(D-2)}$$

$$\frac{y_2^2}{2} = (u-\sin y_{1m})(y_1-y_{1m}) + o[(y_1-y_{1m})^2] \qquad \text{(D-3)}$$

$$y_2 = \pm\{2(u-\sin y_{1m})(y_1-y_{1m})\}^{1/2} + o[(y_1-y_{1m})^{3/2}] \qquad (D\text{-}4)$$

$$\frac{1}{y_2} = \pm\{2(u-\sin y_{1m})(y_1-y_{1m})\}^{-1/2} + o[(y_1-y_{1m})^{1/2}] \qquad (D\text{-}5)$$

$$\frac{1}{y_2^3} = \pm\{2(u-\sin y_{1m})(y_1-y_{1m})\}^{-3/2}$$

$$\pm 3\cos y_{1m}\{2^{-5}(u-\sin y_{1m})^{-5}(y_1-y_{1m})^{-1}\}^{1/2} + o[(y_1-y_{1m})^{1/2}] \qquad (D\text{-}6)$$

where the plus sign is to be used for arcs above the y_1 axis and minus sign for arcs below the y_1 axis. At this point we will need to distinguish between P-arcs and N or O arcs in order to factor such expressions as in (D-4) in a meaningful way.

For a P-arc

$$\{(u-\sin y_{1m})(y_1-y_{1m})\}^{1/2} = (u-\sin y_{1m})^{1/2}(y_1-y_{1m})^{1/2}$$

whereas for an N or O-arc

$$\{(u-\sin y_{1m})(y_1-y_{1m})\}^{1/2} = (\sin y_{1m}-u)^{1/2}(y_{1m}-y_1)^{1/2}$$

in order that we always deal with real numbers. Then assuming we are integrating along an N or O-arc in which case the plus sign is to be used

$$\int_{y_{1s}}^{y_1} \frac{d\sigma}{y_2^3(\sigma)} = \int_{y_{1s}}^{y_1} \left[\frac{1}{y_2^3(\sigma)} - \frac{1}{\{2(u-\sin y_{1m})(\sigma-y_{1m})\}^{3/2}}\right] d\sigma +$$

$$+ \{2(\sin y_{1m}-u)\}^{-3/2} \int_{y_{10}}^{y_1} \frac{d\sigma}{(y_{1m}-\sigma)^{3/2}} \qquad \text{(D-7)}$$

$$= \int_{y_{1s}}^{y_1} \left[\frac{1}{y_2^3(\sigma)} - \frac{1}{\{2(u-\sin y_{1m})(\sigma-y_{1m})\}^{3/2}}\right] d\sigma +$$

$$+ \frac{\sin(y_{1m}-u)^{-3/2}}{\sqrt{2}} \left[\frac{1}{(y_{1m}-y_1)^{1/2}} - \frac{1}{(y_{1m}-y_{1s})^{1/2}}\right]$$

(D-8)

Also

$$\frac{1}{y_{2s}} = \{2(u-\sin y_{1m})(y_{1s}-y_{1m})\}^{-1/2} + o[(y_{1s}-y_{1m})^{1/2}] \qquad \text{(D-9)}$$

Substituting (D-8) and (D-9) into (C-18), we get

$$\lambda_2(\tau) = y_2\Big\{\lambda_{2s}[2(u-\sin y_{1m})(y_{1s}-y_{1m})]^{-1/2} + o[(y_{1s}-y_{1m})^{1/2}] +$$

$$+ (H_B-|u|) \int_{y_{1s}}^{y_1} \left[\frac{1}{y_2^3(\sigma)} - \frac{1}{[2(u-\sin y_{1m})(\sigma-y_{1m})]^{3/2}}\right] d\sigma$$

$$+ \frac{(H_B-|u|)}{\sqrt{2}(\sin y_{1m}-u)^{3/2}} \left[\frac{1}{(y_{1m}-y_1)^{1/2}} - \frac{1}{(y_{1m}-y_{1s})^{1/2}}\right]\Big\}$$

(D-10)

or

$$\lambda_2(\tau) = y_2\Big\{[2(u-\sin y_{1m})^3(y_{1s}-y_{1m})]^{-1/2}[-\lambda_{2s}(\sin y_{1m}-u) +$$

$$+ H_B-|u|] + o[(y_{1s}-y_{1m})^{1/2}] +$$

$$+ (H_B-|u|)\int_{y_{1s}}^{y_1}\left[\frac{1}{y_2^3(\sigma)} - \frac{1}{[2(u-\sin y_{1m})(\sigma-y_{1m})]^{3/2}}\right]d\sigma$$

$$+ \frac{(H_B-|u|)}{\sqrt{2}(\sin y_{1m}-u)^{3/2}} \cdot \frac{1}{(y_{1m}-y_1)^{1/2}}\Big\} \qquad \text{(D-11)}$$

But from (D-2) we have

$$\sin y_{1m} = \sin y_{1s} - \cos y_{1m}(y_{1s}-y_{1m}) + o[(y_{1s}-y_{1m})^2] \qquad \text{(D-12)}$$

The expression $-\lambda_{2s}(\sin y_{1m}-u) + H_B-|u|$ becomes

$$-\lambda_{2s}(\sin y_{1s}-u)+H_B-|u|-\lambda_{2s}\cos y_{1m}(y_{1s}-y_{1m})+o[(y_{1s}-y_{1m})^2] \qquad \text{(D-13)}$$

$$= -\lambda_{1s}y_{2s}-\lambda_{2s}\cos y_{1m}(y_{1s}-y_{1m}) + o[(y_{1s}-y_{1m})^2] \qquad \text{(D-14)}$$

$$= -\lambda_{1s}[2(u-\sin y_{1m})(y_1-y_{1m})]^{1/2} + o[(y_{1s}-y_{1m})] \qquad \text{(D-15)}$$

Substituting (D-15) into (D-11) we get

$$\lambda_2(\tau) = y_2\left\{\frac{\lambda_{1s}}{(\sin y_{1m}-u)} + o[(y_{1s}-y_{1m})^{1/2}] + \right.$$

$$+ (H_B-|u|)\int_{y_{1s}}^{y_1}\left[\frac{1}{y_2^3(\sigma)} - \frac{1}{[2(u-\sin y_{1m})(\sigma-y_{1m})]^{3/2}}\right]d\sigma$$

$$\left. + \frac{(H_B-|u|)}{\sqrt{2}(\sin y_{1m}-u)^{3/2}} \cdot \frac{1}{(y_{1m}-y_1)^{1/2}}\right\} \qquad \text{(D-16)}$$

If we now allow the initial point S to approach M we obtain in the limit

$$\lambda_2(\tau) = \frac{\lambda_{1m}}{(\sin y_{1m}-u)} + \frac{(H_B-|u|)}{[2(u-\sin y_{1m})^3(y_1-y_{1m})]^{1/2}} +$$

$$+ (H_B-|u|)\int_{y_{1m}}^{y_1}\left[\frac{1}{y_2^3(\sigma)} - \frac{1}{[2(u-\sin y_{1m})(\sigma-y_{1m})]^{3/2}}\right]d\sigma \qquad \text{(D-17)}$$

where now the integral is finite for any finite y_1.

FINAL POINT ON THE y_1 AXIS

Looking at our expression for $\lambda_2(\tau)$

$$\lambda_2(\tau) = y_2\left[\frac{\lambda_{2s}}{y_{2s}} + (H_B-|u|)\int_{y_{1s}}^{y_1}\frac{d\sigma}{y_2^3(\sigma)}\right] \qquad \text{(D-18)}$$

we seek the limit as $y_1 \to y_{1m}$ of

$$\lim_{y_1\to y_{1m}} y_2\int_{y_{1s}}^{y_1}\frac{d\sigma}{y_2^3(\sigma)} = \lim_{y_1\to y_{1m}}\frac{y_2}{\left[\int_{y_{1s}}^{y_1}\frac{d\sigma}{y_2^3(\sigma)}\right]^{-1}} \qquad \text{(D-19)}$$

Applying L'Hospital rule

$$\lim_{y_1 \to y_{1m}} \frac{y_2}{\left[\int_{y_{1s}}^{y_1} \frac{d\sigma}{y_2^3(\sigma)}\right]^{-1}} = \lim_{y_1 \to y_{1m}} \frac{\dfrac{\sin y_1 - u}{-y_2}}{\dfrac{\frac{1}{y_2^3}(-y_2)}{\left[\int_{y_{1s}}^{y_1} \frac{d\sigma}{y_2^3(\sigma)}\right]^2}} \tag{D-20}$$

$$= (\sin y_1 - u)\left\{\lim_{y_1 \to y_{1m}} \left[y_2 \int_{y_{1s}}^{y_1} \frac{d\sigma}{y_2^3(\sigma)}\right]\right\}^2 \tag{D-21}$$

From (D-19) and (D-21)

$$\lim_{y_1 \to y_{1m}} y_2 \int_{y_{1s}}^{y_1} \frac{d\sigma}{y_2^3(\sigma)} = \frac{1}{(\sin y_1 - u)} \tag{D-22}$$

Therefore

$$\lambda_{2m} = \lim_{\substack{y_1 \to y_{1m} \\ y_2 \to 0}} \lambda_2 = \frac{H_B - |u|}{(\sin y_1 - u)} \tag{D-23}$$

Now for $y_2 \neq 0$

$$\lambda_1(\tau) = -\frac{(H_B - |u|) + \lambda_2(\tau)(\sin y_1 - u)}{y_2} \tag{D-24}$$

or using (D-18)

$$\lambda_1(\tau) = -\frac{H_B - |u|}{y_2} + (\sin y_1 - u)\left[\frac{\lambda_{2s}}{y_{2s}} + (H_B - |u|)\int_{y_{1s}}^{y_1} \frac{d\sigma}{y_2^3(\sigma)}\right] \tag{D-25}$$

Now we seek the value of $\lambda_1(\tau)$ at the singular point M. Near $M(y_{1m},0)$ we have

$$\frac{1}{y_2} = -[2(u-\sin y_{1m})(y_1-y_{1m})]^{-1/2}+o[(y_1-y_{1m})^{1/2}] \qquad (D\ 26)$$

$$\frac{1}{y_2^3} = -[2(u-\sin y_{1m})(y_1-y_{1m})]^{-3/2} -$$

$$- 3\cos y_{1m}[2(u-\sin y_{1m})]^{-5/2}+o[(y_1-y_{1m})^{1/2}] \qquad (D\text{-}27)$$

If we again assume we are on an N or O-arc so as to factor square roots properly then

$$\int_{y_{1s}}^{y_1} \frac{d\sigma}{y_2^3(\sigma)} = \int_{y_{1s}}^{y_1} \left[\frac{1}{y_2^3(\sigma)} + \frac{1}{[2(u-\sin y_{1m})(\sigma-y_{1m})]^{3/2}}\right] d\sigma -$$

$$- [2(\sin y_{1m}-u)]^{-3/2} \int_{y_{1s}}^{y_1} \frac{d\sigma}{(y_{1m}-\sigma)^{3/2}} \qquad (D\text{-}28)$$

$$= \int_{y_{1s}}^{y_1} \left[\frac{1}{y_2^3(\sigma)} + \frac{1}{[2(u-\sin y_{1m})(\sigma-y_{1m})]^{3/2}}\right] d\sigma -$$

$$- \frac{(\sin y_{1m}-u)^{-3/2}}{\sqrt{2}} \left[\frac{1}{(y_{1m}-y_1)^{1/2}} - \frac{1}{(y_{1m}-y_{1s})^{1/2}}\right]$$

$$(D\text{-}29)$$

Substituting (D-26) and (D-29) into (D-25) we get

$$\lambda_1(\tau) = (H_B-|u|)[2(u-\sin y_{1m})(y_1-y_{1m})]^{-1/2}+o[y_{1m}-y_{1m})^{1/2}] +$$

$$+ (\sin y_1-u)\left\{\frac{\lambda_{2s}}{y_{2s}} + (H_B-|u|)\int_{y_{1s}}^{y_1}\left[\frac{1}{y_2^3(\sigma)} +\right.\right.$$

$$\left.\left. + \frac{1}{[2(u-\sin y_{1m})(\sigma-y_{1m})]^{3/2}}\right] d\sigma +\right.$$

$$\left. - \frac{(H_B-|u|)}{\sqrt{2}(\sin y_{1m}-u)^{3/2}}\left[\frac{1}{(y_{1m}-y_1)^{1/2}} - \frac{1}{(y_{1m}-y_{1s})^{1/2}}\right]\right\} \qquad \text{(D-30)}$$

Collecting and rearranging terms we obtain

$$\lambda_1(\tau) = (\sin y -u)\left\{\frac{\lambda_{2s}}{y_{2s}} + (H_B-|u|)\int_{y_{1s}}^{y_1}\left[\frac{1}{y_2^3(\sigma)} +\right.\right.$$

$$\left.\left. + \frac{1}{[2(u-\sin y_{1m})(\sigma-y_{1m})]^{3/2}}\right] d\sigma\right\} +$$

$$+ \frac{(H_B-|u|)}{[2(\sin y_{1m}-u)(y_{1m}-y_{1s})]^{1/2}} + o[(y_1-y_{1m})^{1/2}] \qquad \text{(D-31)}$$

as $y_1 \to y_{1m}$ then

$$\lambda_{1m} \triangleq \lim_{y_1 \to y_{1m}} \lambda_2(y_1) = (\sin y_{1m} - u)\left\{ \frac{\lambda_{2s}}{y_{2s}} + \right.$$

$$+ (H_B - |u|) \int_{y_{1s}}^{y_{1m}} \left[\frac{1}{y_2^3(\sigma)} + \frac{1}{[2(u - \sin y_{1m})(\sigma - y_{1m})]^{3/2}} \right] d\sigma \Bigg\}$$

$$+ \frac{(H_B - |u|)}{[2(\sin y_{1m} - u)(y_{1m} - y_{1s})]^{1/2}} \qquad \text{(D-32)}$$

where as before the integral is now finite. If we now consider first the point $M(y_{1m}, 0)$ as the end point of an arc and then use that value of λ_{1m} given by (D-32) as the new initial condition on $\lambda_1(\tau)$ (as new λ_{1s}) for continuing the integration across the y_1 axis into the upper half of plane via (D-17), we obtain

$$\lambda_2(\tau) = \left\{ \frac{\lambda_{2s}}{y_{2s}} + (H_B - |u|) \int_{y_{1s}}^{y_{1m}} \left[\frac{1}{y_2^3(\sigma)} + \right. \right.$$

$$\left. \left. + \frac{1}{[2(u - \sin \mathbf{y}_{1m})(\sigma - y_{1m})]^{3/2}} \right] d\sigma \right\} +$$

$$+ \frac{(H_B - |u|)}{[2(\sin y_{1m} - u)^3 (y_{1m} - y_{1s})]^{1/2}} + \frac{(H_B - |u|)}{[2(u - \sin y_{1m})^3 (y_1 - y_{1m})]^{1/2}} +$$

$$+ (H_B - |u|) \int_{y_1}^{y_{1m}} \left[\frac{-1}{y_2^3(\sigma)} + \frac{1}{[2(u - \sin y_{1m})(\sigma - y_{1m})]^{3/2}} \right] d\sigma$$

$$\text{(D-33)}$$

The expression (D-34) is valid for $\lambda_2(\tau)$ for $y_2 > 0$. If the initial point $S(y_{1s}, y_{2s})$ is a P-0 corner, i.e.,

$$\lambda_{2s} = 1 \tag{D-34}$$

and we are integrating along an 0-arc so that

$$u = 0 \tag{D-35}$$

We obtain (3-23) after noting that

$$y_2^2(\sigma) = y_{2s}^2 + 2(\cos\ \sigma - \cos\ y_{1s}) \tag{D-36}$$

along the 0-arc through the point S.

APPENDIX E

COMPLETION OF PROOF OF LEMMA 3-4

Herein we will demonstrate that given (y_{1s},y_{2s}) and (y_{1r},y_{2r}) as first and second switch points of a P-O-P$\cdots$ pseudoextremal, the term $F(y_{1r})$ satisfies

$$F(y_{1r}) > 0 \quad \text{for} \quad y_{1r} > y_{1s} \tag{E-1}$$

from (3-117) we have

$$F(y_{1r}) = -\frac{\lambda_{1s}}{y_{2s}^2} - 2A\int_{y_{1s}}^{y_{1r}} \frac{\lambda_1(\sigma)y_2(\sigma)}{y_2^5(\sigma)}\,d\sigma \tag{E-2}$$

where λ_{1s} is that value of the adjoint λ_1 at the first switching which produces a second switching at (y_{1r},y_{2r}). For a particular O-arc λ_{1s} becomes a function of y_{1r} alone. Along such an O-arc y_{2s} and $y_2(\sigma)$ do not depend upon y_{1r} but $\lambda_1(\sigma)$ is actually y_{1r} dependent

$$\lambda_1(\sigma) = \lambda_1(\sigma,y_{1r}) \tag{E 3}$$

for $\lambda_1(\sigma)$ is that value of the adjoint λ_1 at $y_1 = \sigma$ which produces a switching at y_{1r}. Our notation in (E-2) is thereby justified.

We first note that for $y_{1r} = y_{1s}$ the second switching point R coincides with the first switching point S. This limiting case

corresponds to the adjoint λ_2 being tangent to the line $\lambda_2(\tau) \equiv 1$ from above. At the tangent point y_{1s} the derivative λ_{1s} vanishes. Hence

$$F(y_{1r})\Big|_{y_{1r}=y_{1s}} = 0 \tag{E-4}$$

If now the variation δF due to a positive variation δy_{1r} (corresponding to moving the second switch point to the right an amount δy_{1r} along the fixed 0-arc) is always positive, then relation (E-1) will be verified once we note that every term of (E-2) is of continuous variation. From (E-2) we have

$$\delta F = -\frac{\delta\lambda_{1s}}{y_{2s}^2} - \frac{2A\lambda_{1r}}{y_{2r}^4} - 2A\int_{y_{1s}}^{y_{1r}} \frac{\delta\lambda_1(\sigma)y_2}{y_2^5}\, d\sigma \tag{E-5}$$

where $\delta\lambda_1(\sigma)$ is the change in λ_1 at $y_1 = \sigma$ necessary to move the point of second switching by δy_{1r}. With $\delta\lambda_2(\sigma)$ likewise defined we have

$$(\lambda_1+\delta\lambda_1)' = -\cos y_1(\lambda_2+\delta\lambda_2) \tag{E-6}$$

or since

$$\lambda_1'(\tau) = -\cos y_1\lambda_2(\tau) \tag{E-7}$$

the relation

$$\delta\lambda_1' = -\cos y_1\delta\lambda_2 \tag{E-8}$$

holds exactly. In like manner we have

$$\delta\lambda_2' = \delta\lambda_1 \tag{E-9}$$

$$\delta H_B = \delta\lambda_2 \sin y_1 - \delta\lambda_1 y_2 \tag{E-10}$$

where δH_B is the change in the Hamiltonian producing a change δy_{1r} in the second switch point. Noting that for $\delta y_{1r} > 0$ (via an argument similar to that in the proof of theorem 3-3)

$$-\frac{\delta\lambda_{1s}}{y_{2s}^2} > 0 \tag{E-11}$$

It will be sufficient to show that

$$-2A\left(\frac{\lambda_{1r}}{y_{2r}^4} + \int_{y_{1s}}^{y_{1r}} \frac{\delta\lambda_1(\sigma)y_2(\sigma)}{y_2^5(\sigma)}\, d\sigma\right) > 0 \tag{E-12}$$

in order to guarantee that δF be positive. Using (E-10) this is equivalent to

$$\frac{\lambda_{1r}}{y_{2r}^4} + \int_{y_{1s}}^{y_{1r}} \frac{-\delta H + \delta\lambda_2(\sigma)\sin y_1(\sigma)}{y_2^5(\sigma)}\, d\sigma < 0 \tag{E-13}$$

Now

$$\int_{y_{1s}}^{y_{1r}} \frac{\delta\lambda_2 \sin y_1}{y_2^5}\, d\sigma = \int_{y_{1s}}^{y_{1r}} \delta\lambda_2 \frac{d}{d\sigma}\left(\frac{1}{3y_2^3(\sigma)}\right) d\sigma \tag{E-14}$$

$$= \frac{1}{3y_2^3}\delta\lambda_2 \Big|_{y_{1s}}^{y_{1r}} - \int_{y_{1s}}^{y_{1r}} \frac{1}{3y_2^3(\sigma)} \frac{\delta\lambda_1(\sigma)}{(-y_2(\sigma))}\, d\sigma \tag{E-15}$$

where the last equality is obtained by integration by parts. From (E-10), (E-14), and (E-15) then

$$\int_{y_{1s}}^{y_{1r}} \frac{\delta\lambda_1 y_2 + \delta H_B}{y_2^5}\, d\sigma = \frac{1}{3}\left[\frac{\delta\lambda_{2r}}{y_{2r}^3} + \int_{y_{1s}}^{y_{1r}} \frac{\delta\lambda_1 y_2}{y_2^5}\, d\sigma\right] \tag{E-16}$$

or

$$2\int_{y_{1s}}^{y_{1r}} \frac{\delta\lambda_1(\sigma) y_2(\sigma)}{y_2^5(\sigma)}\, d\sigma = \frac{\delta\lambda_{2r}}{y_{2r}^3} - 3\delta H_B \int_{y_{1s}}^{y_{1r}} \frac{d\sigma}{y_2^5(\sigma)} \tag{E-17}$$

But from Appendix C we have along an O-arc

$$\delta\lambda_2 + \lambda_2 = y_2\left[\frac{\lambda_{2s} + \delta\lambda_{2s}}{y_{2s}} + (H_B + \delta H_B)\int_{y_{1s}}^{y_1} \frac{d\sigma}{y_2^3(\sigma)}\right] \tag{E-18}$$

from which

$$\delta\lambda_2 = y_2\left[\frac{\delta\lambda_{2s}}{y_{2s}} + \delta H_B \int_{y_{1s}}^{y_1} \frac{d\sigma}{y_2^3(\sigma)}\right] \tag{E-19}$$

and since $\delta\lambda_{2s} = 0$

$$\delta\lambda_{2r} = y_{2r}\delta H_B \int_{y_{1s}}^{y_{1r}} \frac{d\sigma}{y_2^3(\sigma)} \tag{E-20}$$

Since $\delta\lambda_{2r} < 0$ we must have

$$\delta H_B < 0 \tag{E-21}$$

Substituting for $\delta\lambda_{2r}$ into (E-17) we obtain

$$2\int_{y_{1s}}^{y_{1r}} \frac{\delta\lambda_1(\sigma)y_2(\sigma)}{y_2^5(\sigma)}\,d\sigma = \delta H_B\left[\frac{1}{y_{2r}^2}\int_{y_{1s}}^{y_{1r}} \frac{d\sigma}{y_2^3(\sigma)} + \right.$$

$$\left. - \int_{y_{1s}}^{y_{1r}} \frac{d\sigma}{y_2^5(\sigma)}\right] - 2\delta H_B \int_{y_{1s}}^{y_{1r}} \frac{d\sigma}{y_2^5(\sigma)} \qquad \text{(E-22)}$$

or

$$2\int_{y_{1s}}^{y_{1r}} \frac{\delta\lambda_2(\sigma)\sin y_1(\sigma)}{y_2^5(\sigma)}\,d\sigma =$$

$$\delta H_B\left[\frac{1}{y_{2r}^2}\int_{y_{1s}}^{y_{1r}} \frac{d\sigma}{y_2^3(\sigma)} - \int_{y_{1s}}^{y_{1r}} \frac{d\sigma}{y_2^5(\sigma)}\right] \qquad \text{(E-23)}$$

Because

$$y_{2r}^2 \geq y_2^2(\sigma) \qquad \text{(E-24)}$$

the bracketed term of (E-23) is positive. This together with (E-21) means

$$\int_{y_{1s}}^{y_{1r}} \frac{\delta\lambda_2(\sigma)\sin y_1(\sigma)}{y_2^5(\sigma)}\,d\sigma < 0 \qquad \text{(E-25)}$$

We have just shown one term of (E-13) to be negative. It will suffice to show

$$\frac{\lambda_{1r}}{y_{2r}^4} + \int_{y_{1s}}^{y_{1r}} -\frac{\delta H_B}{y_2^5(\sigma)}\,d\sigma < 0 \qquad \text{(E-26)}$$

as well. From (3-83) we have

$$H_B = \frac{\left(\frac{1}{y_{2r}} - \frac{1}{y_{2s}}\right)}{\int_{y_{1s}}^{y_{1r}} \frac{d\sigma}{y_2^3(\sigma)}} \tag{E-27}$$

from which

$$\delta H_B = \frac{dH_B}{dy_{1r}} = \frac{-\frac{1}{y_{2r}^2}\left(\frac{\sin y_{1r}}{-y_{2r}}\right)\int_{y_{1s}}^{y_{1r}} \frac{d\sigma}{y_2^3(\sigma)} - \frac{1}{y_{2r}^3}\left(\frac{1}{y_{2r}} - \frac{1}{y_{2s}}\right)}{\left(\int_{y_{1s}}^{y_{1r}} \frac{d\sigma}{y_2^3(\sigma)}\right)^2} \tag{E-28}$$

or using (E-27)

$$\delta H_B = \frac{(\sin y_{1r} - H_B)}{y_{2r}^3 \int_{y_{1s}}^{y_{1r}} \frac{d\sigma}{y_2^3(\sigma)}} \tag{E-29}$$

Since at the switching R

$$H_B = -\lambda_{1r} y_{2r} + \sin y_{1r} \tag{E-30}$$

(E-29) may be rewritten

$$\delta H_B = \frac{\lambda_{1r}}{y_{2r}^2 \int_{y_{1s}}^{y_{1r}} \frac{d\sigma}{y_2^3(\sigma)}} \tag{E-31}$$

Our goal of verifying that (E-26) is infact negative is thereby reduced to showing

$$\frac{\lambda_{1r}}{y_{2r}^4}\left[1 - \frac{y_{2r}^2 \int_{y_{1s}}^{y_{1r}} \frac{d\sigma}{y_2^5(\sigma)}}{\int_{y_{1s}}^{y_{1r}} \frac{d\sigma}{y_2^3(\sigma)}}\right] < 0 \qquad \text{(E-32)}$$

Since $\lambda_{1r} > 0$ for an 0-P corner we must verify that

$$1 < \frac{y_{2r}^2 \int_{y_{1s}}^{y_{1r}} \frac{d\sigma}{y_2^5(\sigma)}}{\int_{y_{1s}}^{y_{1r}} \frac{d\sigma}{y_2^3(\sigma)}} \qquad \text{(E-33)}$$

The fact that

$$y_{2r}^2 > y_2^2(\sigma) \qquad \text{(E-34)}$$

for $y_{1s} < \sigma < y_{1r}$ completes the proof.

If we first note that on the interval $[\pi, 2\pi]$, $\cos \sigma$ is monotonicly increasing then $y_2^2(\sigma)$ also increases monotonicly on the same interval

$$y_{2r}^2 > y_2^2(\sigma) \qquad \pi \leq \sigma < y_{1r} \leq 2\pi \qquad \text{(E-35)}$$

since

$$y_{2r}^2(\sigma) = \cos \sigma + K \qquad \text{(E-36)}$$

Likewise for $0 \leq y_{1s} < \sigma \leq \pi$

$$y_{2s}^2 > y_2^2(\sigma) \tag{E-37}$$

But we must require that

$$y_{2r}^2 \geq y_{2s}^2 \tag{E-38}$$

in order that the backward time Hamiltonian H_B be nonpositive. See relation (E-27). Therefore

$$y_{2r}^2 \geq y_{2s}^2 > y_2^2(\sigma) \tag{E-39}$$

for all σ less than π as well and (E-34) is verified.

REFERENCES

[1] Pontryagin, L.S., Boltyanskii, V.G., Gamkrelidze, R.V. and Mishchenko, E.F., The Mathematical Theory of Optimal Processes, Interscience Publications, John Wiley and Sons, New York, N.Y., 1962.

[2] Almuzara, J.L. and Flügge-Lotz, I. "Minimum Time Control of a Nonlinear System," SUDAAR Report No. 271, Department of Aeronautics and Astronautics, Stanford University, Stanford, California, May 1966. Also Journal of Differential Equations, Vol. 4, No. 1, 1968, pp. 12-39.

[3] Coddington, E.A., and Levinson, N., Theory of Ordinary Differential Equations, McGraw-Hill, New York, N.Y., 1955.

[4] Rozonoer, L.I., "L.S. Pontryagin's Maximum Principle in the Theory of Optimal Systems," Automation and Remote Control, Vol. 20, Oct., Nov., Dec., 1959, pp. 1288-1302, 1405-1421, 1517-1532.

[5] Dunn, J.C., "On the Classification of Singular and Nonsingular Extremals for the Pontryagin Maximum Principle," Journal of Mathematical Analysis and Applications, Vol. 17, No. 1, 1967, pp. 1-36.

[6] Gelfand, I.M. and Fomin, S.V., Calculus of Variations, Prentice-Hall, Englewood Cliffs, New Jersey, 1963.

[7] Kalman, R.E., "The Theory of Optimal Control and the Calculus of Variations," RIAS Technical Report 6-13, Research Institute for Advance Studies (RIAS), Baltimore, 1961. Also, Mathematical Optimization Techniques, Edited by R. Bellman, 1963.

[8] Kane, T.R., Force and Energy (The second of three parts of a preliminary edition from a forthcoming text on dynamics), Holt, Rinehart and Winston, New York, 1966.

[9] Flügge-Lotz, I., and Marbach, H., "The Optimal Control of Linear Systems for a Minimum Effort Performance Criteria," SUDAER No. 153, Department of Aeronautics and Astronautics, Stanford University, Stanford, California, April, 1963.

[10] Bushaw, D.W., Unpublished Ph.D. dissertation, Department of Mathematics, Princeton University, 1952. Also, "Differential Equations with a Discontinuous Forcing Term," Report No. 469, Experimental Towing Tank, Stevens Institute of Technology, Hoboken, N.J., January, 1953. Also, "Optimal Discontinuous Forcing Terms," Contributions to the theory of Nonlinear Oscillations," Vol. 4, Princeton University Press, Princeton, N.J., 1958, pp. 29-52.